PORPHYRINS AND METALLOPORPHYRINS

A new edition based on the original volume by J. E. Falk

Edited by

KEVIN M. SMITH

University of Liverpool

1975

ELSEVIER SCIENTIFIC PUBLISHING COMPANY
AMSTERDAM – OXFORD – NEW YORK

ELSEVIER SCIENTIFIC PUBLISHING COMPANY
335 Jan van Galenstraat
P.O. Box 211, Amsterdam, The Netherlands

AMERICAN ELSEVIER PUBLISHING COMPANY, INC.
52 Vanderbilt Avenue
New York, New York 10017

Universitäts-
Bibliothek
München

Bayerische
Staatsbibliothek
München

Ausgeschieden
aus den Beständen
der BSB München

Library of Congress Cataloging in Publication Data
Main entry under title:

Porphyrins and metalloporphyrins.

Includes bibliographical references and index.
1. Porphyrins and porphyrin compounds.
I. Falk, J. E. Porphyrins and metalloporphyrins.
II. Smith, Kevin M.
QD401.P7 1975 547'.593 75-26551
ISBN 0-444-41375-8

ISBN 0-444-41375-8

Copyright © 1975 by Elsevier Scientific Publishing Company, Amsterdam

All rights reserved. No part of this publication may be reproduced, stored in a retrieval system, or transmitted in any form or by any means, electronic, mechanical, photocopying, recording, or otherwise, without the prior written permission of the publisher, Elsevier Scientific Publishing Company, Jan van Galenstraat 335, Amsterdam

Printed in The Netherlands

PREFACE

In 1964, J.E. Falk was able to give one man's view of the porphyrin and metalloporphyrin field at possibly the last time that such a major task was possible. Since then the area has mushroomed outwards and blossomed in a quite remarkable manner, and this may in no small way be due to the stimulus provided by the appearance of *Porphyrins and Metalloporphyrins.* Around the time of his death, Falk was addressing himself to the task of updating and revizing his highly successful book, and realizing the magnitude of the undertaking, had begun to gather about him various colleagues who might be willing to contribute to a multi-authored Second Edition. Alas, all of this came to nothing, but the demand for a new and expanded edition of *Falk* remained.

The present book represents an attempt by some of the leading authorities in the field to fill the gap left by the progress of porphyrin chemistry past the account written by Falk. It differs considerably from the original, mainly in size, but also in the organization of the chapters into eight sections. A detailed description of the content of each section would be out of place here, but it is worth commenting that sections dealing with synthetic and biological aspects have been added, as well as chapters dealing in depth with many spectroscopic methods which were only in their infancy in 1964. In the whole book Falk's 'systematic and rational exposition which would have been quite impossible some years ago' has been carried to the boundaries of present research.

An attempt has been made to retain the idea of a 'Laboratory Handbook' which was the underlying concept in *Falk.* Though the book has grown dramatically in size, a substantial section dealing with laboratory methods has been included. Many of the procedures have not been noticeably improved since 1964, and in these cases there are few changes from the account written by Falk; however, in other respects, the Laboratory Methods Section has been expanded and revized.

The manuscript deadline for the present book was 1st January 1975, and with the exception of a few chapters which arrived in late March 1975, literature published after December 1974 has not been considered. However, as always when accounts are written by active research workers in the field, the chapters contain abundant references to unpublished work, or work in press, as well as personal communications from other researchers. In order to preserve the timeliness of the contributions in this book, it was necessary to proceed to publication without two manuscripts which were estimated, by the authors, to be one month or more from completion on 1st June 1975.

It is a pleasure to record my thanks to Professor G.W. Kenner, F.R.S., for his advice and encouragement during the past two years. In contributed volumes of this type with about twenty chapters, crises arise at fairly regular intervals; I would like to thank Professor Dr J.W. Buchler (Aachen) and Dr J.-H. Fuhrhop (Stöckheim über Braunschweig) for unhesitating assistance during these difficult times, and for providing the encouragement to go ahead in the formative days of this project.

Liverpool, June 1975 Kevin M. Smith

CONTENTS

Preface V

SECTION A: GENERAL AND SYNTHETIC ASPECTS

Chapter 1 *General features of the structure and chemistry of porphyrin compounds*

Kevin M. Smith

1.1 Structures and nomenclature 3
- 1.1.1 Nomenclature 5
- 1.1.2 Related structures 6
  - 1.1.2.1 Reduced porphyrin macrocycles 6
  - 1.1.2.2 Oxidized porphyrin macrocycles 8
  - 1.1.2.3 Porphyrin analogs 8
- 1.1.3 Isomerism in porphyrins 9

1.2 General chemistry 9
- 1.2.1 Aromaticity of the macrocycle 9
- 1.2.2 Tautomerism in the macrocycle 10
- 1.2.3 Ionization of porphyrins 11
  - 1.2.3.1 Nitrogen atoms 11
  - 1.2.3.2 Carboxylic acid side-chains 14
  - 1.2.3.3 Acid (HCl) numbers 15
  - 1.2.3.4 Complexation with metal ions 15
- 1.2.4 Stability of porphyrin compounds 15
  - 1.2.4.1 General features 15
  - 1.2.4.2 Instability to light 16
  - 1.2.4.3 Other examples of instability 16

1.3 Occurrence of porphyrin compounds 16
- 1.3.1 Metal complexes 16
- 1.3.2 Metal-free porphyrins 18

1.4 Chromophores of porphyrin systems 19
- 1.4.1 Porphyrins 20
  - 1.4.1.1 In neutral solvents 20
    - 1.4.1.1.1 Etio type spectra 20
    - 1.4.1.1.2 Rhodo type spectra 21
    - 1.4.1.1.3 Oxorhodo type spectra 23
    - 1.4.1.1.4 Phyllo type spectra 23
    - 1.4.1.1.5 Spectra of porphyrins containing isocyclic rings 23
  - 1.4.1.2 In acidic solvents 24
  - 1.4.1.3 In alkaline solvents 24

1.4.2 Chlorins 25
1.4.3 Metalloporphyrins 25
1.4.4 Phlorins and oxophlorins 25
References 27

Chapter 2 Synthesis and preparation of porphyrin compounds
Kevin M. Smith

2.1 Scope 29
2.2 Syntheses of dipyrrolic intermediates 30
  2.2.1 Pyrromethenes 30
  2.2.2 Pyrromethanes 31
  2.2.3 Pyrroketones 31
2.3 Syntheses of porphyrins 32
  2.3.1 By polymerization of monopyrroles 32
  2.3.2 From dipyrrolic intermediates 33
    2.3.2.1 From pyrromethenes 33
    2.3.2.2 From pyrromethanes 35
    2.3.2.3 From pyrroketones 36
  2.3.3 From open-chain tetrapyrrolic intermediates 36
    2.3.3.1 From bilanes and oxobilanes 37
      2.3.3.1.1 Using bilane intermediates 37
      2.3.3.1.2 Using *a*-oxobilane intermediates 38
      2.3.3.1.3 Using *b*-oxobilane intermediates 40
    2.3.3.2 From bilenes 41
      2.3.3.2.1 Using 1′,8′-dimethyl-*b*-bilenes 41
      2.3.3.2.2 Using *b*-bilene-1′,8′-diesters 42
      2.3.3.2.3 Using other *b*-bilenes 43
    2.3.3.3 From *a,c*-biladienes 44
      2.3.3.3.1 Using 1′,8′-dimethyl-*a,c*-biladienes 44
      2.3.3.3.2 Using 1′-bromo-8′-methyl-*a,c*-biladienes 46
      2.3.3.3.3 Using other *a,c*-biladienes 46
  2.3.4 General conclusions 47
2.4 Preparation of porphyrins by degradation of natural pigments 48
  2.4.1 From hemoglobin 48
    2.4.1.1 Protohemin 48
    2.4.1.2 Hematoporphyrin-IX 49
    2.4.1.3 Protoporphyrin-IX 49
    2.4.1.4 Mesoporphyrin-IX 50
    2.4.1.5 Deuteroporphyrin-IX and its derivatives 50
    2.4.1.6 Coproporphyrin-III 51
    2.4.1.7 Other porphyrins of biological significance 51
  2.4.2 From the plant chlorophylls 52
References 55

SECTION B: BIOLOGICAL ASPECTS

Chapter 3 Biosynthesis of porphyrins, chlorins, and corrins
A.R. Battersby and E. McDonald

3.1 Introduction 61
3.2 The biosynthesis of porphobilinogen 62

3.2.1 Historical background and fundamental studies 62
3.2.2 ALA synthetase 66
3.2.2.1 Mechanistic studies 66
3.2.2.1.1 Cofactor requirement 66
3.2.2.1.2 Binding and activation of glycine 68
3.2.2.1.3 Binding of succinyl coenzyme A and the acylation step 70
3.2.2.1.4 The decarboxylation step 70
3.2.2.2 Inhibition of ALA synthetase in vivo 72
3.2.3 ALA dehydratase 72
3.2.3.1 Binding of ALA 73
3.3 Conversion of porphobilinogen into uroporphyrinogen-III 74
3.3.1 Porphyrinogens as biosynthetic intermediates 74
3.3.2 Outline of the problem 75
3.3.3 Porphobilinogen deaminase 77
3.3.4 Uroporphyrinogen-III cosynthetase 78
3.3.5 Enzymic formation of uroporphyrinogen-I 78
3.3.5.1 Stoichiometry 78
3.3.5.2 Intermediates 79
3.3.5.3 Possible mechanistic scheme 82
3.3.6 Enzymic formation of uroporphyrinogen-III 83
3.3.7 Analysis of hypotheses regarding formation of the type-III isomer 85
3.3.8 Basic studies with carbon-13 n.m.r. and integrity of the type-III macrocycle 87
3.3.9 Nature of the rearrangement process from experiments with $^{13}C_2$-PBG 89
3.3.10 Enzymic studies with pyrromethanes 92
3.3.10.1 The AP · PA pyrromethane 92
3.3.10.2 The PA · PA pyrromethane 93
3.3.10.3 The AP · AP pyrromethane 93
3.3.10.4 The PA · AP pyrromethane 94
3.3.10.5 Conclusions 95
3.3.11 Enzymic studies with a tripyrrole and a bilane 96
3.3.12 Conclusions 96
3.4 Side-chain modifications and aromatization to protoporphyrin-IX 96
3.4.1 Decarboxylation of uroporphyrinogen-III 96
3.4.1.1 The partially decarboxylated intermediates 97
3.4.2 Oxidative decarboxylation of coproporphyrinogen-III 99
3.4.2.1 Enzymic studies 100
3.4.2.2 Mechanistic studies 101
3.4.2.3 Intermediates 102
3.4.3 Aromatization of protoporphyrinogen-IX 104
3.4.3.1 Intermediates 105
3.5 The iron, magnesium, and cobalt branches 106
3.5.1 The iron branch 106
3.5.1.1 Formation of protoheme 106
3.5.1.2 The hemoproteins 106
3.5.2 The magnesium branch 107
3.5.2.1 Chelation of magnesium 109
3.5.2.2 Esterification of magnesium protoporphyrin-IX 109
3.5.2.3 Reduction of the vinyl group at position-4 109
3.5.2.4 Oxidative formation of the carbocyclic ring 110
3.5.2.5 Reduction of ring D 111
3.5.2.6 Formation of chlorophyll-*a* 111

3.5.2.7 Chlorophyll-*b* 111
3.5.2.8 Bacteriochlorophyll 112
3.5.3 The cobalt branch 112
3.5.3.1 Studies using precursors labeled with carbon-14 and carbon-13 112
3.5.3.2 Intermediates in corrin biosynthesis 115
Epilog 116
References *116*

Chapter 4 *Heme cleavage: biological systems and chemical analogs*
Pádraig O'Carra

4.1 Introduction 123
4.1.1 Chemical and biological derivation of bilins from hemes 123
4.1.2 Mammalian heme catabolism 127
4.2 Coupled oxidation of hemes and hemoproteins 130
4.2.1 General characteristics and requirements 130
4.2.2 Role of axial ligands and effect of heme environment 131
4.2.3 Chemical pathway and intermediates 132
4.2.4 Specificity of bridge cleavage 137
4.3 Biological heme cleavage 142
4.3.1 Pathway in vivo 142
4.3.2 Causative factors 144
References *150*

SECTION C: COORDINATION CHEMISTRY OF METALLOPORPHYRINS

Chapter 5 *Static coordination chemistry of metalloporphyrins*
J.W. Buchler

5.1 Introduction 157
5.2 Classification of metalloporphyrins 163
5.3 Equatorial coordination chemstry 171
5.3.1 Stages in the development of the periodic table of metalloporphyrins 171
5.3.2 Problems associated with metal insertion 174
5.3.3 Examples and scopes of selected successful insertion procedures 177
5.3.3.1 The acetate method 180
5.3.3.2 The pyridine method 182
5.3.3.3 The acetylacetonate method 183
5.3.3.4 The phenoxide method 184
5.3.3.5 The benzonitrile method 185
5.3.3.6 The dimethylformamide method 185
5.3.3.7 The metal organyl method 186
5.3.3.8 The metal carbonyl method 186
5.3.4 Criteria of successful metal insertion; absorption spectroscopy in the visible region and other methods 187
5.3.5 Oxidation states of the central metal ions 191
5.3.6 Demetalation, transmetalation, and stability orders 195
5.3.6.1 Stability classes 196
5.3.6.2 Appraisal of a stability index 199
5.3.6.3 Demetalation 199

5.3.6.4 Transmetalation 201
5.3.6.5 Correlations of spectra data and stability 203
5.3.7 The influence of structurally modified porphyrin ligands on the stability of metalloporphyrins 205
5.4 Axial coordination chemistry 207
5.4.1 General remarks 207
5.4.2 Preparation of metalloporphyrins with specific axial ligands 210
5.4.3 Axial coordination chemistry of metalloporphyrins containing group VIII metals 215
5.4.4 Identification of axial ligands 221
References *224*

Chapter 6 Dynamic coordination chemistry of metalloporphyrins
Peter Hambright

6.1 Introduction 233
6.2 Acid-base properties 234
6.3 Isotopic exchange of the central metal ion 239
6.4 Reactions of metalloporphyrins with free-base porphyrins 239
6.5 Electrophilic substitution reactions 240
6.6 Acid solvolysis reactions 243
6.7 Metal ion incorporation reactions 247
6.7.1 Equilibrium constants 247
6.7.2 Sitting-atop complexes 248
6.7.3 Non-aqueous, mixed solvent, and detergent kinetics 249
6.7.4 Aqueous solutions 252
6.7.5 Mechanisms of incorporation 253
6.8 Electron transfer, exchange and catalysis 255
6.9 Stability constants — thermodynamics 259
6.9.1 Cu, Zn, Cd, Hg, and VO 259
6.9.2 Mg, Ni and Fe(II) 260
6.9.3 Fe(III), Mn(III), and Co(III) 263
6.9.4 Co(II) 264
6.10 Dimerization and hydrolysis 265
6.11 Solvent exchange 268
6.12 Ligand substitution mechanisms 268
References *271*

Chapter 7 Metalloporphyrins with unusual geometry
Minoru Tsutsui and Glenn A. Taylor

7.1 Introduction 279
7.2 Syntheses 282
7.2.1 Traditional method 282
7.2.2 Carbonyl method 282
7.2.3 Hydride method 283
7.2.4 Organometallic method 286
7.2.5 Acetylacetone derivatives 286
7.2.6 Using solvents with high dielectric constants 287
7.2.7 Progress 287
7.3 Structures 288

- 7.3.1 Bridged and metal-metal bonded species 288
  - 7.3.1.1 Nitrogen bridged 289
  - 7.3.1.2 Oxygen bridged 290
  - 7.3.1.3 Halide bridged 292
  - 7.3.1.4 Metal-metal bonds 292
- 7.3.2 Unusual geometries 295
  - 7.3.2.1 Monometallic 295
  - 7.3.2.2 Dimetallic 300
  - 7.3.2.3 Trimetallic 310

References *310*

SECTION D: DETERMINATION OF MOLECULAR STRUCTURE

Chapter 8 Stereochemistry of porphyrins and metalloporphyrins

J.L. Hoard

- 8.1 General considerations 317
  - 8.1.1 Nomenclature 317
  - 8.1.2 Historical notes 320
  - 8.1.3 Considerations of symmetry 321
- 8.2 Stereochemistry of the porphinato core in metalloporphyrins 327
- 8.3 The free-base porphyrins and related metal-free species 336
  - 8.3.1 Free-bases 336
  - 8.3.2 Related free-bases 341
  - 8.3.3 Porphyrin acids 341
- 8.4 Stereochemistry of the coordination groups in metalloporphyrins 343
  - 8.4.1 The d^{10} and d^0 metalloporphyrins 344
  - 8.4.2 The d^9 and d^8 metalloporphyrins 349
  - 8.4.3 The d^1, d^2, and d^3 metalloporphyrins 351
  - 8.4.4 The $4d^5$ and $4d^6$ metalloporphyrins 351
  - 8.4.5 The manganese, iron, and cobalt metalloporphyrins 351
    - 8.4.5.1 The high-spin iron and manganese metalloporphyrins 352
    - 8.4.5.2 The low-spin iron and cobalt porphyrins 359
    - 8.4.5.3 The nitrosylmetal(II) metalloporphyrins 364
    - 8.4.5.4 The iron(II) derivatives of the 'picket fence' porphyrin 366
  - 8.4.6 Stereochemistry of the protoheme in hemoglobin 368
  - 8.4.7 The axial connection in deoxycobaltohemoglobin 371
  - 8.4.8 Porphinato complexes of unconventional coordination geometry 373

Appendix I 373

References *376*

Chapter 9 Mass spectrometry of porphyrins and metalloporphyrins

Kevin M. Smith

- 9.1 Introduction 381
- 9.2 Porphyrins and chlorins 382
  - 9.2.1 The molecular ion 382
  - 9.2.2 Side-chain fragmentations 388
    - 9.2.2.1 Peripheral side-chains 388
    - 9.2.2.2 *meso*-Substitutents and carbocyclic rings 391
    - 9.2.2.3 *N*-Methylporphyrins 394

9.2.3 Doubly charged ions 394
9.3 Metalloporphyrins 395
9.4 Anomalies 396
References *397*

Chapter 10 Nuclear magnetic resonance spectroscopy of porphyrins and metalloporphyrins

Hugo Scheer and Joseph J. Katz

10.1 Introduction 399
  10.1.1 The chemical shift 400
  10.1.2 The aromatic ring current 402
    10.1.2.1 Ring current in related macrocycles 405
    10.1.2.2 Ring current and structure 409
  10.1.3 Practical considerations for ^{1}HMR of porphyrins 411
10.2 ^{1}HMR spectra 412
  10.2.1 The ^{1}HMR spectra of diamagnetic porphyrins 412
    10.2.1.1 Porphin 412
    10.2.1.2 Octaethylporphyrin 416
    10.2.1.3 *meso*-Tetraphenylporphyrin 416
    10.2.1.4 Protoporphyrin-IX dimethyl ester 417
    10.2.1.5 Chlorin-e_6 trimethyl ester 417
    10.2.1.6 Chlorophyll-*a* 418
  10.2.2 β-Substitution 418
  10.2.3 *meso*-Substitution 426
  10.2.4 *N*-Substitution 437
  10.2.5 Chlorins and related structures 440
  10.2.6 Systems with interrupted conjugation 448
  10.2.7 Porphyrin acids 457
  10.2.8 Metal-porphyrin complexes 459
    10.2.8.1 Diamagnetic 1 : 1 metal complexes 460
    10.2.8.2 The chlorophylls 462
      10.2.8.2.1 Chlorophylls c_1 and c_2 465
      10.2.8.2.2 Bacteriochlorophyll-*b* 465
      10.2.8.2.3 Bacteriochlorophyll *c*, *d*, and *e* 466
      10.2.8.2.4 Chlorophyll related structures 467
    10.2.8.3 Unusual metalloporphyrins with central metal 468
    10.2.8.4 Peripheral complexes 471
    10.2.8.5 Paramagnetic metal complexes 473
      10.2.8.5.1 Fe complexes 476
      10.2.8.5.2 Metals other than Fe 480
10.3 Nuclei other than ^{1}H 481
  10.3.1 ^{13}CMR of porphyrins 482
    10.3.1.1 ^{13}CMR of diamagnetic porphyrins 482
    10.3.1.2 ^{13}C of paramagnetic metalloporphyrins 490
  10.3.2 ^{15}NMR of porphyrins 491
  10.3.3 Magnetic resonance of central metals in metalloporphyrins 492
  10.3.4 ^{2}HMR of porphyrins 492
10.4 Introduction to applications section 493
  10.4.1 Aggregation 493
    10.4.1.1 Porphyrin self-aggregation 494
    10.4.1.2 Hetero- or exogamous aggregation 498

10.4.2 Dynamic processes 501
    10.4.2.1 NH tautomerism 501
    10.4.2.2 Conformation of β-pyrrole substituents 503
    10.4.2.3 Conformation of *meso*-substituents 504
10.4.3 Stereochemistry 505
    10.4.3.1 The macrocycle 505
    10.4.3.2 Metalloporphyrins 506
    10.4.3.3 Non-centrosymmetric stereoisomerism 508
    10.4.3.4 Asymmetric carbon atoms 509
10.4.4 Miscellaneous 513
References *514*

Chapter 11 Vibrational spectroscopy of porphyrins and metalloporphyrins
Hans Bürger

11.1 Introduction 525
11.2 Vibrations of the porphin macrocycles 526
11.3 Vibrations of non-porphyrin macrocycles 527
11.4 Vibrations of peripheral groups 530
11.5 Metal-nitrogen vibrations 531
11.6 Vibrations of axial ligands 533
References *534*

SECTION E: ELUCIDATION OF ELECTRONIC STRUCTURE

Chapter 12 Mössbauer spectroscopy and magnetochemistry of metalloporphyrins
Peter Hambright and Alan J. Bearden

12.1 Mössbauer spectroscopy 539
    12.1.1 Introduction 539
    12.1.2 High spin ferric porphyrins 541
    12.1.3 Ferrous porphyrins 545
    12.1.4 Oxy-bridged ferric porphyrin dimers 545
12.2 Magnetic susceptibility 545
    12.2.1 Introduction 545
    12.2.2 Oxidation states 546
    12.2.3 Theoretical predictions 548
    12.2.4 Spin state equilibria and magnetic exchange 549
References *551*

Chapter 13 Electron paramagnetic resonance spectroscopy of porphyrins and metalloporphyrins
J. Subramanian

13.1 General background 555
    13.1.1 Introduction 555
    13.1.2 Basic principles and information obtainable from EPR spectroscopy 555
        13.1.2.1 g-Values and symmetry 555

13.1.2.2 Fine structure and zero field splitting 556
13.1.2.3 Nuclear hyperfine interaction 557
13.1.2.4 The concept of a spin Hamiltonian 558
13.1.2.5 Spin relaxation and linewidths 558
13.1.3 Experimental aspects 559
13.2 Porphyrins which contain paramagnetic metals 560
13.2.1.1 Copper and silver porphyrins 562
13.2.1.2 Vanadyl and molybdyl porphyrins 567
13.2.2 d^2 and d^8 systems 567
13.2.3 d^3 and d^7 systems: Co(II) porphyrins and related systems 568
13.2.4 d^4 and d^6 systems: Fe(II) and Mn(III) porphyrins 571
13.2.5 d^5 systems: Mn(II) and Fe(III) porphyrins 574
13.3 Porphyrins with unpaired electrons on the ligand 576
13.3.1 Radical cations of free-base and metalloporphyrins 576
13.3.1.1 A brief review of the electronic structure of the porphyrin ligand 576
13.3.1.2 Radical cations from *meso*-tetraphenyl- and octaethylporphyrin systems 577
13.3.1.3 Chlorins and chlorophylls 579
13.3.2 Radical anions from porphyrins and related systems 580
13.3.2.1 Metalloporphyrins 580
13.3.2.3 Phlorins 580
13.3.3 Triplet states of porphyrins and metalloporphyrins 581
13.4 Porphyrins with unpaired electrons in the metal as well as in the ligand 582
13.41 Oxidation products of Cu porphyrins and chlorins 582
13.4.2 Oxidation products of iron porphyrins 583
13.4.3 Oxidation products of vanadyl porphyrins 583
13.5 Biological applications 584
References *586*

SECTION F: CHEMICAL REACTIVITY

Chapter 14 Reversible reactions of porphyrins and metalloporphyrins and electrochemistry

Jürgen-Hinrich Fuhrhop

14.1 Introduction 593
14.2 Chemical oxidation and reduction potentiometry 594
14.3 Polarography and voltammetry with a rotating platinum electrode 599
14.4 Cyclic voltammetry 603
14.5 Preparative electrolysis of metalloporphyrins 607
14.6 Differentiation between reactions of central ions and the porphyrin periphery 609
14.7 Redox potentials and chemical reactivity of the porphyrin ligand 610
14.8 Properties of porphyrin π-radicals 612
14.9 Phlorins, porphodimethenes, and porphyrinogens 614
14.10 Aggregation through interactions of the porphyrin π-electron core with other π-electron systems 618
References *620*

Chapter 15 Irreversible reactions at the porphyrin periphery (excluding photochemistry)
Jürgen-Hinrich Fuhrhop

15.1 General aspects of reactivity at the porphyrin periphery 625
  15.1.1 Electronic reactivity parameters of reaction sites 625
  15.1.2 Stereochemical aspects 627
  15.1.3 Influence of central metal ions 629
15.2 Oxidation 629
  15.2.1 Introduction 629
  15.2.2 Oxyporphyrins, oxophlorins, and their π-radicals 630
    15.2.2.1 Structure 630
    15.2.2.2 Reactivity 633
    15.2.2.3 Metal complexes of oxyporphyrins 636
  15.2.3 Dioxoporphodimethenes 636
  15.2.4 Xanthoporphyrinogens (*meso*-tetraoxoporphyrinogens) 638
  15.2.5 Oxaporphyrins 638
  15.2.6 β—β'-Dihydroxychlorins and β-oxochlorins 639
15.3 Peripheral (β-β') hydrogenation 640
  15.3.1 Introduction 640
  15.3.2 Chlorins 641
  15.3.3 *a* and *b* Tetrahydroporphyrins 643
  15.3.4 Hexahydroporphyrins and corphins 644
15.4 Electrophilic substitution and addition reactions 645
  15.4.1 General aspects 645
  15.4.2 Deuteration 647
  15.4.3 Acylation and methylation 648
  15.4.4 Reactions with carbenes, nitrenes, and nitrogen tetroxide/dichloromethane 650
  15.4.5 Nitration 651
  15.4.6 Halogenation 653
  15.4.7 Thiocyanation 653
15.5 Nucleophilic substitution and addition reactions 654
15.6 Reactions of carbon substituents 654
  15.6.1 Ethyl groups 654
  15.6.2 Vinyl groups 655
  15.6.3 Carboxylic and propionic acids 656
  15.6.4 Miscellaneous 659
15.7 Degradation of the porphyrin nucleus 659
References *662*

Chapter 16 Photochemistry of porphyrins and metalloporphyrins
Frederick R. Hopf and David G. Whitten

16.1 Introduction 667
  16.1.1 Excited states of porphyrins and metalloporphyrins 667
    16.1.1.1 Luminescence of porphyrins and metalloporphyrins 667
      16.1.1.1.1 General 667
      16.1.1.1.2 Luminescence of specific types of metalloporphyrin complexes 670
    16.1.1.2 Porphyrin excited states as studied by flash photolysis 672

16.1.2 Porphyrin photochemistry — summary of emerging reaction patterns 673
16.2 Energy transfer, complex formation, quenching phenomena: porphyrins as photosensitizers 675
  16.2.1 General, quenching phenomena and intermolecular energy transfer 673
  16.2.2 Intramolecular energy transfer 675
  16.2.3 Sensitization of singlet oxygen and photodynamic deactivation 676
  16.2.4 Electron transfer and complex formation in the excited state 677
16.3 Photoreduction reactions 677
  16.3.1 Free-base porphyrins 678
  16.3.2 Metalloporphyrins 680
    16.3.2.1 Reduction of the porphyrin ligand 680
    16.3.2.2 Photoreduction of the central metal 687
16.4 Photo-oxidation 687
  16.4.1 Free-base porphyrins 687
  16.4.2 Metalloporphyrins 689
16.5 Ligand photoejection 694
References *695*

Chapter 17 Photochemistry of porphyrins in membranes and photosynthesis

David Mauzerall and Felix T. Hong

17.1 Introduction 701
17.2 Electron transfer 701
  17.2.1 Photosynthesis 701
  17.2.2 Theory 702
  17.2.3 Reduction 704
  17.2.4 Oxidation 705
17.3 Cyclic reactions in solution 706
  17.3.1 Porphyrin-phlorin 706
  17.3.2 Metalloporphyrin-acceptor 707
17.4 Sensitization 708
17.5 Colloidal systems 709
17.6 Monolayers 709
  17.6.1 Air—water 709
  17.6.2 Solid—water 710
17.7 Bilayer lipid membranes 712
  17.7.1 Structure 712
  17.7.2 Photoelectrical effects 713
  17.7.3 Methodology 715
  17.7.4 Results 717
  17.7.5 Discussion 719
  17.7.6 Relation to photosynthesis 721
References *722*

SECTION G: STRUCTURAL ANALOGS OF PORPHYRINS

Chapter 18 Structural analogs of porphyrins

A.W. Johnson

Nomenclature 729
18.1 Porphyrin analogs with mixed hetero-atoms 729

18.2 Corroles and tetradehydrocorrins 732
  18.2.1 Synthesis 732
  18.2.2 Physical properties of corroles and metal tetradehydrocorrins 736
  18.2.3 Chemical properties of corroles and their metal complexes 737
  18.2.4 Chemical properties of nickel 1-methyltetradehydrocorrins 740
  18.2.5 Chemical properties of metal 1,19-disubstituted tetradehydrocorrin salts 741
    18.2.5.1 Protonation 741
    18.2.5.2 Removal of angular ester groups 741
    18.2.5.3 Thermolysis 742
    18.2.5.4 Hydrogenation 743
    18.2.5.5 Hydroxylation 746
    18.2.5.6 Substitution and redox reactions of nickel salts 747
    18.2.5.7 Substitution and redox reactions of cobalt salts 748
18.3 Corroles with mixed hetero-atoms 749
18.4 Sapphyrins and related ring systems 750
18.5 Corphins 751
References *752*

SECTION H: LABORATORY METHODS

Chapter 19 Laboratory methods

Jürgen-Hinrich Fuhrhop and Kevin M. Smith

19.1 Introduction 757
19.2 Typical synthetic procedures 757
  19.2.1 Porphobilinogen 758
  19.2.2. Coproporphyrin-III tetramethyl ester 761
  19.2.3 Etioporphyrin-I 765
  19.2.4 Octaethylporphyrin 766
  19.2.5 *meso*-Tetraphenylporphyrin 769
    19.2.5.1 Crude material 769
    19.2.5.2 'Chlorin-free' *meso*-tetraphenylporphyrin 770
19.3 Porphyrins derived from protoheme 770
  19.3.1 Protoporphyrin-IX 770
  19.3.2 Hematoporphyrin-IX and derivatives 771
    19.3.2.1 Hematoporphyrin-IX 771
    19.3.2.2 Hematoporphyrin-IX dimethyl ester 772
    19.3.2.3 Hematoporphyrin-IX dimethyl ether 772
    19.3.2.4 Hematoporphyrin-IX dimethyl ester dimethyl ether 772
  19.3.3 Mesoporphyrin-IX
  19.3.4 Deuteroporphyrin-IX 773
  19.3.5 Deuteroporphyrin-IX 2,4-disulfonic acid 774
    19.3.5.1 Dimethyl ester 774
    19.3.5.2 Tetramethyi ester 774
19.4 Compounds derived from chlorophylls 774
  19.4.1 Chlorophylls from plant tissue 774
  19.4.2 Pheophytins 775
    19.4.2.1 Separation of pheophytins *a* and *b* 775
  19.4.3 Pheophorbides 776
  19.4.4 Purpurin-7 trimethyl ester 776
  19.4.5 Purpurin-18 methyl ester 776

19.4.6 2-Vinylrhodoporphyrin-XV dimethyl ester 777
19.4.7 Rhodoporphyrin-XV dimethyl ester 777
19.4.8 Methyl pyropheophorbide-*a* 777
19.4.9 Chlorin-e_6 trimethyl ester and rhodin-g_7 trimethyl ester 777
19.4.10 Phylloerythrin methyl ester 777
19.4.11 2-Vinylpheoporphyrin-a_5 dimethyl ester 778
19.4.12 Pheoporphyrin-a_5 dimethyl ester 778
19.5 Porphyrins in natural materials 778
19.5.1 Coproporphyrins 778
19.5.2 Uroporphyrins 778
19.5.3 Detection in biological materials 779
19.5.3.1 Determination of protoporphyrin and uro- (or copro)porphyrin in whole blood 779
19.5.4 Concentration from biological materials 780
19.5.4.1 The calcium phosphate method of Sveinsson et al. 780
19.5.4.2 The Kieselguhr method 780
19.5.4.3 The talc method 781
19.5.5 Analysis by solvent extraction 781
19.5.5.1 Copro- and proto-porphyrins and porphyrinogens 781
19.5.5.2 Zinc(II) coproporphyrin 782
19.5.5.3 Spectrophotometric determinations 782
19.5.5.4 Fluorimetric determination of uro-, copro- and protoporphyrins 783
19.5.5.5 Uroporphyrins 783
19.5.5.5.1 The cyclohexanone method 783
19.5.5.5.2 The ethyl acetate method 785
19.5.5.5.3 The alumina column method 785
19.5.5.5.4 Determination 785
19.5.6 Porphyrins in petroleum and shale 785
19.6 Porphyrin precursors 785
19.6.1 Aminolevulinic acid 785
19.6.1.1 Determination in biological materials 785
19.6.1.1.1 Elliott's picric acid method 786
19.6.1.1.2 Mauzerall and Granick's acetylacetone method 786
19.6.1.1.3 Mauzerall and Granick's ethyl acetoacetate method 787
19.6.1.2 Chromatographic separation of ALA and PBG 787
19.6.1.2.1 Separation of PBG and ALA on the Dowex-2 column 787
19.6.1.2.2 Concentration of ALA by a Dowex-50 column 787
19.6.1.3 Paper chromatography of ALA 788
19.6.2 Porphobilinogen 788
19.6.2.1 Isolation from urine 788
19.6.2.2 Preparation of PBG hydrochloride 789
19.6.2.3 Microbial preparation of PBG from ALA on a large scale 789
19.6.2.4 Qualitative identification 790
19.6.2.4.1 The Ehrlich reaction 790
19.6.2.5 Quantitative determination by Ehrlich's reagent 791
19.6.2.6 Paper chromatography 791
19.6.3 Porphyrinogens 792
19.6.3.1 Preparation with sodium amalgam 792
19.6.3.2 Preparation with sodium borohydride 793

19.6.3.3 Detection of enzymically formed porphyrinogens 793
19.6.3.4 Analysis of urinary porphyrinogens 794
19.7 Preparation of metalloporphyrins from porphyrins and isolation from natural sources 795
19.7.1 Insertion of metal ions other than iron 795
19.7.1.1 Li, Na, K (Ba, Rb, Cs) 795
19.7.1.2 Mg, Ca, Cd 796
19.7.1.2.1 Magnesium protoporphyrin-IX dimethyl ester 796
19.7.1.2.2 Dipotassium salt of magnesium protoporphyrin-IX 796
19.7.1.3 Method 3 797
19.7.1.3.1 Al(III) 797
19.7.1.3.2 Si(IV) [Ge(IV), Ga(III) and In(III)] 797
19.7.1.3.3 Sn(IV), Mn(III), Pd(II) and Pt(II) 797
19.7.1.3.4 Zn(II), [Co(II), Ni(II) and Cu(II)] 798
19.7.1.3.5 Vanadyl 798
19.7.1.3.6 Ag(II), Pb(II), Hg(II) 798
19.7.1.4 Metal diketones 798
19.7.1.4.1 Sc(III), Al(III) 798
19.7.1.4.2 Lanthanides, e.g., Eu(III) 799
19.7.1.5 Method 5 799
19.7.1.5.1 O=Mo(V), Cr(II), O=Ti(IV) 799
19.7.2 Insertion and removal of iron 800
19.7.2.1 Removal of iron from hemins 800
19.7.2.1.1 The ferrous sulfate method 800
19.7.2.1.2 The ferrous acetate—acetic acid method 801
19.7.2.1.3 The iron-powder method 802
19.7.2.1.4 The formic acid method 802
19.7.2.1.5 Removal of iron with concurrent esterification 802
19.7.2.2 Insertion of iron 803
19.7.2.2.1 The ferrous sulfate method 803
19.7.2.2.2 The ferrous acetate—acetic acid method 804
19.7.3 Hemes 804
19.7.3.1 Determination as pyridine hemochromes 804
19.7.3.2 Solvent extraction from tissues 807
19.7.3.2.1 Ether—acetic acid or ethyl acetate—acetic acid 807
19.7.3.2.2 Acid—acetone 807
19.7.3.2.3 Methyl ethyl ketone 808
19.7.3.3 Protohemin 808
19.7.3.3.1 Preparation of crystalline hemin 808
19.7.3.3.2 Formiatohemin and other hemin-anion complexes 810
19.7.3.4 Splitting the heme from cytochrome-*c* 811
19.8 Reactions at the *meso* and peripheral positions of porphyrins and metalloporphyrins 811
19.8.1 Oxidation 812
19.8.1.1 Metalloporphyrin π-cation radicals 812
19.8.1.2 Octaethyloxophlorin 812
19.8.1.3 Octaethyloxophlorin π-radical 812
19.8.1.4 Octaethylxanthoporphyrinogen 813
19.8.1.5 1,2,3,4,5,6,8,8-Octaethyl-7-oxochlorin 813
19.8.1.6 Conversion of an oxyhemin into a biliverdin derivative 813
19.8.1.7 Zinc octaethyl-1′-formylbiliverdin 814

19.8.2 Hydrogenation and reductions 814
    19.8.2.1 β-Phlorin of chlorin-e_6 trimethyl ester 814
    19.8.2.2 *trans*-Octaethylchlorin 815
    19.8.2.3 *cis*-Octaethylchlorin 815
    19.8.2.4 Uroporphyrinogen-III 815
    19.8.2.5 Conversion of an oxophlorin into a porphyrin 816
19.8.3 Reactions at the *meso*-positions of porphyrins and metalloporphyrins 816
    19.8.3.1 Deuteration 816
        19.8.3.1.1 *meso*-Tetradeutero-octaethylporphyrin 816
        19.8.3.1.2 *meso*-Tetradeuterocoproporphyrin-I tetramethyl ester 817
        19.8.3.1.3 γδ-Dideutero-*trans*-octaethylchlorin 817
    19.8.3.2 Vilsmeier formylation of copper octaethylporphyrin and Knoevenagel condensation 818
    19.8.3.3 Mono-nitration of octaethylporphyrin 818
    19.8.3.4 α-Nitro-etioporphyrin-I 818
    19.8.3.5 Mono- and di-chlorination of octaethylporphyrin 819
    19.8.3.6 Mono-thiolation of copper octaethylporphyrin 819

19.9 Modification and identification of porphyrin side-chains 819
19.9.1 Methoxyl groups 820
19.9.2 Active hydrogen atoms 821
19.9.3 Vinyl side-chains 821
    19.9.3.1 Reduction to ethyl 821
    19.9.3.2 Reaction with diazoacetic ester 821
    19.9.3.3 Hydration by HBr—acetic acid 821
    19.9.3.4 Removal in the resorcinol melt 822
    19.9.3.5 Oxidation of vinyl to formyl groups 822
    19.9.3.6 Conversion of vinyl into β-hydroxypropionic acid 822
    19.9.3.7 Protection of vinyl groups 823
19.9.4 Hydroxyethyl groups in side-chains 824
    19.9.4.1 Acetylation 824
    19.9.4.2 Oxidation to a keto group 824
19.9.5 Carboxylic acid side-chains 825
    19.9.5.1 Decarboxylation of acetic acid side-chains 825
    19.9.5.2 Decarboxylation of propionic acid side-chains 826
    19.9.5.3 Formation of amide bonds in propionic side-chains 826
19.9.6 Keto side-chains 827
19.9.7 Formyl side-chains 827
    19.9.7.1 Oxime formation 827
    19.9.7.2 Hydrazone formation 828
    19.9.7.3 Reaction with bisulfite 828
    19.9.7.4 Acetal formation 828
    19.9.7.5 Reduction to hydroxymethyl groups 828
    19.9.7.6 Reduction to a methyl group 829
    19.9.7.7 Oxidation to a carboxyl group 829
    19.9.7.8 Conversion into ethylene epoxide groups 829
    19.9.7.9 Reaction with Girard's reagent 829

19.10 Special techniques 829
19.10.1 Solubilities 829
    19.10.1.1 Aqueous acids 829
    19.10.1.2 Transference from aqueous acid to ether 830
    19.10.1.3 Aqueous alkalies 830
    19.10.1.4 Solubilization in aqueous detergents 831

19.10.1.5 Organic solvents 832
19.10.1.6 Acidified organic solvents 833
19.10.2 Separations by solvent-partition 833
19.10.2.1 Partition between ether and water 833
19.10.2.2 Partition between ether and aqueous HCl 833
19.10.2.3 Countercurrent distribution 834
19.10.2.4 Partition between ether and aqueous buffers 834
19.10.3 Esterification and hydrolysis of esters 834
19.10.3.1 Esterification of porphyrins using diazomethane 834
19.10.3.2 Esterification of porphyrins using alcohols with mineral acid 835
19.10.3.3 Esterification of hemins 836
19.10.3.4 Hydrolysis of esters 836
19.10.3.4.1 Aqueous HCl 836
19.10.3.4.2 KOH-methanol 837
19.10.3.4.2 KOH-water/tetrahydrofuran 837
19.10.4 Crystallization and melting points 837
19.10.4.1 Crystallization 837
19.10.4.1.1 Porphyrin salts 837
19.10.4.1.2 Porphyrins 837
19.10.4.1.3 Porphyrin esters 837
19.10.4.2 Crystal form and melting points 838
19.11 Chromatography 839
19.11.1 Paper chromatography of porphyrins and hemins 839
19.11.1.1 Introduction 839
19.11.1.2 Porphyrin free acids (lutidine method) 841
19.11.1.3 Coproporphyrin isomers (lutidine method) 843
19.11.1.4 Coproporphyrin isomers (n-propanol method) 844
19.11.1.5 Uroporphyrin isomers (dioxan method) 846
19.11.1.6 Dicarboxylic porphyrins 848
19.11.1.7 Hemins 850
19.11.2 Column chromatography 851
19.11.2.1 Introduction 851
19.11.2.2 Porphyrin esters 852
19.11.2.2.1 Al_2O_3, MgO, $MgCO_3$, $CaCO_3$ 852
19.11.2.2.2 Celite (Hyflo Supercel) 853
19.11.2.2.3 Silicic acid 855
19.11.2.3 Porphyrin free-acids 855
19.11.2.4 Hemins 856
19.11.2.4.1 Silicic acid 856
19.11.2.4.2 Silicagel 857
19.11.2.5 Dry column chromatography 857
19.11.3 Thin layer chromatography 858
19.11.4 High pressure liquid chromatography 859
19.11.5 Electrophoresis 860
19.11.5.1 Paper electrophoresis 860
19.11.5.2 Agar gel electrophoresis 861

References *862*

APPENDIX: ELECTRONIC ABSORPTION SPECTRA 871

Table 1 Electronic absorption spectra of porphyrins in organic solvents 872
Table 2 Electronic absorption spectra of *meso*-substituted porphyrins in chloroform 878
Table 3 Electronic absorption spectra of chlorins in organic solvents 880
Table 4 Electronic absorption spectra of representative monometallic metallo-octa-alkylporphyrins in organic solvents 884
Table 5 Electronic absorption spectra of hemins and hematins in ether 887
Table 6 Electronic absorption spectra of porphyrins in aqueous sodium dodecyl sulfate 888
Table 7 Electronic absorption spectra of porphyrin monocations in aqueous sodium dodecyl sulfate 888
Table 8 Electronic absorption spectra of porphyrin dications in aqueous sodium dodecyl sulfate 889

10

NUCLEAR MAGNETIC RESONANCE SPECTROSCOPY OF PORPHYRINS AND METALLOPORPHYRINS*

HUGO SCHEER** and JOSEPH J. KATZ

Chemistry Division, Argonne National Laboratory, Argonne, Illinois, 60439, U.S.A.

10.1. Introduction

The rapid development of proton nuclear magnetic resonance (n.m.r.) spectroscopy since about 1960 has had a strong influence on the study of almost all classes of organic compounds[1]. There are, however, few categories of compounds for which such a wealth of information can be obtained by n.m.r. as for porphyrins. This circumstance arises for the most part from the large magnetic anisotropy (ring current) of the aromatic macrocycle of these compounds[2,3]. The ring current functions as a built-in chemical shift reagent, and spreads the proton magnetic resonance (^{1}Hmr) spectrum of porphyrins over the unusually large range of more than 15 p.p.m. This in consequence generally renders the ^{1}Hmr spectra first order, simplifying interpretation and assignment, and makes ^{1}Hmr a very sensitive probe of structural modifications. The ring current effects, in addition, allow detailed studies of molecular interactions of porphyrins in solution.

In the early applications of n.m.r. to porphyrins, ^{1}Hmr was the most widely used as an analytical tool, and the new structural insights that resulted were a major reason for the revival of interest in porphyrin chemistry. A few examples of important pioneering work may be cited here. The first ^{1}Hmr spectra of porphyrins were reported by Becker and Bradley[2a], and by Ellis et al.[2b], and an early survey on a variety of porphyrin structures was carried out by Caughey and Koski[4]. Based on the extensive synthetic work of Jackson, Kenner, and Smith[5], a series of researches was carried out by Abraham on a number of special aspects of porphyrin behavior, especially

---

* Work performed under the auspices of the U.S. Energy Research and Development Administration.

** Stipendiate of the Deutsche Forschungsgemeinschaft, Bonn—Bad Godesberg, W. Germany; present address: Institut für Botanik der Universität, D 8000 München 19, W. Germany.

Porphyrins and Metalloporphyrins, ed. Kevin M. Smith
© 1975, Elsevier Scientific Publishing Company, Amsterdam, The Netherlands

the effects of substitution[8a,8b], the self-aggregation[6–8] in solution, isomerism of porphyrins[6,8,9], and interactions of nucleophiles with the central metal atom of metalloporphyrins[10,11]. Inhoffen et al.[12] investigated a great variety of chlorophyll derivatives, and widely applied octaethylporphyrin H_2(OEP) as a powerful model compound for the naturally-occurring porphyrins. Closs et al.[13] studied molecular interactions in chlorophylls and chlorophyll derivatives, and were able to delineate many of the salient features of the self-aggregation of the chlorophylls in the convenient form of aggregation maps. In addition to studies undertaken on porphyrins themselves, ligand molecules bound to them have been the subject of investigation by n.m.r. The ring current induced shifts (RIS) by the porphyrin macrocycle on the chemical shifts of axial ligands serve as an alternative probe and thus supplement and complement the pseudocontact shift produced by lanthanide shift reagents (LIS) so important for conformational and stereochemical studies[14–19].

Kowalsky's[20] early report of sharp proton resonance lines in the porphyrin moiety of cytochrome-*c* that lie far outside the usual chemical shift range for protons led to an extensive study of paramagnetic metal complexes[21–29]. The extremely large proton chemical shifts observed in these compounds are produced by hyperfine nuclear interactions with the unpaired electrons of the central metal atom. As these hyperfine shifts are dependent on oxidation state, spin state, and axial ligands coordinated to the central metal ion, n.m.r. has been used as a probe in structural and functional studies of heme and hemoproteins[21,22].

In recent years, nuclei other than protons, especially ^{13}C, have become important in n.m.r. spectroscopy[30]. Although of the same absolute magnitude, the ring current effect in ^{13}Cmr is small relative to the magnitude of the intrinsic chemical shifts and the ring current plays only a minor role[31], whereas paramagnetic contributions from low-lying excited states make a decisive contribution to the ^{13}C chemical shifts[30]. The influence of metalation on the electronic structure of porphyrins has been studied in some detail[32,33], and two n.m.r. publications focus on the conjugation pathway in porphyrins[32,34].

In contrast to the unusual chemical shifts often observed, coupling constants in porphyrins are quite normal. The ^{1}Hmr subspectra of various substituents are in most cases first order, and long range coupling constants are usually only observed in porphyrins with unsubstituted peripheral (β)-positions. Recently, some data on ^1H coupling constants with ^{13}C[35–37], ^{15}N[33], and ^{205}Tl[8,9,11,32] have been published and have been given straightforward explanations.

10.1.1. *The chemical shift*

The magnetic resonance frequency ν of a nucleus is given by

$$\nu = \frac{\gamma}{2\pi} \cdot \tag{1}$$

The gyromagnetic ratio γ is a natural constant for a particular nucleus, and H is the magnetic field experienced by it. Although the latter is usually very close to the external magnetic field, H_0, applied in the experiment, the field at a particular nucleus is modified by its chemical environment. The additional local magnetic field produced by neighboring nuclei with magnetic properties are proportional to H_0, and eq. (1) can then be rewritten as:

$$\nu = \frac{\gamma}{2\pi} H_0(1-\sigma)\,, \tag{2}$$

where the shielding constant σ is a measure of the modification of the external magnetic field H_0 by the chemical environment.

Shielding of a particular proton from the external magnetic field results from currents induced within the electron system of the atom and its surroundings (Larmor precession)[1,38], and the overall shielding is usually divided into several contributions to the chemical shift* experienced by a particular nucleus[1]. Local magnetic effects arise from changes (with respect to the free atoms) in the density and the shape of the electron cloud surrounding a particular proton, and long-range magnetic effects occur from magnetically anisotropic groups in the neighborhood of a particular proton or group of protons. Both of these effects contain diamagnetic contributions, which reflect changes in the magnitude of the electron density, and paramagnetic contributions that originate from changes in the shape of the electron cloud**. In an alternative and equivalent representation, paramagnetic shifts arise from distortions of the ground state orbitals from the mixing of the wave functions of the ground state and low-lying excited states. In compounds containing unpaired electrons, hyperfine interactions result from contact shifts (non-zero spin density at the nucleus) whose effects are transmitted through the chemical bonds in the molecule, and pseudocontact shifts transmitted through space. Proton chemical shifts arising from the presence of unpaired spins can be orders of magnitude larger than those observed in diamagnetic molecules. In addition to all of these internal effects, solvent-induced proton chemical shifts may occur from more or less specific interactions of solute molecules with a solvent that possesses magnetic anisotropy*.

---

* Due to the small magnitude of the shielding constant σ ($\sim 10^{-5}$) and the difficulties in measuring its absolute value, it is usually expressed as the *chemical shift* relative to that of a reference compound. Throughout this chapter, the chemical shift is given in δ units (parts per million, p.p.m.) where $\delta = -10^6\,(\sigma - c)$, and c is the shielding constant for the protons in the usual internal standard tetramethylsilane (TMS). Another commonly employed internal standard is hexamethyldisiloxane (HMS), whose protons come into resonance at slightly higher field than TMS. In some publications, τ is used instead of δ as a measure of chemical shift. These two quantities are related by $\tau = 10 - \delta$.

** The terms paramagnetic and diamagnetic shifts are sometimes used in a different sense designating low-field and high-field shifts, respectively. On the other hand, paramagnetic as well as diamagnetic contributions (as defined above) describe shielding mechanisms which can be both positive (= shielding, high-field shift) and negative (= deshielding, low-field shift).

10.1.2. The aromatic ring current

In the ^{1}Hmr spectra of diamagnetic porphyrins, the long-range diamagnetic contribution of the aromatic macrocyclic system to the chemical shift is the most important single factor that distinguishes porphyrins from similar non-aromatic structures. Consequently, we shall describe this ring current term in somewhat more detail.

If a closed loop of electrons is subjected to an external magnetic field, a Larmor precession[1] of the entire π-cloud is induced. The circulation of the electrons (ring current) gives rise to a secondary magnetic field that is shown in Fig. 1. This effect is strongly anisotropic, it does not average out to zero by random tumbling of the molecule, and thus the ring current gives rise to an anisotropic shielding effect on protons within the range of the ring cur-

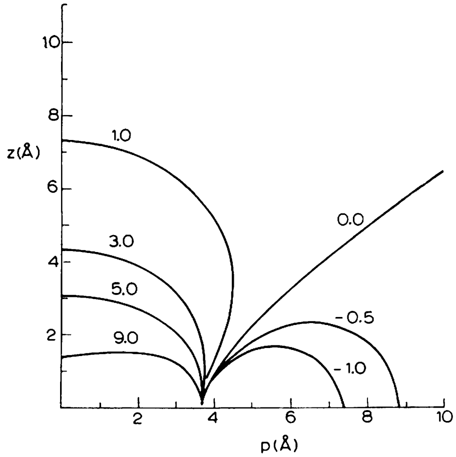

Fig. 1. The magnetic anisotropy of the porphyrin ring system (from Ref. 40). The iso-shielding lines (incremental shift Δ[p.p.m.]) were obtained by a classical ring current calculation (*vide infra*) with two circular loops above and below the macrocyclic plane. The radius '*r*' and spacing '*s*' (see Fig. 2) and π-electron number were adjusted to fit the ^{1}Hmr data observed for the stacked system (10) (see text). The calculation included four additional loop-pairs for the peripheral benzene rings of the phthalocyanine, but only the contribution of the inner tetra-azaporphyrin system is shown here. The abcissa gives the radial distance from the center of the macrocycle, and the ordinate, the *z* (out-of-plane) coordinate. The three dimensional picture is obtained by rotating this cross-section around the *z*-axis.

---

* Bulk magnetic susceptibility changes due to the geometry of the sample and the magnetic properties of the solvent system employed are usually dealt with by use of internal standards, or, where practical, by appropriate susceptibility corrections[1].

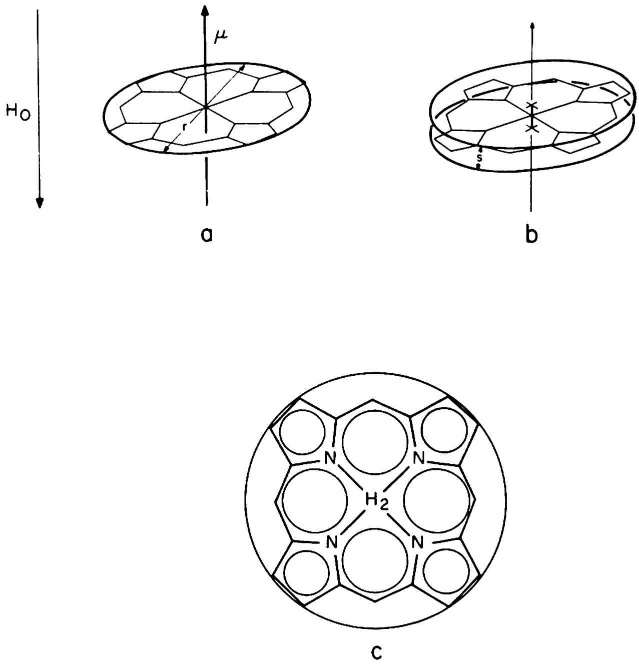

Fig. 2. Schematic drawings of the classical ring current models for porphyrins. (a) The single-loop approach with the radius 'r' and the π-electron number as variables, approximated by the magnetic point dipole μ; (b) the loop-pair approach with the spacing 's' as additional variable; (c) the network or multi-loop pair approach, viewed from the top, with each circle representing a pair of loops above and below the macrocycle. For discussion see text.

rent. This classical 'ring current' model of Pauling[39] has been widely used as a criterion for aromaticity or anti-aromaticity, depending on the sign and magnitude of the related shielding constant. (For a detailed discussion, see Ref. 41.) For an aromatic system such as the porphyrins, the magnetic shielding resulting from the ring current is positive for nuclei on the outside of the loop, and negative for nuclei positioned within the loop (Fig. 1). The first approach to the calculation of the shielding of aromatic nuclei by this classical picture was made by Pople[42]. He assumed a single loop in the plane of the aromatic system, the magnetic field of which can be treated approximately (for protons at the periphery) by a point-dipole in the center of the loop (see Fig. 2a). This treatment has been refined by Waugh and Fessenden[43] and by Johnson and Bovey[44], who used instead two separate loops situated symmetrically at 0.45 Å and 0.65 Å, respectively, above and below the plane of the aromatic ring (Fig. 2b).

Based on the work of London[45], a molecular orbital treatment was developed by Pople[46], McWeeney[47], and Hall and Hardisson[48a] that essentially gives a similar picture as the classical ring current approach, but is more

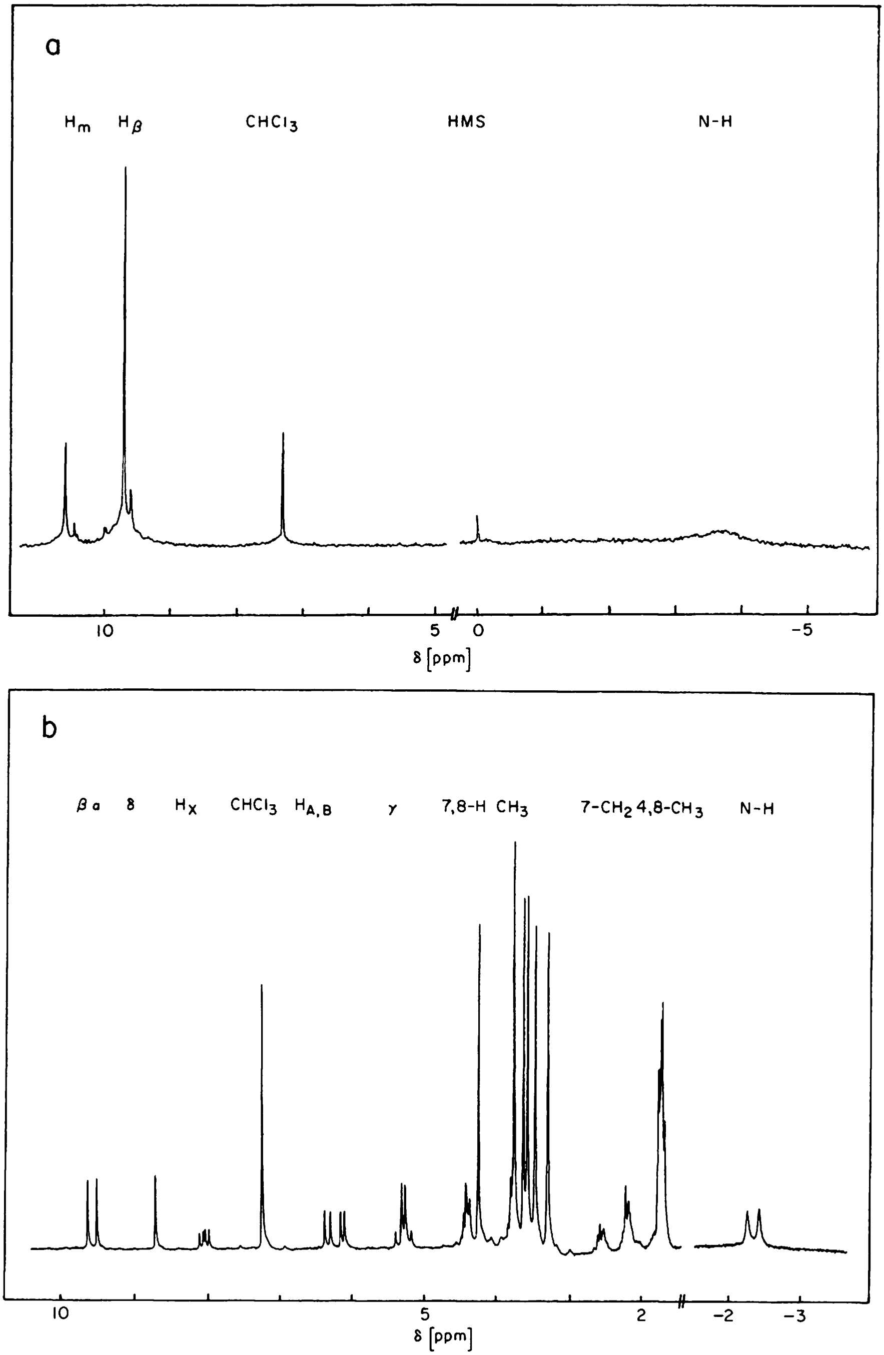

Fig. 3. ^{1}Hmr spectra (220 MHz pulse FT) of (a) porphin (1), saturated solution (~5 × 10^{-5} M) in C^2HCl_3, 2000 pulses, repetition rate 0.49 sec, spectrum width 4500 Hz; and (b) chlorin-e_6 trimethyl ester (14), 5 × 10^{-3} M in C^2HCl_3, 1000 pulses, repetition rate 2.45 sec, spectrum width 3500 Hz.

versatile in complex systems. Although the ring current approach neglects other contributions (i.e., paramagnetic or σ-system terms) and gives results that are often only in qualitative agreement with experiment, this approximation has proved most useful for the qualitative and even semi-quantitative interpretation of chemical shifts in various aromatic and anti-aromatic systems. (For a recent review on a discussion of the limitations of the ring current approach, see Ref. 41.)

The sizeable ring current effect associated with the π-system of the aromatic porphyrin macrocycle was recognized as a dominant feature of the first ^{1}Hmr studies of porphyrins[2–4]. In the ^{1}Hmr spectrum of porphin (1) (Fig. 3a), the resonances of the peripheral protons are shifted about 5 p.p.m. to lower field as compared to those of pyrrole[1], whereas the resonances of the inner N protons are shifted about 11 p.p.m. to higher field. Becker et al.[2a] used both the single loop (point dipole) and double loop model, assuming a radius of 3.3 Å for the 18 π-electron loop, and a variable spacing for the loop pair in the latter (Fig. 2a,b). Ellis et al.[2b] used a double loop pair model (Fig. 2b) to provide a semi-quantitative description of the ring current effect. These authors obtained a self-consistent model with loops of a radius of 3.7 Å, a spacing of 1.28 Å and an effective ring current of 18.8 π-electrons*. In contrast to these studies, which consider only a single pair of loops, Abraham[3] used a network approach[39], in which auxiliary pyrrole loops and chelate hexagon loops as well are all explicitly taken into account in addition to the main macrocycle loop itself (Fig. 2c). The calculated chemical shifts obtained by this procedure are too large by the same factor of 1.5 that was observed earlier in the application of this model to other polycyclic compounds. A similar approach has been used more recently by Mamaev[48b] for the study of some principal porphyrins and of substituent effects. While earlier investigations were focussed on the ring current effect on protons within the plane of the macrocycle, its effect on protons above (and below) the macrocycle plane was studied experimentally by Storm et al.[16], Katz et al.[51] and Janson et al.[52] From the chemical shifts for N-substituents in porphyrins and axial ligands in metalloporphyrins, a semi-empirical formula was deduced that gives with fair accuracy the chemical shift of protons within the ring current loop but above or below its plane[16,17].

10.1.2.1. *Ring current in related macrocycles*

The porphyrin macrocycle can formally be regarded as a bridged diaza[18]annulene (2) with two isolated peripheral double bonds, or as a tetraaza[16]annulene dianion (3) with four isolated double bonds (for leading references, see Refs. 12, 18, 19 and 32).

---

* The 'best self consistent fit' obtained in this semi-empirical approach characteristically gives fictitious or unreal values for the number of electrons in the ring current (Section 10.1.2.2).

TABLE 1

^{1}Hmr chemical shifts (δ[p.p.m.] from TMS) of 18 π-aromatic compounds related to the porphyrins.

Compd.							Ref.
(4)	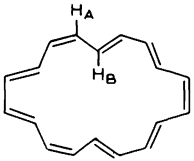		H_A (quadruplet)	H_B (quintuplet)			
		obsd.	9.03	−2.26		THF—$^2H_8$, 0°C	53,54
		calcd.	11.06	−12.6			50
(5)	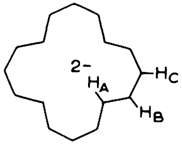		H_A	H_B	H_C		
		obsd.	−8.07	8.77	7.40	THF—$^2H_8$, −30°C, Li^+ as gegenion	50
			(J_{AB} = 13 Hz, J_{BC} = 9.5 Hz)				
		calcd.	−10.9	10.2	10.2		
(6)	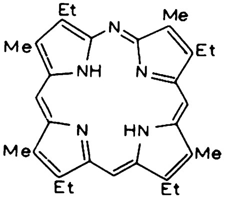	Methine—H:	γ: 10.02			C^2HCl_3	55
			β,δ: 9.90				
		Ring—CH_3:	3.58, 3.50				
		CH_2—CH_3:	3.91, 1.83				
(7)	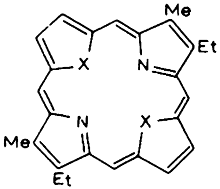	Methine—H			β-furane or β-thiophene—H		
		a) X = O, Y = O: 11.71			10.98	Dihydrobromide	56
		b) X = O, Y = S: 10.59, 10.05			10.01, 9.69	in TFA	56
		c) X = S, Y = S: 10.68, 10.71					57

			H_A	H_B		
(8)	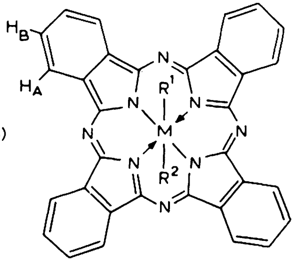	M=Si R^1=CH_3 R^2=OSi $CH_3[OSi(CH_3)_3]_2$ −6.31 −2.99 −1.26	9.60	8.27	C^2HCl_3	52
		M=Si R^1=R^2=OSi$CH_3[OSi(CH_3)_3]_2$ −2.90 −1.22	9.63	8.30		
		M=Si R^1=R^2=OSi$(CH_2CH_3)_3$ −2.48 −1.25	9.68	8.36		
		M=GeR^1=R^2=OSi(CH_2CH_3) −2.42 −1.24	9.70	8.38		

			Methine—H	β-thiophene or β-furane	N—H		
(9)	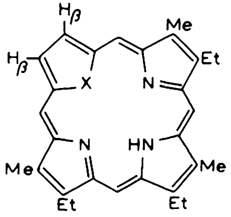	X=O	10.12, 9.98	9.69	—	C^2HCl_3	56
		X=S	10.06, 10.00	9.98	−4.98		

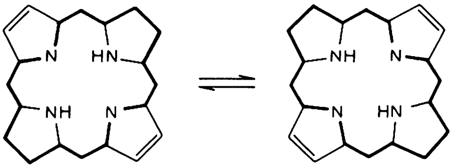

(2)

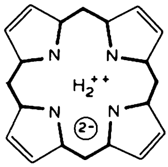

(3)

Indeed, striking similarities in electronic transition and magnetic resonance spectroscopy are evident between porphyrins and the [16]-annulene di-anion (5)*[49,50].

As far as electron states are concerned, porphyrins may be regarded as only a special case of bridged 18 π-heteroannulenes. The n.m.r. properties of several related structures are listed in Table 1. All compounds show strongly shielded inner protons and strongly deshielded outer protons (relative to similar structures with interrupted macrocyclic conjugation, Section 10.2.6) in a manner characteristic of protons of aromatic systems. Replacement of one N—H group in a pyrrole ring of porphyrins by O or S (see Chapter 18) leaves the methine proton resonances of the macrocycle almost unchanged (see Table 1), while in the disubstituted porphyrins the methine protons are more strongly deshielded. As substitution in these compounds is accompanied by local structural changes implicit in the synthesis (i.e., removal of alkyl side chains, change in the entire geometry of the molecule), the chemical shift effects resulting contain contributions other than ring current effects.

The [16]-annulene di-anion (5) and the [18]-annulene (4) have been thoroughly investigated by Oth et al.[50] (Table 1). Based on the 'normal' value of $\delta = 5.8$ p.p.m. for olefinic protons[50], the chemical shifts for both systems were calculated assuming contributions only from the diamagnetic ring current (based on London's treatment[45]) and the negative charge in the case of the di-anion. The agreement with the experimental data is good for the [16]-annulene di-anion and fair for the [18]-annulene, although again in both cases the influence of the ring current is exaggerated.

The ring current effect in silicon and germanium phthalocyanines was studied by Janson et al.[52] These authors circumvented the difficulties involved in defining a reference system in an elegant way. Silicon and germanium phthalocyanines can form stacked complexes of the general structure (10), where *X* can vary from 0 to 4. In this way, the influence of a new ring added to the stack at one end on the phenyl protons and the axial substituent R of the successive porphyrin macrocycles could be measured for various

---

* It should be noted that in solutions of the di-anion, structure (5) is present in the 85 configuration characteristic for porphyrins, while the annulene (4) assumes a configuration different from the one present in porphyrins (Table 1) and thus cannot be directly compared.

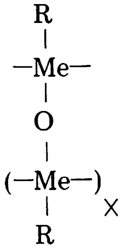

$$\begin{array}{c} R \\ | \\ -Me- \\ | \\ O \\ | \\ (-Me-)_{X} \\ | \\ R \end{array}$$

(10)

$R = OSiCH_3[OSi(CH_3)_3]_2$
$M = Si, Ge$
$X = 0–4$

stack heights. Semi-empirical calculations of the ring current (according to the treatment of Johnson and Bovey[44]) led to a self-consistent set of parameters for a five double loop ring current model. In the model of Janson et al.[52] four benzenoid loops[44] were added to the central macrocycle loop, which has a diameter of 3.90 Å, a separation of 0.64 Å, and an effective ring of 8.43 electrons*. The ^{1}Hmr spectrum of tetrabenzoporphin, the parent compound of the phthalocyanines, was reported recently[60]. Due to the common presence of paramagnetic impurities[58], no systematic study has been done on this class of porphyrins.

10.1.2.2. Ring current and structure

Almost any structural modification to the macrocyclic system changes its ring current, as indicated by changes in the chemical shifts of protons remote from the point of structural change. In spite of its success in describing the general features and in providing good estimates of the proton shifts observed in some porphyrins, the ring current model has to be used carefully, however, in attempts to make quantitative predictions for the consequences of structural modifications in porphyrins. Several reasons can be adduced for this situation. First, although the ring current is a major contributor to the chemical shift, it is not the only source for the unusual shifts observed in aromatic compounds (see above). Second, the ring current is not localized as in a wire, but in orbitals that are subject to hybridization changes. It is thus characteristically found that the 'best self-consistent fit' in ring current calculations is usually obtained with fictitious or unreal values for π-electron number as well as the ring current radius and the distance of π-cloud separation. Third, porphyrins are polycyclic systems, and therefore the true ring current may be affected not only in intensity but also in position by changes in the relative contributions within the various loops into which the total ring current is decomposed[3]. In principle, a much better insight into the relative distribution of the ring current can be provided by ^{13}C spectra.

---

* See footnote on p. 405.

However, the relatively small ring current effects on ^{13}C chemical shifts make separation of the ring current contributions from other operative factors very difficult[31], and the two publications on the subject arrive at opposite conclusions[32,34]. Fourth, local changes can lead to conformational changes in the macrocycle as a whole (Section 10.4.3) thereby changing the magnetic environment of a proton remote from the site of structural modification.

In spite of these limitations, the simple double loop ring current model (Fig. 3b) has been extremely useful from a practical point of view in the interpretation of the ^{1}Hmr spectra of various classes of porphyrins. To evaluate the contribution of the ring current to the ^{1}Hmr of structurally altered porphyrins the following criteria are usually helpful: (a) only well-assigned signals of protons close to the aromatic systems, but far from the locus of modification should be used; (b) resonances of protons inside versus outside the aromatic macrocycle ought to experience opposite shifts; (c) side effects from conformational changes of the ring system have to be taken into account.

Some general aspects of the ring current model as applied to porphyrins may also be summarized here: (a) the ring current is larger in both metal complexes (for some exceptions, see Section 10.2.8.1) and di-cations of porphyrins (Section 10.2.7). This effect is explained by Abraham[3] as a result of increased resonance stabilization in these classes of compounds. (For an alternative explanation, see Ref. 41) (b) Steric hindrance, that is, effects that reduce π—π overlap by distorting the planar macrocycle structure causes a decrease in ring current. This point is further elaborated below (see N-substitution, (Section 10.2.4), *meso*-substitution (Section 10.2.3), and stereochemistry (Section 10.4.3)). (c) Decrease in the electron density of the π-system diminishes the ring current and may thus cause up-field proton shifts, even though a decrease in electron density generally leads to a reduced shielding and down-field shifts. The latter behavior, a down-field shift upon introduction of electron-withdrawing groups, is usually observed in benzene derivatives, where, for example, the ortho, meta, and para proton signals in benzaldehyde are shifted to lower field by 0.58, 0.21 and 0.27 p.p.m., respectively, as compared to the protons in benzene itself[1]. In porphyrins, however, the deshielding effect of electron withdrawal is usually overcompensated by the simultaneous decrease in ring current that results from lowering of the electron density. Thus, the peripheral α, β, and δ methine proton signals in 9-keto pheophorbides are shifted by 0.43, 0.26, and 0.41 p.p.m., respectively, to lower fields as compared to the respective 9-desoxo compound (Tables 5, 11, 12). This effect was first investigated by Caughey et al.[4] and is quite general in porphyrin ^{1}Hmr. As expected from these considerations, the interior N—H proton signals move in just the opposite direction when the ring current is lowered, and are deshielded by 1.5 p.p.m. in the above cited case.

10.1.3. Practical considerations for ^{1}Hmr of porphyrins

The ^{1}Hmr spectra of porphyrins, especially some of the metalloporphyrins, are strongly solvent, concentration and temperature dependent. This is due to the tendency of porphyrins to experience self-aggregation, and this, in combination with the strong magnetic anisotropy of the porphyrins has major consequences for the ^{1}Hmr spectra (Section 10.4.1). In the free porphyrin bases, aggregation is weak, and parallels the π—π aggregation behavior generally observed in aromatic molecules[6]. In metalloporphyrins, self-aggregation or ligation to donor (Lewis base) molecules is usually much stronger and more specific, and occurs by interaction of polar side chains or donor groups in one molecule with axial interaction sites on the central metal ions of another[13,59]. Aggregates of both types have been very useful in the study of molecular interactions with porphyrins (see Section 10.4.1). The formation of self-aggregates on the one hand, or coordination interaction products with extraneous nucleophiles on the other, however, presents a serious problem in making structural deductions from n.m.r. data. Under aggregating conditions the accurate determination and assignment of chemical shifts becomes especially important, as aggregation shifts of more than 2 p.p.m. may occur for the resonances of particular protons as a result of close proximity to the ring current of another macrocycle. A rigorous approach to the problems proposed by aggregation requires mapping the concentration-dependence of the chemical shifts and extrapolation to infinite dilution, but this procedure is really practical only for certain important compounds. The aggregation problem in the assignment of chemical shifts can in general be circumvented by recording the spectra in trifluoroacetic acid (TFA), in which both π—π and coordination-aggregates are broken down by dication formation or by preferential ligation of the metal axial coordination sites with TFA. For sufficiently stable compounds this is a very useful approach, particularly because TFA is an excellent solvent even for otherwise only poorly soluble free base porphyrins.

For compounds unstable in TFA, however, other solvent systems must be used. In metalloporphyrins, strong self-aggregation caused by donor—acceptor interactions involving the central metal ion can be avoided by addition of small amounts of bases (tetrahydrofuran, methanol) to chloroform (or other nonpolar solvents) to compete for the metal coordination site. For free base porphyrins, the concentration should be maintained as low as possible and constant for a series of compounds. Several laboratories use standard concentrations for recording porphyrin spectra whenever possible. For example, the Braunschweig group uses 0.05 M in C^2HCl_3 as their standard, a concentration that is usually on the monomer side for free porphyrin bases, and gives a reasonable signal-to-noise (S/N) ratio in single scan continuous-wave (cw) n.m.r. experiments. However, this requires about 10 mg of material dissolved in 0.3 ml of solvent in a 5 mm n.m.r. sample tube, a concentra-

TABLE 2

Incremental shifts (Δ [p.p.m.]) in C^2HCl_3 due to the aromatic ring current in porphyrins

N	1	2	3	4	5
Methine	−9.5	−3.8	−1.2	−0.6	n.e.
β-pyrrole	−8.5	−3.3	−1	−0.3	n.e.
N	+4	+5.9	+3.7	+2.8	+1.9
Chlorin	−4	−0.9	−0.2	—	—

The expected chemical shift for a proton or a substituent in various positions of the porphyrin can be estimated from its chemical shift in the related aliphatic compound, R—CH_3, and the listed increments. N is the number of bonds between the respective proton and the indicated C or N atom, respectively. Upon reduction of the ring current the increments are reduced proportionally.

tion sometimes not accessible because of insolubility or unavailability of material.

As lower concentrations, down to less than 5×10^{-4} M, are sufficient for routinely recording ^{1}Hmr spectra in modern n.m.r. equipment by pulse Fourier transform spectroscopy, a lower standard concentration is probably useful where a broad range of compounds are to be investigated. In any case, the solvent system should always be quoted together with the concentrations at which the ^{1}Hmr spectra have been recorded.

In ^{13}Cmr, ring current effects are relatively less important, and weak self-aggregation of free porphyrin bases plays a lesser role in determining the relative magnitude of chemical shifts. Consequently, solubility limitations and the sizeable amount of material needed for ^{13}Cmr spectra at natural abundance are the major problems for a broad application of this technique. Concentrations of 0.1 M are desirable for ^{13}C natural abundance work, more if a high S/N ratio is desired.

10.2. ^{1}HMR spectra

10.2.1. The ^{1}Hmr spectra of diamagnetic porphyrins

The ^{1}H chemical shifts of six important porphyrins selected to illustrate the n.m.r. behavior of typical porphyrins are given in Table 3, and two typical spectra are shown in Fig. 3.

10.2.1.1. Porphin

The spectrum of free base porphin (1), the parent compound of the porphyrins, was obtained only recently because of its poor solubility[60]. Porphin shows three signals (Fig. 3a), two at low field assigned to the methine and the β-protons, and one at high field assigned to the NH protons. At room temperature, the N—H exchange between the possible tautomeric

TABLE 3

^{1}Hmr chemical shifts (δ [p.p.m.] from TMS) of some principal porphyrins

			Remarks	Ref.
(1) 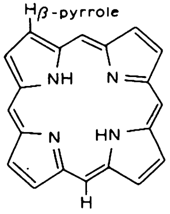	$H_{Methine}$: $H_{\beta\text{-pyrrole}}$: NH:	10.58 9.74 −3.76	Satd. solution in C^2HCl_3	60,67
(11) 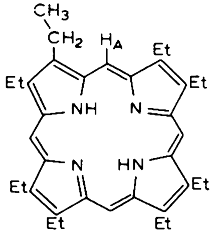	$H_{Methine}$: CH_2: CH_3: NH:	10.18 4.14 1.95 −3.74	RT, C^2HCl_3	71
(12) 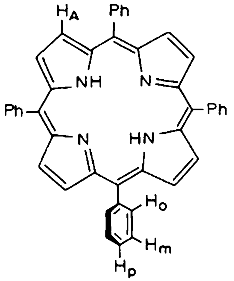	H_A: H_o: H_m: H_p: NH:	8.75 8.30 (m) 7.80 (m) 7.80 (m) —	30°, C^2HCl_3/ CS_2	74

TABLE 3 (continued)

			Remarks	Ref.
(13) 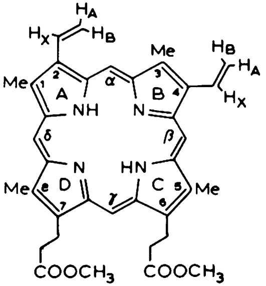 HA HX HB Me HB HA HX Me 1 2 α 3 4 A B NH N δ β N HN Me 8 D C 5 Me 7 γ 6 COOCH3 COOCH3	Methine—H: α, β, γ, δ (*s*):	9.96, 9.95 9.83, 9.82	220 Mz, C^2HCl_3	68
	2-vinyl: H_X, H_A, H_B:	8.10, 6.09 6.26		
	4-vinyl: H_A, H_A, H_B:	8.14, 6.09 6.26		
		ABX, $J_{AB} = 2$ $J_{AX} = 12$ $J_{BX} = 19$		
	6,7-CH_2—CH_2—$COOCH_3$:	3.59, 3.16 3.59		
	Arom. CH_3; 1, 3, 5, 8:	3.48, 3.48 3.54, 3.55		
	NH:	—4.08		
(14) 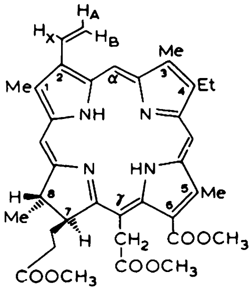 HA HX HB Me Me 1 2 α 3 4 Et NH N N HN H 8 Me 7 γ 5 6 Me H CH2 COOCH3 COOCH3 COOCH3	β, α, δ—H:	9.65, 9.50, 8.70 (*s*)	0.05 m in C^2HCl_3	72,73
	H_A, H_B, H_X:	6.07, 6.28, 8.00 (ABX) $J_{AB} = 2$, $J_{AX} = 12$, $J_{BX} = 18$ Hz		
	γ-CH_2—$COOCH_3$:	5.27 (AB, $J = 17$ Hz), 3.73 (*s*)		
	7,8-H:	4.38 (*m*), 4.40 (*q*, 7Hz)		
	4-CH_2—CH_3:	3.73 (*q*, 7Hz), 1.69 (*t*, 7Hz)		
	1,3,5-CH_3:	3.43, 3.24, 3.55 (*s*)		
	6,7′ ″-$COOCH_3$:	4.23, 3.60 (*s*)		
	8-CH_3:	1.73 (*d*, 7Hz)		
	NH:	—1.40		

(15)

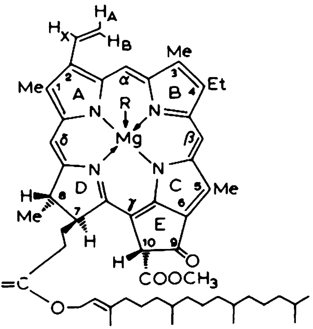
H_A
H_X
H_B
Me
Me
Et
A
B
C
D
E
R
Mg
N
N
N
N
α
β
γ
δ
1
2
3
4
5
6
7
8
10
9
H
Me
H
H
O
COOCH₃
O=C
O

β, α, γ—H:	9.50, 9.23, 8.28	C^2HCl_3/ $C^2H_3O^2H$	13
H_A, H_B, H_X:	5.97, 6.13, 7.92 (ABX, $J_{AB} = 1.7$, $J_{AX} = 11.2$, $J_{BX} = 18.1$)		
10-H:	6.22 (*s*)		
7,8-H:	4.14 (m), 4.27 (q), $J_{7H,8H} \leqslant 2$ Hz		
4-CH_2—CH_3:	3.75 (*q*), 1.72 (*t*)		
10 *a*-CH_3:	3.97 (*s*)		
1,3,5-CH_3:	3.28 (*s*), 3.25 (*s*), 3.60 (*s*)		
8-CH_3:	1.78 (*q*)		
P-1 H_2:	4.30 (*d*)		
P-2-H:	5.10 (*t*)		
P-3-CH_3:	1.52 (*s*)		
P-7, 11, 15-CH_3:	0.71—0.75 (*s*)		

For details see Section 10.2.1; for chlorophyll-*a* (15) see Section 10.2.8. The numbering system for the substituents indicated in structures (13—15) is used throughout this chapter.

forms is fast on the n.m.r. time scale and only one resonance is observed for each group of protons. At low temperatures the β-pyrrole proton signal is split, however, and the exchange kinetics can be studied by ^{1}Hmr[61].

The β-protons in porphin are magnetically equivalent, but in asymmetrically substituted porphyrins the following vicinal coupling constants of the β-pyrrole protons ($^3J_{H\beta-H\beta}$) were obtained: $J = 4.5$ Hz in a partially alkyl-substituted porphyrin[62], $J = 5$ Hz in a Re(I) complex of *meso*-tetraphenylporphyrin H_2(TPP)[63], and $J_1 = 4.70$ Hz, $J_2 = 4.83$ Hz in an isoporphyrin[64], and $J_1 = 4.5$ Hz[65] and $J_2 = 4.7$—5.3 Hz[66] in some *meso*-tetraphenylchlorins. The long-range coupling constant of the β-pyrrole H with the N—H ($^4J_{H-NH} = 1$ Hz) was observed in a Re(I) TPP complex[63], and the splitting of 2 Hz which was observed[65] for the β-pyrrole protons in tetrahydro-*meso*-tetraphenylporphyrin is probably also due to coupling with N—H.

10.2.1.2. Octaethylporphyrin

Octaethylporphyrin [H_2(OEP) (11)] is today the most widely used model compound for structural studies related to the naturally occurring porphyrins. The assignment of the H_2(OEP) n.m.r. spectrum proceeds directly from ring current considerations and the multiplet structure of the resonances[71]. The decrease of the ring current induced low-field shift with increasing distance of the peripheral protons from the macrocycle is clearly evident in the methine, methylene, and the methyl protons, which appear at increasingly high field in that order (Table 3).

One of the major reasons for the use of H_2(OEP) as a model compound is its high symmetry. Because of fast N—H exchange, the parent compound has four-fold symmetry and only one signal is observed for each group of protons. Although this four-fold symmetry is often reduced by chemical modifications, many derivatives retain two-fold symmetry, and in these compounds the ^{1}Hmr spectra can often be interpreted by inspection on the basis of multiplet structure, relative intensities, and symmetry arguments.

10.2.1.3. meso-Tetraphenylporphyrin

meso-Tetraphenylporphyrin[H_2(TPP) (12)][70] is the parent of a variety of compounds not related structurally to the naturally-occurring porphyrins. The ^{1}Hmr spectrum of *meso*-tetraphenylporphyrin shows two resonances (β-pyrrole H, N—H) for the macrocyclic protons, and two signals for the three phenyl protons well separated from the first two. Due to steric hindrance, the phenyl rings in H_2(TPP) are out of the plane of the macrocycle, they do not rotate freely (see Section 10.2.3 and 10.4.2.), and mesomeric interactions between the four phenyl groups and the macrocycle are efficiently reduced. The very similar chemical shifts for the *m*- and *p*-protons of the phenyl groups can be explained on this basis. Although the *m*-protons are closer to the macrocycle, they are out of its plane, and are thus positioned in a less deshielded region. As in porphin (1) the N—H tautomerism is again rapid at ambient temperature on the ^{1}Hmr time scale, but can be studied at low temperatures[69,74–76].

10.2.1.4. *Protoporphyrin-IX dimethyl ester*

Protoporphyrin-IX dimethyl ester [H_2(Proto-IX-DME), (13)] is the principal porphyrin from which most of the naturally-occurring tetrapyrrole pigments are derived. Except for the porphyrin plane, the compound lacks a symmetry element, and under suitable conditions[68], all of the expected resonances are resolved. Although the assignment to a certain group of substituents (i.e., β-pyrrole CH_3 groups) is straightforward, precise assignment within these groups is a difficult task. In the case of (9) it was accomplished by a careful aggregation study[68]. Again, only one set of N—H signals is observed in all instances at ambient temperature because of fast exchange in the N—H tautomers.

10.2.1.5. *Chlorin-e_6 trimethyl ester*

Chlorin-e_6 trimethyl ester (14) is a key compound in chlorophyll chemistry and was the ultimate goal of Woodward's chlorophyll synthesis[77]. Chlorin-e_6 trimethyl ester serves to some extent as the prototype of chlorin-type molecules in which one of the pyrrole rings is reduced (see Section 10.2.5). Assignment of part of the ^{1}Hmr spectrum of chlorin-e_6 trimethyl ester (Fig. 3b) was carried out by Woodward[78] and later by Caughey[4]. To clarify some contradictory assignments, the ^{1}Hmr spectrum of chlorin-e_6 trimethyl ester was reassigned by Jeckel et al.[72,73], whose data are included in Table 3. The order β, α, δ for the three methine proton resonances, in the order of increasing field, is characteristic of a great variety of chlorophyll-*a* derivatives, which have no deshielding substituents in the 2-position. The vinyl group at position 2 in chlorin-e_6 trimethyl ester gives rise to a characteristic ABX subspectrum[1]. All aromatic and ester methyl groups in this compound occur as well-resolved singlets in a narrow range between $\delta = 3$ and 4 p.p.m. The protons in the 4-ethyl group gives rise to a quadruplet and a triplet, both of which are assignable by inspection. The γ-CH_2 protons are magnetically anisotropic because of the neighboring ring asymmetric center. These protons give rise to an AB subspectrum, which is generally observed for γ-CH_2 substituents in the phorbin series (Section 10.2.3). The most complex part of the ^{1}Hmr spectrum arises from the substituents at the reduced pyrroline ('chlorin') ring D. Due to the sp^3 hybridization of the 7 and 8 positions, all protons in the alkyl side-chains are one bond more remote from the aromatic system than in the true porphyrins, and their signals are thus less deshielded by the ring current. The signals are further complicated by the asymmetric centers at C-7 and C-8 and the resulting complex spin systems. The 8-CH_3 group gives rise to a doublet ($J = 7$ Hz), and the neighboring 8-H proton shows the expected quadruplet structure. The small additional coupling of the 8 to the 7 proton, from which the 7,8 *trans*-configuration was inferred[14], is rarely resolved. The 7-proton is coupled to three nonequivalent protons (8-H, 7'-H_A, 7'-H_B), but its resonance peak shows up very often as a characteristic pattern of two broad signals separated by 7 Hz[79]. All four protons of the propionic acid side-chain are magnetically nonequivalent due to the neighboring asymmetric centers at C-7 and C-8. Although potentially useful for conformational studies, no complete assignment for the chemical shifts of these protons has been reported as yet. Recently, the 7b-methylene resonances have been observed as an AB double doublet (δ = 2.50, 2.18 p.p.m., J = 16 Hz) in a selectively deuterated pyropheophorbide-*a*[80]. In the 100 MHz spectrum, only one N—H signal is observed at high-field for (14), but upon cooling[75] or in the 220 MHz spectrum at low concentration (5×10^{-3} M)[80] two N—H signals are well resolved (Fig. 3b). This splitting is typical for chlorins, and is in particular very pronounced in the phorbins (Section 11.2.3). It is indicative of a more pronounced localization of the N—H protons in chlorins than in porphyrins[72,73] (Section 10.4.2).

10.2.1.6. Chlorophyll-a

For a discussion of the n.m.r. spectrum of the chlorophyll-*a* (Chl-*a*, (15)) and the other chlorophylls, the reader is referred to Section 10.2.8.2.

10.2.2. β-Substitution

Porphyrins derived from natural pigments usually have substituents at all of the eight β-pyrrole (peripheral) positions, and n.m.r. spectra recorded on β-substituted porphyrins are so numerous that we can only try to show here some general trends in chemical shifts as observed in some characteristic examples.

Substitution of all β-pyrrole positions of porphyrin with alkyl groups shields the methine protons by 0.20—0.24 p.p.m., and the N—H protons by 0.36 to 0.46 p.p.m., a shielding that is identical within experimental error for different alkyl groups (methyl, ethyl, *n*-propyl)[8b]. The shielding effect may be discussed in terms of a long range (dipole) effect of the alkyl groups, but in addition a ring current change (via an inductive effect) is possible[8b]. For compounds substituted only by alkyl groups or by acetic or propionic acid side-chains, the effects on the methine positions are additive with respect to the next neighbors, but even in these cases a polarization of the entire macrocycle that results in long-range effects can already be observed. Incremental shifts of the methine proton resonance (in TFA) of +0.11, +0.02, and +0.11 p.p.m. for a neighboring alkyl, 2-carbomethoxyethyl and vinyl group, respectively, are reported by Abraham et al.[8b].

Both nearest neighbor and ring current effects are much more pronounced with substituents other than the ones cited above, and for such compounds a simple nearest-neighbor incremental treatment is no longer possible. In an early review on the n.m.r. of various β-substituted porphyrins, Caughey[4] detected a decrease in ring currents with increasingly electron withdrawing

TABLE 4

^{1}Hmr chemical shifts (δ[p.p.m.] from TMS) of β-pyrrole substituted oligomethylporphyrins, selected from the work of Clezy et al.[81–85]

Parent Compound, Substituents	Methine—H	Substituent—H	Propionic Ester Protons [CH_2CH_2-(COOR)]	Ester, Ring-CH_3	Ref.
Porphin	11.22				8a
Octamethylporphyrin	10.98			3.77	8a
Hexamethyl-Porphin					
6,7-diP^{Me}	11.20(1)		4.72, 3.32	3.79	81
	11.06(3)			3.84	
2,3-diAc	11.87(1)			4.02	81
	11.05(2)			3.69	
	10.91(1)				
2-Ac, 5P^{Me}	11.51(1)	3.58 (Ac)	4.65, 3.35	4.13(1)	81
	11.15(1)			3.80(1)	
	10.95(2)			3.81(2)	
				3.72(3)	
2-COOEt, 5-P^{Me}	11.88(1)	5.12, 1.95	4.65, 3.35	4.13(1)	81
	11.21(1)	($COOC_2H_5$)		3.82(2)	
	11.01(2)			3.80(1)	
				3.77(3)	
2-CHOH—CH_3, 3-COOEt	12.26	6.90 (*q*)		4.09(1)	81
	11.13	3.30 (*d*)		3.80(1)	
	10.92	($CHOHCH_3$)		3.72(4)	
	10.90	5.10 (*q*)			
		1.87 (*t*)			
		($COOC_2H_5$)			
2-Ac, 3-COOEt	12.22(1)	5.07 (*q*)		4.05(2)	81
	11.11(2)	1.86 (*t*)		3.70(4)	
	10.98(1)	($COOC_2H_5$)			
		3.57			
		($COCH_3$)			
1-OCH_3, 3-H	11.07(1)	9.62 (β_{pyrr} H)		3.78(2)	82,83
	10.88(3)			3.70(4)	
4-$NHCOCH_3$, 7-P^{Me}	11.08	3.93 ($NHCOCH_3$)	4.67, 3.30	3.82(1)	84
	11.05			3.77(2)	
	11.02			3.80(2)	
	10.97			3.72(2)	
Pentamethyl-Porphin					
5,8-diP^{Me}, 2-CN	11.21(1)		4.65, 3.21	4.01(1)	81
	11.01(3)			3.82(2)	
				3.80(4)	
2-Ac, 3-COOEt, 8-Br	12.17(1)	5.06, 7.88		4.05(2)	81
	11.12(1)	(OC_2H_5)		3.69(2)	
	11.04(1)	3.55 (Ac)		3.74(1)	
	10.91(1)				

TABLE 4 (continued)

Parent Compound, Substituents	Methine—H	Substituent—H	Propionic Ester Protons [CH_2CH_2 (COOR)]	Ester, Ring CH_3	Ref.
2,3-Ac, 5-Et	11.83(1)	3.54 (Ac)		4.02(2)	81
	11.02(2)	4.20 (*q*)		3.69(3)	
	10.90(1)	1.78 (*t*)			
		(C_2H_5)			
1-OCH_3, 3-Ac, 7-P^{Me}	11.28(1)	4.98 (OCH_3)	4.58, 3.26	4.05(1)	82,8
	10.98(1)	4.23, 1.26		3.74(1)	
	10.90(1)	(OC_2H_5)		3.69(3)	
	10.82(1)	3.52 (Ac)			
4-$NHCOCH_3$, 6,7-P^{Et}	11.23	3.88 ($NHCOCH_3$)	4.62, 3.18	3.68(5)	84
	11.12				
	11.08				
	11.04				
2-$NHCOCH_3$, 4-COOEt, 7-P^{Et}	11.76(1)	2.91 ($NHCOCH_3$)	4.67, 3.28	4.02(1)	84
	11.15(1)	5.09, 1.90		3.76(2)	
	10.98(2)	($COOC_2H_5$)		3.72(2)	
				3.61(1)	
1-COOEt, 6,7-C_2H_5	11.75	5.10, 1.85		4.09(1)	85
	11.12	($COOC_2H_5$)		3.72(4)	
	10.92	4.25, 1.85			
	10.88	(C_2H_5)			
	11.42	3.52($COCH_3$)		4.05(1)	85
1-$COCH_3$, 6,7-C_2H_5	11.09	4.20, 1.79		3.70(4)	
	10.89	(CH_2CH_3)			
	10.84				
1-CHOH—CH_3; 6,7-C_2H_5	11.28(1)	7.00, 3.30		3.82(1)	85
	10.99(3)	($CHOHCH_3$)		3.75(4)	
		4.25, 1.82			
		(CH_2CH_3)			
5-vinyl; 2,3-C_2H_5	11.03(2)	8.30, 6.50		3.80(1)	85
	10.98(2)	($CHCH_2$)		3.71(4)	
		5.25, 1.80			
		(CH_2CH_3)			
4-Ac; 6,7-P^{Et}	11.10(1)	3.52 ($COCH_3$*)	4.63, 3.22	4.07(1)	85
	11.03(1)			3.71(4)	
	10.88(2)				
Tetramethyl-Porphin					
6,7-diP^{Me}, 2,3-COOEt	12.57(1)	5.09 (*q*)	4.68, 3.39	4.08(2)	81
	11.18(1)	1.79 (*t*)		3.78(4)	
	11.12(2)	(OC_2H_5)			
6,7-diP^{Me}, 2,3-diCN	11.30(1)		4.70, 3.30	4.08(2)	81
	11.08(3)			3.72(4)	

TABLE 4 (continued)

Parent Compound, Substituents	Methine—H	Substituent—H	Propionic Ester Protons $[CH_2CH_2(COOR)]$	Ester, Ring CH_3	Ref.
2,3,6,7-tetraP^{Me}	11.22(2)		4.75, 3.35	3.84(4)	81
	11.08(2)			3.78(4)	
6,7-diP^{Me}, 2,3-diAc	11.88(1)	3.55(OAc)	4.60, 3.30	4.05(2)	81
	11.16(1)			3.78(4)	
5,8-diP^{Me}, 2-COOEt, 1-H	11.91(1)	10.48 (β_{pyrrol} H)	4.70, 3.35	3.83(6)	81
	11.03(1)	5.13			
	11.35(1)	1.93 (OC_2H_5)			
	10.99(1)				
2,3-diNHAc, 6,7-diP^{Me}	11.28(1)	2.95 ($NHCOCH_3$)	9.70, 3.35	3.82(2)	84
	11.07(3)			3.75(2)	
				3.71(2)	
2,3-diNH_2, 6,7-diP^{Me}	11.13(1)		4.60, 3.30	3.78(2)	84
	10.79(1)			3.73(2)	
	10.72(2)			3.62(2)	
2,3-diNHCOOEt, 6,7-diP^{Et}	11.22(1)	4.65, 1.50	4.65, 3.31	3.80(2)	84
	11.18(1)	($COOC_2H_5$)		3.75(4)	
	11.04(2)				
2-H, 4-Ac, 6,7-diP^{Et}	11.50(1)	9.61 (H)	4.68, 3.29	4.10(1)	85
	11.10(2)	3.58 ($COCH_3$*)		3.80(2)	
	10.95(1)			3.78(1)	
2-H, 4-C_2H_3, 6,7-diP^{Et}**	9.81(1)	8.51, 6.10	4.16, 3.09	3.52(1)	85
	9.72(2)	($CHCH_2$)		3.44(1)	
	9.66(1)	8.75(H)		3.39(2)	

* Tentative assignment

** In C^2HCl_3

For the numbering system, see structure (13). If not otherwise indicated, all spectra were recorded with TFA as solvent. Abbreviations: Et = C_2H_5, P^{Me} = $CH_2CH_2CO_2Me$, P^{Et} = $CH_2CH_2CO_2Et$, Ac = $COCH_3$.

substituents at the pyrrole β-positions. This general trend is clearly visible in Table 4, which lists a selection of chemical shift data of synthetic porphyrins collected from the work of Clezy et al. Although in most cases the basic features of the spectra can be discerned, it is clear from these data that a detailed interpretation of the spectra is not possible without a complete assignment of all signals. This is especially true for the methine and aromatic methyl proton signals, which appear in the spectra as singlets, and which cannot be assigned from their multiplicity.

As the effects of substitution are at best difficult to estimate per se, a careful choice of a completely assigned reference compound from which the substituent effects can be deduced by stepwise structural modifications is necessary in any particular investigation. Inhoffen et al.[72] completely assigned the spectrum of chlorin-e_6 trimethyl ester (14), which is a suitable reference compound for chlorins and pheophorbides, by a systematic variation of certain substituents (for details, see Ref. 73). As an example of a different approach, the careful study of aggregation shifts made possible the chemical shift assignment of chlorophyll-*a* (15)[13] and of a series of three type IX isomer porphyrins[68]. These can now serve as reference compounds for other chlorophylls and porphyrins.

The ^{1}Hmr data of Inhoffen et al.[86] was used to deduce the substituent effects of $-CHO$, $-COOCH_3$, $-COCH_3$ and $-CHOHCH_3$ in positions 2 and 4 in mono- and disubstituted deuteroporphyrins-IX*. The reference compound used was deuteroporphyrin-IX DME (16), whose ^{1}Hmr spectrum was completely assigned by Janson et al.[68] As the latter data were obtained in C^2HCl_3, the first step was to assign the signals observed for the reference compound in TFA. The same order with respect to field for the methine and methyl resonances of H_2(Deut-IX-DME) was assumed for dilute solutions in both $CDCl_3$[68] and in TFA[86]. For the assignment of the protons in the substituted compounds, an incremental shift similar in size for the two most remote resonances was assumed, a slightly different increment for the closer group, and the most strongly deviating increment for the nearest neighbor. Although some of the assignments so obtained are still not completely unambiguous, a self-consistent set of data was obtained by this procedure (Table 5).

The β-substitution effects for $-CHO$, $-COOCH_3$, $COCH_3$ and $-CHOHCH_3$ can be summarized as follows: 1) All of these substituents decrease the ring current substantially, and the incremental shift for remote proton signals is of comparable size for all four substituents; 2) different chemical shift increments are observed for the same substituent in position 2 or 4; 3) the substituent effects are not additive, as shown by the chemical shifts in the disubstituted compounds; 4) different relative increments for the signals of the propionic acid side-chain indicate changed conformations of the latter and/or the ring system for different substituents; 5) the most pronounced effects, which vary characteristically for the substituents, are the neighboring group effects due to long-range shielding. The adjacent methine proton signal is strongly deshielded by the substituents cited, and this effect increases in the order $-CHOHCH_3 \leqslant -COCH_3 < -CHO < -COOCH_3$. The effect on the nearest methyl group is similar, with one

---

* The original assignment of Fischer et al.[87] for the 2- and 4-monoformyldeuteroporphyrin-IX dimethyl ester was revised[88] after the publication of the n.m.r. data[86], hence, the interchanged substituents in Table 5.

TABLE 5

^{1}Hmr chemical shifts (δ[p.p.m.] from TMS in TFA) of H_2(Deut-IX-DME) (16) and its mono- and di-substituted derivatives; and incremental shifts (Δ[p.p.m.]) as compared to the respective signals in the parent compound (16).

(16)

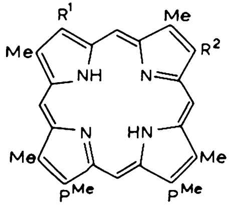

R^1		H	H	CHO	$COOCH_3$	$COCH_3$	$CHOHCH_3$	H	H	H	H	CHO	$COCH_3$
R^2		H*	H	H	H	H	H	CHO	$COOCH_3$	$COCH_3$	$CHOHCH_3$	CHO	$COCH_3$
Methine—H,	α	10.06	11.09	11.61	11.73	11.43	11.42	11.02	11.08	10.96	10.95	11.51	11.63
	β	10.03	11.02	10.82	10.79	10.74	10.88	11.43	11.73	11.37	11.41	11.51	11.34
	γ	10.10	11.21	11.10	11.03	11.00	11.12	11.02	11.08	10.96	11.03	11.01	10.97
	δ	9.99	10.98	11.15	11.09	11.00	10.95	10.89	10.94	10.79	10.91	11.01	10.96
Δ	α			—0.52	—0.64	—0.34	—0.33	+0.07	+0.01	+0.13	+0.14	—0.42	—0.54
	β			+0.20	+0.23	+0.28	+0.14	—0.41	—0.71	—0.35	—0.39	—0.47	—0.32
	γ			+0.11	+0.18	+0.21	+0.09	+0.19	+0.13	+0.25	+0.18	+0.20	+0.24
	δ			—0.17	—0.11	—0.02	+0.03	+0.09	+0.04	+0.19	+0.07	—0.03	+0.02
Arom. CH_3,	1	3.60	3.83	4.16	4.61	4.06	3.72	3.77	3.78	3.71	3.72	4.10	4.01
	3	3.57	3.80	3.77	3.74	3.75	3.66	4.13	4.61	4.06	3.84	4.08	4.01
	5	3.68	3.86	3.77	3.77	3.75	3.66	3.77	3.78	3.74	3.79	3.78	3.71
	8	3.70	3.87	3.77	3.77	3.75	3.66	3.77	3.78	3.74	3.79	3.78	3.66
Δ	1			—0.33	—0.78	—0.23	+0.11	+0.06	+0.05	+0.12	+0.11	—0.28	—0.18
	3			+0.03	+0.06	+0.05	+0.14	—0.33	—0.81	—0.26	—0.04	—0.27	—0.21
	5			+0.09	+0.09	+0.11	+0.20	+0.09	+0.08	+0.12	+0.07	+0.08	+0.15
	8			+0.10	+0.10	+0.12	+0.21	+0.10	+0.09	+0.13	+0.08	+0.09	+0.21
6′,7′-CH_2		4.38	4.72	4.61	4.62	4.58	4.60	4.61	4.61	4.59	4.65	4.58	4.56
Δ				+0.11	+0.10	+0.14	+0.12	+0.11	+0.06	+0.13	+0.07	+0.14	+0.16

TABLE 5 (continued)

R^1 R^2	H H*	H H	CHO H	$COOCH_3$ H	$COCH_3$ H	$CHOHCH_3$ H	H CHO	H $COOCH_3$	H $COCH_3$	H $CHOHCH_3$	CHO CHO	$COCH_3$ $COCH_3$
6″,7″-CH_2	3.24	3.30	3.29	3.25	3.24	3.17	3.27	3.26	3.23	3.26	3.23	3.20
Δ			+0.01	+0.05	+0.06	+0.13	+0.03	+0.04	+0.07	+0.04	+0.07	+0.10
β-pyrrolic—H	9.06	9.66	9.53	9.50	9.45	9.60	9.58	9.60	9.57	9.57		
Δ	9.04											
			+0.13	+0.16	+0.21	+0.06	+0.08	+0.06	+0.09	+0.09		
Substituent			11.66	3.83	3.54	6.86/ 2.19	11.57	3.84	3.52	6.84/ 2.30	11.54/ 11.79	3.48/ 3.50

* 0.004 m in C^2HCl_3

For details see text.

TABLE 6

Expectation ranges (δ [p.p.m.] from TMS in C^2HCl_3) of β-pyrrole substituents in positions 1, 3, and 5 of porphyrins

(17)

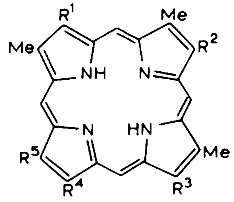

R^4 = Me, Et, P^{Me}
R^5 = Me, Et

R^1			
H	8.78—8.87		
$CHCH_2$	7.8—8.2 (8.2—8.3 in TFA) (H_X) 5.9—6.3 (6.4—6.5 in TFA) ($H_{A,B}$) ABX, $J_{AB} \sim 2$, $J_{AX} \sim 17$, $J_{BX} = 12$		
$COOCH_3$	4.3 (4.6 in TFA) (*s*)		
CHO	10.4—11.1 (*s*)		
$CH_2CH_2OCOCH_3$	3.8—4.4	4.5—4.8	1.9—2.1
CH_2CH_2OH	3.8—4.5 (4.6 in TFA), 3.20		
CH_2CH_2CN		3.21	
CH_2CH_2Cl	4.1—4.6	3.20	
CH_2CH_2Br	4.3—4.5		
$CO—CH_2—(CH_2)_6CH_3$	2.0	1.5—0.8	
CH_2CHO	4.77 (*d*)	10.12 (*t*)	$J = 3$ Hz
$CH_2CH(OCH_3)_2$	4.2—4.3	5.0—5.1	3.4—3.5
CH_2CH_2OTS	4.75 (*m*)	4.90 (*m*)	7.64 (*d*), 7.29 (*d*) 2.38 (*s*)

R^2			
H	8.83—8.93		
$CHCH_2$	7.8—8.2 (8.2 in TFA)	6.0—6.4 (6.4—6.5 in TFA)	
$COOCH_3$	4.3		
$CH_2CH_2OCOCH_3$	4.0—4.4 (3.08 for β-OAc)	4.6—4.8	2—2.1
CH_2CH_2OH	3.8—4.5 (4.6 in TFA)	3.20	
CH_2CH_2Cl	3.9—4.4	3.20	
CH_2CH_2Br	4.35		
CHO	11.08		
$CH_2CH(OCH_3)_2$	4.32	5.13	3.4—3.5

R^3			
$COOCH_3$	4.4—4.6		
$COCH_2COOCH_3$	4.4—4.6	3.5—3.6	
$C(OH)=CH—COOCH_3$	3.3	6.1—6.2	
$C(OCH_3)=CH—COOCH_3$	3.88*	5.81	3.91*
$C(OAc)=CH—COOCH_3$	2.46	6.56	3.93

TABLE 6 (continued)

R^3			
CO—O—CO—Bu^t	1.6—1.7		
CO—O—CO—Et	4.76	1.66	
CO—N—CH=CH—N=CH	8.3—8.4*	7.8—7.9	7.2—7.3*

* Signals assigned to either one of the indicated positions.

Selected from the work of Jackson, Kenner, Smith et al.[91–99]. If not otherwise indicated, the chemical shifts are listed according to the proton sequence in the substituent formula (from left to right, i.e., $-CH_2$ before $-CH_3$).

exception: the $-CHOHCH_3$ group has a strong neighbor group effect on the nearest methine proton resonance, and a negligible effect on the nearest methyl resonance. As both the methine and the methyl protons are at comparable distances to the substituents, the discrepancy is probably due to a preferred conformation of the substituent (or its solvate) (see Section 10.4.2.2).

The chemical shifts of β-pyrrole substituents can be estimated from the incremental shifts listed in Table 2. The expectation ranges for a variety of β-pyrrole substituents in porphyrins of the general structure (13), are listed in Table 6, and some further examples can be found in Table 8 and in the appropriate column in Table 4. Conjugated β-dicarbonyl substituents (Table 7) are usually present both in the keto and the enol form[89,90]. As the total ring current is affected by this (generally slow) tautomerism, the n.m.r. spectrum shows two sets of lines characteristic of a slowly equilibrating mixture. The assignment of the tautomers is possible by temperature dependent studies and by the relative intensities of the signals.

Some n.m.r. data of H_2(TPP) derivatives substituted at β-pyrrole positions (Table 8) have been reported by Callot[100,101]. The shielding effect of the phenyl rings (Section 10.2.3.) shifts the signals of the substituents to considerably higher field as compared to the respective substituents in *meso*-unsubstituted porphyrins (Tables 6 and 7). A further noteworthy feature is the nonequivalence of β-pyrrole methylene protons, which is indicated by the multiplet rather than a triplet structure in the methylene resonances of the ω-bromo-octyl derivatives. This nonequivalence, as well as the centrosymmetric structure discussed for the tetra-substituted products, are judged to be strong indications for a nonplanar structure of the macrocycle.

10.2.3. Meso substitution

Meso-substitution changes the ^{1}Hmr spectrum of porphyrins in three important ways: 1) The ring current is reduced, and within broad limits the extent of the reduction is independent of the nature of the substituents; 2)

TABLE 7

^{1}Hmr chemical shifts (δ[p.p.m.] from TMS) of porphyrins with conjugated β-dicarbonyl substituents.

Compd.		Keto-form		Enol-form	Solvent	Ref.
a) R=CO–CH(OCH$_3$)COOCH$_3$ b) R=C(OH)=C(OCH$_3$)COOCH$_3$ (18) 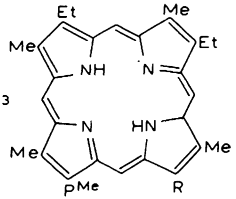 Et Me Me Et NH N N HN Me Me pMe R	Methine—H	10.52 (2)		10.34 (2)		90
		9.96		10.12		
		9.72		9.88	C^{2}HCl$_3$	
	R: OH	—		12.2		
	CH	5.83		—		
a) R=CO–CH$_2$–COOCH$_3$ b) R=C(OH)=CH–COOCH$_3$ (19) 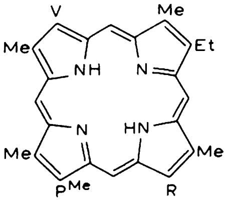 V Me Me Et NH N N HN Me Me pMe R	Methine—H	10.33		10.20		89
		9.46		9.62		
		9.39		9.56		
		9.30		9.39		
	Vinyl—H$_{ABX}$		7.93		C^{2}HCl$_3$	
			6.08			
	R: CH$_{(2)}$	4.57		6.08		
	CH$_3$		3.61			
	OH	—		13.30		
	5-CH$_3$	3.92		4.03		
a) R=CO–CH$_2$–COOCH$_3$ b) R=C(OH)=CH–COOCH$_3$ (20) 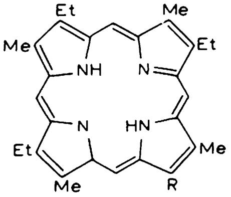 Et Me Me Et NH N N HN Et Me Me R	Methine—H	10.68		10.48	C^{2}HCl$_3$	89
		9.82 (2)		10.01		
		9.80		9.91 (2)		
	R: CH$_{(2)}$	4.59		6.15		
	CH$_3$	3.88		3.99		
	OCH$_3$	3.57 (2)		3.71		
		3.50		3.67		
		3.42		3.54		
				3.46		

See also Sections 10.2.8.2. and 10.2.8.4.

TABLE 8

^{1}Hmr chemical shifts (δ[p.p.m.] from TMS in C^2HCl_3) of β-pyrrole substituents in H_2(TPP) derivatives substituted at β-pyrrole positions

Substituent(s)	Substituent Resonances	Remarks References
1-$CHCH_2$	H_X: 6.35, H_A: 5.68, H_B = 5.17 J_{AB} = 2.3, J_{AX} = 17.3, J_{BX} = 11.8	100
1-$CHCH_2$	H_X: 6.35, H_A: 5.86, H_B = 4.97 J_{AB} = 2.2, J_{AX} = 16.6, J_{BX} = 10.6	100 (Ni-complex)
1-CHO	9.20, 9.33; for 1-CHO and 2-H	100
1,3-di-Br	β-pyrrole—H: 8.80(1); 8.82(1); 8.70(4)	101
1,5-di-Br	β-pyrrole—H: 8.63(2); 8.50, 8.70 (d, J = 5.1)	101
1,3,5,8-tetra-Br	β-pyrrole—H: 8.50	101
1-$(CH_2)_8$-Br	CH_2—$(CH_2)_6$—CH_2Br: 2.8 (*m*), 1.2—2 (*m*), 3.40 (*t*) Phenyl-H: 7.7—8.2 β-pyrrole-H: 8.6—8.85 (*m*)	101
1,3-di-$(CH_2)_8$-Br	CH_2—$(CH_2)_6$—CH_2Br: 2.8 (*m*), 1.2—2 (*m*), 3.40 (*t*) Phenyl—H: 7.75—8.15 β-pyrrole—H: 8.5—8.8 (*m*)	101
1-OC_2H_5	CH_2CH_3: 4.20 (*q*), 1.08 (*t*) Phenyl—H: 7.7—8.2 β-pyrrole—H: 8.75	101
1-O-$(CH_2)_6$-Br	O—CH_2—$(CH_2)_4$—CH_2Br: 4.17 (*t*), 1.25—1.80, 3.43 Phenyl—H: 7.7—8.2 β-pyrrole—H: 8.75	101
1,3,5,7-tetra-CN	β-pyrrole—H: 8.69	101 (Ni-complex)

If not otherwise indicated, chemical shifts are listed according to the proton sequence in the substituent formula (from left to right).

the methine proton opposite to the *meso* substituent is more strongly shifted to higher field than the neighboring methines; 3) protons in the vicinity of the substitutent experience additional shielding effects.

The overall reduction of the ring current can be rationalized[3] in terms of the network theory[39], because a barrier to conjugation at the *meso* position affects the full ring current rather than only one branch of it[3]. The principal reason for the reduced ring current in *meso*-substituted porphyrins appears to be steric hindrance between the *meso*- and β-pyrrole substituents, an explanation which is well supported by the decrease in the effect on the ring current with decrease in the size of the β-substituent[102]. If the neighboring β-pyrrole position is unsubstituted, only a minor decrease (~3%) in ring current is observed on *meso*-substitution[8a], which is somewhat more than the decrease observed for the introduction of a β-substituent.

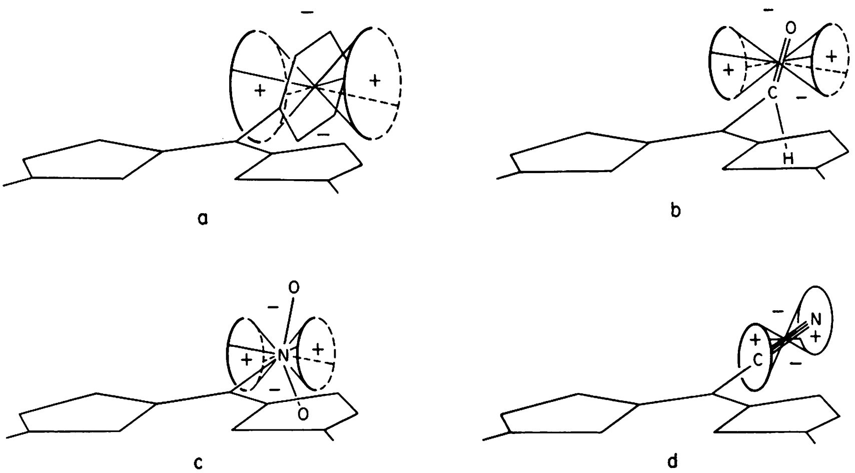

Fig. 4. Magnetic anisotropy of *meso*-substituents. Schematic representation of the porphyrin macrocycle and the zero shielding surface. (a) Phenyl; (b) CHO; (c) NO_2; and (d) CN.

For similar steric reasons, non-linear substituents such as -phenyl, -NO_2 or -CHO are not coplanar with the macrocycle ring, which efficiently reduces mesomeric interactions (Fig. 4). Thus, the shielding effect of a nitro[103,104] or a carbonyl group[71] on the resonances of the remaining methine protons is comparable to that of a methyl[8a] or hydroxymethyl[71] group. There are, however, two outstanding exceptions to this rule, and these are the amino[103,104] and the hydroxyl groups. Upon introduction of a *meso*-NH_2 substituent, the methine proton resonances are more shielded by about 1 p.p.m. than by other *meso*-substituents. This is likely due to contributions from imino-phlorin-like tautomeric structures (21a), in which the ring current is interrupted (see Section 10.2.7). The presence of these mesomeric iminophlorin structures, which are protonated at the opposite methine position, is evidenced by the ready ^1H—^2H exchange in *meso*-amino porphyrins[103]. It is interesting to compare the ^{1}Hmr spectrum of derivatives with *N*-pyrrole substituents in a *meso*-position for which cross conjugated phlorin-like structures have also been discussed[85]. These compounds exhibit a normal n.m.r.

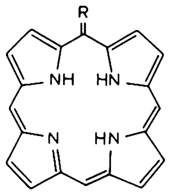

(21)

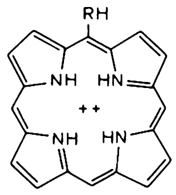

(22)

a R = N—H
b R = O

spectrum, however, indicating that the bulky pyrrole substituent cannot assume the coplanar conformation.

The second exception is the *meso*-hydroxy group. In acidic solutions the di-cation of the *meso*-hydroxyporphyrin is observed, while in neutral solutions[93,105,106] the tautomeric oxophlorin free base or monocation (see Section 10.2.7). can be observed. (For leading references, see Ref. 49.) Hydroxyporphyrin-cations present in TFA exhibit well-resolved ^{1}Hmr spectra with the characteristics of *meso*-substitution, and various *meso*-hydroxy porphyrins[93,106a,107–109] and similar structures with thiophen and furan rings[106] have been studied in detail in acidic media. In contrast, the ^{1}Hmr spectra of the free base oxophlorins present in neutral solutions are generally[105,106] difficult to observe[93,109,110] and exhibit line-broadening because of the presence of small amounts of the oxophlorin π-radical[111] (see Section 10.2.7).

The strong shielding of the methine resonance opposite to the *meso*-substituent can be ascribed to a conformational change in which the entire macrocycle is folded across the two opposite *meso* positions[8a]. This would be expected to reduce the deshielding effects most efficiently at the substituted *meso* position and at the one opposite to it. An indication for the presence of this preferred conformation is the stronger deshielding of the methine resonance in α,γ-disubstituted porphyrins as compared to the α,β-isomers[103,104]. This interpretation of the *meso* effect is further supported by the stability of α,γ-porphodimethenes relative to other systems with interrupted ring current (see Ref. 112 and Section 10.4.3 for X-ray results).

Protons in the vicinity of the *meso*-substituent experience additional shielding effects. These are partly steric in origin, because these groups are forced out of the plane of the macrocycle, but magnetic anisotropies of the *meso*-substituent appear to play the predominant role (Fig. 4). With —CHO[71], phenyl[8a] or —NO_2 groups[104], the neighboring β-substituents are in a region of positive shielding because of the preferred out-of-plane conformation of the *meso*-substituent. Just the opposite is true for the *meso*-cyanoporphyrins, in which the neighboring β-substituent are in a region of strong negative shielding[71].

The most prominent signals for some selected *meso*-substituted porphyrins are listed in Table 9, with references to further examples listed for every substituent. Some δ-alkyl substituted porphyrins related to structures postulated for *Chlorobium* chlorophylls have been reported by Cox et al.[118], and various β-alkoxy porphyrins have been characterized by Clezy et al.[62,93,107,109].

The influence of *meso*-substitution in chlorins is similar to that in porphyrins, but only if the substitution is at a position distant from the reduced ring (see Clezy, Ref. 62). If the *meso*-substituent is adjacent to the pyrroline ring, the effects are less pronounced and more complex. (See, for example,

TABLE 9

^{1}Hmr chemical shifts (δ[p.p.m.] from TMS) of *meso*-substituted derivatives of principal porphyrins

Parent Compound	*Meso* Substituent (Position)	Methine—H [a]	NH	Substituent Resonances	Cond.	Ref. [b]
H_2(OEP)	H	10.18	−3.74	—	C^2HCl_3	113
H_2(OEP)	H	10.98	−4.65	—	CF_3COOH	114
H_2(OEP)	Cl	10.71, 10.58	−2.96, −3.74	—	CF_3COOH	114
	$Cl_2(\alpha,\gamma)$	10.47	−2.62		CF_3COOH	114
	Cl_4	—	−0.92		C^2HCl_3	114
H_2(OEP)	Br	10.43, 10.38	−2.68, −3.63	—	CF_3COOH	114
H_2(OEP)	NO_2	10.85, 10.76	−3.17, −3.66	—	CF_3COOH	104
	$(NO_2)_{2,\alpha,\beta}$	10.49	−2.07	—	CF_3COOH	(103)
	$(NO_2)_{2,\alpha,\gamma}$	10.75	−2.31	—	CF_3COOH	
	$(NO_2)_3$	10.51	−1.37	—	CF_3COOH	
H_2(OEP)	NH_2	9.40, 8.95	1.01, −0.35	—	CF_3COOH	104 (103)
H_2(OEP)	NHCOOEt	10.2, 10.0		—	CCl_4	115
H_2(OEP)	CHO	9.98, 9.87	−2.95	12.74	C^2HCl_3, 0.05 m	71
H_2(OEP)	CN	9.98, 9.89	−3.30	—	C^2HCl_3, 0.05 m	71
H_2(OEP)	CH_2OH	10.07, 9.88		6.79	C^2HCl_3, 0.05 m	71
H_2(OEP)	$CH_2OSO_2—CH_3$	10.18, 9.98	−3.00	6.45 (α-CH_2) 3.92 (CH_3)	C^2HCl_3	122
H_2(OEP)	$CH_2OC_2H_5$	10.14, 10.05	−3.00	6.43 (α-CH_2) 3.95 (*q*), 1.61 (t)	C^2HCl_3	122
H_2(OEP)	CH_3	10.07, 9.87	−2.86	4.63	C^2HCl_3	122
H_2(OEP)	OH	10.36, 10.09	−2.20, −3.03	—	CF_3COOH	106a (116)
H_2(OEP)	$OCOCH_3$	10.04, 9.88	−3.4	2.83	C^2HCl_3	113 (96, 62 89)
H_2(OEP)	$OCOCF_3$	10.4, 9.84	−3.56	8.56 p.p.m. from CF_3CCl_3	C^2HCl_3	116
H_2(OEP)	OCOPh	10.17, 9.99	−3.36	8.92—8.70 (o) 7.79—7.63 (m, p)	C^2HCl_3	106a (117)

TABLE 9 (continued)

Parent Compound	*Meso* Substituent (Position)	Methine—H [a]	NH	Substituent Resonances	Cond.	Ref. [b]
H_2(OMP)	H	10.98	—4.82	—	CF_3COOH	8a
H_2(OMP)	CH_3	10.62, 10.48	—3.57, —4.33	4.83	CF_3COOH	8a (118, 102, 119)
	$(CH_3)_2$ α, γ	10.39	—3.66	4.66	CF_3COOH	
H_2(OMP)	Ph_4	—	—0.76	8.32, 7.90 (Ph), 1.84 (CH_3)	C^2HCl_3/TFA	120
Porphin	H	11.22	—4.40	9.92 (β-H)	CF_3COOH	8a
Porphin	$(CH_3)_4$	—	—3.01	4.73 (meso-CH_3) 9.55 (β-H)	CF_3COOH	8a
Porphin	$(C_6H_5)_4$	—	—2.07	8.59 (o), 8.08 (m, p), 8.85 (β-H)	CF_3COOH	8a (120)
H_2(Etio-I)	$NHCOCH_3$	10.68, 10.59	—3.3, —3.48, —4.3, —4.4		CF_3COOH	103
H_2(Copro-II-TME)	SCN (β)	10.94, 10.64		—	CF_3COO^2H	121
H_2(Copro-II-TME)	SH (β)	10.08, 8.45		—	C^2HCl_3	121
A Hexamethyl-P	S-$COCH_3$	9.65	—4.0	2.06	C^2HCl_3	123
A Hexamethyl-P	A substituted pyrrole	10.81		—	CF_3COO^2H	85

[a] The low field resonance is always due to the proximate, the high field one for the opposite methine protons.

[b] References in brackets ( ) indicates additional information regarding the same substituent.

Ref. 114 for halogen-substituted chlorins.) One reason for this is certainly the diminished steric interaction[77] of this *meso*-substituent with the neighboring group when the β-carbon atoms in the pyrroline group change hybridization from sp^2 to sp^3. More indirect effects involve conformational changes of the more mobile reduced (pyrroline) ring, which are exemplified in the detailed analysis of δ-chloro-chlorins[124] and of peripheral complexes of pheophorbides[80]. The ^{1}Hmr spectra of three isomeric mono-*meso* acetoxy derivatives of the H_2(OEP) mono-geminiketone (35) were studied by Inhoffen et al.[105]. An incremental shift of Δ = 0.16 to 0.18 p.p.m. for the sets of opposed methine protons were observed; the magnitude of the shifts was independent of the position of the *meso*-acetoxy group. The ^{1}Hmr spectra of the *meso* hydroxy isomers are also reported in the same publication[105]. While two of the isomers are present in neutral solution ($CDCl_3$) as oxophlorins, the isomers in which the gemini ketone carbonyl groups and the hydroxy substituent are adjacent has a spectrum typical for a *meso*-substituted porphyrin. To our knowledge, this is the first instance of a metal-free neutral *meso*-hydroxyporphyrin, the stability of which is attributable to hydrogen-bond formation between the two neighboring oxygen functions[105].

Most of the chlorins derived from the chlorophylls have *meso*-substituents. The spectrum of chlorin-e_6 trimethyl ester (14) is discussed in detail at the beginning of this section (10.2.1.5), and the spectra of some selected compounds of similar structure are listed in Table 10. Some examples in which the γ- and the 6-substituents are linked together by ring formation are also listed in Table 10. The isocyclic five-membered ring so formed is the principal characteristic of the phorbin structure common to all chlorophylls. (For a discussion of the n.m.r. spectra of the chlorophylls, see Section 10.2.8.2.) As a consequence of the new bond, which is formed between carbon atom 6 and the γ methine carbon, the steric interaction of the substituents at C-γ and C-6 is efficiently reduced[77] and they become essentially co-planar[128]. This is principally expected to enhance the macrocycle ring current. At the same time, however, considerable strain is introduced into pyrrole ring C[128c,d,129] and the conformation of its substituents at position 6 (i.e., C-9) is changed in such a way that conjugation with the aromatic system of the macrocycle is facilitated. In the compounds listed in Table 10, the first effect is clearly overcompensated by the latter, and the methine protons are shielded by an additional 0.2—0.3 p.p.m. relative to compounds lacking a ring E.

As evidenced by the marked increase in ring current upon reduction of the C=O function to a CH_2 group (Δ methine $\simeq$ 0.45 p.p.m.), a major contribution to the shielding comes from the keto C=O group at position 9. This general principle is clearly visible from the data in Tables 11 and 12, in which some changes in the n.m.r. spectra of phorbins (Table 11) and pheoporphyrins (Table 12) upon substitution of the isocyclic ring E are listed. These

TABLE 10

^{1}Hmr chemical shifts (δ [p.p.m.] from TMS in C^2HCl_3) of γ-substituted 7,8-chlorins

(23)

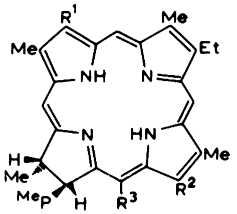

R^2	R^3	Methine—H (β, α, δ)	N—H	γ-CH_2[a]	$2'$-H_x	Ref.
		R^1 = Vinyl				
CH_2COOCH_3	H	9.70, 9.70, 8.81	−2.02	5.35	8.10	73
CH_2COOCH_3	$COOCH_3$	9.65, 9.50, 8.70	−1.04	5.27	8.00	73
CH—— $COOCH_3$	C=O	9.36, 9.24, 8.50	−1.80	4.93	7.86	125
		R^1 = H			2-H	
CH_2COOCH_3	H	9.73, 9.54, 8.81	−2.20, −2.34	5.39	8.81	73
CH_2COOCH_3	$COOCH_3$	9.69, 9.36, 8.72	−1.58	5.31	8.72	73
		R^1 = Ethyl			$2'$-CH_2	
CH_2COOCH_3	H	9.70, 9.53, 8.74	−2.08	5.35	3.90	73
CH_2COOCH_3	$COCH_3$	9.65, 9.37, 8.65	−1.50	5.20	3.85	73
CH_2COOCH_3	$COOCH_3$	9.64, 9.32, 8.61	−1.36	5.25	3.83	73
H_3COOC—CH——	C=O	9.39, 9.14, 8.43	−1.83	5.13	3.64	126
		R^1 = Acetyl			$2''$-CH_3	
CH_2COOCH_3	H	9.62, 10.20, 8.92	−1.84, −2.16	5.34	3.27	73
CH_2COOCH_3	$COCH_3$	9.64, 10.11, 8.90	−1.42, −1.64	5.22	3.26	73
CH_2COOCH_3	$COOCH_3$	9.65, 10.09, 8.88	−1.60	5.30	3.23	73
H_3COOC—CH——	C=O	9.42, 9.86, 8.68	—	5.12	3.19	127

[a] γ-CH_2: AB, J = 17 Hz, Δv = 0.08—0.13 p.p.m.

changes can generally be interpreted in terms of the electron-withdrawing effect of the substituents. Thus, introduction of (electron-withdrawing) carbonyl groups in the 9 or in the 9 and 10 positions leads to a pronounced decrease in the ring current[125,127,130]. These changes are about twice as large as for a conjugated carbonyl substituent in position 2, 4 or 6 (see Section 10.2.2), which is not a part of an additional ring[72,131,132]. This clearly reflects the coplanar conformation of the 6 and γ-substituents in the

TABLE 11

^{1}Hmr chemical shifts (δ[p.p.m.] from TMS in C^2HCl_3) of pheophorbides with various substituents at the isocyclic ring E

(24)

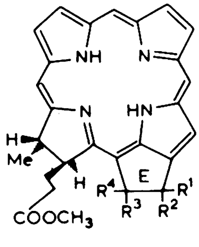

R^1	R^2	R^3	R^4	Methine—H	Vinyl—H_x[a]	NH	Remarks	Ref.
H	H	H	H	9.77, 9.58, 8.87	—	−1.68 −3.53	2-Ethyl	127
=O		H	H	9.32, 9.23, 8.47	7.90	−1.80	—	79
H	OH	H	H	9.83, 9.56, 8.86	8.15	—	$3\text{-}CH_2OH$	133
=O		H	$COOCH_3$	9.36, 9.24, 8.50	7.87	−1.72	10(R)	79
H	OH	H	$COOCH_3$	9.86, 9.86, 8.93	8.20	−3.2	9(R), 10(R)	125
=O		OCH_3	$COOCH_3$	9.53, 9.36, 8.58	7.92	−1.80	10(S)	79, 134
H	OH	OCH_3	$COOCH_3$	9.89, 9.70, 8.94	8.18	−3.0	9(S), 10(S)	130
=O		H	OCH_3	9.51, 9.39, 8.65	7.94	−2.08	10(S)	79
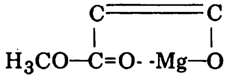 $\overset{C=\!=\!=C}{H_3CO{-}C{=}O\cdots Mg{-}O}$				9.01, 8.83, 8.00	7.77	—	Mg-chelate	135
H	$O{-}C(CH_3)_2{-}O$		H	9.69, 9.69, 8.83	—	—	2-Ethyl	136
H	OH	H	CH_2OH	9.79, 9.53, 8.85	8.07	—	$3,7''\text{-}CH_2OH$	136

[a] See Formula (13).

pheophorbides imposed by the additional ring E. In the absence of X-ray structural information on 9-desoxo-pheophorbides[128d], the steric effect on the geometry of rings C and E that accompanies the change from sp^3 to sp^2 configuration of C-9 is much more difficult to estimate, but can probably not be neglected. The isocyclic five-membered ring E has two potentially asymmetric centers. Although stereoisomers at C-9 and C-10 influence the resonances of neighboring substituents in a characteristic way (Section 10.4.3), long-range effects via the ring current are generally negligible.

Some systems with a fused ring between a *meso* and a β-pyrrole position other than the isocyclic five-membered ring of the phorbins have been investigated by n.m.r. The relief in steric strain resulting from enlargement of ring E in phorbins is clearly demonstrated by the increased ring current in pheophorbide lactones[129]. The ^{1}Hmr spectra of isopheoporphyrins are

TABLE 12

^{1}Hmr chemical shifts (δ[p.p.m.] from TMS) of pheoporphyrins with various substituents at the isocyclic ring E.

(25)

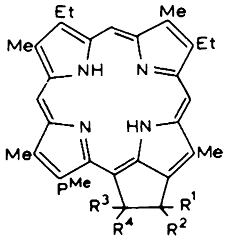

R^1	R^2	R^3	R^4	Methine—H	NH	R^3-Resonance	Remarks	Ref.
H	H	H	H	9.88, 9.79, 9.72	—	—	0.05 m, C^2HCl_3	127
keto C=O		H	H	9.72, 9.67, 9.26	—	—	0.05 m, C^2HCl_3	132
keto C=O		keto C=O		9.70, 8.95, 8.89	—	—	0.1 m, C^2HCl_3	137
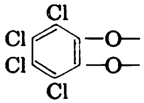		keto C=O		11.28(1), 11.12(2)	—	—	CF_3COO^2H	137
keto C=O		OCH_3	$COOCH_3$	10.15, 10.05, 9.81	—2.75	—	0.03 m, C^2HCl_3	126
keto C=O		OC_2H_5	H	9.97, 9.82, 9.80	—3.2/—4.1	~3.85/1.25	0.03 m, C^2HCl_3	135
keto C=O		OC_3H_7	H	9.96, 9.84, 9.77	—	~4.20/1.40/0.72	0.03 m, C^2HCl_3	135
keto C=O		O-i-prop	$COOCH_3$	9.96, 9.79, 9.50	—3.7	5.10/1.32/0.71	0.05 m, C^2HCl_3 2-vinyl	138

reported by Dougherty et al.[139] and establish a structure in which the γ-substituent is linked to C-7 rather than to C-6[77]. A thiacyclic structure in rapid tautomeric exchange with its mirror image is proposed by Clezy and Smythe[123] to account for the unusual chlorin-like ^{1}Hmr spectrum of the product obtained by hydrolysis of a *meso*-thioacetoxy-porphyrin.

10.2.4. N-Substitution

The n.m.r. spectra of *N*-alkylated porphyrins are generally interpreted in terms of the steric hindrance imposed on the macrocycle by central substituent(s) that do not fit into the inner cavity of the macrocycle. The chemical shift changes observed appear to arise from three different effects which can all be attributed to steric distortions. These include decrease in the ring current, changed local shielding patterns due to conformational changes, and an increased sp^3 hybridization at the substituted *N*-atom(s). These effects were first analyzed by Caughey et al.[140] for *N*-methyl- and *N*-ethyl-etioporphyrin-II (26).

Caughey et al.[140] discuss a conformation of the macrocycle in which the N-substituted ring and the neighboring rings are twisted out of the macrocycle plane, the latter to a smaller extent and in the opposite direction, while the opposite ring remains in the plane of the macrocycle. Confirmation of this interpretation was recently obtained by X-ray analysis[141], although the X-ray structural data showed a similar tilt of the opposite ring C as well. The resonances of the protons in the side chains of the (opposite) ring C are slightly shifted to higher field because of the reduced ring current, and the shielding is even more pronounced in the resonance signals of the protons of ring A, which are considerably tilted out-of-plane. The methine resonances under these circumstances are expected to move to higher field, which is indeed observed for the β and γ protons. This effect is partially compensated, however, by the less effective shielding by the out-of-plane alkyl substituents on the α and δ protons.

A series of *N*-mono-, di- and tri-substituted porphyrins (27—29) was investigated by Jackson et al.[142]. While the interpretation of the spectra for the *N*-monosubstituted porphyrins is similar to the one given above[140], it should be noted that the methine resonances were assigned the opposite way. The ring current of *N*-alkyl porphyrins is increased stepwise by formation of the mono- and di-cation (27a,b,c) although in the latter the conformation is changed as well[142]. The free bases do not aggregate, and the spectra are concentration independent. The mono-cation, however, forms a complex with the free base, the kinetics of which were studied by ^{1}Hmr[142]. In addition to the mono-substituted compounds, three *N,N*-dimethylporphyrin isomers (28a,29a,b), as well as their dications, were investigated and their spectra were again interpreted in terms of conformational and ring current changes arising from steric hindrance[142].

As the *N*-alkyl groups are in the center of the macrocycle, their proton

TABLE 13

^{1}Hmr chemical shifts (δ [p.p.m.] from TMS) of *N*-alkylporphyrins and their cations

(26)
a) R = H
b) R = CH_3
c) R = C_2H_5

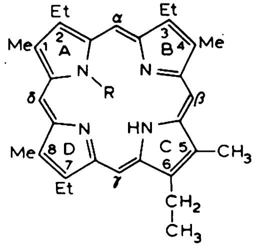
Et
α
Et
Me
2
1
A
3
B
4
Me
N
R
N
δ
β
N
HN
Me
8
D
C
5
CH_3
7
6
Et
γ
CH_2
CH_3

Compound	Formula	Nmr Data a	b	c	Ref.
(26)	N—CH_3	—	—4.89	—2.37	140
	N—CH_2	—	--	—5.16	
	N—H	—3.79	—3.12	—	
	1-CH_3		3.20	3.22	
	4,8-CH_3	3.62	3.50	3.52	
	5-CH_3		2.66	3.65	
	2-CH_2		3.96	3.94	
	3,6,7-CH_2	4.11	4.14	4.12	
	2′-CH_3		1.42	1.39	
	3′, 6′, 7′-CH_3	1.87	1.85	1.86	
	α,δ-H		10.01	10.08	
	β, γ-H	10.11	9.97	9.96	

(27)
a) Free base
b) Mono cation (ClO_4^-)
c) Dication
d) Zn-Complex (Cl^-)
e) Zn-Complex (I^-)

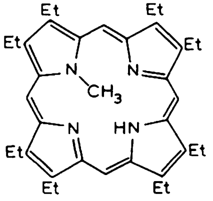
Et
Et
Et
Et
N
CH_3
N
N
HN
Et
Et
Et
Et

Compound	Formula	Nmr Data a	b	c	d	e	Ref.
(27)	N—CH_3	—4.76	—5.18	—5.20	—4.61	—6.05	142
	N—H	—	—	—3.96	—	—	
	1′,2′-CH_3	1.48	1.44	1.54	1.75	0.90	
	3′,4′,7′,8′-CH_3						
	5′,6′-CH_3	1.90	1.91	1.94	1.94	1—1.5	
		1.91	2.00	2.00			
	1,2-CH_2	3.72	4.84	3.94	3.98	3.08	
	3,4,7,8-CH_2	3.96	to	4.40	4.04	3.7—4.2	
	5,6-CH_2	4.00	3.85		4.08		
	α,δ-H	9.89	10.55	11.00	10.22	9.65	
	β,γ-H	9.94	10.64	11.12	10.31	8.65	

(28)
a) R = H
b) R = CH_3 (up); Cl^-

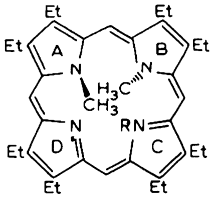
Et
Et
Et
Et
A
B
N
N
H_3C
CH_3
N
RN
D
C
Et
Et
Et
Et

(29)
a) CH_3/CH_3 *trans*
b) CH_3/CH_3 *cis*

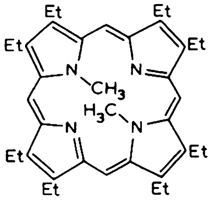
Et
Et
Et
Et
N
N
CH_3
H_3C
N
N
Et
Et
Et
Et

	28a	28b	29a	29b	
$N_{A,C}—CH_3$		−3.92	−5.30	−3.52	142
$N_B—CH_3$	−5.8	−7.08			
CH_3	1.55	1.27	1.71	1.28	
	1.71	1.50	1.94	1.84	
	1.98	1.63			
	1.99	1.89			
CH_2		3.3—4.1	3.8—4.2	3.39—3.98	
Meso—H	10.20	9.96	9.80	9.68	
	10.39	9.92			

TABLE 14

^{1}Hmr chemical shifts (δ [p.p.m.] from TMS) of some *N*-substituted derivatives of (OEP).

				Ref.
29c	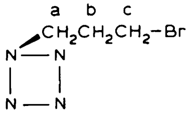	a: b: c:	−4.9 (*t*) −1.5 (*m*) 1.5 (*t*)	143a
29d	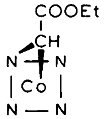	CH:	−2.25 (*s*)	143b
29e	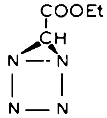	CH:	−5.78 (*s*)	143b
29f	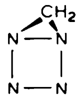	CH_2:	−8 (broad)	143b

Schematic representation of the porphyrin system.

resonance occurs at extremely high field due to the strong shielding provided by the aromatic system in this region. The *N*-alkyl resonances of some principle N-substituted porphyrins are listed in Table 13. The *N*-alkyl incremental shifts were used by Storm and Corwin[16] as a probe from which an empirical formula was derived for the ring current shifts of central, out-of-plane substituents[17]. The decreasing shielding effect with increasing distance from the macrocyclic plane (Fig. 1) is clearly visible in the *N*(ω-bromopropyl)octaethylporphyrin and alkyl-Co-porphyrins[143a,b,199a], which are listed in Table 14 together with some unusual *N*-substituted H(OEP) derivatives. The spectrum of *N*-methyl-*meso*-tetraphenylporphyrin was recently reported[143c].

10.2.5. Chlorins and related structures

In chlorins (30) and bacteriochlorins (31,32) one or two of the macrocycle peripheral double bonds are reduced without loss of the macrocyclic ring current. In most natural products, both carbon atoms in the reduced pyrrole ring(s) become sp^3 hybridized, but bacteriochlorophyll-*b* (41)[231] and several synthetic compounds (54,56) contain an exocyclic double bond at one of the chlorin positions.

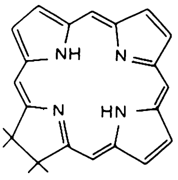

(30)

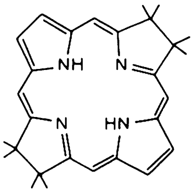

(31)

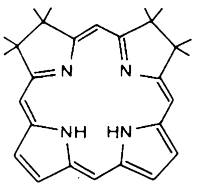

(32)

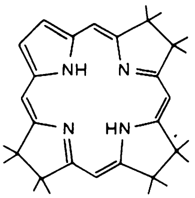

(33)

Removal of one of the peripheral double bonds leads to a decrease in the ring current, as indicated by the upfield shift of peripheral proton signals and a down field shift of the N—H signals (Table 15). The decrease is moderate in chlorins and bacteriochlorins, but very pronounced in the isobacteriochlorins (32). In the latter compounds, the two N—H protons are for the most part located at the two neighboring (non-reduced) pyrrole rings, a structure which is unfavorable for a large ring current for both steric and electronic reasons. A similar trend is observed in the gemini-porphin-diketones[143] with neighboring pyrroline rings (isomers 35a—c) *vs.* the 'opposite' isomers (35d) and (35e) (Table 17). A strongly decreased ring current is also observed in the gemini-porphin-triketones[143], which are examples of the dihydro-bacteriochlorin structure (33).

The ^{1}Hmr spectra of the basic chlorins and bacteriochlorins are listed in Table 15, and some selected examples of chemical shifts in chlorins are compared in Table 16 with those of the corresponding porphyrins. While the fully unsaturated porphyrins generally exhibit one set of closely spaced methine resonances, chlorins (30) show two sets about 0.8—1.0 p.p.m. apart even in the absence of highly anisotropic substituents. The high field set is assigned to the methine protons next to the reduced ring, the low field set to the remote methine protons. The low-field set reflects a moderate decrease in the macrocyclic ring current (Δ = +0.38 p.p.m. for octaethylchlorin *vs.* octaethylporphyrin (11)), and corresponding increments in chemical shift are observed for the resonances of substituents not attached to the reduced ring. The unusual shift of the neighboring methine resonances is best explained by a picture of the macrocycle introduced by Woodward[78,151]. In this model, the four pyrrole rings are considered to remain to some extent autonomous aromatic subunits that borrow electron density from the methine positions. Removal of a peripheral double bond (as by addition of 2H to ring D) results in the loss of an aromatic subunit, and an increase in the electron density at

TABLE 15

^{1}Hmr chemical shifts (δ[p.p.m.] from TMS) of some principal chlorins, bacteriochlorins, and isobacteriochlorins (see structures (30—33)).

	Methine—H	$\beta_{pyrrole}$—H		N—H	Chlorin—H	Remarks	Ref.
Porphin	10.58	9.74		—3.76	—	C^2HCl_3	60
Chlorin (7,8)	9.62 (α, β) 8.92 (γ, δ)	9.03 (3,4) 8.63 (2,5) 8.52 (1,6)		—2.75	4.25	C^2HCl_3	60
Octaethyl		CH_2	CH_3				
Porphyrin	10.18	4.14	1.95	—3.74	—	C^2HCl	71(144)
Chlorin (7,8-H) (*trans*)	9.80 (α, β) 8.95 (γ, δ)	3.88 (2 X CH_2) 3.91 (2 X CH_2) 4.01 (2 X CH_2) 2.20 (7,8-CH_2)	1.81 (2 X CH_3) 1.77 (2 X CH_3) 1.75 (2 X CH_3) 1.05 (7′,8′-CH_3)	—2.46	4.54*	0.05 m in C^2HCl_3	126(145, 146,65,147, 127,144)
Bacteriochlorin (3,4,7,8-H)	8.82	1.9—2.3(M, 3,4,7,8-CH_2) 3.73(1,2,5, 6-CH_2)	0.97 (3′,4′,7′, 8′-CH_3) 1.70 (1′,2′,5′, 6′-CH_3)	—1.88	4.2—4.35	0.05 m in $C_6{}^2H_6$	111,147
Iso-Bacteriochlorin (1,2,7,8-H)	6.80, 6.82 (δ) 7.40, 7.42 (α, γ) 8.46, 8.48 (β)	1.6—2.3 (M,1, 2,7,8—CH_2) 3.25 (3.6-CH_2) 3.37 (4,5-CH_2)	0.98(1′,8-CH_3) 1.03 (2′,7′-CH_3) 1.46 (3′,6′-CH_3) 1.50 (4′,5′-CH_3)	+2.96	3.4—3.8	0.05 m in C^2HCl_3	147(127,144 146,148)
Tetraphenyl-	$\beta_{pyrrole}$—H	Phenyl—H (o, m, p)		N—H	Chlorin—H	Remarks	Ref.
Porphyrin	8.75	8.30 7.80	7.80	—	—	C^2HCl_3	74
Chlorin (7,8-Dihydro)	8.34 (*s*,3,-4-H) 8.10, 8.49	7.6—8.5		1.3	4.10	C^2HCl_3	65

	(AB,1,2, 5,6-H, J=4.5)					
Bacteriochlorin (3,4,7,8-Tetrahydro)	7.85 (d, J=2,1,2, 5,6-H)	7.52	1.3	3.92	C^2HCl_3	65

---

* X-part of an ABX spectrum, J_{AX} = 4, J_{BX} = 6.8.

TABLE 16

^{1}Hmr chemical shifts (δ [p.p.m.] from TMS) of some selected chlorins as compared to the respective porphyrins.

Selected Chlorins			Porphyrin	Chlorin	Remarks	Ref.
(37)	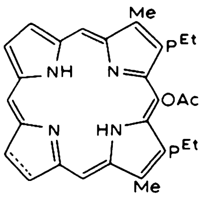 Me p^Et NH N OAc N HN p^Et Me	Methine—H	11.08, 10.98	9.80, 8.53	TFA	62
		$\beta_{pyrrole}$—H	9.83	9.02, 8.55		
		Aromatic CH_3	3.69	3.30, 3.22		
		Chlorin—H	—	4.70		
		N—H	—	—3.0		
(38)	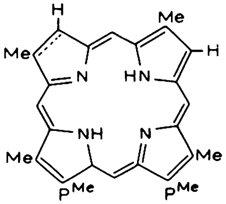 H Me Me H N HN NH N Me Me p^Me p^Me	Methine—H	9.46 (3), 9.37 (1)	9.50, 9.52 8.41 (2, α, δ)	C^2HCl_3	149,150
		$\beta_{pyrrole}$—H	8.61, 8.54	8.60 (4-H) 3.77—4.77 (2-H)		
		Ar., Ester CH_3	3,39, 3.30 3.25, 3.14	3.29 (3) 1.75 (1—CH_3) (*d*, *J* = 7)		
		Chlorin—H	—	3.77—4.77		
		N—H	—4.70	—2.75		
(39)	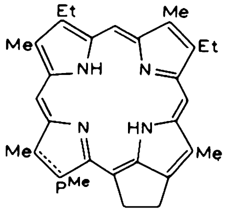 Et Me Me Et NH N N HN Me Me p^Me	Methine—H	9.88, 9.79 9.72	9.77, 9.58 8.87 (δ)	0.05 m, C^2HCl_3	127
		9-CH_2	4.00	3.99		
		Ar., Ester CH_3	3.67, 3.59 3.47, 3.41 3.32	3.43 (2) 3.53 (2) 1.80 (8-CH_3) (d, *J* = 7)		
		Chlorin—H	—	4.3—4.6		
		N—H	—	—1.68, —3.53		

TABLE 17

^{1}Hmr chemical shifts (δ[p.p.m.] from TMS in C^2HCl_3) of the geminiporphin mono-, di-, and tri-ketones of $H_2(OEP)$

(34)
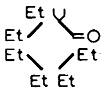
Et
Et
Et
Et
Et
Et
O

(35c)
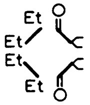
Et
Et
Et
Et
O
O

(36a)
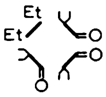

(35a)
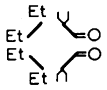
Et
Et
Et
Et
O
O

(35d)
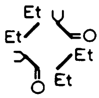
Et
Et
Et
Et
O
O

(36b)
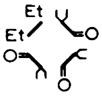

(35b)
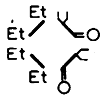
Et
Et
Et
Et
O
O

(35e)
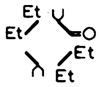

Compound	N—H	Methine—H	Nuclear		Geminal	
			$CH_2(q)$	$CH_3(t)$	$CH_2(q)$	$CH_3(t)$
34	−2.8	9.13	4.0 (m)	1.9 (m)	2.76	0.46
		9.86				
		9.88				
		9.96				
35a	−1.58	8.83 2X	3.86	1.74	2.60	0.48
		9.59	3.95	1.80		
		9.79				
35b		8.39	3.7 (m)	1.67	2.56	0.42
		8.58		1.70		0.54
		9.24		1.72		
		9.37				
35c		7.42 2X	3.52	1.61	2.5 (m)	0.49
		8.81	3.57	1.62		
		9.05				
35d	−1.84	8.78 2X	3.84	1.76	2.63	0.44
		9.59 2X	3.89	1.78		
35e	−2.63	9.05 2X	3.94	1.80	2.70	0.44
		9.71 2X	3.98	1.83		
36a		8.10	3.62	1.63	2.5 (m)	0.49
		8.36				
		8.45				
		8.86				
36b		7.78	3.51	1.57	2.36	0.45
		8.01	3.56	1.60		0.55
		8.08				0.58
		8.90				

Schematic representation of the porphyrin ring system. The heavy bars correspond to the peripheral bonds between adjacent β-pyrrole carbons. From Ref. 143.

the neighboring methine positions, which accounts for the high field shift of the signals for the neighboring methine protons[152].

In the bacteriochlorins (31) all four methine protons are adjacent to a (reduced) pyrroline ring. The methine resonances thus occur in the same chemical shift range as the high field set in chlorins, and the additional (small) high field shift reflects an additional decrease in ring current. In the isobacteriochlorins (32) one methine proton is between two reduced pyrroline rings, two protons are next to one reduced ring each, and one proton is situated between two pyrrole rings. Thus, three sets of methine resonances are observed, each about 0.8—1.0 p.p.m. apart from the next set for the reasons set forth above.

In the gemini-porphin-ketones (34—36) one of the chlorin positions in each pyrroline ring is part of a carbonyl group. All known isomeric gemini-porphin-mono- (34), di- (35) and tri-ketones (36) are listed in Table 17. In a detailed ^{1}Hmr investigation, Inhoffen and Nolte[143] showed that the position of a methine proton resonance is mainly determined by its nearest neighbors. For the methine protons next to one or two geminal diethyl substituents, incremental shifts of $\delta = 0.8$ and 1.6 p.p.m., respectively, could be deduced[143]. (For *meso*-substituted gemini-porphin-ketones, see Section 10.2.3.)

In contrast to the generally straightforward interpretation of the substituent subspectra in porphyrins, the subspectra of substituents of the (reduced) pyrroline ring in chlorins are often very complex. One reason is the reduced ring current shifts. All protons of substituents attached to the pyrroline ring are one C—C bond further removed from the aromatic system than in the corresponding porphyrins. The subspectra are, therefore, less spread out and are often not first order. The spectra are further complicated by the magnetic non-equivalence of the methylene protons of alkyl side-chains because of the asymmetric quaternary β carbon atoms of the pyrroline ring[13]. An additional complicating factor in these compounds is the possibility of spin—spin coupling between the substituents. Finally, structural isomers can be encountered. (The stereochemical aspects of chlorins are dealt with in Section 10.4.3, and the ^{1}Hmr spectra of compounds related to chlorophylls are treated in Section 10.2.8.2.)

Some further examples of chemical shifts associated with reduced pyrroline ring(s) are listed in Table 18. Chlorins in nature generally have one alkyl substituent and one proton at either one of the quaternary chlorin positions, and coupling between the two protons is observed[13]. Corresponding dioxychlorins (40), in which the chlorin protons are replaced by hydroxy and alkoxy-substituents, have been investigated by Inhoffen et al.[153]. Bacteriochlorophyll-*b* (41) has an ethylidene group[155] attached to a pyrroline ring (see also Section 10.2.8.2), and synthetic chlorins with a methylene substituent have been reported by Jackson et al.[91]. These authors[91] also studied some compounds (44,45) in which a methylpyrroline ring is spiroannelated

TABLE 18

Chemical shifts (δ[p.p.m.] from TMS in C^2HCl_3) of substituents of the (reduced) pyrroline ring in chlorins and bacteriochlorins

			Ref.
(40[a])	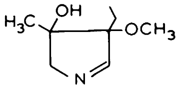	2.95 (3-OCH$_3$) 1.58 (3-CH$_3$) 4.50 (4-OH) 1.48 (4'-CH$_3$)	153
(41[b])	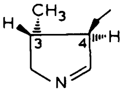	1.77 (3-CH$_3$) 4.24 (3-H) 4.20 (4-H) 1.09 (4'-CH$_3$)	154
(42[c])	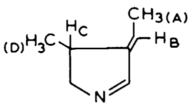	2.01 (CH$_{3(A)}$), d, J_1 = 7 6.84 (H$_B$), *dq*, J_2 = 2 4.93 (H$_C$), *dq*, J_3 = 7 1.66 (CH$_{3,D}$), *d*	155
(43[d])	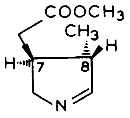	1.82 (*d*, 8-CH$_3$) $J_{8,8'}$ = 7 4.40 (*q*, 8-H) $J_{7,8} \leqslant 2$ 4.13 (*m*, 7-H) 2.1—2.8 (*m*, 7a—CH$_2$), (*m*, 7b—CH$_2$) $J_{7b_A-7b_B}$ = 19	156
(44[e])	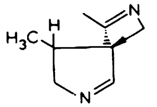	1.67 (*s*, CH$_3$) 1.39 (*m*, CH$_2$CH$_3$) 3.05 (*d*, CH$_3$) 4.20 (*m*, CH)	91
(45[e])	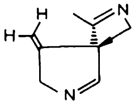	6.73, 5.67 (CH$_2$) 1.67 (*s*, CH$_3$) 1.6 (*m*, CH$_2$CH$_2$)	91
(46[f]) a) R$_B$=H$_B$, R$_C$=H$_C$ b) R$_B$=H$_B$, R$_C$=COOCH$_3$ c) R$_B$=COOCH$_3$, R$_C$=H$_C$ d) R$_B$=R$_C$=COOCH$_{3(B,C)}$	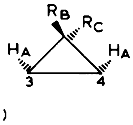	a) 3.88 (H$_A$), 1.65 (H$_B$), 0.60 (H$_C$) J_{AB} = 8.2, J_{AC} = 3.3, J_{BC} = 3.0 b) 4.34 (H$_A$), 2.68 (H$_B$), J_{AB} = 8.1 2.74 (COOCH$_3$) c) 4.47 (H$_A$), 1.58 (H$_C$), J_{AC} = 2.6 3.76 (COOCH$_3$) d) 4.79 (H$_A$), 3.82 (CH$_{3,B}$), 2.34 (CH$_{3,C}$)	66
(47[g]) a) Isomer I b) Isomer II	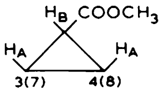	a) 3.70 (H$_A$), 1.42 (H$_C$), 3.70 (CH$_3$) b) 3.72 (H$_A$), 1.40 (H$_C$), 3.63 (CH$_3$)	66

Only a partial structure is shown; the compounds are derived from: (a) methyl bacteriopheophorbide-*a*; (b) Bchl-*a*; (c) Bchl-*b*; (d) pheophytin-*a*; (e) an Etio-type chlorin; (f) *meso*-tetraphenylchlorin; and (g) *meso*-tetraphenylbacteriochlorin.

to one of the chlorin positions. A group of chlorins with condensed cyclopropane rings (46,47) was investigated in some detail by Callot et al.[66,157,158], who showed that their stereochemistry can be deduced both by chemical shift and spin—spin coupling arguments (cf. Section 10.4.3). A substituted octaethylchlorin, in which one ‘extra’ hydrogen is replaced by a methyl group, is reported by Fuhrhop[158a], and recently the spectrum of 7,8-diethyl-octamethylchlorin has been studied[158b].

10.2.6. Systems with interrupted conjugation

Tetrapyrrole structures related to porphyrins, in which the ring current is more or less reduced or abolished, are currently of great interest because of their biochemical importance. We confine our discussion in this section to structures in which the porphyrin skeleton is retained*. In the non-aromatic** structures which contain the porphyrin skeleton, but not the conjugation, the conjugation is usually interrupted at one or more of the bridging methine positions. The resulting subunits have either four (one interruption) or two (two interruptions at opposite positions) pyrrole rings in conjugation, or the pyrrole subunits are isolated. While the system with four conjugated pyrrole rings may show indications of a residual ring current across the interrupted methine bridge, the ^{1}Hmr spectra of the other compounds are very similar to those of pyrromethenes (two conjugated pyrrole subunits) and pyrroles, which are representative non-macrocycle systems. Although the appropriate linear oligopyrrole systems are unlikely to be in the same cyclic conformations as the porphyrins, the chemical shifts are similar to those of porphyrin-derivatives with interrupted conjugation.

For systems without strongly anisotropic groups, the following ranges for the proton chemical shifts are observed: methine-H: δ = 5.8—6.8 p.p.m.; β-pyrrole H: δ = 6—7 p.p.m.; peripheral ethyl groups: δ = 2.5—2.9 p.p.m. (CH_2), and δ = 1.2—1.3 p.p.m. (CH_3); peripheral CH_3: δ = 1.8—2 p.p.m. Significant deviations from these chemical shift values indicate either an aromatic (diamagnetic) or an anti-aromatic (paramagnetic) ring current.

A characteristic feature of these conjugation-interrupted systems is a very large (up to 12.6 p.p.m.) shift to lower field frequently observed for the N—H protons. In contrast to the porphyrins with an aromatic macrocycle, the N—H protons in the interrupted systems occupy peripheral positions with respect to the aromatic subunits, and are subjected to their combined deshielding influence. Although no systematic ^{1}Hmr data are available, the strong variation of the N—H resonance within a given system indicates an additional structural dependence of the N—H shift, probably involving a change in hydrogen bonding.

---

* For leading references to the ^{1}Hmr spectroscopy of corrins and related structures, in which two of the pyrrole rings are directly linked together, see Ref. 159. For a discussion of bile pigments, see Ref. 160. Illustrative of other porphyrin-like systems with interrupted conjugation, a homoazaporphyrin has been reported by Grigg[161], hemiporphyrazines have been studied in detail by Kenney et al.[162a], and a series of related structures is reviewed by Haddon et al.[41].

** The ring current criterion is generally used to determine whether or not a macrocycle aromatic system is present.

One hetero porphyrin, a *meso*-thia-porphyrin[57] (54) in which the ring current is interrupted by substitution at a *meso* carbon, is described in the literature. The resonances of (54) occur at considerably lower field than in linear tetrapyrroles[160], and the chemical shifts are indicative of a residual ring current, suggesting that the non-bonding sulfur electrons participate to a certain extent in the aromatic π-system. A porphyrin-like character for (54) is also consistent with the methine chemical shift pattern, which shows two resonances at lower field, and one originating in the C—H group opposite to the sulfur bridge at higher field. This pattern is characteristic of *meso*-substituted porphyrins (Section 10.2.3) and is opposite to that observed in biliverdins[160a]. The possibility of participation by the non-bonding electrons of heteroatoms is clearly demonstrated by an oxaporphyrin reported by Besecke and Fuhrhop[162], the cation of which shows a typical aromatic ^{1}Hmr spectrum.

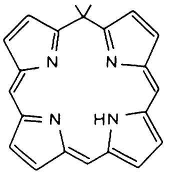

(48)

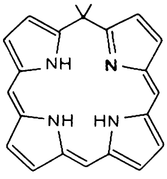

(49)

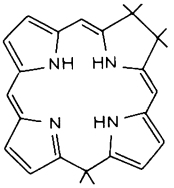

(50)

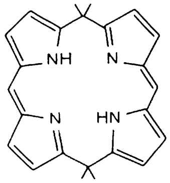

(51)

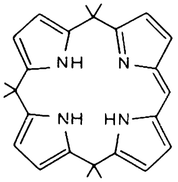

(52)

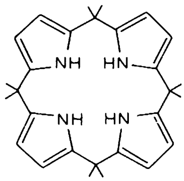

(53)

Isoporphyrins (48)[64,163], phlorins (49)[151] and chlorin-phlorins (50)[153] are isomers of the porphyrins, chlorins (30) and bacteriochlorins (31), respectively, in which the conjugation in the ring is interrupted by quaternization of one methine bridge. Very often the more stable cross conjugated oxo- or imino-derivatives are studied instead of the corresponding structure with a quaternized *meso*-carbon (Table 19). The loss of the aromatic ring current in Zn(iso-TPP) (55) is clearly indicated[64] by the high field shift of the β-pyrrole protons and the presence of only one high field multiplet for the aromatic phenyl protons, whose chemical shifts cover a considerable range in H_2(TPP)[8a,120]. Similar shifts are reported for an *iso*-OEP Pd com-

TABLE 19

^{1}Hmr chemical shifts (δ [p.p.m.] from TMS) of porphyrin derivatives with interrupted conjugation.

		Chemical shifts, δ		Solvent	Ref.
(54) a) R = H b) R = CH_3 c) Dication of a	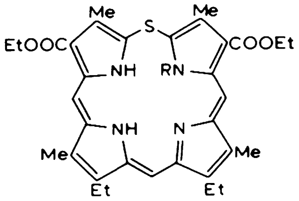 Me Me S EtOOC COOEt NH RN NH N Me Me Et Et	a) Methine—H:	7.57 (β, δ), 6.30 (γ)	a and b:	57
		N—H:	4.56	C^2HCl_3	
		b) Methine—H:	8.83, 7.84, 6.06	c: TFA	
		N—CH_3:	2.92		
		c) Methine—H:	8.30, 7.58 (γ, δ)		
			5.05 (2H, β)		
(55)	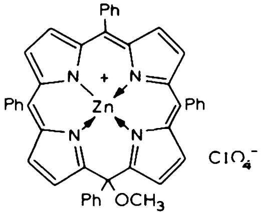 Ph N + N Ph Zn Ph N N ClO_4^- Ph OCH_3	Phenyl—H:	7.04 (m)	$C_6{}^2H_6$	64
		β-H:	6.25, 6.52/6.51, 6.57		
			2 × AB, J_1 = 4.70, J_2 = 4.85		
(56)	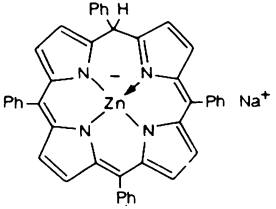 Ph H N - N Ph Zn Ph Na$^+$ N N Ph	$\beta_{pyrrole}$—H:	6.97—6.77	$C_6{}^2H_6$	165

(57)	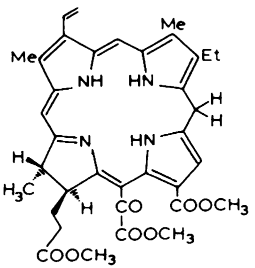	Methine-H:	6.73, 5.45	C^2HCl_3	166
		β-CH_2:	3.80		
		Vinyl ($H_{X,A,B}$):	6.70, 5.40, 5.35		
		OCH_3:	3.58(1X), 3.56 (2X)		
		CH_3 (ring):	2.17 (1X), 2.08 (2X)		
		8, 4′-CH_3:	1.28, 1.16		
		NH:	8.60 (1), 5.9 (2)		
(58)	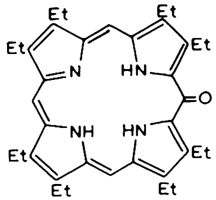	Methine—H:	7.85 (2), 6.98 (1)	C^2HCl_3	93
		CH_2:	3.31, 2.98		
		CH_3:	1.38		
(59)	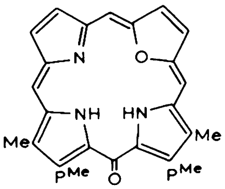	Methine—H:	7.3—8	C^2HCl_3 (aromatic in TFA)	106
		Ring—CH_3:	2.6		
		NH:	1.6		
(60)	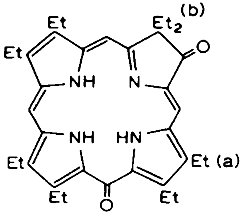	Methine—H:	7.87, 7.50 (β, δ), 6.65 (α)	C^2HCl_3 (aromatic in TFA)	105
		CH_2CH_3(a):	3.60—2,94, 1.54—1.14		
		CH_2CH_3(b):	2.07, 0.67		

TABLE 19 (Continued)

		Chemical shifts, δ		Solvent	Ref.
(61)	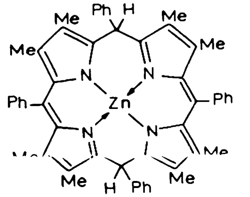	Methine—H: Phenyl: CH_3:	5.52 (*s*) 7.40, 7.21, 7.01 (*m*) 1.90, 1.77 (*s*)	C^2HCl_3	120
(62)	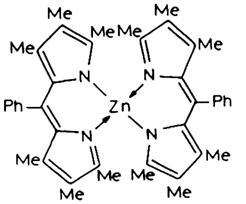	Methine—H: Phenyl: CH_3:	5.52 (*s*) 7.40, 7.21, 7.01 (*m*) 1.90, 1.77 (s)	C^2HCl_3	120
(63)	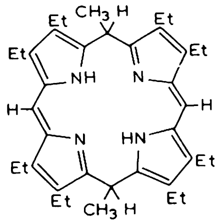	Methine—H: CH_3: CH_2CH_3 (a): CH_2CH_3 (b): NH:	6.58 (*β*, *δ*), 4.08 (*q*, *α*, *γ*) 1.69 (*d*) 2.51, 1.13 2.41, 1.10 12.58	$C_6{}^2H_6$	119
(64) a) $R^1=R^2=O$, $M=H_2$ b) $R^1=O$, $R^2=NH$, $M=Zn$	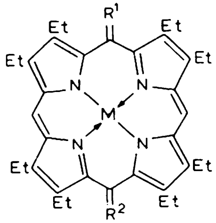	a) Methine—H: CH_2: CH_3: b) Methine—H: NH:	6.68 2.71, 2.50 1.14, 1.12 6.47, 6.81 9.73	C^2HCl_3 C^2HCl_3	174 175

(65) a) R=H_2 b) R=O	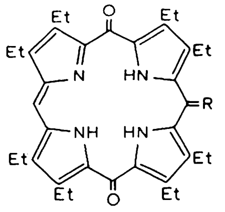 Et O Et Et Et N HN R NH HN Et Et Et O Et	a) Methine—H:	6.86	C^2HCl_3	167
		Methylene—H:	3.83		
		CH_2:	2.77, 2.59, 2.45		
		CH_3:	1.28, 1.09		
		N—H:	10.33		
		b) Methine—H:	6.96	C^2HCl_3	174
		CH_2CH_3:	2.4—3.0, 1.0—1.4		
		N—H:	10.33		
(66) a) R=H b) R=CH_3	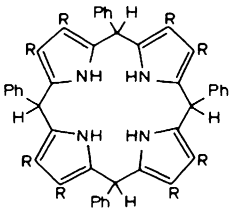 R Ph H R R R NH HN Ph Ph H H NH HN R R R Ph H R	a) Methine—H:	5.38 (*s*)	C^2HCl_3	120
		Phenyl:	7.24 (*m*)		
		β_{pyrrole}—H:	5.68, 5.78 (2 X d, $J = 6$)		
		N—H:	8.2 (*b*, *m*)		
		b) Methine—H:	5.34 (*s*)		
		Phenyl:	7.0 (*m*)		
		CH_3:	1.77 (*s*)		
		N—H:	6.41 (*b*, *s*)		
(67) a) R=O b) R=H_2	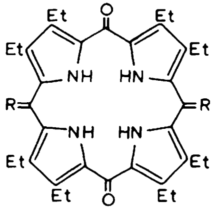 Et O Et Et Et NH HN R R NH HN Et Et Et O Et	a) CH_2:	2.98	$C_5{}^2H_5N$	167
		CH_3:	1.26		
		N—H:	11.9		
		b) Methylene—H:	3.83 (*s*)		
		CH_2CH_3	2.71, 2.42/1.17, 1.06		
		N—H:	8.72		
(70) a) R=R^1=Et,OH b) R=O,R^1=Et_2	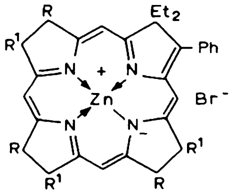 R Et_2 R^1 Ph N + N Zn Br^- N N R R^1 R^1 R	a) Methine—H:	5.97, 6.07, 6.12 6.18	C^2HCl_3	177
		b) Methine—H:	6.47, 6.63, 6.80, 7.14		

TABLE 19 (continued)

		Chemical shifts, δ		Solvent	Ref.
(71)	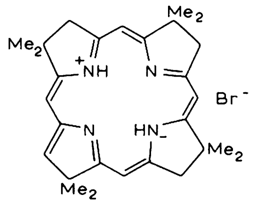 Me$_2$ Me$_2$ +NH N Br$^-$ N HN Me$_2$ Me$_2$	CH_3:	1.37, 1.47, 1.48, 1.50 (*s*, each 2 X CH_3)	C^2HCl_3	178
		CH_2:	3.06, 3.17, 3.27 (*s*, each 1 X CH_2)		
		CH:	5.86, 5.90, 6.10, 6.24, 6.29 (*s*, each 1H)		
		N—H:	10.1, br.		
(72)	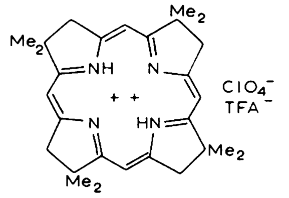 Me$_2$ Me$_2$ NH N + + ClO_4^- TFA$^-$ N HN Me$_2$ Me$_2$	CH_3:	1.34	TFA	178
		CH_2:	2.79		
		CH:	5.47		

plex[163]. Phlorins (49) were first characterized by Woodward[151]. They are in acid-base equilibrium with chlorins (30)[164] and are unstable against oxidants[111]. Only marginal ^{1}Hmr information is available on phlorins[165], but a series of 7,8-chlorin-β-phlorins ((50), see Table 19)[153,166] as well as a 7,8-chlorin-γ-phlorin have been studied in detail[166a]. Both phlorins and chlorin-phlorins show strongly deshielded N—H protons and shielded peripheral protons characteristic of a ring current that has all but vanished. The hydroxyporphyrin ⇌ oxophlorin tautomeric systems (21b ⇌ 22b) have been extensively studied[93,106,106a,108,109,167]. The equilibrium is shifted at higher pH towards the isomer (21b) with interrupted conjugation. The 'olefinic' ^{1}Hmr spectrum in neutral solution indicates an oxophlorin structure. Upon addition of acid, the ring current gradually increases as the monocation is formed and converted to the fully aromatic hydroxyporphyrin dication[69,106a] (see also Section 10.2.3). The n.m.r. spectra of the oxophlorins are generally difficult to observe[109–111,117], because oxophlorins are extremely easily oxidized and the ^{1}Hmr lines are broadened by spin exchange with the oxophlorin radical[111] present in small amounts[110]. Both the position and the pattern of the methine proton resonances again indicate that a residual ring current is present in these cross-conjugated systems.

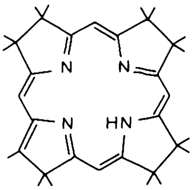

(68)

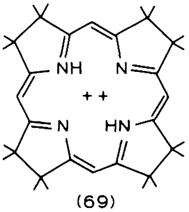

(69)

Porphodimethenes (51) are tautomers[168] of phlorins (49) in which the ring current is interrupted at two opposite methine bridges. This structure contains two isolated pyrromethene subunits, and in fact the ^{1}Hmr spectrum of the Zn complex (59) is very similar to that of the Zn-pyrromethene (60)[120]. Metal complexes of α,γ-dimethyl-octaethyl-β,δ-porphodimethenes (63) have been extensively investigated by Buchler et al.[169,170]. A structure[171] in which the macrocycle is folded like a roof and the *meso*-methyl and axial ligands occupy 'chimney' positions is deduced from steric and n.m.r. considerations[170]. Only one doublet and quadruplet, respectively, for the two methyl groups and the protons at the quaternized bridges are observed, and variations in the chemical shifts of these protons are related to the folding angle and long-range shielding effects of the axial ligands. The N—H signals in the free base occur at extremely low field (δ = 12.58 p.p.m.) indicating strong ring current shifts from the pyrromethene subunits and H-bonding. One of the isomers formed by photo-reduction of α,γ-dimethyl OMP-Zn was proved by ^{1}Hmr to be the corresponding β,δ-porphodimethene[172], and the structure of the Krasnovskii photoreduction product of chlorophyll-*a* (see Section 10.2.8.2) was also shown to be an α,γ-porphodimethene (reduced at the β,δ-positions)[173]. Dioxo- and iminooxo-porphodimethenes (64) were studied by Smith[174] and Fuhrhop[175], respectively. The chemical shifts reported for these compounds agree with those cited in the above examples. An interesting feature is the observation of two methine signals in the spectrum of the imino-oxophlorin (64b), indicating that the molecule has no σ_v plane because of the nonlinear C = NH substituent.

In the porphomethenes (52), the conjugation is interrupted at all but one bridge. ^{1}Hmr spectra of the dioxo- and trioxo-OE-porphomethenes (65) show signals for the peripheral protons that fall in the same range as those observed in oxo-porphodimethenes[167,174]. In contrast to the latter compounds reported only as metal complexes, the free bases were measured in the case of the porphomethene (65). The N—H resonances occur at very low field, and are about 2.6 p.p.m. more strongly deshielded than in pyrrole. The ^{1}Hmr spectrum of a true porphomethene has been reported by Shulga et al.[174a].

In the porphyrinogens (53) the ring current is interrupted at all four methine bridges, and as a result, the porphyrinogen spectra are very similar to those obtained from pyrroles. The most significant difference between the TPP-porphyrinogen (66a) and its octamethyl-derivative (66b), is the shift to higher field of the phenyl protons and the shift to lower field of the N—H proton upon methyl-substitution of the peripheral pyrrole positions[120]. As the N—H shift is especially dependent on molecular structure and intermolecular interactions, no structural conclusions or generalizations can be drawn from the few data available. However, the observation of two doublets (J = 6 Hz) for the β-pyrrole protons in (66a) clearly indicates a symmetry lower than C_4 for these porphyrinogens.

The main spectral feature of the oxoporphyrinogens (67) (xanthoporphyrinogens)[167,176] is the extreme low field shift of the N—H resonance, and to a lesser extent, of the —CH_2 quadruplets, a shift which increases with increasing oxo-substitution. The extreme nature of the shifts in the oxo-compounds has already been noted in the oxo-porphomethenes (65), and must somehow be related to the presence of *meso* carbonyl groups. While the shift of the resonances of the peripheral groups can be accounted for by the magnetic anisotropy of the C = O group, the N—H signals must be subject to additional shifts, presumably by (intermolecular) hydrogen-bonding.

In the corphins (68)[177,178] (see Chapter 18) the ring current is interrupted in an essentially different manner at one α-pyrrolic carbon atom and at one *N* atom. The former efficiently blocks the macrocyclic conjugation, and thus olefinic spectra are observed for (70) and (71). The considerable high-field shift for the methine protons ($\Delta \sim$ 0.5—1.0 p.p.m.) in the oxo-substituted corphin (70)[177] is probably due to the long range deshielding effect of the β-pyrrole carbonyl groups.

The ^{1}Hmr spectra of the corphin[178] and metallocorphin[177,178] mono-cations are characteristic of a highly asymmetric structure and indicate localized double bonds rather than rapid tautomerism. On the other hand, the di-cation (72) exhibits only one signal each for all of its methyl, methylene, and methine protons, indicative of protonation at carbon to form the symmetric structure (69). The tetraaza[16]annulene conjugated system which results is anti-aromatic, and the ^{1}Hmr spectrum shows the expected high-field shift of all peripheral signals (Δ_{CH_3} = +0.4—0.8 p.p.m., Δ_{CH_2} = 0.3—0.5 p.p.m., Δ_{CH_3} = +0.03—0.16 p.p.m.) as compared to the free base mono-cation[178].

10.2.7. Porphyrin acids

Because of aggregation and the frequent low solubility of porphyrins in organic solvents, trifluoroacetic acid is widely used as a solvent for ^{1}Hmr measurements. In this strongly acidic solvent system, the porphyrins are usually present as *N,N'*-diprotonated di-cations, the resonances of which are considerably changed with respect to the free base. The C—H resonances are shifted to lower field by 0.8—1.0 p.p.m. in the protonated species, the N—H resonances to higher field by 0.4—1.0 p.p.m. This effect was first discussed by Abraham[3], who proposed an enhanced ring current from the larger resonance energy (and therefore higher aromaticity) associated with the D_{4h} symmetry of the di-cation as compared with the D_{2h} symmetry of the free base. This argument is identical to that advanced to account for the high basicity of porphyrins[179]. While the increased ring current in the di-cation is the principal contributor to the methine proton chemical shifts, the effect on the N—H protons is partly compensated for by the deshielding resulting from the positive charges at the nitrogen atoms. Expansion of the π-system to the periphery of the macrocycle may play an additional role[180]. An alternative explanation for the protonation effect was put forward by Haddon et al.[41]. In this view, the positive charges at nitrogen lead to a general deshielding that is more than compensated for in the case of the N—H protons by the abolition of hydrogen-bonding[1] and the (anisotropic) nitrogen lone-pairs. The effect of hydrogen-bonding was recently distinguished from other contributions by Ogoshi et al.[180], who reported the ^{1}Hmr spectra of $H_4(OEP)^{2+}$ diacids in chloroform-$^2H_1$. The ^{1}Hmr spectra of the di-cations in a neutral solvent are distinctly different from those of the di-cation in TFA, and the spectra also show marked variations that depend on the gegenions present. This is especially true for the resonances of the N—H signals, and the close correlation of the N—H stretching vibration to the magnitude of the chemical shifts suggested hydrogen-bonding to the gegenion as the main factor in this effect[180].

Judged from the examples cited in Table 20, the effect of protonation is quite general for porphyrins, and the spectra in TFA provide a valuable basis for correlations. The effects are more complicated, however, in porphyrins

TABLE 20

^{1}Hmr chemical shifts (δ[p.p.m.] from TMS) of some porphyrins and their dications

	Methine	β-H		NH	Solvent	Ref.
$H_2(P)$	10.58	9.74		−3.76	C^2HCl_3	60
$H_4(P)^{2+}$	11.22	9.92		−4.40	TFA	8b
	β-H	o-H	m,p-H			
$H_2(TPP)$	8.75	8.3	7.80		C^2HCl_3	74
$H_4(TPP)^{2+}$	8.67	8.67	8.01		C^2HCl_3/TFA	69
	Methine	CH_2 (q, J = 7Hz)	CH_3 (t, J = 7Hz)			
$H_2(OEP)$	10.18	4.14	1.95	−3.74	C^2HCl_3	71
$H_4(OEP)^{2+}$	10.98	4.28	1.87	−4.65	TFA	113
$H_4(OEP)Cl_2$	10.49	4.04	2.04	−2.07	C^2HCl_3	180
$H_4(OEP)(ClO_4)_2$	10.58	4.10	1.80	−4.58	C^2HCl_3	180
$H_4(OEP)(BF_4)_2$	10.61	4.13	1.83	−4.92	C^2HCl_3	180
$H_2(OEC)$ [a]	9.68	3.88	1.80	−2.49	C^2HCl_3	144
$H_4(OEC)^{2+}$ [b]	8.84	2.22	1.06			
	9.95	3.78	1.60	−0.28	TFA	144
	8.80	2.33	1.17	−1.04		
$H_2(OEBC)$ [c]	8.49	3.42	1.53	—		
	7.47	3.30	1.50			
	6.86	1.91	1.05		C^2HCl_3	144
			1.01			
$H_4(OEBC)^{2+}$ [d]	8.98	3.41	1.44	—	TFA	144
	7.73		1.40			
	7.07 (d)	2.02	1.12			
		CH_3	$CH_2(P)$			
H_2(Copro-I-TME)	9.96	3.55	4.32	−3.89	C^2HCl_3	3
H_4(Copro-I-TME)$^{2+}$			3.20			
	11.11	3.83	4.67	−4.26	TFA	8b
			3.32			
		CH_2	CH_3	N—CH_3		
$H_2[(CH_3)_2OEP]$ [e]	9.80	3.8—4.2	1.94	−5.30	C^2HCl_3	169
			1.71			
$H_4[(CH_3)_2OEP]^{2+}$ [f]	11.40	4.37	1.97	−5.11	TFA	169
		4.56	2.20			

[a] *trans*-octaethylchlorin

[b] Dication of a

[c] Octaethyl-iso-bacteriochlorin (see structure (32)).

[d] Dication of c

[e] α, γ-dimethyl-octaethylporphyrin

[f] Dication of e

with reduced peripheral bonds or for those with *N*-substituents. The influence of protonation on the ^{1}Hmr of *N*-mono-, di- and tri-alkyl substituted porphyrins was studied by Jackson et al.[142]. Although the influence of *N*-substitution on the ring current is not very pronounced[140], the rigidity of the macrocyclic ring is changed, which in turn changes the ring behavior on protonation. The spectra of both mono- and di-cations can be interpreted on this basis. The ^{1}Hmr spectra of two peripheral reduced OEP derivatives, H_2(OEC) and a,b-H_2(OEBC)*, and their di-cations have been reported by Bonnet et al.[144] (Table 20). The methine protons remote from the reduced rings are again deshielded, but the other signals do not follow the usual precedents, and the *N*-protons for example are strongly deshielded in these instances.

The behavior of H_2(TPP) is unusual because the β-protons are shielded when the di-cation is formed[69], an effect which is probably to be attributed to conformational changes of the anisotropic *meso*-phenyl groups. H_2(TPP) shows an unusually slow exchange of the N—H protons in TFA, which has been explained[69] in terms of pronounced changes in the geometry of the macrocycle accompanying di-cation formation[181,182]. *X*-ray diffraction reveals the macrocycle in TPP free base to be fairly planar[183,184], while the di-cation shows extreme deviations from planarity[182]. It is these structural changes that probably account for the decrease in ring current implied by the low-field shift of the β-protons.

10.2.8. *Metal-porphyrin complexes*

The primary effect of metal complex formation in porphyrins is similar to that of di-cation formation in that the symmetry of the complex is enhanced and thus the strength of the ring current increased. However, metalation has an additional pronounced influence that depends on the ligand structure and type of axial ligation, the electronegativity of the metal, and the spin state of the central metal ion. The spin state of the metal is highly important, for the hyperfine shifts from interaction of protons with unpaired (electron) spins on the central metal may have consequences that outweigh any of the other contributions.

Metal complexes of porphyrins can occur in a variety of stoichiometric relations, and they can exist in a variety of structures. (For a characterization and classification of metal porphyrins, see Chapter 5 and Refs. 48, 169.) Factors important in determining the structure of metal porphyrins are: the stoichiometry, by which the common 1 : 1 metalloporphyrins are differentiated from bridged structures (μ-porphinato- or μ-metallo-complexes) or layered structures such as compounds (10) and (82); the size of the metal ion and the number of axial ligands, which largely determine whether the metal is in-plane or out-of-plane (Section 10.4.3); and the nature of the axial ligand(s), by which the ligand field is determined. N.m.r. has been widely used, sometimes as the decisive tool, to characterize metal complexes over the entire range of compounds that can be prepared. Here, only some characteristic features of the n.m.r. spectroscopy of these compounds will be described.

---

* See footnotes in Table 20 for nomenclature.

10.2.8.1. Diamagnetic 1 : 1 metal complexes

In these compounds, one metal ion is chelated by the four central *N*-atoms of the one porphyrin macrocycle. The basic questions that arise for this type of metal complex are the identity and the number of the axial ligand(s) and whether or not the metal is in the plane of the macrocycle. The answer to both questions is considerably assisted by n.m.r. The axial ligand occupies a region strongly shielded by the ring current, and thus the proton signals of the ligand occur at unusually high field*. A quantitative study of this effect based on ring current data and comparison with nonporphyrin complexes, can yield, among other information, the extent of the out-of-plane displacement of the metal[17]. The magnetic anisotropy of side-chain methylene protons in alkyl-substituted porphyrins and of the phenyl ring protons in H_2(TPP) can be used as additional criteria for the position of the metal ion (Sections 10.4.2.2 and 10.4.2.3). Such an anisotropy in magnetic environment is observed for several out-of-plane complexes and for asymmetric ligated structures[11,185], and has been studied in detail by Abraham et al.[186]. The arguments based on such magnetic anisotropy are valid even in cases where the ligand protons cannot be seen by n.m.r.

Complexes of octaethylporphyrin with various metals (1 : 1) are listed in Table 21. With a few exceptions, the chemical shifts of the resonances cover a narrow range that extends from $\delta = 10$ to 10.7 p.p.m. for the methine protons, $\delta = 4$—4.3 p.p.m. for the CH_2 quadruplet, and $\delta = 1.8$—2 p.p.m. for the CH_3 triplet. Although to our knowledge the ^{1}Hmr spectrum of low spin Fe^{II}(OEP) is not known, several compounds related to Fe^{II} protoporphyrin-IX have been investigated by Caughey et al.[199,200]. While the chemical shift data recorded in pyridine solution for the methine protons fall in the above range[200], the spectra obtained in pyridine/water mixtures show a strong high-field shift for all proton signals influenced by the ring current[199]. With only a few exceptions, the chemical shifts of the peripheral protons are determined by the oxidation state of the central metal, and there is a well-marked trend toward increased chemical shift with increased oxidation state of the metal. This conclusion is consistent with Caughey's[4] original statement that complexation decreases the porphyrin ring current, because, in his pioneer investigation of metalloporphyrins, only complexes of divalent Zn^{II}, Ni^{II} and Pd^{II} were investigated, and so the effect of oxidation state of the metal could not be detected. According to the oxidation state of the central

---

* Although many ligands bear protons, it is sometimes difficult to detect the ligand signals by ^{1}Hmr, which is especially true for water[11,185]. In one case[11], an $-OCOCF_3$ ligand has been detected by ^{19}Fmr.

TABLE 21

^{1}Hmr chemical shifts (δ[p.p.m.] from TMS) of 1:1 metal complexes of octaethylporphyrin H_2(OEP), (11)

Central Metal	Methine—H	CH_2	CH_3	Ligand(s) (δ_H)	Solvent	Reference
H_2	10.18	4.14	1.95	—	C^2HCl_3	187
Mg^{II}	10.06	4.08	1.91	$(quinoline)_2$ (5.1, 5.7, 6.5, 7.02, 7.45)	C^2HCl_3	185 [a]
Al^{III}	10.31	4.14	1.86	OPh (5.60)	C^2HCl_3	189
	10.38	4.13	1.94	OMe	C^2HCl_3	189
	10.2	4.09	1.91	OH (−1.82)	C^2HCl_3	189
Ga^{III}	10.13	4.05	1.87	OPh (5.61)	C^2HCl_3	189
In^{III}	10.30	4.14	1.95	OPh (2.59, 5.80)	C^2HCl_3	189
Tl^{III}	10.32	4.23, 4.17	1.95	OH, H_2O	C^2HCl_3	11
	10.30	~4.1	1.92	OAc (0.05), H_2O		
	10.34	~4.1	1.94	$OCOCF_3$		
	10.32	~4.1	1.91	I		
	10.24	~4.1	1.93	CN		
Sc^{III}	10.39	4.16	1.90	Acac (0.04)	C^2HCl_3	185
Si^{IV}	9.85	4.14	1.99	$(OMe)_2$ (−2.95)	C^2HCl_3	189
	10.07	4.12	1.90, 1.93	$(OPh)_2$ (1.33, 5.49)	C^2HCl_3	189
Ge^{IV}	10.36	4.17	1.98	$(OMe)_2$ (−3.01)	C^2HCl_3	189
	10.30	4.15	1.93	$(OPh)_2$ (1.35, 5.43)	C^2HCl_3	189
Sn^{II}	10.48	4.11, 4.13	1.87	—	$C_5{}^2H_5N$	175a, 190, 191
Sn^{IV}	10.32			$(OAc)_2$	C^2HCl_3	187
	10.40	4.20	2.01	$(OMe)_2$(−2.57)	C^2HCl_3	189
	10.32	4.15	1.93	(OPh_2) (1.45, 5.40)	C^2HCl_3	189
	10.66	4.30	2.10	Cl_2	C^2HCl_3	190,191
Pb^{II}	10.44	4.14, 4.16	1.90	—	$C_5{}^2H_5N$	190,191
Zn^{II}	10.05				C^2HCl_3	187
Cd^{II}	9.99	4.05	1.86		Dioxan	122
Ti^{IV}	10.48	4.18	1.99	=O	C^2HCl_3	192
Re^{V}	10.55	4.19	1.95	=O,OPh, (1.35, 5.26)	C^2HCl_3	189
Mo^{IV}	10.58	4.20	1.98	=O	C^2HCl_3	185
Co^{III}	10.00	4.09	1.83	Br, Py (6.3—5.7 (2), 4.9—4.6 (3))	C^2HCl_3	117
Co^{III}	10.08	4.00	1.88	CH_3 (−5.20)	C^2HCl_3	198 (199,200)
Ni^{II}	9.77	3.93	1.83	—	C^2HCl_3	122
Pd^{II}	10.08	4.03	1.90	—	C^2HCl_3	122
Ru^{II}	9.75	3.88	1.82	CO, Py (1.07, 4.76, 5.65, 2:2:1)	C^2HCl_3	193,194
Rh^{III}	10.31	4.15	1.99	Cl	C^2HCl_3	195
Rh^{III}	9.96	4.01	1.90	CH_3(−6.47, $J_{H\text{-}RH}$ =3 Hz)	C^2HCl_3	196
Os^{VI}	10.75	4.25	2.13	=O	C^2HCl_3	197

[a] See also Refs. 13, 16 and 188 and Section 10.2.8.2.

metal, the methine-resonances are observed in the following well-defined ranges: $\delta = 9.75$—10.08 p.p.m. for divalent metals, $\delta = 10.13$—10.39 p.p.m. for trivalent metals, $\delta = 10.30$—10.58 p.p.m. for tetravalent metals, $\delta = 10.55$ p.p.m. for pentavalent Re and $\delta = 10.75$ for hexavalent Os. Exceptions are observed for the complexes with the large, out-of-plane ions Sn^{II} and Pb^{II} [86,175a], which show the methine resonances at usually low field, and for Co^{III} [140] and Rh^{III} [89] complexes, which show resonances at unusually high field. The latter complex (Rh^{III}) shows a pronounced dependence of the chemical shifts on the axial ligand[89,241], which is probably related to the kind of axial bond involved: Cl (ionic) lies within the regular range[241], CH_3 (covalent) lies in the range of divalent metals[89]. In first order, this chemical shift dependence can be explained by the same electrostatic model invoked by Fuhrhop[200a] for the redox potentials of porphyrins. More highly charged central metal ions will reduce the electron density on the porphyrin ligand and thus deshield the peripheral protons*.

The metal complexes of (OEP) are characteristic for the metal complexes of the naturally-occurring β-pyrrole substituted porphyrins. The properties of metal complexes of *meso*-tetraphenylporphyrin including a Co^{I}(TPP)[202] are reported by several groups[11,63,201]. The publications on some metal complexes of octaethylchlorin[187,190] and of Sn^{IV} octaethyl—isobacteriochlorin[190] should be mentioned for leading references on reduced porphyrins. (For chlorophylls, see next section.) The metal complexes of two cyclic systems with interrupted conjugation have been investigated; these are the Tl^{III}-dioxoporphodimethenes[174] and extensive series of porphodimethene complexes[169].

10.2.8.2. The chlorophylls

Chlorophylls are magnesium complexes of the phorbin system, which are characterized by an isocyclic five-membered ring attached to the γ-carbon and carbon 6. The chlorophylls are derived from true porphyrins, chlorins, or bacteriochlorins. Because of the essential role chlorophylls play as the primary photo-acceptors in plant and bacterial photosynthesis, a great deal of work has focused on their molecular structure, their interactions in solution, and their structure-function relationships. N.m.r. work to 1966 has been reviewed[188], and some basic features of the n.m.r. spectroscopy of the phorbin system are discussed in Sections 10.2.3 and 10.2.5. Here, we wish first to review ^{1}Hmr spectral data of some recently characterized important chlorophyll structures. Spectral parameters of these newly characterized

---

* It should be noted that in the metalloporphyrins, electron withdrawal has the opposite (deshielding) effect as compared to the shielding upon withdrawal of electrons by peripheral substituents. This discrepancy might be explained by a contraction and expansion of the main loop, respectively, but it shows the ambiguities that can arise from the ring current approach (see Section 10.1.2).

TABLE 22

^{1}Hmr chemical shifts (δ [p.p.m.] from TMS) of the chlorophylls

	Chl-*a*[e] (15)	Chl-*b*[e]	Chl-*c*$_1$[d] (74)	Chl-*c*$_2$[d] (74)	Bchl-*a*[f,i]	Bchl-*b*[f] (75)	Bchl-*d*[g] (76a)	Bchl-*c*[g] (76b)	Bchl-*e*[h] (76c)
Methine α	9.23	9.87	9.95*	10.10*	9.40	9.41	9.67	9.78	9.41*
β	9.50	9.55	9.90*	10.00*	8.52	8.93	9.34	9.41	10.63*
δ	8.28	8.18	9.80*	9.92*	8.38	8.39	—	9.20	—
3-CHO	—	10.92	—	—	—	—	—	—	~11.1
2-Vinyl[a] H_X	7.92	7.85	8.28	8.33	—	—	—	—	—
H_A	5.97	5.98	6.34	6.35	—	—	—	—	—
H_B	6.13	6.15	6.04	6.06	—	—	—	—	—
4-Vinyl[a] H_X	—	—	—	8.33	—	—	—	—	—
H_A	—	—	—	6.32	—	—	—	—	—
H_B	—	—	—	6.04	—	—	—	—	—
7-Acrylic[b]									
7a	—	—	8.89	8.99	—	—	—	—	—
7b	—	—	6.61	6.67	—	—	—	—	—
10-$H_{(2)}$	6.22	6.10	6.72	6.84	6.44	6.43	4.92(*s*)	~5.18[h]	5.18(A,B)
3-H	—	—	—	—	4.10	4.93(*dd*)	—	—	—
4-H	—	—	—	—	3.86	—	—	—	—
7-H	4.14[j]	4.15[j]	—	—	4.10	4.10	n.r.	n.r.	n.r.
8-H	4.27[j]	4.45[j]	—	—	4.21	4.21	n.r.	n.r.	n.r.
2a-H	—	—	—	—	—	—	6.58	n.r.	6.54(*q*)
4a-H	—	—	—	—	—	6.84(*dd*)	—	—	—
1-CH_3	3.28	3.22	3.5—4[c],*	3.5—4[c],*	3.33*	3.34*	3.33*	3.34*	3.51
2a-CH_3	—	—	—	—	3.00*	2.99*	n.r.	n.r.	1.49(*d*)
3-CH_3	3.25	—	3.5—4[c],*	3.5—4[c],*	1.58(*d*)	1.66(*d*)	3.40*	3.50*	—
4a-CH_3	1.72(*d*)	n.r.	1.67	—	n.r.	2.01(*d*)	n.r.	n.r.	n.r.
5-CH_3	3.60	3.52	3.5—4[c],*	3.5—4[c],*	3.44*	3.45*	—	3.70*	—
8-CH_3	1.78(*d*)	n.r.	3.5—4[c],*	3.5—4[c],*	1.41(*d*)	1.41(*d*)	n.r.	n.r.	n.r.
10a-CH_3	3.97	3.95	3.5—4[c],*	3.5—4[c],*	3.66*	3.66*	—	—	3.60
δ-CH_3	—	—	—	—	—	—	3.75*	—	3.84
4-CH_2	3.75(*d*)	n.r.	4.26[c]	—	~2.5		n.r.	n.r.	n.r.

TABLE 22 (continued)

	Chl-*a* [e] (15)	Chl-*b* [e]	Chl-c_1 [d] (74)	Chl-c_2 [d] (74)	Bchl-*a* [f,i]	Bchl-*b* [f] (75)	Bchl-*d* [g] (76a)	Bchl-*c* [g] (76b)	Bchl-*e* [h] (76c)
5-CH_2	—		—	—	—	—	n.r.	n.r.	3.99(*q*)
7-CH_2	2.0—2.5	~2.35	n.r.	n.r.	~2.5	~2.4	n.r.	n.r.	n.r.
7a-CH_2	2.0—2.5	~2.35	n.r.	n.r.	~2.5	~2.4	n.r.	n.r.	n.r.

* Tentative assignment from intercomparison with other chlorophylls.

[a] ABX spectrum with $J_{AB} \sim 2$ Hz, $J_{AX} \sim 12$ Hz, $J_{BX} \sim 18$ Hz.

[b] AX spectrum with $J \sim 16$ Hz

[c] in TFA[139].

[d] in tetrahydrofuran-$^2H_8$.[139,203]

[e] in $C^2HCl_3/C^2H_3O^2H$ [13].

[f] in pyridine—$^2H_5$[80,155].

[g] Resonances of one of the pheophorbides of the homologues, in C^2HCl_3, Ref. 207.

[h] See Ref. 206.

[i] See Ref. 204 and footnote p. 466 for the esterifying alcohols in Bchl *a*.

[j] in pyridine.

All spectra are obtained in disaggregated (monomeric) solution.

chlorophylls are listed in Table 22 together with those of chlorophylls-*a* and -*b*, and bacteriochlorophyll-*a*, the principal natural chlorophylls. The chlorophylls show very pronounced solvent and concentration dependence, which result from chlorophyll self-aggregation (see Section 10.4.1.1) and chlorophyll—solvent interactions (Section 10.4.1.2). All chemical shift values referred to in this section were obtained on disaggregated monomeric chlorophyll solutions, and are thus typical of chlorophyll · L_1 and for chlorophyll · L_2 species[59].

10.2.8.2.1. Chlorophylls-c_1 and -c_2

The chlorophylls-*c* (74) are minor accessory pigments in diatoms and many marine micro-organisms and brown algae, and are closely related to the chlorophylls found in other photosynthetic organisms. Early ^{1}Hmr results were obtained on a mixture of the two pigments, which are difficult to separate by the usual sugar column chromatography, and the results were later confirmed on the fully separated compounds[139,203]. Both of these closely related pigments are *porphyrin* free acids, which lack an esterifying alcohol. The ^{1}Hmr spectra of the chlorophylls-*c* as compared to all other chlorophylls derived from chlorins and bacteriochlorins show a low field shift of the methine signals and the spectra are simple in the medium and high field region. The broad unresolved high-field resonance associated with the aliphatic protons of the long chain esterifying alcohol, as well as all signals typical of reduced pyrroline rings are missing from the c_1 and c_2 spectra. Apart from the CH_3 singlets, Chl-c_2 shows no resonances at high field below $\delta = 6$ p.p.m., and chlorophyll-c_1 shows only the ethyl proton resonances in this region. The low field region in both compounds is dominated by the complex patterns of the vinylic protons. Both compounds show an AX pattern[1] for one *trans*-acrylic side-chain proton, and ABX patterns[1] for one (Chl-c_1), or two vinyl groups (Chl-c_2). Although the vinyl signals of Chl-c_1 and -c_2 do overlap, a quantitative analysis of Chl-*c* mixtures is possible by ^{1}Hmr.

10.2.8.2.2. Bacteriochlorophyll-b

Bchl-*b* (75) is the pigment responsible for the extreme long wavelength absorption of *Rhodopseudomonas viridis* and some other photosynthetic bacteria[211]. Bchl-*b* has an ethylidene side-chain in position 4 in place of the ethyl side-chain present in Bchl-*a*[155]. Thus, the main difference in the ^{1}Hmr spectrum of *b* as compared to that of Bchl-*a* are the resonances of ring B protons. Both the 3- and the 4a-protons give rise to double doublets ($J_1 = 2$ Hz, $J_2 = 7$ Hz) at low field ($\delta = 4.93$ and 6.84 p.p.m.). By double resonance experiments these were proved to be coupled to each other ($J = 2$ Hz) and to a high field methyl group each ($J = 7$ Hz) at higher field and assigned to protons 3 and 4a, respectively. As a further consequence of the 4,4a double bond, the β-proton resonance is shifted to lower field, while all other resonances are essentially identical to those of Bchl-*a* (Table 21)*. Obviously, the small shielding effect expected to result from the introduction of the conjugated double bond is compensated for by (possibly steric) effects.

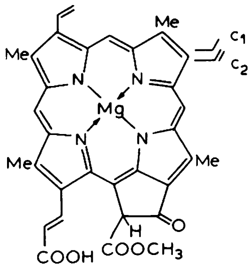
Me
Me
C1
C2
N
N
Mg
N
N
Me
Me
H
O
COOH
COOCH3

(74)

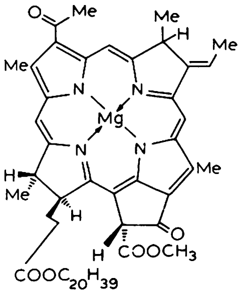
O
Me
Me
H
Me
Me
N
N
Mg
N
N
H
Me
Me
H
O
H
COOCH3
COOC20H39

(75)

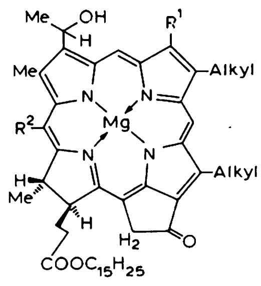
Me
OH
H
R1
Me
Alkyl
N
N
R2
Mg
N
N
Alkyl
H
Me
H
H2
O
COOC15H25

(76) ǃ

a; $R^1 = R^2 = Me$

b; $R^1 = Me, R^2 = H$

c; $R^1 = CHO, R^2 = Me$

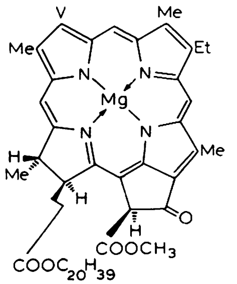
V
Me
Me
Et
N
N
Mg
N
N
H
Me
Me
H
O
H
COOCH3
COOC20H39

(77)

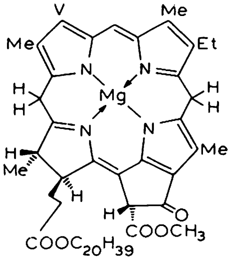
V
Me
Me
Et
H
H
N
N
H
H
Mg
N
N
H
Me
Me
H
H
O
COOCH3
COOC20H39

(78)

V = CH=CH$_2$

10.2.8.2.3. Bacteriochlorophyll-c, -d, and -e

The bacteriochlorophylls-*c*, -*d*, and -*e* present in the green photosynthetic bacteria (*Chlorobium* species) are unique among all natural chlorophylls in that they appear to be a mixture of various homologs[205]. All *Chorobium* chlorophylls have a 2(α-hydroxyethyl)-substituent characterized by a low-field quadruplet (2a-H) at 6.1—6.6 p.p.m. and a high field doublet. These chlorophylls lack a 10-COOCH$_3$ group, but the typical (Section 10.2.3) AB double doublet[206] expected for the 10-methylene protons is often only poorly resolved[207]. Finally, all *Chlorobium* chlorophylls have farnesol as the esterifying alcohol, which was characterized among other criteria by the olefinic CH_3 singlets at about 1.6 p.p.m. and the 1-methylene doublet at 3.96 p.p.m.[208].

---

* Bchl-*b* from *Rh. viridis* as well as Bchl-*a* from *Rhodopseudomonas* strains contain phytol as the esterifying alcohol. In contrast, Bchl-*a* from *Rhodospirillum rubrum* contains geranyl-geraniol instead[204]. The latter alcohol contains four double bonds. In the ^{1}Hmr spectrum, this is manifested by a general deshielding of all resonances from the esterifying alcohol (as compared to phytol), and additional olefinic resonances at δ = 4—5 p.p.m.

Bchl-*d* (*Chlorobium* chlorophyll '650')* is a mixture of homologues of structure (76b). The ^{1}Hmr spectrum of one of the pheophorbides (Table 22) is reported by Mathewson et al.[207]. The spectrum shows only three low-field methyl singlets, the signal position indicating homologation at position C-5. The methine protons show a very unusual pattern as compared to 2-desvinyl-2-hydroxyethyl-pyromethylpheophorbide-*a*[135]. The α-proton is deshielded by 0.23 p.p.m., the β-proton by 0.18 p.p.m., and the γ-proton by 0.78 p.p.m. These differences are unexpected. They may be due, however, to the unusual aggregation behavior of 2-(α-hydroxyethyl)-pheophorbides[213].

Bacteriochlorophyll-*c* (*Chlorobium* chlorophyll '660' (76a)) is considered to have an alkyl substituent at one of the methine bridges, as deduced from the presence of only two methine signals in the pheophorbides. The position of this alkyl substituent was discussed[207,209,210] mainly on the basis of n.m.r. arguments. While the loss of the high-field methine-signal suggested a δ-substituent[210], the presence of one acid-exchangeable methine proton indicated the δ-proton was still present and indicated substitution in the α or β position[207,209]. (For unsuccessful attempts to correlate the structure of porphyrins derived from Bchl-*c* with synthetic δ- and β-alkylporphyrins, see Ref. 118.) Substitution of the δ position was shown recently to be the correct assignment, a conclusion supported by n.m.r. studies (aggregation, substituent induced shifts) of model compounds[206,212,213].

Very recently, still another series of at least three *Chlorobium* chlorophylls, designated Bchl-*e* (76c) was investigated and described by Brockmann[206]. This family of chlorophylls has the same relationship to Bchl-*c* as does Chl-*b* to Chl-*a*. The spectra have features similar to those of Bchl-*c*, but the presence of a CHO group is proven by the appropriate CHO resonance in both the ^{1}Hmr and ^{13}Cmr spectra.

10.2.8.2.4. Chlorophyll related structures

A variety of structures related to the chlorophylls have been characterized by ^{1}Hmr. In the chlorphyllides, the propionic ester side-chain is transesterified, usually with methanol or ethanol. Besides the loss of all signals related to the long chain alcohols in chlorophylls and the appearance of the signals related to the introduced alcohol, the ^{1}Hmr spectrum remains unchanged upon transesterification. The spectral changes observed upon substitution at C-10[129,212], removal of the 10-$COOCH_3$ group[214], the reduction of the 9-CO to a CH_2 group[80], cleavage of ring E[212], or the hydrogenation of the

---

* The number indicates the wavelength (nm) of the absorption band in the red, measured in ether solution.

2-vinyl group[80] are similar to those observed in the (metal free) pheophorbides (Section 10.2.3).

The structure of two long known chlorophyll derivatives has been proven recently by ^{1}Hmr; Chl-*a*′ (and other 'prime' chlorophylls) were identified as C-10 epimers[215], and the product of the Krasnovskii photoreduction was shown to be β,δ-dihydro Chl-*a*[173]. Chlorophyll-*a*′ (Chl-*a*′, (77)) is the 10-epimer of Chl-*a*[215] which is present as an artifact in equilibrium amounts of about 15% in chlorophyll preparations[216]. Its presence is manifested in the ^{1}Hmr spectrum by small satellite peaks or shoulders at the high field side of the methine-H, and by a distinct satellite peak accompanying the 10-H resonances at about 0.12 p.p.m. towards higher field. Similar satellites are observed for Chl-*b* and Bchl-*a*, as well as for their pheophytins and some related structures. They are absent, however, in compounds without an asymmetric C-10. The 10-epimeric structure of Chl-*a*′ was proved[215] by comparison of the distinctly different chemical shifts of the C-10 protons in Chl-*a* and -*a*′ with the ones in pyropheophorbides[79], and by equilibration and aggregation experiments of the epimers. These experiments were substantially facilitated by carrying out the experiments with ^{2}H-chlorphyll-[10-^{1}H], in which the 10-H resonances can be studied without interference from other signals.

The Krasnovskii photoreduction was the first[217] and probably most widely studied photoreaction of the chlorophylls, and porphyrins in general[126,218]. The structure of the Krasnovskii reaction product of Chl-*a* was recently shown to be β,δ-dihydro Chl-*a* (78) by carrying out the reaction in dilute chlorophyll solution with hydrogen sulfide as reductant directly in a sealed n.m.r. tube[173]. The ^{1}Hmr spectrum of the porphodimethene that is formed shows the typical high field shifts observed for systems with interrupted ring current (see Section 10.2.6). The *meso*-methine and methylene signals and the protons at the reduced *meso* positions were assigned by using ^2H_2S as the reducing agent, and correlating signals in the reduction product with the signals in the regenerated Chl-*a* from the isotope content and position.

10.2.8.3. *Unusual metalloporphyrins with central metal*

Several porphyrin—metal complexes with a stoichiometry deviating from 1 : 1 have been characterized by n.m.r. recently (Table 23). The most useful aids in rationalizing the ^{1}Hmr spectra of these substances were again symmetry and ring current arguments. The appearance of four methine proton resonances testifies to the coordination of two neighboring *N*-atoms to the two metal atoms in the non-axial dirhodium complex (80), otherwise a spectrum consistent with higher symmetry would be observed[196]. The mirror plane in the Re complex (81) is established by the pattern of the β-proton signals, the inner hydrogen by a resonance at the very high field of —4.0 p.p.m. and by its spin coupling with the β-protons in the same ring[63]. Two

TABLE 23

^{1}Hmr chemical shifts (δ[p.p.m.] from TMS) of metalloporphyrins with stoichiometries other than 1:1.

				Solvent	Ref.
(80) (OEP)	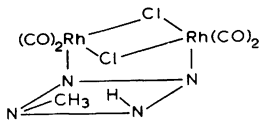	Methine—H:	10.35, 10.50, 10.55, 10.58	C^2HCl_3	196
		Ethyl—CH_3:	1.72, 1.77, 1.80, 1.84, 1.87, 1.89, 1.96, 1.98		
		N—H:	—3.74		
		N—CH_3:	—5.90		
(81) (TPP)	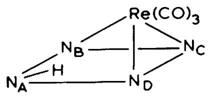	β-pyrrole protons:		C^2HCl_3	63
		Ring A:	8.88 (*d*, J_{H-NH} = 2Hz)		
		Ring B, D:	9.11 (AB, *J* = 5Hz, Δ = 0.12 p.p.m.)		
		Ring C:	8.72 (*s*)		
		Phenyl—H:	7.87 (*m*, *p*); 8.30 (o)		
		N—H:	—4.0		
(82) (Etio I – IV; Copro I – IV TME)	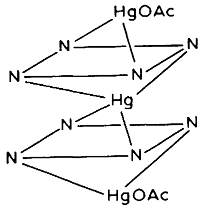	Etio-I:			
		meso-H:	8.97 (J_{H-Hg} = 10Hz)	C^2HCl_3	219
		ring—CH_3:	3.48; 3.45 (*s*)		
		OAc:	—0.24 (*s*)		
		^{199}Hg (Indor):	17.8866 17.8854 (2 : 1)		223
(83) (OEP)	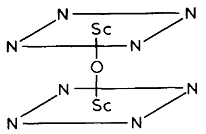	Methine—H:	9.55 (*s*)		220
		CH_2:	1.65 (*t*), 1.89 (*t*)		
		CH_3:	3.94, 3.98		

TABLE 23 (continued)

				Solvent	Ref.
(84) (OEP)	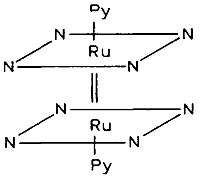	Methine—H: CH_2CH_3: Pyridine—H: (geometry not discussed)	7.61 (*s*) 5.92, 1.45 (*t*) 2.6, 5.3 (2 : 2)		193
(85) (OEP)	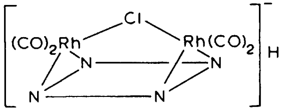	Methine—H: CH_2: CH_3:	10.04, 10.35 4.00, 4.10 1.89, 1.67	C^2HCl_3	195
(86) (OEP)	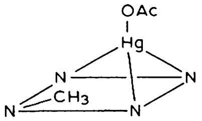	Methine—H: CH_2: CH_3: $N—CH_3$: OAc:	10.03, 10.00 3.95 (*m*) 1.95 (*m*), 1.72 (*t*) —5.0 ($J_{^1H—^{199}Hg}$ = 10 Hz) 0.1	C^2HCl_3	223

isomers (meso, racemic) account for the splitting of the ring-methyl group resonances in the stacked Hg_3P_2 complex (82); the high field acetate resonance is characteristic of inner protons, and the two ^{199}Hg indor* lines indicate the presence of one and two equivalent Hg atoms, respectively[219,223] (see Section 10.4.3).

A characteristic feature of the sandwich structures is the pronounced shielding effect of one ring on the other. This shielding increases the closer the rings are to each other. The incremental shift for the methine protons is about +0.8 p.p.m. in the μ-oxo Sc complex (83)[220], [as compared to Sc(OEP)[185]], 1.3 p.p.m. in the layered Hg complex (82)[219], and 2.1 p.p.m. [as compared to Ru^{II}(OEP)[193]] in the dimeric ruthenium complex (84)[193]. The latter value serves as an additional argument for the proposed direct metal—metal bond. Like the stacked phthalocyanines[18], complexes with stacked porphyrins may serve as a useful probe for the ring current effect in the spatial region above the conjugated system, which is otherwise only accessible with axial ligands, porphyrin cyclophanes[221], or structures like the fused cyclopropano-chlorins (46) and (47).

10.2.8.4. Peripheral complexes

While in all metalloporphyrins so far discussed the metal is bound to the inner nitrogen atom, two new types of metal complexes have been recently characterized in which the metal is bound to peripheral substituents of the macrocyclic system. Logan et al.[222] investigated π complexes of $Cr(CO)_3$ with one or more of the phenyl rings in H_2(TPP). Hyperfine interactions are essentially confined to the ring(s) to which the chromium is bound, with the chemical shifts in the latter comparable in magnitude to those observed in the chromium carbonyl—benzene complex.

A second group of complexes related to the chlorophylls, but with the metal bound at the periphery, was recently investigated by Scheer et al.[80]. In these compounds, the metal ion is chelated by the β-keto-ester function present in ring E. The ^{1}Hmr spectrum of the peripheral Mg complex of methylpheophorbide-*a* indicates a uniformly reduced aromatic ring current, presumably arising from the electron-withdrawing effect of the chelate. Most signals are shifted to higher fields, with $\Delta\delta$ values similar for protons in similar environment. However, the 8-CH_3 doublet, the 7-H multiplet, as well as the 10b-CH_3 singlet, are deshielded.

These deshielding effects in the vicinity of the isocyclic ring E can be rationalized in terms of conformational changes. In the chelate, the β-keto-ester system is essentially coplanar with the macrocycle. This brings the 10b-CH_3 protons into a more deshielding region of the ring current field

---

* In the indor double resonance technique, n.m.r. transitions of a heteronucleus are scanned with a strong RF field, while one line of a coupled (usually proton) multiplet is monitored[1].

TABLE 24

^{1}Hmr chemical shifts (δ [p.p.m.] from TMS) of methyl pheophorbide-*a* (87) and its peripheral Mg complex (88), and incremental shifts ($\Delta\delta$ [p.p.m.]) of (88) vs. (87).

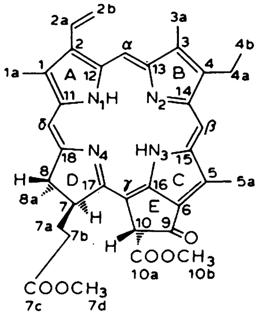
2a
2b
3a
4b
1a
1
2
α
3
4
4a
A
12
13
B
11
N1H
N2
14
δ
β
18
N4
HN3
15
H
8
D
17
γ
16
C
5
5a
8a
7
E
H
10
9
6
7a
7b
H
O
COOCH3
10a
10b
COOCH3
7c
7d

(87)

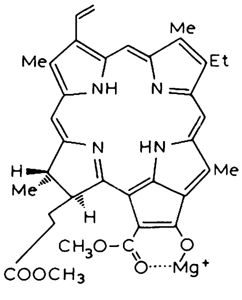
Me
Me
Et
NH
N
N
HN
H
Me
Me
H
CH3O-C
O
COOCH3
O····Mg+

(88)

	Methyl pheophorbide (87)	Peripheral Mg Complex (88)	$\Delta\delta$	Multiplicity
β-H	9.75	9.01	+0.74	*s*
α-H	9.57	8.83	+0.74	*s*
δ-H	8.71	8.00	+0.71	*s*
H_X	8.08	7.77	+0.31	*dd*, J=11,17
Vin H_A	6.23	6.06	+0.17	*dd*, J=2,17
H_B	6.05	5.87	+0.18	*dd*, J=2,11
10-H	6.61	—	—	
7-H	4.29	4.65	—0.36	*m*
8-H	4.42	4.10	+0.32	"*q*"
10b-CH_3	3.76	3.83	—0.07	*s*
7d-CH_3	3.52	3.38	+0.14	*s*
5a-CH_3	3.42	3.11	+0.31	*s*
1a-CH_3	3.21	2.95	+0.26	*s*
3a-CH_3	3.08	2.83	+0.25	*s*
8-CH_3	1.66	1.73	—0.07	*d*, J=7
4-CH_2	3.54	3.29	+0.25	*q*, J=7
4-CH_3	1.53	1.39	+0.14	*t*, J=7
N—H	+0.74	2.44	—1.70	*s*, broad
	—1.48	2.04	—3.52	*s*, broad

2×10^{-3} M in pyridine-$^2H_5$, and pyridine-$^2H_5$ saturated with anhydrous $Mg(ClO_4)_2$; 30°C; Ref. 80a.

(Fig. 1), and the signal at δ = 3.83 p.p.m. is therefore assigned to this group. In addition, the increased steric hindrance of the 10-substituent with the substituents at C-7 induces a conformational change in ring D by which both the 7-H and the 8-CH_3 group are forced into a more deshielding region. This effect is well established in δ-substituted chlorins[124], where incremental shifts of the same magnitude are observed.

Peripheral metal chlorin complexes are unstable to water and competitive Mg^{2+} chelating agents such as acetylacetone or 2-carbethoxy-cyclopentanone. As metal ion exchange in these complexes is slow on the n.m.r. time scale, two distinct sets of resonances are observed during titrations, one set of which corresponds to the free methyl-pheophorbide and the other to its peripheral complex. If part of the complex is destroyed by addition of water, temperature-dependent equilibrium for the reaction of water with the peripheral complex can be determined by n.m.r. Complex formation is favored by higher temperatures. For a 27-(39)fold molar excess of water, the net reaction enthalpy is 5 (9.1) kcal/mole, and equal amounts of free methyl pheophorbide and its Mg^{2+} complex are present at 30° C (90° C), respectively.

10.2.8.5. Paramagnetic metal complexes

The salient features of ^{1}Hmr spectra of compounds with unpaired spins are determined by hyperfine electron-nuclear interactions and by relaxation processes[224]. Although broad n.m.r. lines are observed in many cases, many paramagnetic metalloporphyrins have electron spin relaxation times fast enough to result in sufficiently sharp lines under high resolution conditions[22]. In complexes of porphyrins with paramagnetic metal ions, the large chemical shifts generated by the macrocyclic ring current are often small in comparison to the hyperfine shifts resulting from interactions with the unpaired spins, and in these cases the ^{1}Hmr spectrum can extend over more than 50 p.p.m. The hyperfine shifts in paramagnetic metalloporphyrins leads to a considerably enhanced resolution of signals in very similar chemical environment (as compared to the diamagnetic porphyrins). This fact renders the spectra extremely sensitive to structural and electronic changes, and Fe porphyrins are now widely used as a sensitive n.m.r. probe in hemoproteins. (For an application in the analysis of porphyrin isomers, see Ref. 225.)

The hyperfine interactions can be split into two major components. The first is the contact shift, which results from the leakage of unpaired spin to the nucleus under observation by n.m.r., and the second is the pseudocontact shift, which results from dipole—dipole couplings in molecules with anisotropic g-tensors and/or zero field splitting (ZFS)*. (For a detailed discussion and leading references, see Refs. 224 and 226.)

Pseudocontact interactions occur through space, while contact interactions occur through chemical bonds. The contact term thus allows a detailed

---

* The g-tensor characterizes the spatial distribution of the electron g-factor, and the ZFS parameters D and E characterize the coupling of unpaired electrons in systems with more than one free electron or hole[38,224].

TABLE 25

Incremental hyperfine shifts (Δ [p.p.m.] relative to the respective diamagnetic reference compound) of paramagnetic Fe-porphyrins and of their μ-oxo dimers.

Complex (Reference compound)	Axial Ligand (s)	Hyperfine Shifts (Pseudocontact contribution)		Conditions	Ref.
Low Spin Fe^{III}					
Fe^{III} (P)	$(CN)_2$	Methine—H:	+9	Pyridine—$^2H_5$/^2H_2O,	22
[Zn(P)]		β-H:	+24	46°C	
Fe^{III} (TPP)	im_2 [a]	β-H:	+25.3 (+5.8)	C^2HCl_3, 29°C	27
[Ni(TPP)]		*o*-H:	+3.09 (+3.09)		
		m-H:	+1.49 (+1.44)		
		p-H:	+1.37 (+1.27)		
Fe^{III}(T-*n*-PrP) [b]	im_2 [a]	β-H:	+21.0 (+5.8)	C^2HCl_3, 29°C	27
[Ni(T-*n*-PrP)]		*meso*-CH_2:	−0.6 (+4.5)		
		CH_2:	+0.5		
		CH_3	+1.3		
Fe^{III}(OEP)	im_2 [a]	Methine—H:	+7.0 (+9.3)	$C^2H_2Cl_2$	27
[Ni(OEP)]		CH_3:	−1.97 (+3.2)		
		CH_3:	+1.60		
High Spin Fe^{III}					
Fe^{III}(TPP)	Cl	β-H:	−70.2 (−9.6)	C^2HCl_3, 29°C	
[Ni(TPP)]		*o*-H:	+1.7 (−6.3, −3.2)		
		m-H:	−4.50, −5.62 (−2.6, −2.0)		
		p-H:	+1.45 (−2.1)		
Fe^{III} (T-*n*-PrP) [b]	Cl	β-H:	−76.8 (−9.6)	C^2HCl_3, 29°C	29
[Ni(T-*n*-PrP]		*meso*-CH_2:	−57.2		
		CH_2:	0		
		CH_3:	−1.3		
Fe^{III}(OEP)	Cl	Methine—H:	+65	C^2HCl_3, 29°C	29
[Ni(OEP)		CH_2:	−35.4, −39.0		
		CH_3:	−4.7		

Fe^{III} Dimers					
[Fe^{III}(TPP)]$_2$O	—O—	*β*-H:	−5.02	C^2HCl_3, 29°C	29
{[Sc(TPP)]$_2$O}		*o,m,p*-H:	~+0.05		
[Fe^{III}(T-*n*-PrP)]$_2$O	—O—	*β*-H:	−6.3	C^2HCl_3, 29°C	29
{[Sc(TPP)]$_2$O and		*meso*-CH_2:	~−1.3		
T-*n*-PrP[b]}		CH_2:	~+0.5		
		CH_3:	~0		
[Fe^{III}(OEP)]$_2$O	—O—	Methine-H:	~+3.9	C^2HCl_3, 29°C	29
{[Sc(OEP)]$_2$O}		CH_2:	−2.26, −1.30		
		CH_3:	−0.19		
Co^{II} (Low Spin)					
Co(TPP)	Solvent	*β*-H:	−7.0 (−9.4)	C^2HCl_3, 35°C	28
[Ni(TPP)]		*o*-H:	−5.0 (−5.0)		
		m-H:	−2.15 (−2.3)		
		p-H	−2.03 (−2.03)		
Co(OEP)	Solvent	Methine—H:	−19.0 (−15.0)	C^2HCl_3, 35°C	28
[Ni(OEP)]		CH_2:	−3.55 (−5.2)		
		CH_3:	−4.05		

---

[a] im = imidazole

[b] T-*n*-PrP = *meso*-tetra-*n*-propyl-porphyrinate

insight into the electronic structure of the molecule, especially the spin density distributions and the spin transfer mechanism, while the pseudocontact term can give valuable information on the magnetic anisotropy and the zero field splitting parameters. The magnitude of the pseudo-contact shift induced by paramagnetic shift reagents in favorable circumstances yield information on the solution structure and conformation of a molecule. Next to the assignment of the resonances, the separation of these contributions to the spectrum is therefore of considerable interest in most investigations.

Since the first detection of sharp hyperfine-shifted lines in the ^{1}Hmr spectrum of cytochrome-c[20], a great deal of ^{1}Hmr work has been done on heme-proteins and related structures primarily directed to the structures in solution and structure-function relationships. The reader is referred to two excellent reviews[21,22] for a description of these studies. A recent series of publications by Perutz et al.[227–229] shows the potentialities and limitations of the n.m.r. method in hemoprotein studies when used in conjunction with other methods. Here we propose to focus on some of the basic investigations which have been carried out on iron porphyrins, and on some porphyrin complexes containing other paramagnetic metals.

10.2.8.5.1. Fe-complexes

Several types of iron complexes are observed in porphyrins, depending on oxidation state and ligand field: (a) low-spin complexes in which the ligand field splits the energy levels of the d-orbitals sufficiently far apart that a maximal number of the d-electrons are paired, resulting in a net spin of $S = 0$ for $\mathrm{Fe^{II}}$ and $S = 1/2$ for $\mathrm{Fe^{III}}$; (b) high-spin complexes with a net spin of $S = 4/2$ for $\mathrm{Fe^{II}}$ and $S = 5/2$ for $\mathrm{Fe^{III}}$; (c) $\mathrm{Fe^{IV}}$ complexes with $S = 2$; and (d) $\mathrm{Fe^{I}}$ complexes*. Complexes containing low-spin $\mathrm{Fe^{II}}$ are diamagnetic (see Section 10.2.8.1), all the others are paramagnetic. In addition to these 1 : 1 complexes, some μ-oxo $\mathrm{Fe^{III}}$ dimers are known to show antiferromagnetic coupling ($S_0 = 0$) of the two $\mathrm{Fe^{III}}$ atoms.

(a) *Low-spin* $\mathrm{Fe^{III}}$: The ^{1}Hmr spectrum of low-spin $\mathrm{Fe^{III}}$ protoporphyrin-IX dimethyl ester dicyanide [$\mathrm{Fe^{III}(Proto\text{-}IX\text{-}DME)(CN)_2}$] was first investigated by Wüthrich et al.[22,230] together with some related low spin $\mathrm{Fe^{III}}$ porphyrins. Groups of resonances were originally assigned by intercomparison and by the relative intensities of the resonances, but the assignment of all four β-pyrrole CH_3 signals and some methine proton resonances was recently achieved by total synthesis of selectively deuterated compounds[231,232]. From the chemical shift of the ester protons, which experience only pseudo-contact contributions, small pseudo-contact contributions to the shifts of the hyperfine-shifted protons were originally estimat-

---

* An intermediate spin state ($S = 3/2$) was recently reported for a $\mathrm{Fe^{III}}$ porphyrin[229a].

TABLE 26

^{1}Hmr chemical shifts (δ [p.p.m.] from TMS) of miscellaneous paramagnetic metalloporphyrins

Complex	Chemical Shift (δ [p.p.m.])		Conditions, Remarks	Ref.
$Fe^{IV}(TPP)Cl^+$	β-H:	+68.6	$C^2H_2Cl_2$, 90% Fe^{IV}	246
	Phenyl-H:	+12.3, +5.8		
$[Fe(TPP]_2O^+ClO_4^-$	β-H:	12.2	C^2HCl_3, 40 C	246
	o,p-H:	11.4		
	m-H:	3.4		
meso-tetra-CH_2NO_2-Fe^{III}-$(OEP)^+Cl^-$	*meso*-CH_2:	−1.4(br), +0.2, +1.3, +3.2(br)	C^2HCl_3	245
	CH_2Me:	−40.1, −37.5, −35.2, −33.2		
$Cr^{III}(TPP)^+X^-$ $X=Cl^-, I^-, N_3^-$	Broad peak at δ = −7.5—8 p.p.m.		C^2HCl_3, 35°C	26
$Cr^{III}(TPP)^+ Cl^-$	Aromatic—H:	~—7.5 (br)	C^2HCl_3, 35°C	26
	CH_3:	−2.35(br)		
Mn^{III} (Etio-I)$^+$ Cl^-	CH_3:	−35.3	C^2HCl_3, 35°C	24
	CH_2CH_3:	−22.6, −2.6		
	Methine—H:	+10.5		
Eu^{III}(*p*-CH_3 · TPP)[a]	*o*-H:	−13.31, −8.13	C^2HCl_3, −21°C	259
	m-H:	−9.33, −8.13		
	p-CH_3:	−3.44		
	Acac[a]:	0.88		

[a] Acetylacetonate (Acac) as fifth and sixth ligand.

ed[22,230,233]. Assuming that the hyperfine shifts arise from contact interactions, a high spin density at the β-positions and a much smaller one (perhaps one-third as large) for the *meso* protons were inferred. A spin transfer mechanism mediated predominantly by the π-system was inferred by Shulman et al.[25], Kurland et al.[23], and Hill et al.[234]. The latter investigators correlated increasing hyperfine shifts in dipyridinates of Fe^{III}(Proto-IX-DME) with decreasing basicity of the (suitably substituted) pyridine ligand in the 5th and 6th axial coordination positions. As the electron density at the coordinated Fe^{III} decreases with decreased basicity of the ligand, it was concluded that a spin transfer by charge transfer from the ligand to the metal occurs.

La Mar et al.[27] have investigated the Fe^{III} low-spin complexes of the three key porphyrins H_2(TPP), H_2(OEP), and *meso*-tetra *n*-propylporphyrin. All of these compounds are highly symmetric and this enhances the sensitivity of the ^{1}Hmr data acquisition and facilitates assignments. In addition, this series of compounds makes it possible to compare hyperfine shifts for protons and the —CH_2-methylene group in both the *meso*- and the β-position. Under the assumption that the porphyrin frontier orbitals are identical in all three compounds, the following conclusions are arrived at for the complexes of low spin Fe^{III}: As suggested by other spin-transfer studies[23,25,230,234], the spin-in these compounds is transferred to the π-system of the ligand by charge transfer to the metal, and the spin resides primarily in the highest occupied molecular orbital that has high-spin density at the β-positions and low-spin density at the *meso*-positions. Because the spin transfer from the *meso*-positions to the phenyl ring is hindered, the phenyl protons are expected to experience only pseudo-contact shifts, and therefore their chemical shifts were used to separate the pseudo- from the true contact contribution. In contrast to earlier results[22,230–233,234], both contributions to the chemical shifts are found to be of the same order of magnitude. The dipolar shift is positive throughout, the contact shift can be either positive or negative. Both show Curie ($1/T$) behavior, and deviations observed in OEP were explained by hindered rotation of the ethyl substituents. At ambient temperatures, the effective[25] g-tensor is axial, with the axis perpendicular to the macrocycle plane, a conclusion that follows because only one set of signals for each set of equivalent substituents is observed. In spite of their $1/T$ behavior, the hyperfine shifts usually do not extrapolate to zero at $T = \infty$[22,27,235–237], which is discussed in terms of second order Zeemann effects and mixing in of excited states into the ground state. Both contributions in low-spin Fe^{III} complexes have recently been critically investigated by Horrocks[237].

(b) *High-spin* Fe^{III}: The lines in high-spin Fe^{III} complexes are spread over more than 80 p.p.m. and are generally[26] considerably broadened. The first n.m.r. spectrum of a Fe^{III} (high spin) porphyrin complex, Fe^{III} (TPP)Cl, was published by Eaton et al.[238], and a series of high-spin hemins was studied by Kurland et al.[23]. Broadened lines were observed, and some signals were assigned by their relative intensity and by intercomparison with each other. The assignment of particular resonances in high-spin Fe^{III} porphyrins relative to that of the respective low-spin complexes was investigated by Gupta and Redfield[239,240] by an elegant cross-relaxation double resonance method.

The ligand effect on the hyperfine shift in deuterohemins was studied by Caughey et al.[241], who found a correspondence of the magnitude of the hyperfine shifts to the D value of the zero field splitting parameters, suggesting a pseudo-contact contribution to the observed shifts[226]. In contrast to the low-spin complexes, a significant σ-spin transfer is generally[238] observed in high-spin Fe^{III} complexes[23,29,241,242]. La Mar et al.[29] studied a series of high-spin Fe^{III} complexes of symmetric porphyrins in detail. These investigators proved[238] that the spin transfer occurs from the central metal to the ligand, with about equal spin density at the β- and the methine-positions of the macrocycle. A spin transfer from the metal to the ligand is further supported by the preferred stabilization of the high-spin form in π-complexes of aromatic acceptors with Fe^{III} porphyrins[243]. Although the g-tensor in high-spin Fe^{III} complexes is essentially anisotropic, an appreciable pseudo-contact contribution to the shift was found, the magnitude of which could be evaluated via the phenyl proton shift as described above for the low-spin series[27]. From a $1/T^2$ term in the (non-Curie) temperature dependence of the chemical shifts, the authors[29] concluded that the pseudo-contact shift arises from the zero field splitting as discussed earlier[23,226,241], and the D value calculated from the chemical shift data was in good agreement with the value previously deduced from IR measurements for high-spin Fe^{III} porphyrins[244]. The recently reported[245] spectrum of a fully substituted porphyrin Fe^{III} complex, the *meso*-tetra-CH_2-NO_2 substituted $Fe^{III}(OEP)^+$ shows, surprisingly, four $-CH_2-$ resonances, which might be explained by a ruffling of the molecule caused by steric hindrance and an out-of-plane position of the central metal ion.

Whereas either high- or low-spin complexes are observed in most instances, deviations from the $1/T$ law and the wide range of shifts in some hemin azides has been attributed to a mixture of both forms[246a] in the same compound[22]. The exchange between high- and low-spin hemin was studied together with the ligand exchange (pyridine, water) by Degani and Fiat[233] by relaxation measurements (see Section 10.4.1).

Fe^{IV} complexes are postulated by Felton et al.[246]. The 1 : 1 complex Fe^{IV} $(TPP)Cl^+$ has a net spin of $S = 2$, and shows a broad signal at $\delta = 68.6$ p.p.m. assigned to the resonances of the β-pyrrole protons. A more stable Fe^{IV} compound, the μ-oxo dimer of Fe(TPP) has formally one Fe^{III} and one Fe^{IV} atom, and the removal of one electron from a Fe^{III}-O-Fe^{III} orbital is discussed*. The alternative formulation as a π-cation radical of $Fe^{III}(TPP)$ was discussed critically by Fuhrhop[248] on the basis of the uv-vis spectrum and redox potentials.

(c) Di-nuclear Fe^{III} complexes: μ-Oxo-bridged dinuclear Fe^{III} porphyrins[249] have been the object of attention by several groups[29,246,250–252]. The two iron atoms are anti-ferromagnetically coupled[253], which results in a diamagnetic ground state (S_0) and paramagnetic excited states (S_1,S_2...) the spacing of which is characterized by the exchange parameter J. Boltzmann population of the paramagnetic levels (S_1,S_2...) leads to hyperfine shifts for the protons. Assuming only contact contributions and identical electron-proton coupling constants A_n for all excited states, Boyd et al.[251] determined J from the temperature dependence of the hyperfine shifts. However, Wicholas et al.[252] determined that about 80% of the shift should be attributed to the first excited state, S_1, and 20% to the S_2 state, although the

---

* The unusual redox properties of $[Fe^{III}(TPP)]_2O$ are further illustrated by the report of a Fe^{I} species obtained by reduction with Na/Hg[247].

latter is populated only to the extent of about 3%. These investigators were also able to show that the coupling constants A_1 and A_2 corresponding to S_1 and S_2, are unequal with $A_1 > A_2$. This relative order of coupling constant magnitude has been proved by La Mar et al.[29], who again investigated a series of highly symmetric model compounds. These authors[29] take into account the ring current shifts due to the neighboring ring by using the diamagnetic μ-oxo-scandium complexes for comparison, and evaluated the possibility of dipolar contributions that were neglected in earlier publications[150,246,251,252]. A μ-oxo dimer of hemin-*a* is described by Caughey[250], and the n.m.r. behavior of a heterometallic Fe^{III}-Cu^{II} dimer is reported by Bayne et al.[254].

10.2.8.5.2. Metals other than Fe

The hyperfine shifts of low-spin Co^{II} porphyrins were shown[28,256] to be dominated by the pseudo-contact term[255] (for the application of Co^{II} porphyrins as shift reagents in n.m.r., see Section 10.4.1.2). This term does not follow Curie ($1/T$) behavior, a circumstance that was shown to arise not from zero field splitting, but rather from a temperature (and more important, solvation) dependence of the g-tensor.

Several Mn^{III} porphyrins, including the Mn^{III} complex of a pheophorbide, were studied by Janson et al.[24]. The increased shifts upon increase of the porphyrin donor strength suggest a charge transfer from the ligand to the metal, and spin transfer through the π-system is invoked.

Abraham et al.[10] investigated the ligation of Ni^{II}(Meso-IX-DME). While square planar Ni^{II} porphyrins are usually diamagnetic, paramagnetic complexes are formed upon addition of a fifth ligand[256]. Strong shifts in resonances are observed for the methine protons, much smaller ones (~1/6) for the signals of the protons in the β substituents, and a spin transfer via the π-system is advanced to account for the spectra.

The nuclear spin relaxation mechanism was studied for Cr^{III}, Mn^{III}, and high-spin Fe^{III} complexes of *meso*-tetra-*p*-tolyl-porphyrin by a linewidth analysis[26]. For the Fe^{III} complexes, the linewidth is proportional to the electron spin relaxation time, T_{1e}, which is determined by the modulation of the zero field splitting parameter, D, by the molecular tumbling. It can be varied considerably by the axial ligand. This relaxation mechanism is less important for Mn^{III}, and Cr^{III} shows relaxation times corresponding to the tumbling correlation time. A dependence on D (or rather D^2) could be demonstrated for Fe^{III} and Mn^{III} complexes by variation of the fifth (axial) ligand[26]. Thus, a suitable choice of solvent can aid considerably in the resolution of the ^{1}Hmr spectra. Most of the investigations described here focus on resonances arising from the porphyrins. The broadening of resonance lines of axial ligands in paramagnetic porphyrin complexes, which has been used by several authors[233,257,258] as a probe for the mechanism of ligand exchange is discussed in Section 10.4.1.2.

A Eu^{III} complex of (TPP) was recently reported by Wong et al.[259]. As evidenced by the non-equivalence of the *o*- and *m*-phenyl proton resonances (Sections 10.2.8.1. and 10.4.2.2), the metal ion is considerably out-of-plane. Assuming only pseudo-contact shifts, a considerably larger Eu—N distance than in other Eu complexes was estimated.

10.3. Nuclei other than ^1H

The extensive use of ^1H as the basic n.m.r. probe for large organic molecules such as porphyrins to the exclusion of other nuclei was originally dictated by the high sensitivity of ^1Hmr as compared to that of the other elements present (carbon, nitrogen, and oxygen), which constitute the structural backbone. A combination of one or more of the following properties of a given nucleus (Table 27) is responsible for the problems involved in the n.m.r. spectroscopy of nuclei other than ^1H: (a) low inherent sensitivity at a given magnetic field, which depends on the third power of the gyromagnetic ratio; (b) low natural abundance; (c) spin $S \neq 1/2$, which either completely precludes n.m.r. spectroscopy ($S = 0$), or renders interpretation of spectra difficult because of complex coupling patterns produced when $S \geqslant 1$; (d)

TABLE 27

Nmr characteristics for some nuclei important in porphyrins and metalloporphyrins

Nucleus	Inherent Sensitivity [a]	Natural Abundance (%)	S	T_1 [b]
^1H	100.0	99.9	1/2	++
^2H	0.36	0.015	1	++/+++
^{12}C	0	98.9	0	—
^{13}C	1.6	1.1	1/2	+/++
^{14}N	0.04	99.63	1	+/+++
^{15}N	0.1	0.38	1/2	+
^{16}O	0	99.76	0	—
^{17}O	0.25	0.04	5/2	+++
^{18}O	0	0.20	0	—
^{199}Hg	0.57	16.8	1/2	+/++
^{203}Tl	18.7	29.5	1/2	+/++
^{205}Tl	19.2	70.5	1/2	+/++

Only crude approximations for the spin lattice relaxation time T_1 are given.

[a] As compared to ^1H at the same magnetic field strength.

[b] +: $T_1 > 10^2$ sec; ++: $10^0 < T_1 < 10^2$ sec; +++: $T_1 < 10^0$ sec.

quadrupole-induced line broadening; and (e) long inherent spin lattice relaxation times, T_1, of a nucleus, which easily leads to saturation of the n.m.r. resonances.

Early attempts to increase the spectral sensitivity of exotic nuclei involved enrichment of the nucleus of interest above its natural abundance level, S/N enhancement by signal averaging techniques, methods of circumventing the relaxation problem by adding small amounts of paramagnetic compounds (such as Cr $acac_3$) to facilitate relaxation, the use of cross relaxation techniques (nuclear Overhauser enhancement), and flow methods. The principal technical advance, however, in the n.m.r. spectroscopy of formerly exotic nuclei was made possible by the development of pulse Fourier transform (PFT) n.m.r. spectroscopy in recent years[260], a technique that can be further combined with some of the above-mentioned procedures. In conventional continuous wave (cw) mode for recording n.m.r. spectra, only one frequency at a time is observed, and most of the time spent in recording the spectrum is lost in collecting noise instead of signal. In the PFT mode, all nuclei are excited simultaneously by a strong radio frequency pulse, and the decay of the thus induced magnetization (free induction decay, FID) is observed in the time domain. If the spin—spin relaxation time, T_2, (or better $T_2{}^*$) is comparable to the spin lattice relaxation time, T_1, a signal is collected over most of the measurement time, which is thus used much more efficiently. The Fourier transformation from this time domain signal, (i.e., the FID) into the frequency domain (i.e., the usual spectrum), and any additional necessary processing of the spectrum is then done by a digital computer. The sensitivity enhancement by PFT as compared to cw is usually from one to two orders of magnitude. The sensitivity of PFT can be even further increased by some of the above-cited techniques, particularly the nuclear Overhauser enhancement that results from a simultaneous irradiation of coupled protons while ^{13}C spectra are recorded*. For a detailed discussion of pulse FT spectroscopy[260] and its applications to ^{13}Cmr[30], the reader is referred to recent monographs.

10.3.1. ^{13}Cmr of porphyrins

10.3.1.1. ^{13}Cmr of diamagnetic porphyrins

The majority of n.m.r. studies on nuclei other than ^{1}H have been made on

---

* Although pulse Fourier transform techniques are usually employed in heteronuclear (i.e., nuclei other than ^{1}H) n.m.r., we want to emphasize the advantages of PFT for ^{1}Hmr as well. This is especially true for porphyrins, as the greatly increased sensitivity overcomes their sometimes poor solubility and their pronounced aggregation. For example, the spectrum of porphin shown in Fig. 3a was obtained in our laboratory in about 15 min in a solution estimated to be 0.0005 M. PFT n.m.r. has also been applied[173] for the study of photoreactions directly in n.m.r. sample tubes, which require low concentrations because of the high light absorption of porphyrins.

^{13}C, not only because carbon is a universal component of organic structures (^{13}C is present to the extent of 1.1% of the carbon present), but also because ^{13}C possesses a comparatively high sensitivity (Table 27) and a comparatively low price in high isotopic purity, which makes the synthesis and biosynthesis of ^{13}C enriched compounds a practical proposition.

Only two ^{13}C studies of porphyrins have appeared in which at least some of the spectra were recorded in the cw mode[36,37]. The compounds employed were enriched in ^{13}C to 15 and 95%, respectively, but nonetheless, long signal averaging times were still necessary to obtain reasonable signal-to-noise in the spectra.

By contrast, and illustrating the great technical advances embodied in modern spectroscopic equipment, a wide variety of porphyrins at natural abundance or only moderate ^{13}C enrichment, used at concentrations of less than 0.1 M, have now been investigated by ^{13}C PFT-n.m.r. spectroscopy. The technique of moderate (biosynthetic) enrichment to about 15% ^{13}C has proven especially useful[33,37] .^{13}C—^{13}C Spin—spin coupling in compounds at this enrichment is still negligible, while the gain in sensitivity over natural abundance is considerable. Enrichments higher than 20% are desireable primarily for studies of ^{13}C—^{13}C spin—spin interactions[36], and, to some extent, for selective labeling experiments[35,261,262].

(a) *Assignments*: Due to the favorably spaced and well-assigned ^{1}Hmr spectra of porphyrins, carbon atoms bearing hydrogen atoms can be directly assigned from multiplicity of their resonance, and the assignment can be assisted by either single frequency off-resonance decoupling[34], or (more unambiguously) by single frequency on-resonance decoupling[37]. The very closely spaced methine ^{13}C resonances in H_2(Proto-IX-DME) and (2,4-diacetyl-Deut-IX-DME) were assigned by (synthetic) selective enrichment at these specific positions with ^{13}C[261,262], and Katz et al.[37] and Lincoln et al.[263] used stepwise chemical modifications to clarify questionable assignments.

The assignment of the quaternary carbons in large molecules presented a major challenge, especially as the chemical shifts of these carbons may be expected to yield valuable information otherwise unavailable from ^{1}Hmr. All, or almost all, of the expected quaternary carbon atom resonances are usually observed as resolved singlets, which are easily differentiated by their multiplicity in the undecoupled spectrum and by their relatively low intensity as compared to the proton-bearing carbons in the broad-band ^{1}H decoupled spectrum. The latter effect is due to longer relaxation times and the small nuclear Overhauser enhancement of the quaternary carbons.

Matwiyoff et al.[36] and Abraham et al.[32] discuss the (exchange) broadening of the α-pyrrole ^{13}C signals in free base porphyrins[9,261], by tautomeric N—H exchange[32], as a way to differentiate between α- and β-pyrrole carbon resonances. The latter authors also discuss the effect of metalation on the absolute chemical shifts and spacing of the α- and β-pyrrolic resonances as a potential aid in assigning these resonances (see also Ref. 33). Lincoln et al.[263] use gradual structural changes to assign some of the quaternary ^{13}C resonances, and ^{13}C—^{13}C couplings in highly enriched porphyrins can establish some assignments in the vicinity of *meso*-carbon atoms[36]. The most direct approach to assignment of the quaternary carbon atoms is the modified indor (heteronuclear double resonance) techniques used by Boxer et al.[33] to assign all the macrocyclic quaternary carbons in chlorophyll-*a* and some of its derivatives. In conventional indor spectroscopy, the absorption level or intensity of a satellite line of a (usually proton) multiplet is monitored, while a second radio frequency is swept through the absorption range of the respective nucleus coupled to the proton. In 'center line indor', the absorption intensity at the center of the resonance line is monitored instead. Although no distinct multiplets are observed, the center lines of the proton resonances of the β-pyrrole substituents are broadened by long range spin—spin couplings with the quaternary carbon atoms, and the absorption is increased by collapse of the unresolved proton multiplet when a transition of the coupled quaternary carbon atom is induced. Obviously, the utility of this technique is again enhanced by the use of compounds at moderate ^{13}C enrichment. The assignment of the ^{13}C resonances of chlorophyll-*a* obtained[33] in this way are not only self-consistent, but also confirm the earlier assignment of the ^{1}Hmr spectrum[13] in all respects.

(b) *^{13}C Chemical shifts*: Although the ^{13}C chemical shift can be broken down into the same components as discussed for protons, the relative importance of their contributions is different. The ^{13}C nucleus is comparatively shielded from the surrounding environment, but carbon nuclei have a multitude of accessible hybridization states that affect the ^{13}C shifts strongly and spread ^{13}C resonances over a range of several hundred p.p.m. Thus, ring current effects on the chemical shifts of protons are roughly ±5—10 p.p.m. and this strongly determines the appearance of a proton spectrum that in most instances extends over only a slightly larger range. Although ring current effects are of the same absolute magnitude for ^1H and ^{13}C, they contribute less than 10% to ^{13}C shifts[31], which are spread over about 200 p.p.m. Reliable ring current increments to the chemical shift of carbon atoms in the conjugation pathway of porphyrin macrocycles would be a valuable probe of the magnetic anisotropy in these regions of the molecule that are not accessible to ^{1}Hmr. So far, the ambiguities in the interpretation of ^{13}C shifts do not permit the separation of these terms. Ring current contributions may be responsible, however, for the same order of chemical shifts for both the ^1H and ^{13}C signals of sets of β-pyrrole CH_3 groups.

The ^{13}Cmr spectra (insofar as available) of the same selected archetypical porphyrins discussed at the beginning of this chapter (Section 10.2.1) are summarized in Table 28. Rather than discussing each spectrum in detail we propose to outline such fundamental and general features of porphyrin ^{13}C n.m.r. as can be drawn from the yet very incomplete work. The ^{13}C spectra

TABLE 28

^{13}Cmr chemical shifts (δ[p.p.m.] from TMS) of some principal porphyrins, and ^{15}N spectrum (δ[p.p.m.] rel. to external $^{15}NH_4Cl$) of methyl pheophorbide-*a*-$^{15}N_4$.

				Solvent	Ref.
(11)	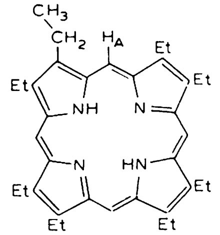	Methine—C: $\alpha_{pyrrole}$—C: $\beta_{pyrrole}$—C: CH_2: CH_3:	96.8 142.2 141.1 19.8 18.0	C^2HCl_3/TFA	32
(13)	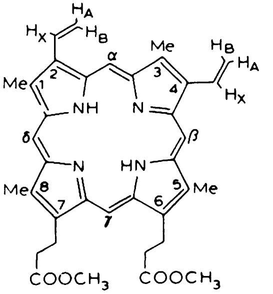	Methine—C (α,β): Methine—C (γ,δ): CH_3: CH_2CH_2: $COOCH_3$: $CHCH_2$:	97.5, 97.0 95.6, 96.6 11.5—12.7 21.8, 36.8 172.8, 51.6 129.8, 120.2	C^2HCl_3	35

C	δ^c	$^1J_{^{13}C-^{13}C}$ ^{d}	C	δ^e	$^1J_{^1H-^{13}C}$ ^{f}
1	131.6	44	1a	11.6	129
2	136.3		2a	128.4	155
3	135.9	45	2b	121.9	160, 68^h

(87)

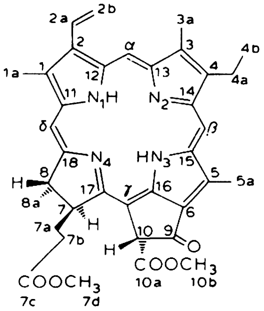
2a
2b
3a
1a
1
2
12
α
13
3
4
4b
4a
11
N1H
N2
14
δ
β
18
N4
HN3
15
5
5a
8
H
8a
17
7
γ
16
6
7a
H
7b
10
9
H
O
COOCH3
COOCH3
7c
7d
10a
10b

C	δ^{c}	$^{1}J_{^{13}C-^{13}C}$ [d]	C	δ^{e}	$^{1}J_{^{1}H-^{13}C}$ [f]
4	144.9	42	3a	10.4	126
5	128.8	44	4a	18.7	125
6	161.2		4b	16.9	160
7	51.0 [a]	129 [b]	5a	11.6	129
8	49.9 [a]	46, 130[b]	10a	169.2	58 [i]
9	189.0 [a]		10b	52.5	148
10	64.6 [a]	136 [b]	7a	30.9	130
11	141.9		7b	29.7	126
12	135.9		7c	172.9	
13	155.3				
14	150.7		8a	22.8	125
15	137.8		α	96.8	155, 70 [g]
16	149.6		β	103.7	145, 70 [g]
17	173.3		γ	104.9	
18	172.0		δ	92.7	157, 70 [g]
N	δ^{j}	J_{N-N} [k]			J_{N-H} [k]
1	102.5	$^{2}J_{12} = 2.0$, $^{2}J_{14} = 2.5$			$^{1}J_{N-H} = 98$
2	219				
3	110.9	$^{2}J_{23} = 5.7$, $^{2}J_{34} = 1.4$			$^{3}J_{N-H} = 3$ [l]
4	272.8				

---

[a] From Ref. 37.

[b] $^{1}J_{^{1}H-^{13}C}$ from Ref. 37.

[c] From Ref. 33 in δ[p.p.m.] relative to internal TMS.

[d] Coupling constant for the β-pyrrolic C and the adjacent substituent C in Hz, from Ref. 36.

[e] In δ[p.p.m.] relative to internal TMS, from Ref. 37.

[f] In Hz, from Ref. 37.

[g] $^{1}J_{^{13}C-^{13}C}$ in Hz between the methine-C and the adjacent α-pyrrolic C, from Ref. 36.

[h] $^{1}J_{^{13}C_{2a}-^{13}C_{2b}}$ in Hz, from Ref. 36.

[i] $^{1}J_{^{13}C_{10}-^{13}C_{10a}}$ in Hz, from Ref. 36.

[j] In δ[p.p.m.] relative to external $^{15}NH_4Cl$, from Ref. 33.

[k] In Hz, from Ref. 33.

[l] Three bond *trans*-coupling between ^{15}N and the methine proton.

of porphyrins can be more or less arbitrarily subdivided into four regions: the aliphatic carbon region with chemical shifts in the range ~10—70 p.p.m.;* the methine carbon region (~90—100 p.p.m.); the aromatic and olefinic carbon region (130—170 p.p.m.); and the carbonyl region in the most strongly deshielded portion of the spectrum (170—190 p.p.m.). Although there may be some overlap in chemical shifts, especially in the low-field regions, such a situation is usually readily resolvable from the number and multiplicity of the resonances.

The signals of all proton-bearing sp^3 hybridized carbon atoms are observed in the high field region between 0 and 70 p.p.m. These chemical shifts fall well within the usual ^{13}C expectation ranges[30]. The resonances of the carbon atoms in the aliphatic side-chains occur in the range of δ = 10—40 p.p.m., and for similar substituents the same order of chemical shifts in both the ^1H and the ^{13}C spectrum is found[33,37]. The chemical shifts for several important β-pyrrole substituents are listed in Table 29, and these shifts seem to be fairly constant in various porphyrins. The 7 and 8 carbons in chlorins come into resonance at about 50 p.p.m.[33,213,263], and the carbon atoms adjacent to ester or carbonyl functions have resonances in the range of 50—70 p.p.m.

The chemical shift range from 90—100 p.p.m. contains the resonances of the methine carbons. These signals are closely spaced in protoporphyrin-IX[35] and related alkyl- or vinyl-substituted porphyrins[32,34,263] but are spread out by β-substitution with other groups[35,263] and in chlorins[33,213,263]. Alkyl-substitution of a β-pyrrole position shifts the neighboring methine carbon resonances upfield by about 3.5 p.p.m.[32], as compared to the β-unsubstituted compounds. In chlorins, the signal(s) of the methine carbons next to the reduced ring occur (as in the proton spectrum) as separate resonances at higher fields, probably because of the high electron density at these sites. However, in pheophorbides the quaternary γ-C methine resonance occurs in the region of the α- and β-methine carbon atom signals. The above-mentioned shielding clearly seems to be compensated for by quaternization and bond angle deformations[128].

In the region between 130 and 170 p.p.m. the resonances of the quaternary α- and β-pyrrole carbons occur, with the latter at higher field and usually without overlap of the α-carbon atoms at lower field. Again, these two sets of α- and β-pyrrole carbon resonances are closely spaced in alkyl-substituted porphyrins[9,32,35], while the resonance peaks are spread out in

---

* All ^{13}C chemical shifts are given in δ [p.p.m.], down-field relative to internal $Si(^{13}CH_3)_4$ (TMS). For conversion of chemical shifts from other internal standards sometimes used in the literature, the following reference values relative to TMS were used here: $^{13}CS_2$: δ = 193.7 p.p.m.; benzene: δ = 128.5 p.p.m.[30]. TMS has the considerable convenience in that both ^1H and ^{13}C chemical shifts are referred to the same internal standard compound.

TABLE 29

Expectation ranges (δ[p.p.m.] from TMS) of the ^{13}Cmr resonances of β-pyrrole substituents in porphyrins

Substituent	Chemical Shift δ[p.p.m]	Ref., remarks
β-pyrrole		
CH_3	10.4—15.7 (22.8—23.1 = 8 CH_3 in chlorins)	9,32,33,34,35,37, 261,263
CH_2CH_3	18.7—22.5/16.9—18.5 (12.8[35])	32,34,36,37,261, 263
$CH{=}CH_2$	128.8—131.6/120.1—122.6	34,35,36,37,261, 263
$CH_2{-}CH_2Br$	18.3	263
$CHOH{-}CH_3$	65.3/26.0	34
$CH_2CH_2COOCH_3$	21.6—23.5/35.8—39.2/172.7—174.7/51.4—53.0	9,32,34,35,37,
in chlorins	30.9—31.1/29.6—29.9/172.9—173.5/51.6—51.7	261,263
CHO	187.4	36,263
$COCH_3$	33.1—34.3	34,35
CO—R	189—196.1	9-CO in chlorins, 37,263
$COOCH_3$	169.4—173.0/52.0—53.1	263
γ-Methine		
CH_2COOCH_3	38.3—38.6/169.4—173.0/52.0—53.1	263

If not otherwise indicated, the chemical shifts are listed according to the carbon atom sequence in the substituent formula (from left to right).

the less symmetrically substituted porphyrins[9,32,34,35,263] and in the chlorins[33,213,263]. (For a recent discussion of the ^{13}C resonances in non-alternant hydrocarbons, see Ref. 264.) Abraham et al.[32] observed a distinct incremental shift of about 2 p.p.m. for β-pyrrole carbon atoms next to a carbomethoxy-ethyl substituent as compared to a methyl substituent. In pheophorbides[33], the α-pyrrole carbon atoms in ring D are more deshielded by almost 20 p.p.m. than those in the remaining pyrrole rings, thus indicating a more pyridine-like character for the pyrroline ring (see below). A similar low-field shift is also observed for carbon 6 in ring C, which not only is subject to shielding by the adjacent 9-carbonyl group, but also has distorted bond angles[128] that change its hybridization.

The unsubstituted β-pyrrole C-2 and C-4 atoms in H_2(Deut-IX) occur on the high-field side of the quaternary carbon resonance region[32,34,35,263] (120—130 p.p.m.), along with the resonances of the carbon atoms in olefinic substituents[33,34,263]. This similarity in chemical shift was considered by Doddrell and Caughey[34] to be a strong hint for the presence of an inner (16-annulene di-anion) conjugation pathway (see formula 4, 5, Section

10.1.2), which makes the peripheral double bonds essentially olefinic. This interpretation was rejected by Abraham et al.[9,32], partly[32] upon the observation of similar chemical shifts for the α- and β-pyrrole carbon atoms, both of which come into resonance at considerably lower field than does the methine carbon atom. Ambiguities in the interpretation of the ^{13}C shifts still remaining do not permit a definitive decision on this point by ^{13}Cmr.

Abraham et al.[32] were able to show that the resonances of the α-pyrrole carbon atoms in the coproporphyrin isomers are close to coalescence at room temperature with respect to N—H tautomerism. This N—H exchange is slower in chlorins (see Section 10.4.2.1) and the more localized N—H protons generate two distinct types of rings as far as the ^{13}C (and ^{15}N) spectrum is concerned. Rings A and C are pyrrole-like, ring B and especially ring D resemble pyridine[33]. Upon metalation, the differences between the chemical shifts of the carbon and the nitrogen atoms in the different pyrrole rings becomes less pronounced, and at the same time the average of the α- and β-pyrrole ^{13}C resonances is shifted to lower field[32,33]. These effects are discussed by Boxer et al.[33] in terms of a redistribution of charge densities upon metalation within the macrocyclic system and a change in its absolute value, which results in part from a leveling effect on the non-bonding nitrogen orbital energies, and a simultaneous increase in their average value. The effect of protonation in ^{13}Cmr spectra has been investigated by Abraham et al.[32]. Upon initial addition of TFA, the α-pyrrole carbons are shielded, and the β-pyrrole (and methine) carbons are deshielded, as in the case of other *N*-heterocyclic compounds. At higher TFA concentrations, all signals are deshielded due to solvent effects and/or further protonation. Shifts of the α and β *meso* carbon lines in chlorin spectra upon addition of TFA have been used[213] to identify these carbons as well as clarify the site of *meso* methylation in the *Chlorobium* chlorophylls '660'.

The signals of the carbonyl carbons are observed in the region from 170 to 190 p.p.m. Katz et al.[37,265] found a pronounced downfield shift of the C-9 carbonyl resonance in chlorophyll-chlorophyll self-aggregates ($\Delta = -2.4$ p.p.m.). An even stronger downfield shift is observed in the resonances of the carbonyl carbon atoms of 2,4-pentanediones upon coordination with Mg^{2+} [37]. Obviously, any shielding from the ring current of the adjacent macrocycle in the chlorophyll dimer is more than compensated for by the deshielding effect of the coordination interactions of the non-bonding $C = O$ orbital with the metal ion. Similar downfield shifts due at least in part to hydrogen bonding are reported for the ester carbonyl carbons in the coproporphyrin isomers[32] in strong acids.

(c) *^{13}C Spin—spin coupling: ^{1}H—^{13}C* — Natural abundance ^{13}C spectra are usually recorded under partial (single frequency off-resonance) or full (broad band) proton decoupling to obtain sensitivity enhancement from the nuclear Overhauser effect. Under these conditions, however, the ^{1}H—^{13}C couplings are reduced or removed, respectively. Although gated decoupling is expected to yield correct coupling constant values, $^1H—^{13}C$ coupling constants are reported to our knowledge only for ^{13}C enriched compounds in spectra recorded without double irradiation. $^1H_{^1H-^{13}C}$ of about 150 and 130 Hz are observed for aromatic and olefinic, and for benzylic carbon atoms, respectively, in chlorins[36,37] and porphyrins (methine carbon atoms only)[35]; these values fall within the usual range expected for these groups[30]. While these coupling constants are fairly consistent, the two non-benzylic methyl groups in methyl pheophorbide-*a* at 4b and 8a, show a marked difference in their coupling constants, viz. 160 and 125 Hz, respectively, which probably reflects differences in steric hindrance in these groups. No long range $^1H—^{13}C$ couplings have thus far been reported; such couplings are usually unresolved and result only in line broadening[32,33]. A small ($J < 2$ Hz) coupling of the α-pyrrole carbons (probably) with the methine protons is observed in the OEP dication[135].

$^{13}C—^{13}C$ — While the enrichment ($\leqslant 20\%$ ^{13}C) optimal for ^{13}Cmr data collection effectively suppresses carbon—carbon couplings, some $^1J_{^{13}C-^{13}C}$ values are reported by Matwiyoff et al.[36] in highly ^{13}C-enriched chlorophyll-*a* and -*b*. Although the aromatic part of the spectrum is obscured by the various extensive couplings, it was possible to extract some $^{13}C—^{13}C$ coupling constants from the multiplets of the β-pyrrole substituents and the methine carbon atoms. The following values for the 1 bond $^{13}C—^{13}C$ constants are reported[36] (Table 28): 44 ± 2 Hz for the coupling of benzylic carbon atoms of the aliphatic side-chain to the ring carbon atoms; 34 Hz for J_{4a-4b}; 50 Hz J_{3-3a} in Chl-*b*; 68 Hz for J_{2a-2b}; 58 Hz for J_{10-11}; and 70 Hz for the coupling constant of the methine carbon atoms with both α-pyrrole neighbors. The values of $^1J_{^{13}C-^{13}C}$ are mainly dependent on the hybridization states of the coupled carbons (for a recent review, see Refs. 30 and 266). The only unusual coupling value, as judged from similarly substituted benzenes[30], is the (equal) coupling constant of 70 Hz observed between the methine carbon atoms and their α-pyrrole carbon neighbors, a value which is closer to that of ethylene (68 Hz) than to that of the benzene carbon atoms (~60 Hz).

$Tl—^{13}C$ — Abraham et al.[9,32] discuss in some detail the (long-range) $Tl—^{13}C$ couplings in Tl^{III}-porphyrins. No difference was noticeable for the two magnetically very similar isotopes ^{203}Tl and ^{205}Tl. Two to four bond couplings are observed in these cases, which are (in accordance with earlier Tl studies)[267] about 60 times larger but in the same relative order as the $^1H—^1H$ couplings, indicative of dominant contact couplings via spin transfer through the σ bond system.

10.3.1.2. ^{13}C of paramagnetic metalloporphyrins

In addition to the ^{1}Hmr spectra of Fe^{III} porphyrins, Wüthrich et al. recently studied the ^{13}Cmr spectra of some low-spin Fe^{III} porphyrins[268,269], as well as the Fe^{III} complexes of Proto-IX[268,270] and Deut-

IX[270]. The chemical shift assignment of carbon atoms bearing protons was achieved by single frequency off-resonance, and, in some cases, by single frequency (on-resonance) decoupling, and the quaternary carbons were assigned by intercomparisons. The treatment of the ^{13}C data is, as in the case of the ^{1}Hmr data, directed to the separation of the hyperfine shifts from all other contributions present in the diamagnetic porphyrins. Furthermore, the separation of the hyperfine shifts into contact and pseudo-contact contributions (Section 10.2.8.5), and the further subdivision of both hyperfine terms into contributions from the σ and π electron framework and the metal ion was attempted. As in the ^{1}Hmr investigations, the Zn complexes were again used as reference compounds to evaluate the diamagnetic shifts* (average value of sets of ^{13}C resonances from chemically equivalent nuclei). It should be noted, however, that the pronounced differences in the ^{13}C chemical shifts of diamagnetic porphyrins observed for different metals[32] make these reference shifts of lesser value than in the case of the ^{1}H spectra, because they are sometimes of similar magnitude as the hyperfine shifts.

A semi-quantitative treatment provides limits for the pseudo-contact shifts, which were calculated from the g-factor anisotropy (see Section 10.2.8.5) in frozen solution (an upper limit), and from values estimated in earlier ^{1}Hmr work (a lower limit).

The results from ^{13}Cmr are in many points complementary to the conclusions derived from ^{1}H hyperfine shifts. The ^{13}Cmr results provide a distinct refinement, as they indicate pronounced differences in the (hyper-conjugation) coupling parameters Q for different substituents[270]. These differences can be interpreted in geometrical terms and in principle yield a better insight into the conformation of the various substituents in solution. It has been further shown that, in contrast to ^{1}H shifts, the ^{13}C pseudo-contact shift contribution from spin transferred to the ligand is no longer negligible.

10.3.2. ^{15}Nmr of porphyrins

^{15}N in magnetic resonance spectroscopy may have such very long relaxation times that acquisition of ^{15}Nmr data may be prevented. The ^{15}N spectrum of highly (95%) enriched ^{15}N pheophytin-*a* (87b) (Table 28) has been recorded by the use of the very long pulse interval of 60 sec[33], and by addition of $Cr^{III}acac_3$ **[271] to induce more rapid relaxation. The ^{15}N shifts of the related Mg-complex (chlorophyll-*a*) were obtained indirectly by heteronuclear (^1H—^{15}N) double resonance experiments[33]. For both chlorophyll-*a* and pheophytin-*a*, the ^{15}N resonances were assigned by single frequency decoupling of the methine proton resonances[33]. The ^{15}N spectrum in the free base pheophytin-*a* shows two sets of resonances, with chemical shifts characteristic for pyrroles (ring A, C) and pyridines (ring D, and somewhat intermediate, ring B). The order of the chemical shifts was interpreted to reflect the relative order of the energy levels of the non-bonding nitrogen orbitals, with ring $D > B \geqslant C \sim A$[33]. This order is in agreement with ESCA data on porphyrins[272]. Various ^{15}N—^{15}N couplings via the inner hydrogen atoms are observed, and the data allow an estimate of the sharing of the inner hydrogen atoms between the nitrogen atoms (Table 28, see also Section 10.4.2.1)[33]. The ^{15}N—^1H coupling constant with the inner hydrogen atoms is $^1J_{^{15}N-^1H}$ = 98 Hz. In addition, long-range (*trans*) coupling of $^3J_{^{15}N-^1H}$ = 3 Hz, with the methine protons (used to assign the ^{15}N resonances) in chlorophyll-*a*, was observed, and five bond couplings ($^5J_{^{15}N-^1H}$) with the methine protons via the central Mg are discussed[33].

---

* In contrast to the usual n.m.r. spectroscopic definition, the diamagnetic shift refers here to all terms (diamagnetic as well as paramagnetic) *except* the hyperfine terms arising from the nuclear interaction of the unpaired spin.

** By comparison with the values given by Boxer et al.[33] the ^{15}N-spectrum of the algal pigment mixture[271] is obviously that of pheophytin-*a* and -*b* (probably demetalated by $Cr^{III}acac_3$) rather than that of the chlorophylls.

10.3.3. *Magnetic resonance of central metals in metalloporphyrins*

In spite of the wide variety of porphyrin metal complexes available for study, only a very few investigations deal with the n.m.r. spectroscopy of these metals and their (nuclear) spin-spin interactions with the porphyrin ligand. Abraham et al. investigated in some detail long-range spin—spin couplings between Tl and ^{13}C[9,32] and ^1H[8,11]. ^{203}Tl and ^{205}Tl are magnetically very similar and their proton coupling constants are identical, in agreement with results of Maher and Evans on Tl organic compounds[267]. The ^{13}Cmr results show a predominant contact coupling mechanism with spin transfer through the σ-system. A similar mechanism was advanced for the long-range ^1H—Tl couplings with the protons of the β-pyrrole sidechains, whereas the methine protons appeared to be coupled *via* the π-system.

The μ-diporphinato—trimercury complex (82) was studied by (^1H-{^{199}Hg}) indor spectroscopy (see Table 23)[219,223]. The observation of two ^{199}Hg in indor lines at 17.8866 and 17.8854 MHz in an intensity ratio of 2 : 1, is one of the basic results acquired to establish the stacked structure proposed for this compound.

10.3.4. ^{2}*Hmr of porphyrins*

^{2}Hmr is of low sensitivity, and the resonance lines are broadened because of quadrupolar relaxation, (for a recent review see Ref. 273). The few ^{2}Hmr studies available, however, indicate certain technical advantages to this spectroscopic technique. For example, the ^{2}Hmr spectra are first order (because of the higher $\Delta\delta/J$ ratio), and resolution is much better in the case of (paramagnetically) broadened lines[274]. Isotope effects on chemical shifts and coupling constants are furthermore of considerable theoretical interest.

In evaluating the potentialities and advantages of bio-molecules of unnatural isotopic composition, the Argonne group reported the ^{2}Hmr spectrum of methyl pheophorbide-*a*-$^2H_{35}$ (7d-CH_3) and chlorophyll-*a*-$^2H_{72}$[293]. Although the ^2H lines are broadened by quadrupolar relaxation, the resolution is good for the former compound (2—7 Hz line widths) and sufficient in Chl-*a* for the identification of the major resonances. The ^2H chemical shifts of the porphyrin moiety of the molecules are very similar to the ^1H shifts, with generally positive (shielding) isotope effects of less than +0.05 p.p.m. The ^2H-phytyl side-chain, however, is strongly shielded. An isotope effect of 0.63 p.p.m. is observed in the ^2H-chlorophyll, which is probably accounted for by the integrated (shielding) isotope effect in the aliphatic chain, although aggregation shifts involving ring current effects cannot be completely excluded.

10.4. Introduction to applications section

In this section, the applications of n.m.r. spectroscopy to three major areas are discussed: the aggregation of porphyrins (including ligand exchange processes) is mainly studied by using ring current induced shifts (RIS) as a probe for molecular interaction; dynamic processes involving tautomerism and rotation of substituents; and the stereochemistry of porphyrins. To complete this somewhat arbitrary selection, pertinent applications outside this scope are listed under miscellaneous without further discussion.

10.4.1. Aggregation

The very early ^{1}Hmr studies of porphyrins revealed a remarkable solvent and concentration dependence of the chemical shifts of the solute (the porphyrins), the solvent, and co-solutes. These effects arise from self-aggregation of the porphyrins, or are the result of more or less specific interactions with nucleophiles that may be present. The reason for aggregation shifts in the porphyrins, in a general way, lies in the combination of the strong magnetic anisotropy of the porphyrins with strong, and often specific, molecular interactions of the porphyrins with each other or with other species (nucleophiles) present in solution. The study of the chemical shift consequences of porphyrin molecular interactions thus provides detailed insight into both self-aggregation (endogamous aggregation)[59] and porphyrin—ligand interactions (exogamous interactions)[59].

Porphyrin aggregation can involve either or both π—π and metal—ligand interactions. The π—π forces are relatively weak (for an exception, see Ref. 276), fairly insensitive to solvent*, and generally produce only upfield shifts of the species ligated to the porphyrins. The sources of these upfield shifts are obvious from the magnetic anisotropy of the macrocycle (Fig. 1), and result from the positioning of protons above or below the plane of another macrocycle. The surface defining zero shielding is not perpendicular to the macrocycle plane, and only associated molecules which are substantially larger in area than the porphyrin itself, can protrude into the deshielding areas. π—π Interactions are the main aggregation forces* in free base porphyrins. In metalloporphyrins, the π—π forces are often outranged in magnitude by metal—ligand coordination interactions, which are strongly solvent dependent and may result (especially in the case of porphyrin self-interactions) in both low and high-field shifts. In diamagnetic metalloporphyrins, aggregation shifts are ring current induced and can amount to as much as 2 p.p.m. or more for proton chemical shifts. In paramagnetic complexes, the chemical shifts in aggregates are dominated by nuclear hyperfine interactions with the unpaired spin(s), and thus can be an order of magnitude larger (see Section 10.2.8.5).

---

* Disaggregation in TFA is a result of dication formation rather than a result of a solvent effect.

In addition to self-aggregated species we also include in this section a discussion of covalently bound axial ligands involving the central metal ion of metalloporphyrins. Molecular aggregates of this kind show exactly the same incremental shifts, and ^{1}Hmr data have proven extremely useful in evaluating and comparing the magnetic anisotropy of the porphyrin macrocycle.

10.4.1.1. Porphyrin self-aggregation

The two self-aggregation extremes studied by ^{1}Hmr are the coproporphyrin tetramethyl esters[6,9] and the chlorophylls[37]. The concentration dependence of the proton chemical shifts in Copro was first noted by Abraham et al.[7] and later investigated in detail by ^{1}Hmr[6] and ^{13}Cmr[9]. As a by-product these studies made possible a useful analytical technique for distinguishing-III and IV isomers of coproporphyrins, thus solving an old problem. From symmetry considerations, both of these isomers are expected to yield similar multiplicity patterns for sets of chemically equivalent protons. This is indeed observed. For example, the methine resonances in the monomers present in TFA solution show three signals with intensities in the ratio 1 : 2 : 1. However, the significantly different geometry of the porphyrin aggregates in C^2HCl_3 solution leads to a partial collapse of the methine resonances to two signals (intensities in the ratio 2 : 2) in the III isomer[6]. In other cases, distinctions between isomers in which not all of the expected resonances are visible can be made from the fine structure in the spectra of the aggre-

---

* This is true only if no strongly aggregating substituents are present. Thus, for example, the recently studied 2a-hydroxypheophorbides show aggregation via H-bonding[132,213,277].

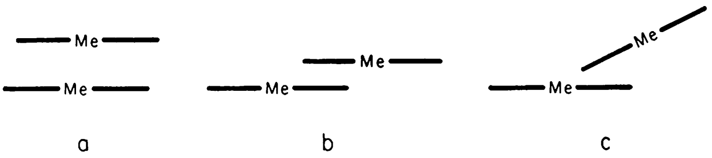

Fig. 5. Endogamous (self)-aggregation in porphyrins. (a) π—π charge transfer interaction, plane-to-plane distance 8—10 A, macrocycles laterally displaced. (From Ref. 68; see also Refs. 6,8,282.); (b) strong π—π interactions between ring A and D in Fe^{III}(Proto-IX)dicyanide (see Ref. 276); (c) strong n.m.r. averaged metal-ligand interaction between the central magnesium atom and the ring E keto carbonyl group in chlorophylls (see Ref. 37).

gates[92]. A quantitative analysis of the concentration dependence of the ^1H chemical shifts[6] indicated that: (a) only a monomer—dimer equilibrium in porphyrin π—π aggregation has to be considered in the concentration range up to about 0.2 m; (b) in the porphyrin dimer, the two porphyrin molecules are parallel to each other and on the average about 8 Å apart; and (c) the dimer components are persuaded by steric interactions of the bulky (propionic ester) side-chains to adopt an orientation such that the side-chains are staggered. Thus, the macrocycles are laterally displaced by about 2 Å (Fig. 5a). Of particular interest, Abraham[6] remarks that the separation distance observed in these dimers is more typical of charge transfer complexes rather than entities generated by generalized π—π interactions. A similar conclusion was reached by Ogoshi et al.[180] from infrared studies of the aggregation of porphyrin di-acids, which were formulated by these workers as cation—anion complexes, and the aggregation of *N*-methyl OEP with its mono-cation[142] provides further support for this view. On the other hand, a separation of only 4.5 Å characteristic for π—π aggregation was recently reported[276] for a low-spin protohemin (Fig. 5b).

A similar aggregation behavior was demonstrated for Meso-, Proto- and Deuteroporphyrins-IX in a high magnetic field study[68]. In these cases, the aggregates show a 10 Å separation of the macrocycle planes. Moreover, it was shown that at 220 MHz all magnetically non-equivalent nuclei were resolved[68]. The self-aggregation of pheophorbides-*a* and -*b* was studied by Closs et al.[13] and that of pyropheophorbide-*a* by Pennington et al.[214]. Because all of the ring proton signals in these compounds are assigned, aggregation in the dimers can be mapped in detail. The dimer structure in these compounds is similar to that of the porphyrins, but here steric interactions in the chlorin rings causes a pronounced lateral displacement of the macrocycles, with ring B showing the strongest overlap in the dimer.

Both the endogamous and exogamous interactions of the chlorophylls, which represent the other extreme of strong (axial) ligand—metal interactions, have been studied in detail by the Argonne group[13,214]. The central magnesium atom in the chlorophylls can be considered to be coordinatively unsaturated, which leads in the absence of extraneous ligands (nucleophiles, Lewis bases) to pronounced chlorophyll—chlorophyll aggregation. In aliphatic hydrocarbon solvents, large chlorophyll—chlorophyll aggregates with aggregation numbers higher than 20 are observed in concentrated chlorophyll solutions (0.1 M)[188,278]. These large oligomers, with molecular weights in excess of 20,000 appear to have linear polymeric structures in which the central Mg atom in one chlorophyll molecule is ligated (principally) to the 9-keto carbonyl group of the next molecule (Fig. 5c). The large aggregates that may be present in aliphatic hydrocarbon solutions not only lead to complex n.m.r. spectra, because of ring current effects, but the resonance lines are broadened by the longer correlation times of the aggregates and by a slow exchange of the subunits. The ^{1}Hmr spectra of these oligomers are of such ill-defined nature as to prohibit detailed analysis. The basic chlorophyll—chlorophyll interaction can be studied, however, in 'soft' non-polar solvents such as chloroform, benzene or carbon tetrachloride. In these less hostile solvents, the chlorophylls are present largely as dimers[279] or small oligomers undergoing fairly fast exchange. Participation of the 9-keto C = O group in chlorophyll-*a* aggregation is demonstrated in the ^{1}Hmr spectra by the strong high-field shifts of all ^{1}H resonances in the vicinity of the isocyclic ring E (see aggregation map, Fig. 6), by the similar aggregation behavior of pyrochlorophylls lacking the 10-carbomethoxy substituent[214], and by the upfield shift of the 9-CO ^{13}C resonance[37] upon disaggregation (see Section 3.1). The dimer and oligomer structure defined by n.m.r. is the weighted average of all the conformers that are present, as the exchange of chlorophyll molecules between the species present is fast on the n.m.r. time scale. Thus, only one set of lines is visible at room temperature*. A structure (Fig. 5c), in which the macrocycle planes form an angle with each other was inferred from (approximate) ring current induced shift (RIS) calculations (for a related CD study, see Houssier and Sauer[280]). These conclusions have received additional support recently from an analysis of the lanthanide induced shifts (LIS) in a Chl-*a* dimer—Eu(fod)$_3$ complex[279]. Although the LIS reagent changes the chlorophyll dimer structure to some extent, small solvent-dependent differences for the average dimer conformation in benzene and carbon tetrachloride were nevertheless inferred.

The ^{1}Hmr spectra of chlorophyll dimers in non-polar solvents are essentially concentration independent, unlike the case for π—π aggregates, whose spectra are strongly concentration dependent. The strong keto C=O···Mg interactions that form aggregates can be disrupted by the addition of bases that compete with the 9-CO group as the fifth (or sixth) axial ligand for the central Mg atom[59]. Disaggregation of chlorophyll oligomers and dimers by titration with base can easily be followed by ^{1}Hmr because of the pronounced proton chemical shift changes caused by disaggregation[13,188,214].

---

* Preliminary results obtained on pyrochlorophyll-*a* indicate the presence of at least three distinct conformers below —45° C, for which both high and low field shifts are observed[80].

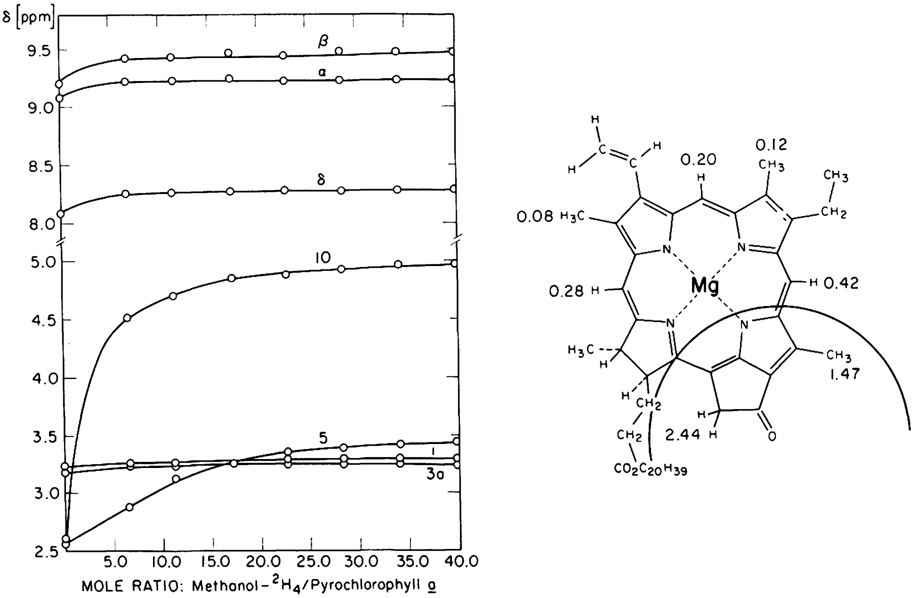

Fig. 6. (a) Titration of pyrochlorophyll-*a* (5×10^{-2} M in CCl_4) with $C^2H_5O^2H$; and (b) aggregation map of pyrochlorophyll-*a*. The chemical shift values indicated in the structural formula refer to the incremental shifts observed upon complete disaggregation of the dimer in CCl_4 solutions by titration with $C^2H_3O^2H$ (from Refs. 80, 214).

The order of base-strength for coordination to Mg relative to the 9-CO function for a variety of bases has been established by both ^{1}Hmr and by uv-vis and infrared measurements[405].

Between the extremes of π—π interactions in the free base porphyrins on the one hand, and the metal coordination interactions in the chlorophylls on the other, a gradual mixing of both effects can be observed in porphyrin complexes with other central metals. A gradual increase in self-aggregation involving ligand—metal interactions was shown to occur in the chlorophylls for the series free base, Ni^{II}, Cu^{II} (by infrared only), Zn^{II}, and Mg^{II} by both ^{1}Hmr and infrared spectra measurements[281]. The presence of both types of interactions in Ni(Meso-IX-DME) was also inferred from n.m.r. aggregation studies by Doughty and Dwiggins[282]. Because of the increased strength of interaction in the metalloporphyrin, separation of the macrocycle planes in the dimer is decreased from 10 Å in the free base dimer[68] to 7.9 Å in the Ni^{II} complex dimer[282]. The four isomeric Tl^{III}-Copro's were studied by Abraham et al.[11]. The geometry of the (weak) metalloporphyrin aggregates is very similar to that of the free bases, but the somewhat increased molecular interaction as compared to the free bases is evidenced by larger equilibrium constants (4.11 vs. 3.55 l/mole^{-1}). A unique type of strong π—π interactions in low-spin Fe^{III} porphyrins was recently reported by LaMar et al.[276]. Quantitative analysis of the selective paramagnetic broadening of ring A and ring D substituents yielded a structure in which ring A and D interact strongly and specifically, and in which the macrocycles are only about 4.5 Å apart (Fig. 5b).

10.4.1.2. Hetero- or exogamous aggregation

As in the preceding section, we again classify the interaction products of porphyrins with nucleophiles by the type of interactions, i.e., metal atom coordination interactions involving the central metal, π—π interactions with the aromatic system, and interactions via certain substituents involving hydrogen-bonding. Only little information is available for specific aggregation of free base porphyrins with non-porphyrin molecules. As a characteristic feature of porphyrin solutions, concentration-dependent chemical shifts are not only observed for the porphyrin themselves, but also for the solvent and the resonances of the protons of the internal standard. Abraham et al.[6] found incremental shifts of —0.65 Hz for the protons in tetramethylsilane (TMS) and about —12 Hz* for chloroform upon dilution of concentrated coproporphyrin solutions (from 100 mg/ml to 34 mg/ml) and extrapolated to infinite dilution. The TMS shift can be accounted for by bulk susceptibility changes with concentration, the $CHCl_3$ shifts by the randomly averaged effect of the ring current on the solvent. Obviously, the latter effect cannot be neglected in quantitative studies[6,11], but it is due to a random process rather than to specific solvent—porphyrin interactions that generate complexes. Assuming fast exchange, an upper incremental shift limit of 1 Hz for the $CHCl_3$ resonance was estimated, which is negligible in most situations. As an example of specific π—π interactions, the aggregation of the strong acceptor 1,3,5-trinitrobenzene with metalloporphyrins has been reported, and a model has been advanced in which pyrrole ring B acts preferentially as the donor[243,255,283].

Specific aggregation interactions are also observed for free base porphyrins with other porphyrins (viz. pheophytins with chlorophylls, J.J. Katz, unpublished results). As an interesting application, Wolf and Scheer[126] determined the enantiomeric purity of chiral pheoporphyrins by adding an excess of another chiral enantiomeric pure porphyrin, in this case pyromethylpheophorbide-*a*, to the solution. The diastereomeric collision complexes that are formed show sufficiently large chemical shift differences in the methine chemical shift region to be of analytical value.

The main interest in porphyrin heteroaggregation with exogamous nucleophiles has focussed on metalloporphyrin interactions because of the stronger and more specific interactions characteristic of such systems. Porphyrin-induced shift (PIS) reagents as a complement and alternative to lanthanide-induced shift (LIS) reagents have been studied by Storm et al.[17], Hill et al.[14,255], and extensively by Kenney, Maskasky, Janson and co-workers

---

* At 100 MHz.

(Ref. 19 and citations therein). Compounds suitable for shift reagent use, which show both ring current and additional pseudo-contact shifts, have been developed and critically examined[19]. Pronounced upfield shifts for methanol CH_3-protons bound to the central Mg in chlorophylls by coordination through oxygen were first reported by Closs et al.[13], and the corresponding incremental shifts of pyridine[16] and other ligands[51] in Mg-porphyrins were used to map the magnetic domain of space above and below the macrocycle plane. From a refined analysis of these data, the displacement of the central metal in some metalloporphyrins in solution from the plane of the macrocycle could be inferred[17], with conclusions as to the position of the metal ion in good agreement with conclusions derived from crystallographic data[128a,284].

The use of group IV metalloporphyrins and phthalocyanines and of the corresponding Fe^{II} and Ru^{II} complexes as shift reagents has recently been summarized by Maskasky and Kenney[19]. The PIS reagents are generally inferior to the LIS reagents as far as the magnitude of the chemical shift is concerned (the maximal shifts are about 8 p.p.m.[15]), but the PIS reagents are more stable and selective. Fe^{II} phthalocyanine[18,19] and its Ru^{II} analog[19] have been shown to interact very selectively with amines and to have ligand exchange kinetics optimal for recording spectra. Although the parent compounds are paramagnetic, the amine complexes are diamagnetic and the complexes show pure ring current shifts. Of the group IV metalloporphyrins, the germanium compound is specially valuable, for it forms covalent bonds with ligands and the products are well-defined compounds that can be purified and crystallized. Compounds of this type can be very valuable for combined X-ray/n.m.r. investigation to obtain the conformation of the adducts in both the crystal and in solution. The magnetic anisotropy is best mapped for the phthalocyanines[40] (see Section 10.1.2), but for better solubility the porphyrin complexes are recommended. The (TPP) complexes are easily accessible, but quantitative interpretation is not only difficult because the ring current properties of this porphyrin is less well known, but is also difficult because the phenyl rings cause steric interactions and additional (benzene) ring current shifts. Germanium porphin is recommended as a shift reagent but its use is restricted by its high price.

The use of Co^{II} porphyrins as pseudo-contact shift reagents has been studied by Hill et al.[14,255]. In the 1 : 1 complex of trinitrobenzene with Co^{II}(Meso-IX), the benzene ring is very probably situated above one of the pyrrole rings[255], indicating the operation of substantial π—π interactions. The hyperfine shifts are interpreted as arising only from pseudo-contact contributions, which add to the smaller ring current contribution. On the basis of these results, complexes of some steroids with Co^{II} porphyrins were studied, and in one case, that of the steroid cortisone, the solution structure was successfully determined by a quantitative analysis of the induced shifts[14].

References, p. 514

Studies of porphyrin or phorbin model systems of biological importance often exhibit complicated sets of overlapping ^{1}Hmr spectra, which may be difficult to analyze. Katz et al.[285] circumvented these problems by the use of mixtures of compounds in which one of the partners is extensively or fully deuterated and thus invisible in ^{1}Hmr, allowing detailed observation of the other component[51,285,286]. The aggregation interaction of lutein, a xanthophyll important in photosynthesis, with chlorophyll-*a*, is an example[285]. Adducts form via ligation of the hydroxyl group of lutein with the central magnesium atom, positioning a portion of the lutein molecule above the macrocycle, with effects clearly visible from the RIS of the lutein proton resonances. This aggregation complex was studied with fully deuterated chlorophyll-*a*, and lutein of normal isotopic composition, while in an inverse isotope experiment, in which chlorophyll interaction with sulfolipids were studied, the ^{1}Hmr resonances of the latter were deleted by the use of fully deuterated sulfolipid obtained by biosynthesis. In the latter type of experiment, however, no specific binding site can be established because the resonances of the ligand are absent in the ^{1}Hmr spectrum.

Ligand—metal interactions and ligation kinetics of Fe-porphyrins and related compounds have received considerable attention because of their biochemical importance in hemoproteins[21,22,227–229]. As in the discussion of the paramagnetic metal complexes (Section 10.2.8.5), we wish to discuss here only some of the principal model systems that have been studied.

The spin state of Fe-porphyrins is determined by the ligand field, which reflects and is determined to a great extent by the ligands present in the axial positions. The effect of axial ligands in complexes of both Fe^{II} and Fe^{III} porphyrins[287] have been studied[199] by ^{1}Hmr and infrared spectroscopy and these studies have been reviewed by Caughey et al.[250]. The results are interpreted in terms of the relative strength of the bonding of the central metal to the porphyrin and to the ligands in the fifth and sixth axial position. For various axial ligands, a gradual increase in the hyperfine shifts is observed from the low-spin complexes with two identical axial ligands to the high-spin complexes to an extent that depends on the binding of the axial ligands.

In addition to equilibrium studies, the ligation kinetics of paramagnetic metalloporphyrins have been investigated in some recent publications. The complexes formed are usually orders of magnitudes less stable than the complexes of the same ligand with the same metal ion not coordinated to a porphyrin[194,257]. Complexes of metal porphyrins with nitrogen bases have been most extensively studied because of interest in these complexes as models for heme—ligand interactions. For a series of substituted pyridines, the stability of the complex increased with increasing pK_a of the amine, but was decreased by steric repulsions[194]. For nitrogen ligands, S_N1 type ligand exchange reactions have been observed in which dissociation is the rate determining step[194,288,289]. For a high-spin chlorohemin, an S_N2 type exchange reaction is reported[290], which has a tetragonal—bipyramidal transition state in which the metal ion moves through the macrocyclic plane. A third process, an intramolecular ligand exchange was proposed by Tsutsui et al.[291] in which the binding site in cyclic diamines is changed. Although this mechanism was shown to be incorrect by cross-relaxation experiments[289] for the case of imidazole as ligand[291], the intramolecular exchange suggested was shown[194] to occur with another ligand, pyridazine. The solvation of high-spin metalloporphyrins was studied by several groups who made use of the paramagnetic contributions to the linewidth of the ligands as the probe[233,257,258,289].

10.4.2. Dynamic processes

10.4.2.1. N—H Tautomerism

Several tautomers involving N—H exchanges can be formulated for the free base porphyrins (Fig. 7), and additional structures are possible in which the protons are shared by two (or more) ring *N*-atoms*. The tautomerism is generally fast on the n.m.r. time scale**. This phenomenon was first dis-

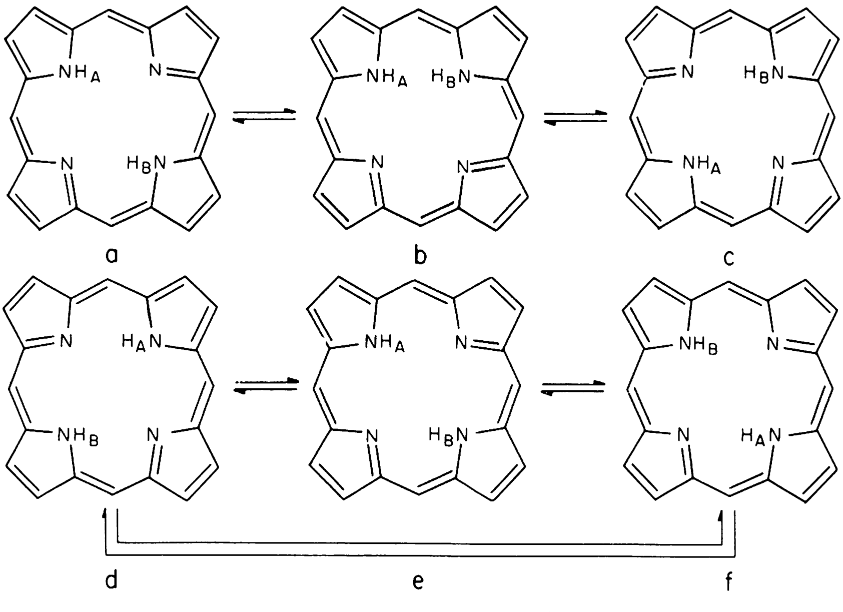

Fig. 7. N—H tautomeric equilibria in porphyrins. Non-concerted mechanism (ab,bc) with both N—H protons exchanging independently, and concerted mechanism with N—H exchanging simultaneously between neighboring (de,*df*), or, opposite nitrogen atoms (*ef*).

---

* In addition to intramolecular N—H exchange, Tsutsui[292] demonstrated recently fluxional behavior in Re^I and Tc^I complexes, in which the interchange of N—H, N—Re tautomers can be observed.

** For a relevant discussion of X-ray results, see Ref. 296.

cussed by Becker et al.[293] who attributed the magnetic equivalence of the methyl groups in H_2(Copro-I) to tautomerism even at low temperatures, and the same explanation was used to explain the methine signals in H_2(Copro-III) studied by Abraham[6].

The non-equivalence of neighboring pyrrole rings due to slow N—H exchange was first observed by Storm et al.[74], who found two resolved lines for the β-protons in H_2(TPP) and deuteroporphyrin-IX dimethyl ester at low temperatures. The signals for H_2(TPP) coalesce at —53°C, and the tautomerism shows an extremely high kinetic isotope effect[74,75] when the inner protons are replaced by deuterium. The tautomerism was explained by a concerted mechanism (Fig. 7b). The much smaller isotope effect for H_2(Deut-IX-DME) was attributed to the decreased symmetry in the latter, which biases the different tautomer equilibria. This problem was critically reinvestigated[61,76], and Abraham et al.[76] attributed the enormous isotope effect observed by Storm to a neglect of the activation entropy. From the ^{13}Cmr coalescence of two different carbon atoms at the same temperature in TPP (N—^{1}H) and TPP (N—^{2}H), respectively, the isotope effect $k_{1\,\mathrm{H}}/k_{2\,\mathrm{H}}$ on the tautomerization was determined to be 12.1 at 35°C. This value is well within the expectation range for such an isotope effect and is compatible with an independent exchange mechanism for the two *N*-hydrogen atoms (Fig. 7a).

In the less symmetric chlorins, the N—H protons are considerably more localized on the nitrogen atoms of rings A and C adjacent to the reduced ring rather than on the nitrogen atoms of rings B and D[74,75,294,295]. The single broad N—H resonances at δ = —1.38 p.p.m. in chlorin-e_6 trimethyl ester (14) splits into two peaks at δ = —1.35 and —1.42 p.p.m. upon cooling[75], and at high magnetic field (Fig. 3b[80]). Similar effects have been noted for several other 7,8-chlorins with γ-substituents[74]. In the phorbins bearing an isocyclic five-membered ring, which may be regarded as substitution at the 6- and γ-positions, (Section 10.2.3), two separate N—H resonances about 1—2 p.p.m. apart are already observed at room temperature[80,127,138]. One N—H resonance occurs in the range usually observed for the N—H signals in chlorins ($\delta \approx$ —1.5 p.p.m.) and bacteriochlorins ($\delta \approx$ —1 p.p.m.), and is thus assigned to the N_1 proton. The other resonance assigned to the N_3 proton is considerably shifted by 1—2 p.p.m. to higher field, which must be related to the steric deformations introduced into ring C by ring E formation[128]. The implication of more or less localized *N*-protons in phorbins at N_1 and N_3 was recently proved by ^{15}Nmr data on pheophorbides of the *a* series[33] (Section 10.3.2).

From the ^{15}N—^{15}N coupling constants (via the inner hydrogen atoms) and the ^{15}N chemical shifts, a decrease in the tendency to protonation in the order $N_1 \geqslant N_3 > N_2 > N_4$ was inferred[33], which corresponds well to X-ray crystal structure data for methyl pheophorbide-*a*[128]. Tautomeric structures similar to those in porphyrins have been advanced on the basis of

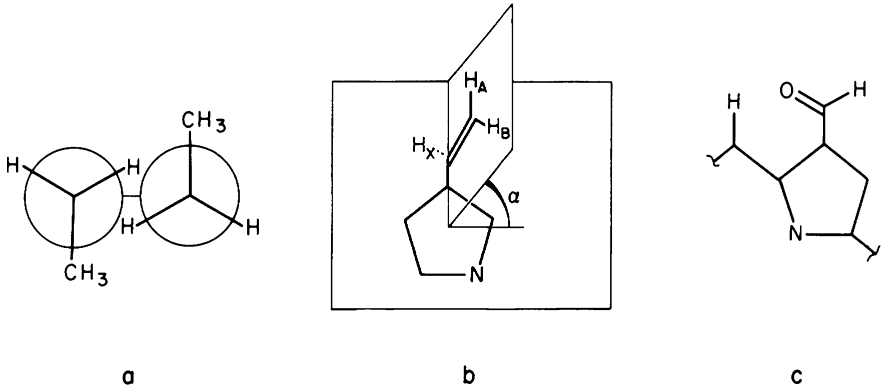

Fig. 8. Conformation of β-pyrrole substituents; only partial structures are shown. (a) Ethyl side-chains in H_2(OEP), schematic representation viewed parallel to the plane of the macrocycle, (from Ref. 296); (b) vinyl group in chlorophylls and (Proto-IX) derivatives, α = dihedral angle between the plane of the macrocycle and the plane of the vinyl group; and (c) 3-CHO in chlorophyll-*b* derivatives (from Ref. 263).

mations with the CH_3-groups of neighboring ethyl substituents out-of-plane and *transoid* to each other (Fig. 8a). Different conformations of vinyl substituents in heme and chlorophyll derivatives, respectively, can be inferred from ^{1}Hmr data. In chlorin-e_6 trimethyl ester (14), for example, the H_B resonance (see Fig. 8b) occurs at lower field than the H_A resonance, while the opposite is true for H_2(Proto-IX-DME) (13, see Section 10.2.1). H_B is closer to the macrocycle* than H_A; in case of a planar substituent it is therefore expected to be more strongly deshielded by the ring current, as observed in the chlorophyll derivatives. If the vinyl group is rotated, H_A remains almost co-planar with the macrocycle, while H_B is forced out-of-plane (Fig. 8b), thus occupying a less deshielding region, which accounts for the observed high field shift of H_B (relative to H_A) in H_2(Proto-IX) and related porphyrins. The conformation of the 2-formyl substituent in chlorophyll-*b* derivatives was investigated by using the pronounced magnetic anisotropy of the carbonyl group as a probe[73,263]. The data support a coplanar conformation with the aldehyde C = O oxygen atom oriented towards the α-methine position (Fig. 8c).

10.4.2.3. Conformation of meso-substituents

On the basis of X-ray structures[48,112,297,298], ^{1}Hmr long-range shielding effects (see Section 10.2.3) and space-filling models, nonlinear substituents have been shown to assume a conformation in which the planes of the macrocycle and the substituent are nearly perpendicular to each other. The rotation of *meso*-phenyl substituents has received considerable attention. Atropisomers of *o*-substituted H_2(TPP) derivatives[299,300–302] have been shown to be stable on the ^{1}Hmr time scale up to 198°C Ni(o-Me-TPP)[248], and a lower limit of 26 kcal has been estimated for the activation enthalpy of rotation. With bulky substituents in the *o*-phenyl positions, the atropisomers are stable even on prolonged refluxing in THF[300].

---

* This is true both for the S-*cis* and the S-*trans* conformation of the vinyl group with respect to the α-H.

In unsubstituted H_2(TPP), the two *o*-(as well as the two *m*-)protons are enantiotopic. This magnetic equivalency is removed, however, in metal complexes with an out-of-plane metal and/or with different axial ligands[29,194,201,303]. For Ru^{II}(TPP)CO, in which the non-equivalency is due to asymmetric ligation, an activation enthalpy of 18 kcal/mole has been determined from the coalescence of the *o*-phenyl proton resonances[183].

10.4.3. Stereochemistry

10.4.3.1. The macrocycle

The stereochemistry of the porphyrin macrocycle has been studied extensively by X-ray diffraction. [See Hoard[298] (Chapter 8) and Fleischer[48] for reviews.] These crystal structure studies show the macrocycle system to be fairly flexible. Planarity of the macrocycle is rather an exception and its shape has been described as domed, ruffled or roof shaped[169,298]. Large deviations from planarity are especially observed in H_2(TPP) derivatives[48]. The pyrrole rings are maximally twisted about 28° out-of-plane defined by the four central nitrogen atoms in the TPP dication[181].

Although about 100 porphyrin X-ray crystal structures have been published, relatively little is known about the stereochemistry and the rigidity of the macrocycle in solution. A first attempt to determine the solution structure of chlorophyll directly by the use of LIS shift reagents[279] gave results consistent with the X-ray parameters, but obviously the accuracy of the method is limited and serves to detect only relatively large deviations from planarity. If it is assumed that the crystal structure represents a conformation that is easily accessible in solution, deviations from planarity in the solid may primarily reflect the response to crystal packing of the macrocycle rather than its actual solution conformation. This is indicated, for example, by the different conformations assumed by H_2(TPP) in the triclinic[183] and tetragonal[297] crystal forms, as well as by the very anisotropic thermal ellipsoids deduced from X-ray diffraction, which show a pronounced out-of-plane mobility of most atoms in the crystal[48,297]. Ring current calculations usually assume the aromatic system to be planar. The consequences of pronounced deviations from planarity have been discussed only for H_2(TPP) in solution[69], which is well-known for its atypical behavior as compared to naturally-occurring porphyrins and the usual model compounds with β-substituents.

The strong incremental ring current shifts observed as a result of structural modifications that increase steric hindrance in the molecule may be taken as

^{1}Hmr data, with the participation of the lone pair on the nitrogen atom of ring D in the conjugated system in structures protonated at N_4[74]. ^{15}N—^{15}N coupling constants (via the inner hydrogen, Section 10.3.2) provide a direct measure for the importance of this mechanism[33]. Sharing of the proton is most prominent between N_2—N_3, it is less for N_1—N_4, even less for N_1—N_2 and N_3—N_4, and negligible for N_1—N_3 and N_2—N_4. The pronounced differences strongly favor a non-converted mechanism (Fig. 7a) and argue especially against hydrogen exchange between opposite *N*-atoms in the pheophorbides studied.

10.4.2.2. Conformation of β-pyrrole substituents

For certain metal complexes of OEP (Tl^{III},[11]; Pb^{II}, Sn^{II},[190]; Al^{III}, Ga^{III}, In^{III}, Ge^{IV}, Sn^{IV},[169]; Fe^{III},[29]) the methylene protons of the ethyl substituents give rise to a complex signal instead of the usually observed quadruplet. The complex pattern observed for the CH_2-signal in Tl^{III}(OEP) was analyzed by Abraham[186] as an ABR_3X, or better, an ABC_3X spectrum[11] and two different coupling constants of the A and B methylene protons to the central Tl^{III} ion (6.1 and 18.1 Hz) have been determined. Two effects are invoked in the interpretation. The rotation of the ethyl side-chains is slow ($\Delta H \sim 20$ kcal) and probably correlated with its next neighbor, and the central metal ion is in an out-of-plane position[296]. While the out-of-plane metal ion is not expected to affect the rotation to any considerable extent, it does increase the magnetic anisotropy of the (diastereotopic) methylene protons sufficiently for differentiation by ^{1}Hmr. Splitting of β-pyrrole methylene groups in (OEP) complexes is, therfore, an indication of an out-of-plane central metal ion, and/or of asymmetric ligation.

Hindered rotation between two distinct conformers was also advanced to account for split signals in some pheoporphyrins and pheophorbides with 2-CHOH—CH_3 substituents[132]. According to recent results of Brockmann and Trowitzsch[277], aggregation plays an additional role in this phenomenon as to enhance the magnetic anisotropy. These authors studied the effect in some detail for compounds related to the *Chlorobium* chlorophylls, which bear a 1-hydroxyethyl substituent at the 2 position (Section 10.2.8.2). Only one set of signals was found for the pure 2′ epimer, while the racemic mixture gave two sets of signals which merge upon dilution. The splitting can, therefore, be attributed to slow rotation of the side-chain combined with formation of diastereomeric aggregates. Recently, the slow rotation of a methyl group in ferric myoglobin was studied by n.m.r.[296a].

Only few n.m.r. data are available on the preferred conformation of β-pyrrole substituents in solution. From comparison of acyclic and cyclic conjugated substituents, a weaker interaction with the aromatic system was inferred for the former from ^{1}Hmr data (see Section 10.2.2), indicating the presence of non-coplanar conformers. The non-equivalence of ethyl CH_2-protons discussed above was interpreted to arise from preferred conforan indication that the assumption of an essentially planar macrocyclic conjugation system in solution for most porphyrins is justified. Many of the examples in the foregoing sections show, moreover, that the conjugation pathway tends to make adjustments that serve to circumvent steric obstacles effectively. While the conformational analysis and assignment of the basic macrocycle chosen as the reference is therefore somewhat ambiguous, some reasonably successful attempts have been made to correlate incremental n.m.r. shifts with conformational changes of the macrocycle in cases where marked deviations in conformation have been observed.

The ^{1}Hmr spectra of *N*-mono-substituted porphyrins have been interpreted in terms of the effects of steric hindrance[140]. A solution structure was inferred in which the *N*-substituted pyrrole-ring is twisted considerably out-of-plane; the neighboring rings are twisted to a lesser extent in the opposite direction; and, the opposite ring remains essentially in-plane. The X-ray structure of *N*-ethoxycarbonyl-OEP[141] provides convincing support for the first two conclusions. The inclination of 11.7° observed for the opposite pyrrole ring, which is intermediate between the *N*-substituted (19.1°) and its neighboring rings (4.6°, 2.2°) contradicts the third conclusion, but this deviation may arise at least in part from packing[141]. Similar sterically induced conformation changes have been invoked in the interpretation of the n.m.r. spectra of mono-, di- and tri-*N*-alkyl porphyrins and their cations, and the results have been interpreted in terms of the conformation and the rigidity of the ring system[142]. In mono-*meso*-substituted porphyrins, the pronounced decrease of the ring-current and the deshielding of the methine proton opposite to the substituent can be rationalized on the basis of a structure folded like a peaked roof along the axis connecting these two positions (see Section 10.2.3). A recent X-ray analysis[112] of *meso*-benzoyloxy-octaethylporphyrin provided some support for a folded structure, for the macrocycle is considerably folded at the substituted methine position, and, to a lesser extent, at the opposite one. In addition, the entire macrocycle is stretched along the fold, and the inner cavity deformed into a rectangle. A similar roof-shaped structure proposed[169,170] mainly on n.m.r. arguments for α,γ-dimethyl-β,γ-porphodimethenes (63) in solution was supported as well by a crystal structure determination[171]. The conformational changes resulting from δ-substitution are especially pronounced in the more flexible reduced ring D of 7,8 chlorins, which provides independent proof of the 7,8-*trans* configuration of the hydrogen atoms of the pyrroline ring D[124].

10.4.3.2. *Metalloporphyrins*

Two other types of stereochemical effects become important in metalloporphyrins. The metal ion can be out-of-plane, and it can be ligated in various distinct ways (Fig. 9). The position of the central metal ion with respect to the macrocycle is determined by the ionic radius of the metal ion

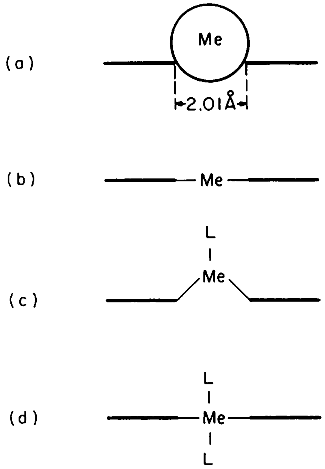

Fig. 9. Stereochemistry of metalloporphyrins. (a) Metal ion considerably larger than 2.01 Å diameter, e.g., Pb^{II} (Refs. 109,191); (b) metal ion $\leqslant$2.01 Å diameter, no axial ligands; (c) metal ion $\leqslant$2.01 Å diameter, one axial ligand; and (d), metal ion $\leqslant$2.01 Å diameter, 2 axial ligands. (See also Tables 21 and 25.) Schematic representation, viewed parallel to the plane of the macrocycle.

and the mode of ligation. The diameter of the central cavity of the macrocycle is fairly restricted[48,298] and the porphyrin cannot easily accomodate metal ions with an ionic radius significantly larger than 2.01 Å (Fig. 9a). Below this critical ionic radius, the type of coordination essentially determines whether the metal is in-plane or out-of-plane. Square planar and tetragonal bipyramidal configuration have the metal ion in-plane (Fig. 9b,d), while in the tetragonal pyramidal configuration (Fig. 9c) the axial ligand forces the metal out-of-plane. (See, for example, Ref. 17 and citations therein.) A qualitative indication for an out-of-plane metal ion is the splitting observed for the *o*-phenyl proton signals in (TPP) metal complexes, and for the multiplicity of the methylene proton signals in the ^{1}Hmr spectra of H_2(OEP) complexes (Section 10.4.2); in H_2(TPP), the splitting is due to hindered rotation[201,302]. Although the methylene protons of the (OEP) complexes are diastereotopic per se, their magnetic non-equivalence is enhanced by the out-of-plane position of the metal and by a correlated rotation of neighboring ethyl groups[186]. A quantitative estimate of the extent of metal ion displacement is possible from the ring-current induced ^{1}Hmr chemical shifts of ligand protons bound in the metal axial positions[16,17,51,52]. Assuming pyridine to be ligated at right angles to the macrocycle in metalloporphyrin-pyridinates, the incremental shift of the 4-pyridine proton can be used to estimate the distance of the ligand from the porphyrin plane. With the metal-N distance and the pyridine geometry well established from known pyridine compounds, the apparent N-to-metal ion distance deduced from ^{1}Hmr makes an estimate of the metal displacement from the macrocycle possible[17]. In Co^{III} (Meso-IX-DME), the metal ion is essentially in plane, while Zn(TPP) and Mg(TPP) have metal ions that are out-of-plane by 0.3—0.5 Å and 0.7—0.8 Å, respectively. Ring current arguments can also be used to estimate the plane-to-plane distances in layered structures with two or more metalloporphyrins parallel to each other (see Section 10.2.8.3).

With metal ions that can assume a paramagnetic state, the ligand field may determine the spin state, which thus can serve as a probe for the metal coordination type (see Section 10.2.8.5 for leading references). Axial ligation of square-planar, diamagnetic Ni-etioporphyrin leads to a paramagnetic tetragonal pyramidal complex[10], and similar behavior is found for Fe^{II} porphyrin complexes when one of the two axial ligands of low-spin Fe^{II} complexes is removed. In Fe^{III} complexes, both the five and six-coordinate states are paramagnetic, but they show differences characteristic of their ligand field. In most cases, even with different axial substituents, a clearly defined spin state is present, but a high-spin, low-spin mixture is often observed for azidohemins[22,246].

10.4.3.3. Non-centrosymmetric stereoisomerism

An interesting new case of stereoisomerism in porphyrins was recently observed by Hudson et al.[219]. The diporphinato-trimercury complex (82) of Etio-I was shown to exist in two diastereomeric forms. In the racemic forms, the two porphyrins are ligated 'face to face', in the meso form they are ligated 'face to back' (Fig. 10). Obviously, isomerism of this kind is not dependent on hindered rotation of the porphyrins around their common axis, and similar isomers are possible for all porphyrins that do not possess a

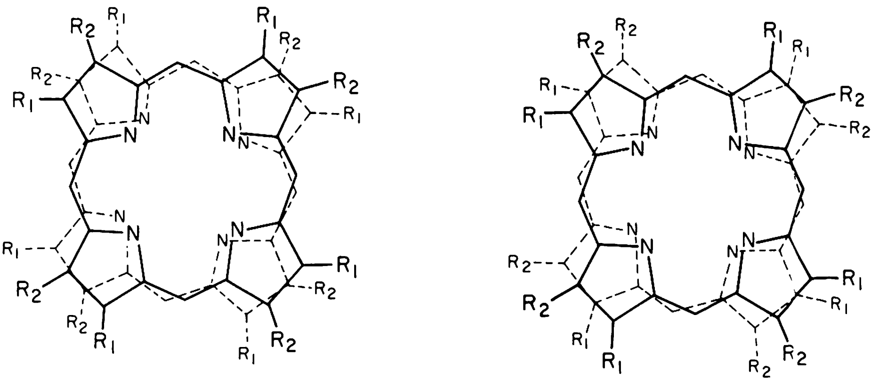

- racemic -

- meso -

Fig. 10. Stereoisomerism in porphyrin dimers with structures similar to (32). For details, see text.

σ_v plane, as for instance, Copro-I and -III, but not Copro-II or -IV. This type of isomerism is generally possible in all diporphinato complexes and could be valuable in studying porphyrin—ligand exchange reactions in these molecules. Such isomerism is likewise a possibility in porphyrin π—π dimers present in concentrated solutions, and may be an alternative explanation (in addition to lateral displacement)[6] for the additional fine structure observed in the ^{1}Hmr spectra of some of porphyrin self-aggregates.

In phenyl-substituted H_2(TPP) derivatives, the hindered rotation around the methine—phenyl bond leads to the possibility of atropisomerism[302]. *meso*-Tetra-*o*-tolyl—porphyrin shows a complex pattern for the *o*-CH_3 resonances, which was attributed by Walker[299] to originate from a statistical mixture of the four possible atropisomers. Recently, the four *meso*-tetra-*o*-aminophenyl—porphyrins have been separated and characterized by ^{1}Hmr[300]. Both the tolyl and *o*-amino H_2(TPP) isomers are stable at room temperature, and even at 180°C no indication of line broadening is observed[299] (see Section 10.4.2).

10.4.3.4. *Asymmetric carbon atoms*

In fully unsaturated porphyrins all macrocyclic carbon atoms are sp^2 hybridized, but asymmetric C-atoms can result from introduction of substituents, or formed by reduction of the macrocycle system to the chlorin or porphodimethene states among others. Pheoporphyrins with one asymmetric C-atom of defined configuration were first described by Wolf et al.[126,138]. The low signal-to-noise ratio of their ORD spectra made the determination of enantiomeric purity difficult, but this problem can be overcome by an absolute determination of enantiomeric purity of the compounds by ^{1}Hmr[126]. In a chiral enantiomeric environment, previously enantiotopic (i.e., indistinguishable by ^{1}Hmr), protons become diastereotopic and thus, in principle, distinguishable by n.m.r.[304a]. This effect was studied in a variety of compounds in chiral aromatic solvents (for leading references, see Ref. 304). The pronounced aggregation exhibited by porphyrins made it possible to use the conventional achiral solvent ($CDCl_3$) and adding a chiral porphyrin as co-solute, which form diastereotopic aggregates with the porphyrin enantiomers. The n.m.r. spectra of the chiral pheoporphyrin showed sufficient differences in the methine region in the presence of excess pyromethylpheophorbide-*a* (with the natural 7S, 8S configuration) to distinguish between the R and S form of the pheoporphyrins, and thus to determine the enantiomeric purity by integration of the appropriate signals[126]. In a similar case, the pronounced aggregation of 2-(α-hydroxyethyl)pheoporphyrins caused by hydrogen-bonding was shown[213] to be responsible for the splitting observed for most of the ^{1}Hmr signals[132]. This splitting occurs only for 2a-epimeric mixtures, but not for the pure epimers[213]. Splitting thus reflects diastereomeric aggregates, in which the chemical shift differences are enhanced by specific aggregation of the systems and by hindered rotation at the 2—2a bond (see Section 10.4.2.2).

The stereochemistry of peripherally-reduced porphyrins has been studied extensively because of their relevance to the chlorophylls. The 7,8-*trans* figuration of the chlorophylls suggested by the racemization experiments of Fischer and Gibian[305] was proved by chromic acid degradation[306,307], and by the small *transoid* vicinal coupling constant ($J \leqslant 2$ Hz) of the 7,8 protons[13]. In the model compound H_2(OEC) the 'extra' hydrogen atoms in the reduced pyrroline ring are essentially equivalent and thus show no coupling, and in some other pheophorbides with unnatural configuration, the 7,8 coupling constants were not observable. In these cases, however, the *cis* and *trans* isomers can be differentiated by other differences in their n.m.r. spectra[126]. In the *cis*-H_2(OEC), the ring current is somewhat reduced by steric hindrance in the *cis* ethyl groups as compared to the *trans* epimer[65,308], and the altered coupling pattern of the extra hydrogen atoms with the neighboring methylene protons indicates a change in the conformation of the reduced ring[126]. The differences between the epimers are much more pronounced in 7,8-*cis* as compared to 7,8-*trans*-mesopyromethylpheophorbide[126]. In the 7,8-*cis* compound, all proton signals, especially those from protons in the vicinity of the reduced ring D, are shifted to higher field. An additional characteristic difference in the pyropheophorbide compounds is the increased anisochrony of the 10-methylene* protons in the 7,8-*cis* ($\Delta(H_\beta - H_\alpha)$ = 0.38 p.p.m.) as compared to the 7,8-*trans* epimer ($\Delta(H_\beta - H_\alpha)$ = 0.11 p.p.m.)[126]. Obviously, the shielding effect of the *transoid* 7,8-alkyl side-chains in the *trans*-pheophorbide are partially compensated. An indirect approach to the relative configuration of chlorins is possible by analysis of the induced conformational changes that result from introduction of a large substituent at a neighboring *meso*-position[124]. Because of the steric interaction of the δ-substituent with the 8-CH_3 group in δ-Cl-chlorin-e_6 trimethyl ester, ring D is tilted out of the macrocycle plane, and the high field shift of both the 8-CH_3 and the 7-H signals thus proves their *cisoid* relationship. Similar changes have recently been observed by perturbation of the γ-position in peripheral complexes of pheophorbides[80] (see Section 10.2.8.4).

In cyclopropano-chlorins and -bacteriochlorins[66] the chlorin substituents are necessarily in the *cis* configuration. The endo- and exo-positions of the cyclopropane substituents show characteristic differences in chemical shift arising from the anisotropy of the ring current shift. Exo-substituents are essentially in the plane of the macrocycle and are thus strongly deshielded, while the endo-substituents are above the plane and resonate at substantially higher field. In the case of protons, a further additional assignment is possible on the basis of coupling constants with the chlorin protons[66].

---

* α and β are used as in terpenes, α designating a substituent below, β a substituent above the plane in the structure shown the conventional way.

Most chlorophylls possess an additional asymmetric center at C-10 in the isocyclic ring E, whose configuration can be linked to that at C-7 and C-8 by means of incremental substituent shifts[138]. For chlorophyll-*a*, the *transoid* configuration of the 7 and 10 substituents was suggested on the basis of the high field shift of the 7-H signal (relative to that of the 8-H) due to the shielding by carbonyl groups in the 10-$COOCH_3$ substituent. This interpretation is somewhat ambiguous because the incremental shift of the anisotropic ester group is difficult to estimate, and because only one of the epimers is readily available in pure form. The *transoid* configuration was proved by a combined ^{1}Hmr and spectropolarimetric[307a] investigation of diastereomeric 10-alkoxy pheophorbides[79,138]. In these compounds, the conformation of the C-10 atom is stabilized, and the two C-10 epimers can thus be studied separately.

With the assumption that incremental shifts are more pronounced for *cisoid* than for *transoid* substituents, the relative position of two substituents can then be determined by n.m.r. as shown in the following example (Fig.

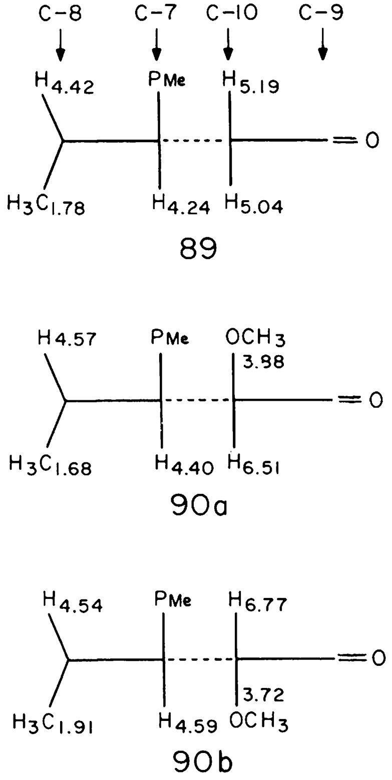

Fig. 11. ^{1}Hmr chemical shifts (δ[p.p.m.] from TMS) of pyromethylpheophorbide-*a* (89), and its enantiomeric (R,S)-methoxy derivatives (90a,b). Schematic representation of the periphery of rings D and E, viewed parallel to the macrocycle (see Ref. 79).

11). Substitution of one of the 10-H protons in pyromethylpheophorbide-*a* (89) by —OCH_3 causes shifts of the 7-H proton signal by —0.16 (—0.35) p.p.m., the 8-H quadruplet by —0.15 (—0.12) p.p.m., and the 8-CH_3 doublet by +0.10 (—0.13) p.p.m. in the two epimers (90a) and (90b). Obviously, the 10-OCH_3 substituent has a pronounced deshielding effect on the neighboring ring protons. This effect is expected to be more pronounced for *cisoid* than for *transoid* substituents, and from the relative magnitude of the shifts *cisoid* configuration to the 8-H can be inferred in the epimer (90a), *cisoid* configuration to the 7-H and 8-CH_3 in the epimer (90b). The different incremental shifts observed for both positions of the 10-OCH_3 groups (i.e., the positive increment for the 8-CH_3 resonance in 90a), indicate that the substituent shifts are accompanied by pronounced shifts due to other (conformational) reasons, clearly demonstrating that an unambiguous analysis requires data on both epimers. In the same way as the configuration at C-10 affects the chemical shifts of the substituents at C-7 and C-8, the configuration at C-7 affects (but to a lesser extent) the chemical shift of the substituents at C-10. Thus, in the compounds cited above the 10-OCH_3 is more strongly deshielded when *cisoid* to the propionic ester side-chain than when it is *transoid* to it, and the stereochemical assignment of the non-equivalent 10-methylene protons in pyropheophorbides[79] and in the chlorophyll 'prime' epimers (i.e., Chl-*a*′, Section 10.2.8.2)[215] can be carried out in the same way. Similar relationships have been observed for the pheophorbide-*b* series as well[309], and the effects are characteristic of a wide variety of 10-alkoxy pheophorbides[130,138].

The configuration of C-9 in 9-desoxo-9-hydroxy-pheophorbides can be linked to that at C-10 in an analogous manner, and the reciprocal influence can again be detected by a careful analysis of the n.m.r. signals[125,130]. In the case of the diastereomeric 9-desoxo-9-hydroxy-methylpheophorbides-*a* (91a—c) (Table 12) the relative configuration at C-9 and C-10 is also deducible from the 9-H, 10-H coupling constants (7 Hz for 9,10-*cis* as compared to ⩽2 Hz for 9,10-*trans*)[125].

In a different approach, configuration correlations can be made by studying specific intramolecular interactions. Hydrogen-bonding of a 9-OH group with substituents at C-10 leads to a broadening of the 9-H signals from residual HCOH coupling, which is removed upon deuterium exchange of the 9-OH group[125,130]. This broadening is obviously characteristic of a hydrogen bond of intermediate strength, for both weak and strong hydrogen bonds are expected to yield sharp signals, with the latter showing a distinct coupling constant[310]. Gradual changes in the strength of the hydrogen bonds as explified in the ^{1}Hmr spectra can be expected to be correlated with the O—H stretch frequency in the infrared spectra[125,130]. In favorable cases, hydrogen-bonding is not only observed to occur between the 9-OH group and the neighboring groups, but also with the carbonyl function in the 7-propionic side-chain (91b)[125,136].

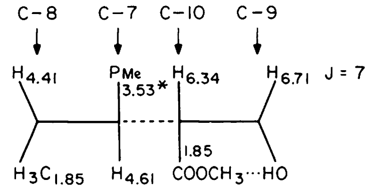
C-8
C-7
C-10
C-9
H4.41
PMe
3.53*
H6.34
H6.71
J = 7
1.85
H3C1.85
H4.61
COOCH3···HO

91a

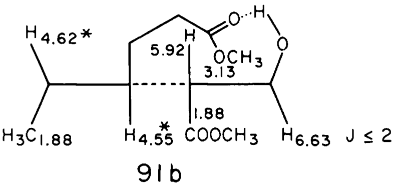
H4.62*
5.92
H
O···H
O
OCH3
3.13
1.88
H3C1.88
H4.55*
COOCH3
H6.63
J ≤ 2

91b

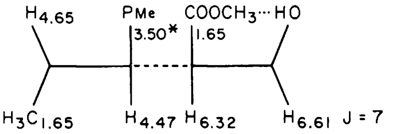
H4.65
PMe
3.50*
COOCH3···HO
1.65
H3C1.65
H4.47
H6.32
H6.61
J = 7

91c

Fig. 12. ^{1}Hmr chemical shifts (δ[p.p.m.] from TMS) of the diastereomeric 9-desoxo-9(R,S)-hydroxy-10(R,S)-methylpheophorbides-*a* (91a,b,c). Schematic representation as in Fig. 11. (See Ref. 125.)

10.4.4. Miscellaneous

^{1}Hmr has been widely used in mechanistic studies by monitoring the ^{1}H/^{2}H exchange with the medium. Pertinent examples include the nucleophilic exchange of the methine protons in acidic media[56,78,144,163,207,209] and during and after metalation[135,311], the exchange of benzylic protons[79,127,135,138,215] and substituents[130], the phlorin-chlorin and related equilibria[57.93,103,121,123,164], the photochemical[90,126,173,311a] and electrochemical[312] reduction of porphyrins and redox processes in hemins[313].

^{1}Hmr has often been used as a decisive tool to distinguish between isomers. For the application of symmetry arguments, the reader is referred to standard monographs[1] as well as to examples cited in Section 10.2.2, 10.2.3, 10.2.8, and 10.4.3.

The application of stable isotopes (^{2}H, ^{13}C, ^{15}N) in conjuction with n.m.r. measurements is of increasing interest in biosynthetic studies. The method is superior to radioactive labeling because the position *and* the amount of the label can be measured directly, provided the n.m.r. resonances are assigned. In a pair of mirror image experiments, ^1H_2O plus succinic acid-$^2H_4$ vs. ^2H_2O + succinic acid-$^1H_4$, the incorporation of $^1H(^2H)$ from the succinic acid and the medium into bacteriochlorophyll-*a* was studied[314], and recently the ^{13}C pathway in Proto-IX biosynthesis was investigated by ^{13}Cmr[35,261,262] (see also Chapter 3).

The photo-oxidation of chlorophyll with quinones has been studied[315] by chemical induced dynamic nuclear polarization[316] of the quinone resonances, and selective ^{1}Hmr line-broadening as a result of triplet energy transfer in photo-excited methyl pyropheophorbide-*a* makes possible the assignment of hyperfine coupling constants in the triplet[317].

Acknowledgments

H.S. acknowledges the grant of a Research Stipendiate from the Deutsche Forschungsgemeinschaft, Bonn-Bad Godesberg. We thank Dr. Thomas R. Janson for helpful discussions in preparing this manuscript. We are indebted to all who have communicated unpublished work.

References

1. L.M. Jackmann, 'Applications of NMR Spectroscopy in Organic Chemistry', 2nd ed., Pergamon, New York (1969); J.A. Pople, W.G. Schneider, and H.J. Bernstein, 'High Resolution NMR', McGraw-Hill, New York (1959); E.D. Becker, 'High Resolution NMR, Theory and Chemical Applications', Academic Press, New York (1969); F.A. Bovey, 'NMR Spectroscopy', Academic Press, New York (1969); J.W. Emsley, J. Feeney, and L.H. Sutcliffe, 'High Resolution NMR Spectroscopy', Pergamon, New York (1965—66).
2. (a) E.D. Becker and R.B. Bradley, J. Chem. Phys., **31**, 1413 (1959).
2. (b) J. Ellis, A.H. Jackson, G.W. Kenner, and J. Lee, Tetrahedron Lett., 23 (1960).
3. R.J. Abraham, Mol. Phys., **4**, 145 (1961).
4. W.S. Caughey and W.S. Koski, Biochemistry, **1**, 923 (1962).
5. K.M. Smith, Quart. Rev., **25**, 31 (1971).
6. R.J. Abraham, P.A. Burbidge, A.H. Jackson, and D.B. Macdonald, J. Chem. Soc., 620 (1966).
7. R.J. Abraham, P.A. Burbridge, A.H. Jackson, and G.W. Kenner, Proc. Chem. Soc., London, 134 (1963).
8. R.J. Abraham, G.H. Barnett, E.S. Bretschneider, and K.M. Smith, Tetrahedron, **29**, 553 (1973).
8. (a) R.J. Abraham, A.H. Jackson, G.W. Kenner, and D. Warburton, J. Chem. Soc., 853 (1963).
8. (b) R.J. Abraham, A.H. Jackson, and G.W. Kenner, J. Chem. Soc., 3468 (1961).
9. R.J. Abraham, G.E. Hawkes, and K.M. Smith, J. Chem. Soc., Chem. Commun., 401 (1973).
10. R.J. Abraham and P.F. Swinton, J. Chem. Soc. C, 903 (1969).
11. R.J. Abraham, G.H. Barnett, and K.M. Smith, J. Chem. Soc., Perkin Trans. 1, 2142 (1973).

12. H.H. Inhoffen, J.W. Buchler, and P. Jäger, Fortschr. Chem. Org. Naturst., **26**, 785 (1968).
13. G.L. Closs, J.J. Katz, F.C. Pennington, M.R. Thomas, and H.H. Strain, J. Am. Chem. Soc., **85**, 3809 (1963).
14. H.A.O. Hill, P.J. Sadler, R.J.P. Williams, and C.D. Barry, Ann. N.Y. Acad. Sci., **206**, 247 (1973).
15. J.E. Maskasky and M.E. Kenney, J. Am. Chem. Soc., **93**, 2060 (1971).
16. C.B. Storm and A.H. Corwin, J. Org. Chem., **29**, 3700 (1964).
17. C.B. Storm, J. Am. Chem. Soc., **92**, 1423 (1970).
18. J.E. Maskasky, J.R. Mooney, and M.E. Kenney, J. Am. Chem. Soc., **94**, 2132 (1972).
19. J.E. Maskasky and M.E. Kenney, J. Am. Chem. Soc., **95**, 1443 (1973).
20. A. Kowalsky, Biochemistry, **4**, 2382 (1965); A. Kowalsky, 'Hemes and Hemoproteins,' 529 (1966).
21. W.D. Philips, in 'NMR of Paramagnetic Molecules', Eds. G.N. LaMar, W. DeW. Horrocks Jr., and R.H. Holm, Academic Press, New York (1973), p. 422.
22. K. Wüthrich, Struct. Bonding Berlin, **8**, 53 (1970).
23. R.J. Kurland, R.G. Little, D.G. Davis, and C. Ho, Biochemistry, **10**, 2237 (1971).
24. T.R. Janson, L.J. Boucher, and J.J. Katz, J. Am. Chem. Soc., **92**, 2725 (1970).
25. R.G. Shulman, S.H. Glarum, and M. Karplus, J. Mol. Biol., **57**, 93 (1971).
26. G.N. LaMar and F.A. Walker, J. Am. Chem. Soc., **95**, 6950 (1973).
27. G.N. LaMar and F.A. Walker, J. Am. Chem. Soc., **95**, 1782 (1973).
28. G.N. LaMar and F.A. Walker, J. Am. Chem. Soc., **95**, 1790 (1973).
29. G.N. LaMar, G.R. Eaton, R.H. Holm, and F.A. Walker, J. Am. Chem. Soc., **95**, 63 (1973).
30. G.C. Levy and G.L. Nelson, '^{13}C Nuclear Magnetic Resonance for Organic Chemists', Wiley, New York (1972); J.B. Stothers, '^{13}C NMR Spectroscopy', Academic Press, New York (1972).
31. H. Günther, H. Schmickler, H. Königshofen, K. Recker, and E. Vogel, Angew. Chem., **85**, 261 (1973); R. du Vernet and V. Boekelheide, Proc. Nat. Acad. Sci. U.S.A., **71**, 2961 (1974).
32. R.J. Abraham, G.E. Hawkes, and K.M. Smith, J. Chem. Soc., Perkin Trans. 2, 627 (1974).
33. S.G. Boxer, G.L. Closs, and J.J. Katz, J. Am. Chem. Soc., **96**, 7058 (1974).
34. D. Doddrell and W.S. Caughey, J. Am. Chem. Soc., **94**, 2510 (1972).
35. A.R. Battersby, G.L. Hodgson, M. Ihara, E. McDonald, and J. Saunders, J. Chem. Soc., Perkin Trans. 1, 2923 (1973).
36. N.A. Matwiyoff and B.F. Burnham, Ann. N.Y. Acad. Sci., **206**, 365 (1973); C.E. Strouse, V.H. Kollman, and N.A. Matwiyoff, Biochem. Biophys. Res. Commun., **46**, 328 (1972).
37. J.J. Katz and T.R. Janson, Ann. N.Y. Acad. Sci., **206**, 579 (1973).
38. A. Carrington and A.D. McLachlan, 'Introduction to Magnetic Resonance', Harper and Row, New York (1967).
39. L. Pauling, J. Chem. Phys., **4**, 673 (1936).
40. T.R. Janson, 'The Ring-Current Effect of the Phthalocyanine Ring', Dissertation, Case Western Reserve University, Univ. Microfilms, Ann Arbor, 72-51, (1971).
41. R.C. Haddon, V.R. Haddon, and L.M. Jackman, Fortschr. Chem. Forsch., **16**, 103 (1971).
42. J.A. Pople, J. Chem. Phys., **24**, 1111 (1956).
43. J.S. Waugh and R.W. Fessenden, J. Am. Chem. Soc., **79**, 846 (1957).
44. C.E. Johnson, Jr. and F.A. Bovey, J. Chem. Phys., **29**, 1012 (1958).
45. F. London, J. Phys. Radium, **8**, 397 (1937).
46. J.A. Pople, Mol. Phys., **1**, 175 (1958).
47. R. McWeeny, Mol. Phys., **1**, 311 (1958).

48. E.B. Fleischer, Acc. Chem. Res., **3**, 105 (1970).
48. (a) G.G. Hall and A. Hardisson, Proc. Roy. Soc. London, Ser. A, **268**, 328 (1962).
48. (b) V.M. Mamaev, G.V. Ponomarev, S.V. Zenin and R.P. Evstigneeva, Teor. Eksp. Khim. **6**, 60 (1970).
49. J.H. Fuhrhop, Angew. Chem., **86**, 363 (1974).
50. J.F.M. Oth, H. Baumann, J.M. Gilles, and G. Schröder, J. Am. Chem. Soc., **94**, 3498 (1972).
51. J.J. Katz, H.H. Strain, D.L. Leussing, and R.C. Dougherty, J. Am. Chem. Soc., **90**, 784 (1968).
52. T.R. Janson, A.R. Kane, J.F. Sullivan, K. Knox, and M.E. Kenney, J. Am. Chem. Soc., **91**, 5210 (1969).
53. F. Sondheimer, Proc. Roy. Soc. London, Ser. A, **297**, 173 (1967).
54. I.C. Calder, P.J. Garratt, and F. Sondheimer, Chem. Commun., 41 (1967).
55. A.M. Shulga, Biofizika, **18**, 32 (1973); Transl. **18**, 30 (1973).
56. M.J. Broadhurst, R. Grigg, and A.W. Johnson, Chem. Commun., 1480 (1969).
57. M.J. Broadhurst, R. Grigg, and A.W. Johnson, Chem. Commun., 807 (1970).
58. C.O. Bender, R. Bonnett, and R.G. Smith, J. Chem. Soc. D, 345 (1969).
59. J.J. Katz, in 'Inorganic Biochemistry,' Ed. G. Eichhorn, Elsevier (1973), p. 1022.
60. K.N. Solov'ev, V.A. Mashenkov, A.T. Gradyushko, A.E. Turkova, and V.P. Lezina, J. Appl. Spectrosc. USSR, **13**, 1106 (1970).
61. A.M. Ponte Goncalves and R.A. Gottscho, J. Am. Chem. Soc., in press.
62. P.S. Clezy, V. Diakiw, and A.J. Liepa, Aust. J. Chem., **25**, 201 (1972).
63. T.S. Srivastava, C.-P. Hrung, and M. Tsutsui, J. Chem. Soc., Chem. Commun., 447 (1974).
64. D. Dolphin, R.H. Felton, D.C. Borg, and J. Fajer, J. Am. Chem. Soc., **92**, 743 (1970).
65. H.W. Whitlock, Jr., R. Hanauer, M.Y. Oester, and B.K. Bower, J. Am. Chem. Soc., **91**, 7485 (1969).
66. H.J. Callot, Tetrahedron Lett., 1011 (1972).
67. T.R. Janson, H. Scheer, and J.J. Katz, unpublished results.
68. T.R. Janson and J.J. Katz, J. Magn. Reson., **6**, 209 (1972).
69. R.J. Abraham, G.E. Hawkes, and K.M. Smith, Tetrahedron Lett., 71 (1974).
70. A.D. Adler, F.R. Longo, J.D. Finarelli, J. Goldmacher, J. Assour, and L. Korsakoff, J. Org. Chem., **32**, 476 (1967).
71. H.H. Inhoffen, J.H. Fuhrhop, H. Voight, and H. Brockmann Jr., Ann. Chem., **695**, 133 (1966).
72. H.H. Inhoffen, G. Klotmann, and G. Jeckel, Ann. Chem., **695**, 112 (1966).
73. G. Jeckel, Dissertation, Technische Hochschule Braunschweig, West Germany (1967).
74. C.B. Storm, Y. Teklu, and E.A. Sokolski, Ann. N.Y. Acad. Sci., **206**, 631 (1973).
75. C. Storm and Y. Teklu, J. Am. Chem. Soc., **94**, 1745 (1972).
76. R.J. Abraham, G.E. Hawkes, and K.M. Smith, Tetrahedron Lett., 1483 (1974).
77. R.B. Woodward, Pure Appl. Chem., **2**, 383 (1961).
78. R.B. Woodward and Škarić, J. Am. Chem. Soc., **83**, 4676 (1961).
79. H. Wolf, H. Brockmann Jr., H. Biere, and H.H. Inhoffen, Ann. Chem., **704**, 208 (1967).
80. H. Scheer and J.J. Katz, unpublished results.
80. (a) H. Scheer and J.J. Katz, J. Am. Chem. Soc., in press.
81. P.S. Clezy and A.J. Liepa, Aust. J. Chem., **24**, 1027 (1971).
82. R. Chong and P.S. Clezy, Aust. J. Chem., **20**, 951 (1967).
83. P.S. Clezy and N.W. Webb, Aust. J. Chem., **25**, 2217 (1972).
84. P.S. Clezy, A.J. Liepa, and N.W. Webb, Aust. J. Chem., **25**, 2687 (1972).
85. P.S. Clezy, A.J. Liepa, and N.W. Webb, Aust. J. Chem., **25**, 1991 (1972).
86. H.H. Inhoffen, H. Brockmann Jr., and K.M. Bliesener, Ann. Chem., **730**, 173 (1969).

87. H. Fischer, and A. Kirstahler, Hoppe-Seyler's Z. Physiol. Chem., **198**, 43 (1931); H. Fischer and G. Wecker, Hoppe-Seyler's Z. Physiol. Chem., **272**, 1 (1941).
88. P.S. Clezy and V. Diakiw, J. Chem. Soc., Chem. Commun., 453 (1973).
89. M.T. Cox, A.H. Jackson, G.W. Kenner, S.W. McCombie, and K.M. Smith, J. Chem. Soc., Perkin Trans. 1, 516 (1974).
90. H. Scheer and H. Wolf, Ann. Chem., 1741 (1973).
91. G.L. Collier, A.H. Jackson, and G.W. Kenner, J. Chem. Soc. C, 66 (1967).
92. A.H. Jackson, G.W. Kenner, and G.S. Sach, J. Chem. Soc. C, 2045 (1967).
93. A.H. Jackson, G.W. Kenner, and K.M. Smith, J. Chem. Soc. C, 302 (1968).
94. G.W. Kenner, S.W. McCombie, and K.M. Smith, Ann. Chem., 1329 (1973).
95. J.A.S. Cavaleiro, G.W. Kenner, and K.M. Smith, J. Chem. Soc., Perkin Trans. 1, 2478 (1973).
96. A.H. Jackson, G.W. Kenner, and J. Wass, J. Chem. Soc. Perkin Trans. 1, 480 (1974).
97. T.T. Howarth, A.H. Jackson, and G.W. Kenner, J. Chem. Soc., Perkin Trans. 1, 502 (1974).
98. G.W. Kenner, S.W. McCombie, and K.M. Smith, J. Chem. Soc., Perkin Trans. 1, 527 (1974).
98. (a) M.T. Cox, T.T. Howarth, A.H. Jackson, and G.W. Kenner, J. Chem. Soc., Perkin Trans. 1, 512 (1974).
99. R.V.H. Jones, G.W. Kenner, and K.M. Smith, J. Chem. Soc., Perkin Trans. 1, 531 (1974).
100. H.J. Callot, Tetrahedron, **29**, 899 (1973).
101. H.J. Callot, Bull. Soc. Chim. Fr., 1492 (1974).
102. P. Burbidge, G.L. Collier, A.H. Jackson, and G.W. Kenner, J. Chem. Soc. C, 930 (1967).
103. A.W. Johnson and D. Oldfield, Tetrahedron Lett., 1549 (1964).
104. R. Bonnett and G.F. Stephenson, J. Org. Chem., **30**, 2791 (1965).
105. H.H. Inhoffen and A. Gossauer, Ann. Chem., **723**, 135 (1969).
106. P.S. Clezy and V. Diakiw, Aust. J. Chem., **24**, 2665 (1971).
106. (a) R. Bonnett, M.J. Dimsdale, and G.F. Stephenson, J. Chem. Soc. C, 564 (1969).
107. P.S. Clezy and A.J. Liepa, Aust. J. Chem., **23**, 2477 (1970).
108. P.S. Clezy and A.J. Liepa, Aust. J. Chem., **23**, 2461 (1970).
109. P.S. Clezy, A.J. Liepa, and G.A. Smythe, Aust. J. Chem., **23**, 603 (1970).
110. R. Bonnett, M.J. Dimsdale, and K.D. Sales, J. Chem. Soc., Chem. Commun., 962 (1970).
111. J.-H. Fuhrhop, S. Besecke, and J. Subramaniam, J. Chem. Soc., Chem. Commun., 1 (1973).
112. M.B. Hursthouse and S. Neidle, J. Chem. Soc., Chem. Commun., 449 (1972).
113. J.-H. Fuhrhop, Dissertation, Technische Hochschule Braunschweig, West Germany (1966).
114. R.Bonnett, I.A.D. Gale, and G.F. Stephenson, J. Chem. Soc. C, 1600 (1966).
115. R. Grigg, Chem. Commun., 1238 (1967).
116. G.H. Barnett, M.F. Hudson, S.W. McCombie, and K.M. Smith, J. Chem. Soc., Perkin Trans. 1, 691 (1973).
117. R. Bonnett and M.J. Dimsdale, J. Chem. Soc., Perkin Trans. 1, 2540 (1972).
118. M.T. Cox, A.H. Jackson, and G.W. Kenner, J. Chem. Soc. C, 1974 (1971).
119. J.W. Buchler and L. Puppe, Ann. Chem., **740**, 142 (1970).
120. D. Dolphin, J. Heterocycl. Chem., **7**, 275 (1970).
121. P.S. Clezy and C.J.R. Fookes, J. Chem. Soc., Chem. Commun., 1268 (1971).
122. O. Somaya, Dissertation, Technische Hochschule Braunschweig, West Germany, 1967.
123. P.S. Clezy and G.A. Smythe, Chem. Commun., 127 (1968).
124. G. Brockmann and H. Brockmann jr., IIT NMR Newsletter, 117-62 (1968).

125. H. Wolf and H. Scheer, Ann. Chem., **745**, 87 (1971).
126. H. Wolf and H. Scheer, Ann. Chem., 1710 (1973).
127. C.D. Mengler, Dissertation, Technische Hochschule Braunschweig, West Germany (1966).
128. M.S. Fischer, Ph.D. Dissertation, University of California, Berkeley (1969), (UCLR-19524); J. Gassmann, I. Strell, F. Brandl, M. Sturm, and W. Hoppe, Tetrahedron Lett., 4609 (1971); R.C. Petersen and L.E. Alexander, J. Am. Chem. Soc., **90**, 3873 (1968); R.C. Petersen, J. Am. Chem. Soc., **93**, 5629 (1971).
129. F.C. Pennington, H.H. Strain, W.A. Svec, and J.J. Katz, J. Am. Chem. Soc., **89**, 3875 (1967).
130. H. Wolf and H. Scheer, Tetrahedron, **28**, 5839 (1972).
131. H. Brockmann, K.-M. Bliesener, and H.H. Inhoffen, Ann. Chem., **718**, 148 (1968).
132. H. Scheer, Dissertation, Technische Universität Braunschweig, West Germany (1970).
133. J. Bode, Dissertation, Technische Universität Braunschweig, West Germany (1972).
134. I. Richter, Dissertation, Technische Universität Braunschweig, West Germany, (1969).
135. H. Scheer, unpublished results.
136. H. Brockmann jr. and J. Bode, Ann. Chem., 1017 (1974).
137. G.W. Kenner, S.W. McCombie, and K.M. Smith, J. Chem. Soc., Perkin Trans. 1, 2517 (1973).
138. H. Wolf, H. Brockmann jr., I. Richter, C.-D. Mengler, and H.H. Inhoffen, Ann. Chem., **718**, 162 (1968).
139. R.C. Dougherty, H.H. Strain, W.A. Svec, R.A. Uphaus, and J.J. Katz, J. Am. Chem. Soc., **92**, 2826 (1970).
140. W.S. Caughey and P.K. Ibers, J. Org. Chem., **28**, 269 (1963).
141. G.M. McLaughlin, J. Chem. Soc., Perkin Trans. 2, 136 (1974).
142. A.H. Jackson and G.R. Dearden, Ann. N.Y. Acad. Sci., **206**, 151 (1973).
143. H.H. Inhoffen and W. Nolte, Tetrahedron Lett., 2185 (1967); H.H. Inhoffen and W. Nolte, Ann. Chem., **725**, 167 (1969).
143. (a) R. Grigg, G. Shelton, A. Sweeney, and A.W. Johnson, J. Chem. Soc., Perkin Trans. 1, 1789 (1972).
143. (b) P. Batten, A. Hamilton, A.W. Johnson, G. Shelton, and D. Ward, J. Chem. Soc., Chem. Commun., 550 (1974).
143. (c) D.K. Lavallee and A.E. Gebala, Inorganic Chem., **13**, 2004 (1974).
144. R. Bonnett, I.A.D. Gale, and G.F. Stephenson, J. Chem. Soc. C, 1168 (1969).
145. J.-H. Fuhrhop and T. Lumbantobing, Tetrahedron Lett., 2815 (1970).
146. H.H. Inhoffen, J.W. Buchler, and R. Thomas, Tetrahedron Lett., 1141 (1969).
147. R. Thomas, Dissertation, Technische Hochschule Braunschweig, West Germany (1967).
148. D.G. Whitten and J.C.N. Yau, Tetrahedron Lett., 3077 (1969).
149. P.S. Clezy and D.B. Morell, Aust. J. Chem., **23**, 1491 (1970).
150. Y. Chang, P.S. Clezy, and D.B. Morell, Aust. J. Chem., **20**, 959 (1967).
151. R.B. Woodward, Ind. Chim. Belge, 1293 (1962).
152. A.E. Pullman, J. Am. Chem. Soc., **85**, 366 (1963).
153. H.H. Inhoffen, P. Jager, R. Mahlop, and C.D. Mengler, Ann. Chem., **704**, 188 (1967).
154. H. Brockmann jr., Habilitation, Technische Hochschule Braunschweig, West Germany (1969).
155. H. Scheer, W.A. Svec, B.T. Cope, M.H. Studier, R.G. Scott, and J.J. Katz, J. Am. Chem. Soc., **96**, 3714 (1974).
156. J.J. Katz, R.C. Dougherty, and L.J. Boucher, in 'The Chlorophylls', Eds. L.P. Vernon and G.R. Seely, Academic Press, New York (1966).
157. H.J. Callot and A.W. Johnson, Chem. Commun., 749 (1969).

158. H.J. Callot, A.W. Johnson, and A. Sweeney, J. Chem. Soc., Chem. Commun., 1424 (1973).
158. (a) J.-H. Fuhrhop, T. Lumbantobing, and J. Ulrich, Tetrahedron Lett., 3771 (1970).
158. (b) G.N. Sinyakov, V.P. Suboch, A.M. Shul'ga and G.P. Gurinovich, Dokl. Akad. Nauk Beloruss. SSR, **17**, 660 (1973).
159. A. Eschenmoser, R. Scheffold, E. Bertele, M. Pesaro, and H.G. Schwend, Proc. Roy. Soc. London, Ser. A, **288**, 306 (1965); R. Bonnett and D.G. Redman, Proc. Roy. Soc. London, Ser. A, **288**, 342 (1965); H.A.O. Hill, J.M. Pratt, and R.P.J. Williams, J. Chem. Soc. C, 2859 (1965); H.A.O. Hill, B.E. Mann, J.M. Pratt, and R.J.P. Williams, J. Chem. Soc. C, 564 (1968); J.D. Brodie and M. Poe, Biochemistry, **10**, 914 (1971); J.D. Brodie and M. Poe, Biochemistry, **11**, 2534 (1972); S.A. Cockle, H.A.O. Hill, R.J.P. Williams, B.E. Mann, and J.M. Pratt, Biochim. Biophys. Acta, **215**, 415 (1970); C.E. Brown, D. Shemin, and J.J. Katz, J. Biol. Chem., **248**, 8015 (1973); A.R. Battersby, M. Ihara, E. McDonald, J.R. Stephenson, and B.T. Golding, J. Chem. Soc., Chem. Commun., 404 (1973).
160. R. Bonnett and A.F. McDonagh, J. Chem. Soc., Perkin Trans. 1, 881 (1973); J.-H. Fuhrhop, P.K.W. Wasser, J. Subramanian, and U. Schrader, Ann. Chem., 1450 (1974); A. Gossauer and W. Hirsch, Ann. Chem., 1496 (1974).
161. R. Grigg, J. Chem. Soc. C, 3664 (1971).
162. S. Besecke, and J.-H. Fuhrhop, Angew. Chem., **86**, 125 (1974); S. Besecke and J.-H. Fuhrhop, Angew. Chem., Int. Ed. Engl., **13**, 150 (1974).
162. (a) J.N. Esposito, L.E. Sutton, and M.E. Kenney, Inorg. Chem., **6**, 1116 (1967).
163. R. Grigg, A. Sweeney, and A.W. Johnson, Chem. Commun., 1237 (1970).
164. H.W. Whitlock and M.Y. Oester, J. Am. Chem. Soc., **95**, 5738 (1973).
165. G.L. Closs and L.E. Closs, J. Am. Chem. Soc., **85**, 818 (1963).
166. R. Mählhop, Dissertation, Technische Hochschule Braunschweig, West Germany (1966); H.H. Inhoffen and R. Mählhop, Tetrahedron Lett., 4283 (1966).
166. (a) V.P. Suboch, A.M. Shul'ga, G.P. Gurinovich, Yu.V. Glazkov, A.G. Zhuravlev and A.N. Sevchenko, Dokl. Akad. Nauk SSSR, **204**, 404 (1972).
167. H.H. Inhoffen, J.-H. Fuhrhop, and F. von der Haar, Ann. Chem., **700**, 92 (1966).
168. D.A. Savel'ev, A.N. Sidorov, R.P. Evstigneeva, and G.V. Ponomarev, Dokl. Akad. Nauk. SSSR, **167**, 135 (1966).
169. J.W. Buchler, L. Puppe, K. Rohbock, and H.H. Schneehage, Ann. N.Y. Acad. Sci., **206**, 116 (1973).
170. J.W. Buchler and L. Puppe, Ann. Chem., 1046 (1974).
171. P.N. Dwyer, J.W. Buchler, and W.R. Scheidt, J. Am. Chem. Soc., **96**, 2789 (1974).
172. A.M. Shul'ga, G.N. Sinyakov, V.P. Suboch, G.P. Gurinovich, Yu.V. Glazkov, A.G. Zhuravlev, and A.N. Sevchenko, Dokl. Akad. Nauk. SSSR, **207**, 457 (1972).
173. H. Scheer and J.J. Katz, Proc. Natl. Acad. Sci. U.S.A., **71**, 1626 (1974).
174. K.M. Smith, J. Chem. Soc., Chem. Commun., 540 (1971).
174. (a) A.M. Shul'ga, I.F. Gurinovich, G.P. Gurinovich, Yu.V. Glazkov and A.G. Zhuravlev, Zh. Prikl. Spektr., **15**, 106 (1971).
175. J.-H. Fuhrhop, J. Chem. Soc., Chem. Commun., 781 (1970).
176. H. Fischer and A. Treibs, Ann. Chem., **457**, 209 (1927).
177. H.H. Inhoffen and N. Müller, Tetrahedron Lett., 3209 (1969).
178. P.M. Müller, S. Farooq, B. Hardegger, W.S. Salmond, and A. Eschenmoser, Angew. Chem., **85**, 954 (1973).
179. A. Neuberger and J.J. Scott, Proc. Roy. Soc. London, Ser. A, **213**, 307 (1952).
180. H. Ogoshi, E. Watanabe, and Z. Yoshida, Tetrahedron, **29**, 3241 (1973).
181. A. Stone and E.B. Fleischer, J. Am. Chem. Soc., **90**, 2735 (1968).
182. S.J. Silvers and A. Tulinsky, J. Am. Chem. Soc., **89**, 3331 (1967).
183. S.J. Silvers and A. Tulinsky, J. Am. Chem. Soc., **86**, 927 (1964).

184. M.J. Hamor, T.A. Hamor, and J.L. Hoard, J. Am. Chem. Soc., **86**, 1938 (1964).
185. J.W. Buchler, G. Eikelmann, L. Puppe, K. Rohbock, H.H. Schneehage, and D. Weck, Ann. Chem., **745**, 135 (1971).
186. R.J. Abraham and K.M. Smith, Tetrahedron Lett., 3335 (1971).
187. J.-H. Fuhrhop, Z. Naturforsch., **25b**, 255 (1970).
188. J.J. Katz, R.C. Dougherty, and L.J. Boucher, 'The Chlorophylls', Eds. L.P. Vernon and G.R. Seely, Academic Press, New York (1966).
189. J.W. Buchler, L. Puppe, K. Rohbock, and H.H. Schneehage, Chem. Ber., **106**, 2710 (1973).
190. D.G. Whitten, J.C. Yau, and F.A. Carrol, J. Am. Chem. Soc., **93**, 2291 (1971).
191. D.G. Whitten, T.J. Meyer, F.R. Hopf, J.A. Ferguson, and G. Brown, Ann. N.Y. Acad. Sci., **206**, 516 (1973).
192. J.-H. Fuhrhop, Tetrahedron Lett., 3205 (1969).
193. G.W. Sovocool, F.R. Hopf, and D.G. Whitten, J. Am. Chem. Soc., **94**, 4350 (1972).
194. S.S. Eaton, G.R. Eaton, and R.H. Holm, J. Organomet. Chem., **39**, 179 (1972).
195. Z. Yoshida, H. Ogoshi, T. Omura, E. Watanabe, and T. Kurosaki, Tetrahedron Lett., 1077 (1972).
196. H. Ogoshi, T. Omura, and Z. Yoshida, J. Am. Chem. Soc., **95**, 1666 (1973).
197. J.W. Buchler and P.D. Smith, Angew. Chem., **86**, 378 (1974); J.W. Buchler and P.D. Smith, Angew. Chem. Int. Ed. Engl., **13**, 341 (1974).
198. H. Ogoshi, E. Watanabe, N. Koketzu, and Z. Yoshida, J. Chem. Soc., Chem. Commun., 943 (1974).
199. W.S. Caughey, C.H. Barlow, D.H. O'Keeffe, and M.C. O'Toole, Ann. N.Y. Acad. Sci., **206**, 296 (1973).
199. (a) D.A. Clarke, R. Grigg, and A.W. Johnson, Chem. Commun., 208 (1966).
200. G.A. Smythe and W.S. Caughey, Chem. Commun., 809 (1970).
200. (a) J.-H. Fuhrhop, K.M. Kadish, and D.G. Davis, J. Am. Chem. Soc., **95**, 5140 (1973).
200. (b) D.A. Clarke, R. Grigg, A.W. Johnson, and H.A. Pinnock, Chem. Commun., 309 (1967).
201. S.S. Eaton and G.R. Eaton, J. Chem. Soc., Chem. Commun., 576 (1974).
202. H.W. Whitlock, Jr. and B.K. Bower, Tetrahedron Lett., 4827 (1965).
203. H.H. Strain, B.T. Cope, G.N. McDonald, W.A. Svec, and J.J. Katz, Phytochemistry, **10**, 1109 (1971).
204. J.J. Katz, H.H. Strain, A.L. Harkness, M.H. Studier, W.A. Svec, T.R. Janson, and B.T. Cope, J. Am. Chem. Soc., **94**, 7938 (1972).
205. A.S. Holt, in 'The Chlorophylls', Eds. L.P. Vernon and G.R. Seely, Academic Press, New York, (1966), Chap. 4.
206. H. Brockmann jr., personal communication (1974); W. Trowitzsch, Dissertation, Technische Hochschule Braunschweig, West Germany (1974).
207. J.W. Mathewson, W.R. Richards, and H. Rapoport, J. Am. Chem. Soc., **85**, 364 (1963).
208. H. Rapoport and H.P. Hamlow, Biochem. Biophys. Res. Commun., **6**, 134 (1961).
209. J.H. Mathewson, W.R. Richards, and H. Rapoport, Biochem. Biophys. Res. Commun., **13**, 1 (1963).
210. A.S. Holt, D.W. Hughes, H.J. Kende, and J.W. Purdie, J. Am. Chem. Soc., **84**, 2835 (1962).
211. K.E. Eimhjellen, O. Aasmundrud, and A. Jensen, Biochem. Biophys. Res. Commun., **10**, 232 (1963); K.E. Eimhjellen, H. Steensland, and J. Traetteberg, Arch. Mikrobiol., **59**, 82 (1967); T. Meyer, S.E. Kennel, S.M. Tedro, and M.D. Kamen, Biochim. Biophys. Acta, **292**, 634 (1974).
212. F.C. Pennington, S.D. Boyd, H. Horton, S.W. Taylor, D.G. Wulf, J.J. Katz, and H.H. Strain, J. Am. Chem. Soc., **89**, 387 (1967).

213. K.M. Smith and J.F. Unsworth, Tetrahedron, **31**, 367 (1975).
214. F.C. Pennington, H.H. Strain, W.A. Svec, and J.J. Katz, J. Am. Chem. Soc., **86**, 1418 (1964).
215. J.J. Katz, G.D. Norman, W.A. Svec, and H.H. Strain, J. Am. Chem. Soc., **90**, 6841 (1968).
216. H.H. Strain and W.M. Manning, J. Biol. Chem., **146**, 275 (1942).
217. A.A. Krasnovksii, Dokl. Akad. Nauk. SSSR, **60**, 421 (1948).
218. G.R. Seely, in 'The Chlorophylls', Eds. L.P. Vernon and G.R. Seely, Academic Press, New York (1966), p. 523; A.N. Sidorov, in "Elementary Photoprocesses in Molecules', Ed. B.S. Neporent, Plenum Press, New York (1968); A.A. Krasnovskii, M.I. Bystrova, and F. Lang, Dokl. Akad. Nauk. SSSR, **194**, 308 (1970).
219. M.F. Hudson and K.M. Smith, J. Chem. Soc., Chem. Commun., 515 (1973).
220. J.W. Buchler and H.H. Schneehage, Z. Naturforsch., **28b**, 433 (1973).
221. H. Diekman, C.K. Chang, and T.G. Traylor, J. Am. Chem. Soc., **93**, 4068 (1971).
222. N.J. Logan and Z.U. Siddiqui, Can. J. Chem., **50**, 720 (1972).
223. M.F. Hudson and K.M. Smith, Tetrahedron Lett., 2223 (1974).
224. G.N. La Mar, W.DeW. Horrocks, Jr., and R.H. Holm (Eds.), 'NMR of Paramagnetic Molecules', Academic Press, New York (1973).
225. A.M. d'A. Rocha Gonsalves, Tetrahedron Lett., 3711 (1974).
226. R.J. Kurland and B.R. McGarvey, J. Magn. Reson., **2**, 286 (1970).
227. M.F. Perutz, J.E. Ladner, S.R. Simon, and C. Ho, Biochemistry, **13**, 2163 (1974).
228. M.F. Perutz, A.R. Fersht, S.R. Simon, and G.C.K. Roberts, Biochemistry, **13**, 2174 (1974).
229. M.F. Perutz, E.J. Heidner, J.E. Ladner, J.G. Beetlestone, C. Ho, and E.F. Slade, Biochemstry, **13**, 2187 (1974).
229. (a) M. Maltempo, J. Chem. Phys., **61**, 2540 (1974).
230. K. Wüthrich, R.G. Shulman, B.J. Wyluda, and W.S. Caughey, Proc. Nat. Acad. Sci. U.S.A., **62**, 636 (1969).
231. J.A.S. Cavaleiro, A.M.d'A. Rocha Gonsalves, G.W. Kenner, K.M. Smith, R.G. Shulman, A. Mayer, and T. Yamane, J. Chem. Soc., Chem. Commun., 392 (1974).
232. J.A.S. Cavaleiro, A.M.d'A. Rocha Gonsalves, G.W. Kenner, and K.M. Smith, J. Chem. Soc., Perkin Trans. 1, 1771 (1974); G.W. Kenner and K.M. Smith, Ann. N.Y. Acad. Sci., **206**, 138 (1973).
233. H.A. Degani and D. Fiat, J. Am. Chem. Soc., **93**, 4281 (1971).
234. H.A.O. Hill and K.G. Morallee, Chem. Commun., 266 (1970).
235. K. Wüthrich, R.G. Shulman, and T. Yamane, Proc. Nat. Acad. Sci. U.S.A., **61**, 1199 (1968).
236. K. Wüthrich, R.G. Shulman, and J. Peisach, Proc. Nat. Acad. Sci. U.S.A., **60**, 373 (1968).
237. W.DeW. Horrocks, Jr. and E.S. Greenberg, Mol. Phys., **27**, 993 (1974).
238. D.R. Eaton and E.A. LaLancette, J. Chem. Phys., **41**, 3534 (1964).
239. R.K. Gupta and A.G. Redfield, Biochem. Biophys. Res. Commun., **41**, 273 (1970).
240. R.K. Gupta and A.G. Redfield, Science, **169**, 1204 (1970).
241. W.S. Caughey and L.F. Johnson, Chem. Commun., 1362 (1969).
242. R.J. Kurland, D.G. Davis, and C. Ho, J. Am. Chem. Soc., **90**, 2700 (1968).
243. G.N. La Mar, J.D. Satterlee, and R.V. Snyder, J. Am. Chem. Soc., **96**, 7137 (1974).
244. G.C. Brackett, P.L. Richards, and W.S. Caughey, J. Chem. Phys., **54**, 4383 (1971).
245. J.C. Fanning, T.L. Gray, and N. Datta-Gupta, J. Chem. Soc., Chem. Commun., 23 (1974).
246. R.H. Felton, G.S. Owen, D. Dolphin, and J. Fajer, J. Am. Chem. Soc., **93**, 6332 (1971).
246. (a) J. Beetlestone and P. George, Biochemistry, **3**, 707 (1964).
247. I.A. Cohen, D. Ostfeld, and B. Lichtenstein, J. Am. Chem. Soc., **94**, 4522 (1972).

248. J.-H. Fuhrhop, Struct. Bonding Berlin, **18**, 1 (1974).
249. N. Sadasivan, H.I. Eberspaecher, W.H. Fuchsman, and W.S. Caughey, Biochemistry, **8**, 534 (1969).
250. W.S. Caughey, J.O. Alben, W.Y. Fujimoto, and J.L. York, J. Org. Chem., **31**, 2631 (1966).
250. (a) W.S. Caughey, Adv. Chem. Ser., **100**, 248 (1971).
251. P.D.W. Boyd and T.D. Smith, Inorganic Chem., **10**, 2041 (1971).
252. M. Wicholas, R. Mustacich, and D. Jayne, J. Am. Chem. Soc., **94**, 4518 (1972).
253. E.B. Fleischer and T.S. Srivastava, J. Am. Chem. Soc., **91**, 2403 (1969).
254. R.A. Bayne, G.A. Smythe, and W.S. Caughey, in 'Probes for Membrane Structure and Function', Eds. B. Chance, M. Cohn, C.P. Lee, and T. Yonetani, Academic Press, New York (1971).
255. H.A.O. Hill, B.E. Mann, and R.J.P. Williams, J. Chem. Soc., Chem. Commun., 906 (1967).
256. B.D. McLees and W.S. Caughey, Biochemistry, **7**, 642 (1967).
257. J. Hodgkinson and R.B. Jordan, J. Am. Chem. Soc., **95**, 763 (1973).
258. L. Rusnak and R.B. Jordan, Inorganic Chem., **11**, 196 (1972).
259. C.-P. Wong, R.F. Venteicher, and W.DeW. Horrocks, Jr., J. Am. Chem. Soc., **96**, 7149 (1974).
260. T.C. Farrar and E.D. Becker, 'Pulse and Fourier Transform NMR', Academic Press, New York (1971).
261. A.R. Battersby, J. Moron, E. McDonald, and J. Feeney, J. Chem. Soc., Chem. Commun., 920 (1972).
262. A.R. Battersby, E. Hunt, E. McDonald, and J. Moron, J. Chem. Soc., Perkin Trans. 1, 2917 (1973).
263. D.N. Lincoln, V. Wray, H. Brockmann, Jr., and W. Trowitzsch, to be published.
264. A.J. Jones, T.D. Alger, D.M. Grant, and W.M. Litchman, J. Am. Chem. Soc., **92**, 2386 (1970).
265. J.J. Katz, T.R. Janson, A.G. Kostka, R.A. Uphaus, and G.L. Closs, J. Am. Chem. Soc., **94**, 2883 (1972).
266. G.E. Maciel, in "Nuclear Magnetic Resonance Spectroscopy of Nuclei Other Than Protons", Eds. T. Axenrod and G.A. Webb, John Wiley and Sons, New York (1974), Chap. 13, p. 187.
267. J.P. Maher, M. Evans, and M. Harrison, J. Chem. Soc., Dalton Trans., 188 (1972).
268. K. Wüthrich and R. Baumann, Ann. N.Y. Acad. Sci., **222**, 709 (1973).
269. K. Wüthrich and R. Baumann, Helv. Chim. Acta, **56**, 585 (1973).
270. K. Wüthrich and R. Baumann, Helv. Chim. Acta, **57**, 336 (1974).
271. A. Lapidot, C.S. Irving, and Z. Malik, Proceedings of the First International Conference on Stable Isotopes in Chemistry, Biology, and Medicine, Argonne, CONF-730525, U.S. Atomic Energy Commission (1973), p. 127.
272. D. Karweik, N. Winograd, D.G. Davis, and K.M. Kadish, J. Am. Chem. Soc., **96**, 591 (1974). H. Falk, O. Hofer and H. Lehner, Monatsh. Chem. **105**, 366 (1974).
273. P. Diehl, in 'Nuclear Magnetic Resonance Spectroscopy of Nuclei Other than Protons', Eds. T. Axenrod and G.A. Webb, John Wiley and Sons, New York (1974), Chap. 18, p. 275.
274. J. Reuben and D. Fiat, J. Am. Chem. Soc., **91**, 1242 (1969); A. Johnson and G.W. Everett, Jr., J. Am. Chem. Soc., **92**, 6705 (1970).
275. R.C. Dougherty, G.D. Norman, and J.J. Katz, J. Am. Chem. Soc., **87**, 5801 (1965).
276. G.N. La Mar and D.B. Viscio, J. Am. Chem. Soc., **96**, 7354 (1974).
277. H. Brockmann, Jr. and W. Trowitzsch, personal communication, (1974).
278. K. Ballschmiter, K. Truesdell, and J.J. Katz, Biochim. Biophys. Acta, **184**, 604 (1969).

279. A.D. Trifunac and J.J. Katz, J. Am. Chem. Soc., **96**, 5233 (1974).
280. C. Houssier and K. Sauer, J. Am. Chem. Soc., **92**, 779 (1970).
281. L.J. Boucher and J.J. Katz, J. Am. Chem. Soc., **89**, 4703 (1967).
282. D.A. Doughty and C.W. Dwiggins, Jr., J. Phys. Chem., **73**, 423 (1969).
283. J.R. Larry and Q. Van Winkle, J. Phys. Chem., **73**, 570 (1969).
284. C.E. Strouse, Proc. Nat. Acad. Sci. U.S.A., **71**, 325 (1974).
285. J.J. Katz, Dev. Appl. Spectrosc., **6**, 201 (1968).
286. J.J. Katz and H.L. Crespi, Pure Appl. Chem., **32**, 221 (1972).
287. C.E. Castro, Bioinorg. Chem., **4**, 45 (1974).
288. G.N. La Mar and F.A. Walker, J. Am. Chem. Soc., **94**, 8607 (1972).
289. J.W. Faller and J.W. Sibert, J. Organometal. Chem., **31**, C5 (1971).
290. G.N. La Mar, J. Am. Chem. Soc., **95**, 1662 (1973).
291. M. Tsutsui, D. Ostfeld, and L.M. Hoffman, J. Am. Chem. Soc., **93**, 1820 (1971).
292. M. Tsutsui and C.P. Hrung, J. Am. Chem. Soc., **96**, 2638 (1974).
293. E.D. Becker, R.B. Bradley, and C.J. Watson, J. Am. Chem. Soc., **83**, 3743 (1961).
294. L.E. Webb and E.B. Fleischer, J. Am. Chem. Soc., **87**, 667 (1965).
295. K.M. Smith, private communication, 1974.
296. J.W. Lauher and J.A. Ibers, J. Am. Chem. Soc., **95**, 5148 (1973); P.W. Codding and A. Tulinsky, J. Am. Chem. Soc., **94**, 4151 (1972).
296. (a) I. Morishima and T. Iizuka, J. Am. Chem. Soc., **96**, 7365 (1974).
297. M.J. Hamor, T.A. Hanmor and J.L. Hoard, J. Am. Chem. Soc., **86**, 1938 (1964).
298. J.L. Hoard, Science, **174**, 1295 (1971).
299. F.A. Walker, Tetrahedron Lett., 4949 (1971).
300. J.P. Collman, R.R. Gagne, T.R. Halbert, J.-C. Marchon and C.A. Reed, J. Am. Chem. Soc., **95**, 7868 (1973).
301. J.P. Collman, R.R. Gagne, H.B. Gray, and J.W. Hare, J. Am. Chem. Soc., **96**, 6522 (1974).
302. L.K. Gottwald and E.F. Ullman, Tetrahedron Lett., 3071 (1969).
303. W. Bhatti, M. Bhatti, S.S. Eaton, and G.R. Eaton, J. Pharm. Sci., **62**, 1574 (1973).
304. M. Raban and K. Mislow, in 'Topics in Stereochemistry', Eds. N.L. Allinger and E.L. Eliel, Vol. 2, Interscience, New York (1967), p. 199; W.H. Pirkle and S.D. Beare, J. Am. Chem. Soc., **91**, 5150 (1969); W.H. Pirkle, S.D. Beare, and R.L. Muntz, Tetrahedron Lett., 2295 (1974).
305. H. Fischer and H. Gibian, Ann. Chem., **550**, 208 (1942); H. Fischer and H. Gibian, Ann. Chem., **552**, 153 (1942).
306. G.E. Ficken, R.B. Johns, and R.P. Linstead, J. Chem. Soc., 2272 (1956).
307. H. Brockmann, Jr., Ann. Chem., **754**, 139 (1971).
307. (a) H. Wolf and H. Scheer, Ann. N.Y. Acad. Sci., **206**, 549 (1973).
308. H.H. Inhoffen, J.W. Buchler, and R. Thomas, Tetrahedron Lett., 1145 (1969).
309. H. Wolf, I. Richter, and H.H. Inhoffen, Ann. Chem., **725**, 177 (1969).
310. W.B. Moniz, C.F. Poranski, Jr., and T.N. Hall, J. Am. Chem. Soc., **88**, 190 (1966) and citations therein.
311. A.M.d'A. Rocha Gonsalves, G.W. Kenner, and K.M. Smith, J. Chem. Soc. D, 1304 (1971); G.W. Kenner, K.M. Smith, and M.J. Sutton, Tetrahedron Lett., 1303 (1973).
311. (a) A.M. Shul'ga, I.F. Gurinovich, Yu.V. Glazkov and G.P. Gurinovich, Zh. Prikl. Spektr., **15**, 671 (1971), A.M. Shul'ga, G.P. Gurinovich and I.F. Gurinovich, Biofizika **18**, 32 (1973).
312. H.H. Inhoffen and P. Jäger, Tetrahedron Lett., 1317 (1964).
313. C.E. Castro and H.F. Davis, J. Am. Chem. Soc., **91**, 5405 (1969).
314. R.C. Dougherty, H.L. Crespi, H.H. Strain, and J.J. Katz, J. Am. Chem. Soc., 88, 2854 (1966); J.J. Katz, R.C. Dougherty, H.L. Crespi, and H.H. Strain, J. Am. Chem. Soc., 88, 2856 (1966), J.J. Katz and H.L. Crespi, in 'Recent Advances

Phytochemistry', Eds. M.K. Seikel and V.C. Runeckles, Vol. II, Appleton-Century-Crofts, New York (1969).
315. M. Tomkiewicz and M.P. Klein, Proc. Nat. Acad. Sci., U.S.A., **70**, 143 (1973).
316. A.R. Lepley and G.L. Closs (Eds.), 'Chemically Induced Dynamic Nuclear Polarization', Wiley, New York (1973).
317. S. Boxer and G.L. Closs, private communication (1974).

SUBJECT INDEX

Absorption spectra, in acidic solvents, 24, table 784
— —, in alkaline solvents, 24
— —, chlorins, 25, table 880—883
— —, in detergents, tables 888—889
— —, etio type, 20
— —, hemochromes, table 805
— —, *meso*-substituted porphyrins, 23, table 878—879
— —, metalloporphyrins, 25, 187—191, table 884—886
— — —, hyper type, 190
— — —, hypso type, 190
— — —, normal type, 189
— — —, in organic solvents, table 872—877
— —, oxophlorins, 26
— —, phlorins, 25
— —, phyllo type, 23
— —, porphyrins in aqueous acid, table 784
— —, porphyrins with isocyclic ring, 23
— —, porphyrin β-keto-esters, 23
— —, porphyrin monocations, 24
— —, rhodo type, 21
— —, substituent effects, 22
— —, tables 871—889
'Accidental' heme cleavage, 146—150
Accumulation of biosynthetic intermediates with ammonium ions or hydroxylamine, 79—82
Acetals from formylporphyrins, 828
Acetate method for metal insertion, 179
meso-Acetoxyporphyrins from oxophlorins, 41, 631, 816
Acetyl acetonate method for metal insertion, 182, 286, preparative method 798
Acetylation of hydroxyl groups, preparative method, 824
—, of oxophlorins, 41, 631, 816
—, step in aminolevulinic acid synthesis, 70
Acetylporphyrins, from α-hydroxyethylporphyrins, preparative method 824
Acid/base properties, 11—15, 234—238
Acid catalyzed conversion of porphobilinogen into uroporphyrinogens, 75, 82
— —, solvolysis of metalloporphyrins, 246
Acid number, 14, 15, 833
— —, table 14
Acid solvolysis reactions of metalloporphyrins, 243—247
Activated oxygen, 134, 135, 142, 629, 676
— —, in heme cleavage, 134, 135, 142
Active H atoms, determination, 821
Acylation, 648
Agar gel electrophoresis, 861
π-π Aggregation, 294, 493—501, 618
Algal bile pigments, origin, 125, 144
Alkali metal insertion, 795
Alkylation, reductive, 659—661
Amide bonds in side-chains, preparative method, 826
Aminolevulinic acid, binding to dehydratase, 73
— —, detection in natural materials, 785—787
— —, dehydratase, 72
— — —, Sepharose-bound, 72
— —, formation, 62—74
— — —, in plants, 66
— —, synthesis 62—74
— — —, acylation step, 70
— — —, decarboxylation step, 70, 71
— —, synthetase, 66
— — —, activity in plants, 66
— — —, properties, 67
— — —, inhibition, 68, 69, 72
— —, paper chromatography, 788
meso-Aminoporphyrins, 636
—, reactivity, 652
Ammonium ions, use for accumulation of biosynthetic intermediates, 79—82

Analysis of coproporphyrin and protoporphyrin, 781—782
—, of natural porphyrins by spectrophotometry, 782
— — — —, by solvent extraction, 781—785
—, of zinc(II) coproporphyrin, 782
Analytical methods for bile pigment isomers, 138—140
π-Anions of metalloporphyrins, 599
Annulenes, ring current in, 405—409
Anodic half-wave potentials, table 601
Anomalous mass spectra, 222, 396
— — —, of metalloporphyrins, 222
Anti-Markownikoff hydration of vinyls, 51, 656, 823 (preparative method)
AP.AP Pyrromethane, enzymic studies, 93
AP.PA Pyrromethane, enzymic studies, 92
Appendix, absorption spectra tables, 871—889
Applications of n.m.r. spectroscopy to porphyrin problems, 493—514
Aqueous acids, hydrolysis of esters, preparative method, 836
Aqueous solvents, effect on heme cleavage, 132
— —, kinetics of metal insertion, 252
Aromaticity, 9
Aromatic nature of porphyrin core, 332, 394, 402—410
— — — —, using mass spectra, 394
— — — —, using n.m.r. 402—410
— — — —, X-ray techniques, 332
Aromatization of protoporphyrinogen-IX, 104, 105
— — —, intermediates, 105
Assignments, ^{13}CMR, 88, 483
Asymmetric carbon atoms, n.m.r. investigations, 509—513
Autoxidation of porphyrinogens, 75, 104
Axial connection in deoxycobaltohemoglobin, 371—373
— —, in hemoglobin, 369—370
—, coordination chemistry of metalloporphyrins, 207—224
—, ligands, identification, 221—224
— —, preparation of metalloporphyrins with specific ones, 210
— —, vibrations, table 533
Azaporphyrins, basicity 13
Bacteriochlorins, 643
—, ^{1}HMR, 440—448
—, radical anions, 580
Bacteriochlorophyll-*a*, 7, 465, 644
Bacteriochlorophyll-*b*, 7, 465
Bacteriochlorophylls, *c*, *d*, and *e*, 466
—, formulae, 112
—, ^{1}HMR, 465—466
Basicity, 12 (Table), 234—238
—, measurements in non-aqueous solvents, 237
—, water soluble porphyrins, table, 238
Benzonitrile method for metal insertion, 185
Benzyl ethyl β-keto-adipate, preparative method, 758
Biladiene, 6
—, metal complexes, 205
a,c-Biladienes in porphyrin synthesis, 44, 47
Bilatriene, 6
Bilane, 6
—, enzymic studies, 96
—, from enzymic inhibition experiments, 81
Bilanes, in porphyrin synthesis, 37
Bilayer lipid membranes (BLM), 712—722
— — —, methodology, 715
— — —, photoelectrical effects, 713
— — —, relation to photosynthesis, 721
— — —, results from, 717—721
— — —, structure, 712
Bile pigment formation, 123—153
Bilene, 6
a-Bilenes, porphyrin synthesis from, 41
b-Bilenes, porphyrin synthesis from, 41—44
b-Bilene-1′,8′-diesters in porphyrin synthesis, 42
b-Bilenes, synthesis 41—44
Bilidiene, 6
Bilinogen, 6
Bilins, metabolic transformations, 128
Bilirubin formation, 124
Bilitriene, 6
Biliverdin-IXγ, 126
Biliverdin derivation, 123
—, formation from oxophlorins, 635, (preparative method, 813)
—, origin of oxygen atoms in terminal rings, 142—144

Binding and activation of glycine in aminolevulinic acid synthesis, 68
—, of aminolevulinic acid to dehydratase, 73
—, of succinyl coenzyme-A, 70
Biological applications of EPR, 584
—, heme cleavage, 142—150
Biosynthesis of hemes, chlorophylls, vitamin-B_{12}, 61—122; broad outline, 61
—, use of ^{13}CMR, 87—92, 513, 514
—, of chlorophylls, 107—112
—, of corrins, 112—116
—, of porphobilinogen, 62—74
—, of vitamin B_{12}, 112—116
Bis-histidine *meso*-hemin, preparative procedure, 826
Bis-porphyrins, 667
Bisulfite reaction of formylporphyrins, 828
1′-Bromo-8′-methyl-*a,c*-biladienes, synthesis and use in porphyrin synthesis, 46
Bridged and metal-metal bonded metalloporphyrins, 228—295

Calcium phosphate, adsorption of porphyrins, 780
Calculations, ring currents, 409
Carbenes, reactions with, 650
Carbon monoxide formation in heme cleavage, 125, 133—136
Carbonyl method for metal insertion, 186, 282, 284 (table), 799 (preparative method)
Carbocyclic ring, chlorophyll biosynthesis, 110
— —, mass spectral fragmentations, 391—394
Carboxylic acid side-chains from formyl groups, preparative method, 829
— — — —, reactions, 656
Catalase, 150, 258
Cathodic half-wave potentials, table, 602
Cation radicals, aggregation, 618—620
— —, of metalloporphyrins, 595—597, 643, 705
— —, EPR, 576—580
— —, preparative method, 812
Causative factors in heme cleavage, 144
Celite, for column chromatography, 853
Cellulose, for column chromatography, 855
Central metal ions, influence of, 629
— — —, oxidation states, 191—195
C_{4h} geometry, 322
C_{2v} geometry, 348
C_{4v} geometry, 326
Chelation of magnesium into protoporphyrin-IX, 109
Chemical intermediates in heme cleavage, 132—137
—, reactivity and redox potentials, 610—612
—, shifts, 400
— —, ^{13}CMR, 484
meso-Chlorination of porphyrins, preparative method, 819
Chlorins, 641—643
—, absorption spectra, 25
—, $\gamma\delta$-dideuteration, preparative method, 817
—, dehydrogenation with quinones, 32, 54; preparative method, 770
Chlorin-e_6 trimethyl ester, ^{1}HMR, 404
— — —, preparation, 54; preparative method, 777
Chlorins, electron densities, 626
'Chlorin-free' *meso*-tetraphenylporphyrin, synthetic method, 770
Chlorins and analogs, ^{1}HMR, 440—448
—, mass spectra, 390
Chlorin-phlorins, ^{1}HMR, 455
— —, preparative method, 814
Chlorins, structure, 6
—, vibrations, 529 (table)
Chlorobium chlorophylls, 661
— —, ^{13}CMR, 489
— —, synthesis of derived phylloporphyrins, 43
Chlorocruoroporphyrin, synthesis from protoporphyrin-IX, 52
Chlorophyllase, 111
Chlorophyll-benzoquinone system, 694
Chlorophyll biosynthesis, 107—112; scheme, 108
Chlorophyll-*b* formation, 111
Chlorophylls c_1 and c_2, ^{1}HMR, 465
Chlorophyll degradation, 52—55; preparative methods, 774—778
Chlorophylls from leaf tissue, 52; preparative method, 774
Chlorophyll formation from chlorophyllide, 111
Chlorophylls, ^{1}HMR, 462—468

Chlorophyll monolayers, 709—712
—, nomenclature, 52
—, photoreduction, 704
—, related structures, ^{1}HMR, 467
Chlorophyllides, from chlorophyll, 53
Choleglobin, 136
Chromatographic separation of aminolevulinic acid and porphobilinogen, 787
Chromatography, 839—860
Chromophores of porphyrin systems, 19
Chloroporphyrin-e_6, preparation, 54
Cis-effects in ruthenium and osmium porphyrins, 220
—, in iron porphyrins, 262
Cis-photohydrogenation, 683
CIDNP studies, 514
Classification of metalloporphyrins, 163—171
Cleavage of non-iron metalloporphyrins, 16, 143, 689, 814
—, of protoheme, 126
Closed-shell metalloporphyrin luminescence, 670
π-Cloud of porphyrins, 402
^{13}CMR, 482—493
—, assignments, 483
— —, *meso*-carbons, 88
—, in biosynthetic studies, 87—92, 513, 514
—, chemical shifts, 484
—, of diamagnetic porphyrins, 482—490
—, of paramagnetic metalloporphyrins, 490
C_t—N radius, 323
Cobalt and low spin iron metalloporphyrins, stereochemistry, 399—364
Cobalt(II) porphyrins, EPR, 568—573
— —, scheme of chemistry, 217
Coboglobins, 223, 264, 371—373
Colloidal preparations of chlorophyll, 709
Column chromatography, 851—858
Complexation with metal ions, 15
Concentration of aminolevulinic acid on Dowex columns, 787
—, of porphyrins from natural material, 780
Conformation of *meso*-substituents, ^{1}HMR, 504
—, of β-pyrrole substituents, ^{1}HMR, 503
Conjugation of phenyl groups with macrocycle in *meso*-tetraphenylporphyrin, 342
Conversion of formyl groups into ethylene epoxides, 829
—, of porphobilinogen into uroporphyrinogen-III, 74—96
Cooperative effect in hemoglobin, 369, 371
Coordination chemistry of metalloporphyrins, dynamic aspects, 233—278
— — —, static aspects, 157—231
— — —, unusual aspects, 279—313
Coordination groups in metalloporphyrins, stereochemistry, 343—373
Copper porphyrins, EPR of oxidation products, 582
'Copper salt' method for cyclization of tetrapyrroles, 42, 44
Copper and silver porphyrins, EPR, 562—567
Copper, silver, and molybdyl porphyrins, EPR tables, 566
Coproporphyrins, 9
—, analysis from natural materials, 781
Coproporphyrin-III, from natural materials, 778
—, from protoporphyrin-IX, 51
—, occurrence, 18
—, from uroporphyrin-III, preparative method, 825
Coproporphyrin isomers, separation by lutidine method on paper, 843
— —, separation by *n*-propanol method on paper, 844
Coproporphyrin-III tetramethyl ester, synthesis 40; preparative method, 761
Coproporphyrinogen-III, mechanism of decarboxylation, 101, 104
—, oxidative decarboxylation, 99—104
Coproporphyrinogenase, properties, 100
Corphins, 7, 645, 751
—, ^{1}HMR, 456
Correlation of spectral data and stability in metalloporphyrins, 203—205
Corrins, 7
—, biosynthesis, 112—116
—, from tetradehydrocorrins, 743—744
—, stability of metal complexes, 205
Corroles, 8
—, chemical properties, 737—740
—, physical properties, 736—737
—, synthesis, 732—736
Countercurrent distribution, 15, 834
Coupled oxidation, 16, 635

— —, of hemes and hemoproteins, 130—142; preparative procedure, 813
Criteria for successful metal insertion, 187—191
—, for site of one-electron oxidation, 609
Crude *meso*-tetraphenylporphyrin, synthetic method, 769
Crystallization, porphyrins, porphyrin esters, 837
Cyclic voltammetry, 603—607
Cyclization of 1′,8′-dimethyl-*b*-bilenes to give porphyrins, 42
Cytochromes, 258, 288
Cytochrome-*c*, splitting heme from, 811
Cytochrome oxidase, 258, 288
Cytochrome-*P*450, 130, 629—630
—, in heme cleavage, 145—150

Decarboxylation, of acetic acid side-chains, 825
—, of propionic acid side-chains, 826
—, in aminolevulinic acid synthesis, 70—71
—, of uroporphyrinogen-III, 96—99
Degradation, of chlorophylls, 52—55
—, of hemoglobin, 48—52
—, of mesoporphyrin-IX, 63, 64, 660
—, of porphyrin nucleus, 659
—, of protoporphyrin-IX, 63, 64
Dehydrocorphin, 752
Dehydroisocorrin, 744—745
Delocalization pathway for π-electrons, 9, 10, 338—341
Demetalation of metalloporphyrins, 195—207, 243—247
Deoxophylloerythroetioporphyrin, synthesis, 43
Derivation of bile pigments, 123—153
Determination of porphyrins in biological material, 779
—, of porphyrinogens, 793
Detergents, effect on porphyrin ionization, 235
—, kinetics of metal incorporation in, 249—252
—, solubility of porphyrins in, 831
Deuteration, 647
—, of chlorins, preparative method, 817
—, of porphyrins, preparative method, 816
Deuterium magnetic resonance, 492
Deuterohemin, from protohemin, 50
Deuteroporphyrin-IX, synthesis, 34, 50
—, from hemin, preparative method, 773
Deuteroporphyrins, 2,4-disubstituted, p*K*'s (table) 236
Deuteroporphyrin-IX disulfonic acid, preparative methods, 774
Development of periodic table of metalloporphyrins, 171—174
Devinylation of vinylporphyrins, 50, 655; preparative method, 773
D_{2d} geometry, 325
D_{4h} geometry, 318
2,4-Diacetyldeuteroporphyrin-III dimethyl ester, ^{13}CMR assignments of *meso*-carbons, 88
—, from deuterohemin, 51
—, from hematoporphyrin-IX, 51
2,3-Diacetyldeuteroporphyrin-III, synthesis, 44
Diacids of porphyrins, ^{1}HMR, 457
— —, stereochemistry, 341—343
Diamagnetic porphyrins, ^{13}CMR, 482—490
— —, ^{1}HMR, 412—473
—, 1 : 1 metalloporphyrins, ^{1}HMR, 460—462
Diastereotopic methylene groups in octaethylporphyrin derivatives, 503, 507
Diazomethane for esterification of porphyrins, preparative method, 834
—, reactions with formyl groups, 829
Dicarboxylic porphyrins, separation on paper, 848
Dications of porphyrins, ^{1}HMR, 457
— —, stereochemistry, 341—343
Dichlorodicyanobenzoquinone (DDQ) reaction with chlorins, 770
—, reaction with porphyrinogens, 41, 816
Didehydrocorrins, 744
2,4-Diformyldeuteroporphyrin-IX from protoporphyrin-IX, 51; preparative method, 822
Dihydrocorrins, 744
Dihydroxychlorins, 639
Di-imide reduction of porphyrins, 643
Dimerization rates of porphyrins and metalloporphyrins, 265—268
Dimetallic porphyrins, 300—310
1′,8′-Dimethyl-*b*-bilenes, synthesis, and use in porphyrin synthesis, 41
Dimethylformamide method for metal insertion, 185
Dinuclear iron(III) porphyrins, ^{1}HMR, 479
Dioxocorroles, 749

Dioxan method for separation of uroporphyrin esters on paper, 846
Dioxaporphyrins, 729—732
Dioxasapphyrins, 750
Dioxoporphodimethenes, 636—637
—, ^{1}HMR, 456
Diprotonation, effect on ^{1}HMR, 457
—, effect on stereochemistry, 341—343
Dithiaporphyrins, 730—732
d^1, d^2, and d^3 metalloporphyrins, stereochemistry, 351
d^2 and d^8 metalloporphyrins, EPR, 567
d^3 and d^7 metalloporphyrins, EPR, 568—571
d^4 and d^6 metalloporphyrins, EPR, 571—574
d^5 metalloporphyrins, EPR, 574—575
$4d^5$ and $4d^6$ metalloporphyrins, stereochemistry, 351
d^{10} and d^0 metalloporphyrins, stereochemistry, 344—348
d^9 and d^8 metalloporphyrins, stereochemistry, 349—350
Doming of porphyrin core, 326
d-Orbitals in iron porphyrins, 561
Doubly charged ions in mass spectra, 394—395
Dowex columns for aminolevulinic acid and porphobilinogen, 787
Dry column chromatography, 857
Duck blood enzyme system, 63—64
Dynamic coordination chemistry of metalloporphyrins, 233—278
Dynamic processes studied by NMR, 501—505

Effect of substituents on stability of metal complexes, 206
Ehrlich reaction and reagent, 790
Ejection of ligands, photochemical, 694
Electrolysis, preparative, 607—608
Electron densities, chlorins, 626
— —, phlorins, 627
— —, porphyrins, 626
—, transfer reactions, 255, 677, 707
Electronic absorption spectra, in acidic solvents, 24; table 784
— — —, in alkaline solvents, 24
— — —, chlorins, 25, table 880—883
— — —, in detergents, tables 888—889
— — —, etio type, 20
— — —, hemochromes, table 805
— — —, *meso*-substituted porphyrins, 23; table 878—879
— — —, metalloporphyrins, 25, 187—191; table 884—886
— — — —, hyper type, 190
— — — —, hypso type, 190
— — — —, normal type, 189
— — —, in organic solvents, table 872—877
— — —, oxophlorins, 26
— — —, phlorins, 25
— — —, phyllo type, 23
— — —, porphyrin dications in aqueous acid, table 784
— — —, porphyrins with isocyclic rings, 23
— — —, porphyrin β-keto-esters, 23
— — —, porphyrin monocations, 24
— — —, rhodo type, 21
— — —, substituent effects, 22
— — —, tables, 871—889
Electronic configuration in iron porphyrins, 320, 327
—, reactivity parameters of porphyrin periphery, 625
—, structure of porphyrin ligand, 576—577
Electrophilic substitution and addition reactions, 645—653
— —, general aspects, 645—647
— —, reactions of metalloporphyrins, 240—243
Electrophoresis, 860
Endogamous self-aggregation, 495
Enzymes for uroporphyrinogen-III formation, 77, 78
Enzymic aromatization of protoporphyrinogen-IX, intermediates, 105
—, conversion of porphobilinogen into uroporphyrinogen-III, nature of the process, 89—92
—, formation of protoporphyrin-IX, side-chain modifications, 96—104
— —, of uroporphyrinogen-I, 78—83
— —, of uroporphyrinogen-III, 83—85
—, inhibition experiments, 79—82
—, studies with a bilane, 96
— —, with pyrromethanes, 92—96
— —, with a tripyrrole, 96
EPR, biological applications, 584
—, of metalloporphyrins with unpaired electrons in the ligand and metal, 582

—, of porphyrins with paramagnetic metals, 560—575
—, of porphyrins with unpaired electrons in the ligand, 576—582
—, spectra, 555—589
Equatorial coordination chemistry, 171—207
Equilibrium constants for metal insertion, 247
Erythrocytes, life span, 129
Erythropoietic protoporphyria, 676
Esterification with alcohols and mineral acids, 835
—, with diazomethane, preparative method, 834
—, of hematoporphyrin-IX, 49
—, of hemin, 49, 836
—, of magnesium protoporphyrin-IX, 109
Ethyl groups, from propionic acid side-chains, 826
— —, reactions of, 654
Ethylene epoxide groups from formylporphyrins, 829
Etioporphyrins, preparation from uro-, copro-, and mesoporphyrins, 826
—, type isomers, 5
Etio type absorption spectra, 20
Etioporphyrin-I, synthetic method, 765
Even-electron ions, mass spectra, 388, 394
Exciplexes, 677
Excited states, 667—673
Excited metalloporphyrins, electron transfer, 707
Exchange of central metal ions, 239
Exogamous aggregation, 495, 498—501

Faraday method for magnetic susceptibilities, 545
Ferrochelatase, 106, 251
Flash photolysis and porphyrin excited states, 672
Fluorescence, 190, 667—672
Fluorimetric determination of uro-, copro-, and protoporphyrins, 783
Formation of aminolevulinic acid, 62—74
—, of bacteriochlorophyll, 112
—, of bile pigments, 123—153
—, of chlorophyll-*a* from chlorophyllide, 111
—, of chlorophyll-*b*, 111
—, constants for metalloporphyrins, 261
—, of the hemoproteins, 106
—, of protoheme, 106
—, uroporphyrinogen-III, 83—85
Formylbiliverdins, 16, 145, 689; preparative method, 814
—, metal complexes, 690
Formyl dihydrobiliverdins, 691
Formyl side-chains from vinyl groups, preparative method, 822
— —, reactions, 827—829
Formiatohemin, preparative method, 810
Formylation, of copper(II) octaethylporphyrin, preparative procedure, 818
Formylporphyrins, reaction with diazomethane, 829
—, reaction with Girard's reagent, 829
Free acid porphyrins, chromatography on columns, 855
Free base porphyrins, photo-oxidation, 687—689
— — —, photoreduction, 678—680
— — —, X-ray studies, 336—341
Friedel-Crafts reactions, 649
Frontier orbital model, 625

Geometry of coordination groups in metalloporphyrins, 343—373
—, of metal-free porphyrins, 336—343
—, unconventional, 373
Geminiketones, 639, 752
—, ^{1}HMR, 445
—, preparative methods, 813
Girard's reagent, reaction with formyl groups, 53; preparative method, 829
Glycine binding and activation in aminolevulinic acid synthesis, 68
Glycine as a biosynthetic precursor of pyrrole pigments, 62—69
Gouy technique for magnetic susceptibility, 545
Green hemin, 131, 630, 638
g-values in EPR, 555—556

Halide bridged metalloporphyrins, 292
Halogenation, 653
Harderian gland, 18, 102
Harderoporphyrin, 102
—, synthesis from protoporphyrin-IX, 52
Hardero- and isoharderoporphyrin, separation by high pressure liquid chromatography, 859

HCl number, 13, (table) 14, 15, 833
Heavy atom effect, 672
Hematinic acid, 63, 661
Hematoporphyrin-IX, from blood, 49
—, from hemin, preparative method, 771
Hematoporphyrin-IX dimethyl ester, from free acid, 772
— — —, from hemin, 772
Hematoporphyrin-IX dimethyl ester dimethyl ether, from hematoporphyrin-IX, 772
Heme cleavage, 123—153
— —, 'accidental' nature, 146—150
— —, bridge specificity, 137—142
— —, causative factors, 144
— —, chemical intermediates, 132—137
— —, effect of aqueous solvents, 132
— —, in vivo, 142—150
— —, role of axial ligands, 131
— —, role of cytochrome P450, 145—150
— —, theories, 127
Heme, coupled oxidation, 130—142
—, from cytochrome-*c*, preparative method, 811
Hemes, detection as pyridine hemochromes, 804
Heme-heme interactions, 369
Heme-α-methenyl oxygenase, 145
Heme oxygenase, 145
Hemes, solvent extraction from tissues, 807
Heme, stereochemistry in hemoglobin, 368—371
Heme synthetase, 251
Hemin-anion complexes, preparative procedures, 810
Hemins, column chromatography, 856
—, esterification of, 49
—, paper chromatography, 850
—, preparation from blood, 808
Hemin, synthesis, 34
Hemoproteins, coupled oxidation, 136—139
—, formation, 106
Hemoglobin, stereochemistry of heme, 368—371
Hepatic catalase, 150
Heptacarboxylic porphyrin in porphyrin biosynthesis, 97—99
Hetero-aggregation, 498—501
Hexahydroporphyrins, 644
High mass cluster of ions in mass spectra, 396
High performance liquid chromatography, 859
High potential quinones, treatment of chlorins, 54, 770
— — —, treatment of porphyrinogens, 41, 816
High pressure liquid chromatography, 859
High spin iron(III) complexes, ^{1}HMR, 478
— —, iron and manganese porphyrins, stereochemistry, 351—358
^{1}HMR of metalloporphyrins, 459—481
—, of paramagnetic (non-iron) metalloporphyrins, 480
^{2}HMR of porphyrins, 492
^{1}HMR of porphyrins, 412—482
—, use in mechanistic studies, 513
Homoazaporphyrin, 650
Hydration of vinyl groups with HBr/HOAc, preparative method, 821
Hydrazone formation from formylporphyrins, 828
Hydride method for metal insertion, 283
Hydrogen overpotential, 599
Hydrogenation, of tetradehydrocorrins, 743—746
—, and reductions, preparative methods, 814—816
Hydrolysis of esters, 836
Hydrolysis and dimerization data for metalloporphyrins, table, 267
Hydroporphyrins, 640—645
Hydroxide, use for hydrolysis of esters, 837
Hydroxylamine, use for accumulation of biosynthetic intermediates, 79—82
Hydroxylation of tetradehydrocorrins, 746
Hydroxymethylporphyrins from formylporphyrins, 828
Hydroxyporphyrins, ^{1}HMR, 455
β-Hydroxypropionic porphyrins and porphyrinogens, 103
— —, from vinyl or formyl side-chains, preparative method, 822
Hyper type metalloporphyrin absorption spectrum, 190
Hyperfine interactions, 558
Hypso type metalloporphyrin absorption spectrum, 190

Incorporation reaction of metal ions, 247—255
Identification of axial ligands, 221—224
Imino-oxoporphodimethenes, ^{1}HMR, 456
Incremental chemical shifts due to ring current, 412
Infrared and Raman spectra, 525—535
—, spectra of metalloporphyrins, 222, 525—535, (table 529)
— —, substituents, table, 530
Inhibition of aminolevulinic acid synthetase, 68—69, 72
—, experiments, bilanes derived from, 81
— —, with amines, 79—82
—, of porphobilinogen deaminase, 77, 78
—, of uroporphyrinogen-III cosynthetase, 78
Insertion of iron, preparative method, 803
—, of lanthanides, 184, 799 (preparative method)
—, metals, 177—187, 795—800, 803—804
— —, dynamic aspects, 247—255
Integrity of type-III macrocycle in biosynthesis, 87
π-π Interaction, 294, 493—501, 618
Interactions with metal ions, general outline, 233
Intermediates in corrin biosynthesis, 115
—, in enzymic aromatization of protoporphyrinogen-IX, 105
—, in heme cleavage, 132—137
—, in oxidative decarboxylation of coproporphyrinogen-III to protoporphyrinogen-IX, 102—103
—, in uroporphyrinogen-I formation, 79
Intermolecular energy transfer, 675
Interrupted conjugation, ^{1}HMR studies, 448—457
Intramolecular energy transfer, 675
Ionization, 234—238
—, at nitrogen atoms, 11, 234—238
—, at carboxylic acid side-chains, 14
Ion-molecule reactions in mass spectra, 396
Ions with m/e values greater than molecular weight, 384, 396
Iron, insertion, preparative method, 803
—, high-spin, and manganese porphyrins, stereochemistry, 351—358
—, low-spin, and cobalt porphyrins, stereochemistry, 359—364
Iron(II) and manganese(III) porphyrins, EPR, 571—574
Iron(III) and manganese(II) metalloporphyrins, EPR, 574
Iron porphyrins, EPR of oxidation products, 583
— —, *cis* and *trans*-effects, 262
— —, d-orbitals, 561
— —, ^{1}HMR, 476—480
Iron(II) porphyrins, Mössbauer spectra, 545
Iron(III) porphyrins, Mössbauer spectra, 541—545
— —, oxo-bridged dimers, 263, 266—268, 290—292
— — — —, ^{1}HMR, 479
— — — —, Mössbauer spectra, 545
— — — —, stereochemistry, 355
Iron porphyrins, scheme of chemistry, 215
Iron, removal from hemins, preparative method, 800—803
Irreversible reactions at porphyrin periphery, 625—666
Isocoproporphyrin, occurrence, 19
—, synthesis, 45
Isocorrins, 744
Isocyclic ring, biosynthesis in chlorophyll, 110
— —, mass spectral fragmentations, 391—394
Isolation of porphobilinogen from urine, 788
Isomer composition of biliverdins from hemes, 138
— — —, from hemoproteins, 140
Isomerism in porphyrins, 9
Isoporphobilinogen, 85
—, lactam, 80
Isoporphyrins, 647
—, ^{1}HMR, 449
Isotopic exchange of central metal ions, 239

Jaundice, 127, 677
'Jumbling' of pyrromethane and bilane rings, 38

Kekulé formula for porphyrin core, 332, 333, 338
Kernicterus, 127
β-Keto-esters of porphyrins, cyclization, 657

— — —, mass spectral fragmentations, 389
— — —, synthesis, 659
Keto-groups on porphyrins, reactions, 827
Kieselguhr method for concentration of natural porphyrins, 780
Kinetics of metal insertion, 249—253
Knoevenagel reaction of formylporphyrins, preparative method, 818
Krasnovskii reaction, 456, 615, 629, 678, 704
Küster's cyclic tetrapyrrole formula, 3

Lability of porphyrinogens, pyrromethanes, and bilanes in acid, 38
Laboratory methods, 757—870
Lanthanide induced shifts (LIS), 498
Lanthanides, insertion into porphyrins, preparative method, 799
Larmor precession, 402
Life span of erythrocytes, 129
Ligand-metal interactions, 500
Ligand photo-ejection, 694
—, substitution reactions, 268—271
Line widths in EPR, 558
Low-spin iron and cobalt porphyrins, stereochemistry, 359—364
— —, iron(III) complexes, ^{1}HMR, 476
— — — —, Mössbauer spectra, 543
Luminescence, 667—672
Lutidine method, paper chromatography, 843

MacDonald's method for porphyrin synthesis, 35
Macrocycles related to porphyrins, 729—754
— — —, ring current, 405—409
Magnesium octaethylporphyrin, titration with oxidants, 596
—, protoporphyrin-IX dimethyl ester, preparative method, 796
— —, disodium salt, preparative method, 796
Magnetic anisotropy, 399, 402—410
—, exchange, 549
—, resonance of central metals in metalloporphyrins, 492
—, susceptibility, 545—550
— —, table, 547
— —, temperature dependence, 548—549
— —, theoretical predictions, 548
Magnetochemistry, 545—550
Maleimide formation, 63, 661
Mammalian heme catabolism, 127—130
Manganese and iron (high spin) metalloporphyrins, stereochemistry, 351—358
Manganese(II) and iron(III) metalloporphyrins, EPR, 574
Manganese(III) and iron(II) porphyrins, EPR, 571—574
Markownikoff hydration of vinyl groups, 49, 655, (preparative method) 821
Mass spectrometry, 222, 381—398
— —, of metalloporphyrins, 222, 395
Mechanism of oxidative decarboxylation of coproporphyrinogen-III, 101, 104
Mechanisms of metal incorporation, 253—255
Mechanistic scheme for uroporphyrinogen formation, 82
—, studies using ^{1}HMR, 513
— —, of porphobilinogen formation, 66—74
Melting points, 9, 838
18-Membered delocalization pathway, 338—341
Membranes, photochemistry in, 701—725
Mesohemin from mesoporphyrin-IX, 50
Mesoporphyrin-IX degradation, 63, 64, 661
Mesoporphyrin isomers, 9
Mesoporphyrin-IX, from protohemin, 50
Mesoporphyrin-IX dimethyl ester, mass spectrum, 387
— — —, preparative method, 773
— — —, synthesis, 39
meso-substituents, conformations from ^{1}HMR, 504
—, ^{1}HMR characteristics, 426—437
Metabolic transformations of bilins, 128
Metal carbonyl method for metal insertion, 186, preparative method, 799
—, diketones, metal insertion, 182, preparative method, 798
Metal-free corphins, 752
Metal insertion, acetate method, 179, preparative method, 798
— —, acetylacetonate method, 182, preparative method, 798
— —, benzonitrile method, 185
— —, criteria of success, 187—191
— —, dimethylformamide method, 185
— —, discussion of problems, 174—176
— —, kinetics, 249—253

— —, mechanisms, 253—255
— —, metal organyl method, 186
— —, metal carbonyl method, 186, preparative method, 799
— —, metal diketone method, 182, preparative method, 798
— —, phenoxide method, 184
— —, procedures, 177—181, preparative methods 791—799, 803—804
— —, pyridine method, 181, 796—797
— —, reactions involved, 247—255
Metal ions, influence exerted by presence, 629
— —, oxidation states in metalloporphyrins, 191—195
Metal-ligand interactions, 500
—, vibrations, 532
Metal-metal bridged metalloporphyrins, 288—295, 471
Metal organyl method for metal insertion, 186
Metalation, general phenomena, 157, 160—163
Metallochlorins, π-cation radicals, 643
Metalloporphyrins, absorption spectra, 25, 187—191, tables, 805, 806, 884—887
—, dynamic coordination chemistry, 233—278
—, general classification of type, 163—171
—, ^{1}HMR, 459—481
—, isotopic exchange of ions, 239
—, magnetochemistry, 545—553
—, mass spectra, 222, 395
—, use in nuclear medicine, 271
—, photoreduction, 680—687
—, preparative procedures, 795—811
—, reactions with free-base porphyrins, 239—240
—, stability constants, 259—264
—, static coordination chemistry, 157—231
—, types, 208—214
—, with unusual geometry, 279—313
Methionine in vitamin B_{12} biosynthesis, 113
Methoxyl group determination, 820
Methyl groups from acetic acid side-chains, preparative method, 825
Methyl pheophorbide-*a*, mass spectrum, 393
Methyl side-chains by reduction of formylporphyrins, 829
Methylation, 649
Methylethylmaleimide, 63, 661
N-Methylporphyrins, ^{1}HMR, 437—440
—, slow protonation, 13; p*K*'s, 237
Microbial preparation of porphobilinogen from aminolevulinic acid, 789
Microsomal cytochrome P450, 130
—, heme cleavage enzymes, 145
Midpoint potentials for metal complexes, 598
M + 2 and M + 4 ions, 390, 396
Mixed solvent kinetics for metal insertion, 249—252
Modifications of porphyrin side-chains, preparative methods, 819—829
Modified porphyrin derivatives, 729—754
— — —, luminescence, 672
— — —, stability of metal complexes, 205—207
Molecular complexes, 618—620
Molecular ions, 382—388
Molecular symmetry, 321
Molybdyl and vanadyl porphyrins, EPR 567
Monometallic porphyrins, unusual examples, 295—300
Mössbauer spectroscopy, 539—545
— —, high spin iron(III) porphyrins, 541—545
— —, iron(II) porphyrins, 545
— —, oxy-bridged iron(III) dimers, 545
— —, parameters for iron porphyrins, table, 544
Myoglobin, effect on heme cleavage, 146—148
—, models, 218, 358, 366, 657

Nature of type-III rearrangement process, 89—92
Nernst equation, 594
Nernstian plots for metalloporphyrins, 597
NH tautomerism, 235, 340—341, 489, 501—503
Nickel(II) octaethylporphyrin, infrared spectrum, 527
Nicolaus oxidation, 661
Nitrenes, reactions of porphyrins with, 650
Nitration, 651; preparative method, 818
Nitrogen bridged metalloporphyrins, 289
Nitrogenase models, 258

Nitrosyl metal(II) porphyrins, stereochemistry, 364—366
N-Methylporphyrins, ^{1}HMR, 437—440
—, mass spectra, 394
—, slow protonation, 13; p*K*'s, 237
NMR spectra, 399—523
— —, of nuclei other than ^{1}H, 481—493
^{15}NMR of porphyrins, 491
NMR spectra, practical considerations, 411
— —, use in studies of self-aggregation, 494
Nomenclature, 5
—, of metalloporphyrins, 317
Non-aqueous solvents, kinetics of metal insertion, 249—252
Non-centrosymmetric stereoisomerism, by NMR, 508
Non-equivalence of methylenes in octaethylporphyrins, 503, 507
—, of ortho-phenyl protons in *meso*-tetraphenylporphyrin derivatives, 505, 507
Non-porphyrin macrocycles, 729—754
— —, vibrations in 527
Normal absorption spectra in metalloporphyrins, 189
Norsapphyrin, 751
Novel metalloporphyrins, 279—313, table 174
N-Substituted porphyrins, ^{1}HMR, 437—440
Nucleated red blood cells, 63
Nuclear hyperfine interactions, 557
—, medicine, use of metalloporphyrins, 271
—, monopole interaction, 540
—, quadrupole interaction, 540
—, Zeeman interaction, 541
Nucleophilic substitution, 654

Occurrence, bacteriochlorophylls, 17
—, chlorocruoroporphyrin, 17
—, *Chlorobium* chlorophylls, 17
—, chlorophylls, 17
—, coproporphyrin, 18
—, harderoporphyrin, 18
—, isocoproporphyrin, 19
—, metal-free porphyrins, 18
—, pemptoporphyrin, 19
—, porphyrin metal complexes, 16—18
—, protoporphyrin-IX, 18
—, *Spirographis* porphyrin and hemin, 17
—, uroporphyrins, 17, 19
cis-Octaethylchlorin, preparative method, 815
trans-Octaethylchlorin, preparative method, 815
Octaethyloxophlorin, preparative method with Tl(III) salts, 812
Octaethylporphyrin, ^{1}HMR, 416
—, mass spectrum, 383
—, synthesis, 33, preparative methods, 766—769
One-electron oxidation of metalloporphyrins, 595—597
Open-shell diamagnetic metalloporphyrins, luminescence, 670
Organic solvents, solubilities of porphyrins in, 832
Organometallic method for metal insertion, 286
Origin of oxygen atoms in biliverdin, 142—144
Osmium porphyrins, *cis* and *trans* effects, 220
— —, scheme of chemistry, 216
Overpotential, 599
Oxacorroles, 749
Oxaporphyrins, 635, 638, 730—732
Oxathiaporphyrins, 730—732
Oxidation, criteria for site of electron abstraction, 609
—, of formylporphyrins to give carboxylic acid porphyrins, preparative method, 829
—, of hydroxyethyl groups, preparative method, 824
—, number (Z_{ox}), 191—195
—, of porphyrins and metalloporphyrins, 63, 661, 812—814
—, at porphyrin periphery, 629—639
—, of pyrromethanes, 30
—, states of central metal ions, 191—195, 546—548
—, of vinyl groups to formyl, preparative method, 822
Oxidative decarboxylation of coproporphyrinogen-III, 99—104
— — —, intermediates, 102, 103
— — —, mechanism, 101, 104
Oxidative degradation of porphyrin nucleus, 63, 659—661
—, formation of carbocyclic ring in chlorophyll, 110

Oxidometric titrations, 597
Oxime formation from formylporphyrins, preparative method, 827
a-Oxobilanes, porphyrin synthesis from, 38
b-Oxobilanes, oxophlorin synthesis from, 40, 41
—, porphyrin synthesis from, 40
μ-Oxo-bridged iron(III) porphyrin dimers, 263, 266—268, 290—292
— — — —, ^{1}HMR, 479
— — — —, Mössbauer spectra, 545
— — — —, stereochemistry, 355
β-Oxochlorins (7-Oxochlorins), 639, preparative method, 813
Oxophlorins, 630—639
—, absorption spectra, 26
—, basicity, 13
—, conversion into porphyrins, 41, preparative method, 816
—, electronic spectra, 632
—, ^{1}HMR, 430, 455
—, metal complexes, 636
—, photo-oxygenation, 635
—, preparative procedures, 812
—, *π*-radicals, 631—633, preparative method, 812
— —, effect on ^{1}HMR, 455
—, reactivity, 633—640
—, removal of oxygen function, 41
—, structure, 8, 630
—, synthesis, 36
— —, from *b*-oxobilanes, 40—41
—, zinc complex, photo-oxidation, 692
Oxorhodo type absorption spectra, 23
Oxo-bridged iron(III) dimers, 263, 290—292
— — —, ^{1}HMR, 479
— — —, Mössbauer spectra, 545
— — —, stereochemistry, 355
Oxygen binding, cobalt porphyrins, 257, 262, 371—373
— —, iron porphyrins, 218, 256, 262, 366—371
Oxygen bridged metalloporphyrins, 263, 290—292
— — —, ^{1}HMR, 479
— — —, Mössbauer spectra, 545
— — —, stereochemistry, 355
Oxyhemes, 133—134
Oxyporphyrins, 630—639
—, metal complexes, 636

Paper chromatography of aminolevulinic acid, 788
— —, lutidine method, 841—844
— —, of porphobilinogen, 791
— —, of porphyrin free acids, 841—844
— —, of porphyrins and hemins, 839—851
Paper electrophoresis, 860
Paramagnetic metalloporphyrins, ^{13}CMR, 490
— —, EPR, 560—575
— —, ^{1}HMR, 473—481
— —, luminescence, 671
— —, with metals other than iron, ^{1}HMR, 480
Partition between ether and aqueous buffers, 834
— — —, and aqueous acid, 833
— — —, and water, 833
Pathway of heme cleavage, 132—137
Peak potentials from cyclic voltammetry, table, 605
Pemptoporphyrin, occurrence, 19
—, synthesis from protoporphyrin-IX, 52
Periodic table of metalloporphyrins, 171—174, 287—288
Peripheral side-chains, conformation by NMR, 503—504
— —, mass spectral fragmentations, 388—391
— —, vibrations, 530
Peripherally complexed porphyrin metal derivatives, ^{1}HMR, 471—473
—, substituted porphyrins, ^{1}HMR, 418—426
Periphery, irreversible reactions at, 625—666
Permanganate oxidation of porphyrin nucleus, 661
Petroporphyrins, 18, 172—173, 785
—, mass spectra, 382
Phenoxide method for metal insertion, 184
Phenyl groups, conjugation with macrocycle in *meso*-tetraphenylporphyrin, 342
Pheophorbides, from chlorophylls, 53
—, preparative method, 776
Pheophytins from chlorophylls, 53, preparative method, 775
—, separation of *a* and *b* series, preparative method, 775
Pheoporphyrins, formation from porphyrin *β*-keto-esters, 657
Pheoporphyrin-a_5 dimethyl ester, preparative method, 778

Phlorins, 6, 614—615, 704
—, absorption spectra, 25
—, electrochemical formation, 641—643
—, electron densities, 627
β-Phlorin from chlorin-e_6 trimethyl ester, preparative method, 814
Phlorin formation by photoreduction, 678
Phlorins, ^{1}HMR, 455
—, radical anions, 580
Phorbins, ^{1}HMR, 433
Phosphorescence, 667—672
Photochemical cleavage of metalloporphyrins, 130
—, reactions, sensitization, 708
Photochemistry, 667—700, 701—725
—, reaction patterns, 673—674
Photodynamic deactivation, 677
Photoejection of ligands, 694
cis-Photohydrogenation, 683
Photolability of vinylporphyrins, 689
Photo-oxidation, 676—677, 687—694,
—, of bilirubin, 677
—, of metalloporphyrins, 689—694, 709
Photo-oxygenation of zinc oxophlorins, 635
Photoprotoporphyrin and its isomer, 16, 688—689
Photoreduction of porphyrins, 16, 615, 677—687, 704
—, of central metals in metalloporphyrins, 687
—, of metalloporphyrins, 680—687
—, of porphyrin ligand in metalloporphyrins, 680—686
Photoredox cycles, 706—708
Photosynthesis, 677, 701—725
—, results from bilayer lipid membranes, 721
—, theory, 702—704
Photosystem I, 702
Photosystem II, 702
Phthalocyanine X-ray data, 320
Phycocyanobilin, 124
Phycoerythrobilin, 124
Phyllo-type absorption spectra, 23
Phylloerythrin, occurrence, 18
—, preparation, 54, preparative method, 777
Phylloporphyrin-XV from chlorophyll, 55
Phyriaporphyrin, 97—99, 847
Phytochrome, 124
'Picket Fence' porphyrin, 218, 262, 358, 366—368
pK, scheme for porphyrins, 11, 234—238
—, water soluble porphyrins, table 238
—, of substituted deuteroporphyrins, table, 236
—, correlation with visible absorption bands, table, 12
Planarity of porphinato core, 324
Polarography, 599
Polymers of metalloporphyrins, 309—310
Polymerization of monopyrroles, 32
—, of porphobilinogen, general biosynthetic considerations, 75
Porphin, 3
—, ^{1}HMR, 404, 412
Porphin macrocycle, vibrations of, 526
Porphinato core, symmetry, 321
iso-Porphobilinogen, 85
Porphobilinogen, acid catalyzed conversion into uroporphyrinogens, 75, 82
—, biosynthesis, 62—74
—, conversion into uroporphyrinogen-III, 74—96
—, deaminase, 77
— —, inhibition, 77, 78
— —, properties, 77
Porphobilinogen, formation, mechanistic studies, 66—74
—, hydrochloride, preparative method, 789
—, isolation from urine, 788
—, lactam, 79
— —, synthetic method, 760
iso-Porphobilinogen lactam, 80
Porphobilinogen, from natural materials, 788
—, paper chromatography, 791
—, polymerization, 617
— —, general biosynthetic considerations, 75
—, preparation from aminolevulinic acid on large scale, 789
—, qualitative identification, 790
—, synthetic method, 758—761
Porphodimethenes, 615—617, 636—637, 687, 705
—, ^{1}HMR, 455
—, stability of metal complexes, 206
Porphomethenes, 7, 616, 687, 705
Porphyria, 19, 676

Porphyrin-208, 97—99
Porphyrin analogs, 729—754
— —, ring current, 405—409
— —, stability of metal complexes, 205—207
Porphyrin basicity, 14
—, compounds from chlorophylls, preparative methods, 774—778
—, ligand, electronic structure, 576—577
—, esters, column chromatography, 852—855
— —, paper chromatography, 844
Porphyrins from hemoglobin, 48—52
Porphyrin induced chemical shifts, 498
Porphyrins with isocyclic rings, absorption spectra, 23
Porphyrin β-keto-esters, absorption spectra, 23
Porphyrin melting points, 9, 838
Porphyrins from natural products, 48—55, preparative methods, 778—785
Porphyrin nomenclature, 5
Porphyrin nucleus, degradation, 63, 659—661
Porphyrins from oxophlorins, preparative method, 816
Porphyrins in petroleum and shale, 172—173, 785
Porphyrin-phlorin photoredox cycle, 706
Porphyrin precursors, laboratory methods, 785—795
Porphyrins from protoheme, synthetic methods, 770—774
Porphyrins, sublimation, 15
Porphyrin synthesis, 32—48
— —, from *a,c*-biladienes, 44, 47
— —, from bilenes, 37, 41, 43
— —, from 1′-bromo-8′-methyl-*a,c*-biladienes, 46
— —, from 1′,8′-dimethyl-*a,c*-biladienes, 44
— —, from 1′,8′-dimethyl-*b*-bilenes, 41
— —, from open-chain tetrapyrroles, 36—47
— —, from *a*-oxobilanes, 38
— —, from *b*-oxobilanes, 40
— —, from oxophlorins, 41, preparative method, 816
— —, from pyrroketones, 36
— —, from pyrromethanes, 35
— —, from pyrromethenes, 33
— —, strategy, 29, 47
— —, from tripyrrenes, 44, 46—47
Porphyrin trivial names, 4
Porphyrinogens, 7, 617
—, analysis from natural materials, 781
—, autoxidation, 75
—, as biosynthetic intermediates, 74
—, detection, 793
—, ^{1}HMR, 456
—, lability in acids, 38
—, laboratory methods, 792—795
—, photo-oxidation, 687
—, preparation with sodium amalgam, preparative method, 792
—, preparation with sodium borohydride, preparative method, 792
—, randomization in acid, 16
—, from urine, analysis, 794
meso-Positions, reactions at, 816—819
Potentiometry, 594—599
Precorphins, 752
Preparation of porphyrins from protoheme, 770—774
Preparative electrolysis of metalloporphyrins, 607—608
n-Propanol method for paper chromatography of porphyrin esters, 844
Properties, of aminolevulinic acid synthetase, table, 67
—, of coproporphyrinogenase, 100
—, of porphobilinogen deaminase, 77
—, of π-radicals, 612—614
Protection of porphyrin vinyl groups, 51, preparative method, 823
Protoheme, from blood, 48
—, formation, 106
—, from hemoglobin, 48
—, in hemoglobin, stereochemistry, 368—371
—, preparation of porphyrins from, 770—774
Protohemin, from blood, 48, laboratory method, 808—809
Proton magnetic resonance spectra, 412—482
Protonation, effect on ^{1}HMR spectra, 457
Protoporphyrin-IX, analysis from natural materials, 781
Protoporphyrin isomers, 9
—, from blood, 49
Protoporphyrin-IX dimethyl ester, ^{13}CMR assignments of *meso*-carbons, 88

Protoporphyrin-IX and chlorophyll biosynthesis, 107
—, degradation, 63—64
—, ^{1}HMR, 417
—, preparative method from hematoporphyrin-IX, 771
—, preparative method from hemin, 771
Protoporphyrinogen-IX, aromatization, 104
Pseudocontact shifts, 499
Pseudouroporphyrin, 97—99, 847
Purification of *meso*-tetraphenylporphyrin, synthetic method, 770
Purpurin reaction, 659
Purpurin-7 trimethyl ester, 53, preparative procedure, 776
Purpurin-18 methyl ester, 53, preparative procedure, 776
Pyridine hemochromes, determination, 804
— —, tables of absorption spectra, 805
Pyridine method for metal insertion, 181
Pyropheophorbides, 54
Pyropheophorbide-*a* methyl ester, preparative method, 777
Pyrroketones, porphyrin synthesis from, 36
—, synthesis of, 31
—, synthesis from pyrromethanes, 31
β-Pyrrole substituents, conformations by ^{1}HMR, 503—504
Pyrrolo-oxygenase, 74
Pyrromethanes as biosynthetic units, 79—80
—, enzymic studies, 92—96
—, oxidation of, 30
—, in porphyrin synthesis, 35
—, synthesis, 31, 79—80
—, synthetic method, 764
Pyrromethenes, porphyrin synthesis from, 33
—, reduction of, 31
—, synthesis, 30
—, vibrations, table, 529
Pyrroporphyrin-XV from chlorophyll, 55

Quantitative determination of porphobilinogen, 791
Quenching phenomena in porphyrin photochemistry, 675
Quinones, dehydrogenation of chlorins, 54, 770
—, dehydrogenation of porphyrinogens, 41, 816

Radical anions, 679
— —, EPR, 580
Radical cations, aggregation, 618—620
— —, from chlorophyll and chlorins, EPR, 579
— —, EPR, 576—580
—, dimers, 294
π-Radicals, properties, 612—614
Radius of central porphinato hole, C_t—N, 323
Raman and infrared spectra, 525—535
Rate data, metalloporphyrin substitution reactions, 240
— —, solvolysis of metalloporphyrins, 246
Rates of dimerization of porphyrins and metalloporphyrins, table, 265
Reaction of chlorophyll-*b* with Girard's reagent, 53, preparative method, 775
Reactions of metalloporphyrins with free-base porphyrins, 238—240
—, of porphyrins with carbenes and nitrenes, 650
—, of porphyrins and metalloporphyrins at *meso*-positions, preparative methods, 816—819
—, of porphyrin side-chains, 654—659, preparative methods, 819—829
Reactivity parameters, 625
—, at porphyrin periphery, 625—666
—, and redox potentials, 610—612
Rearrangement process in type-III problem, 89—92
Redistribution of bilanes, porphyrinogens, and pyrromethanes, 38
Redox potentials and chemical reactivity, 610—612
— —, of metalloporphyrins, 505—506
—, potentiometry, 594—599
—, reactions of cobalt tetradehydrocorrins, 748
— —, of nickel tetrahydrocorrins, 747
Reduction of formylporphyrins to hydroxymethylporphyrins, preparative method, 828
—, of oxophlorin carbonyl group, 41
—, of pyrromethenes, 31
—, of ring D in chlorophyll biosynthesis, 111
—, of 4-vinyl group in chlorophyll biosynthesis, 109
—, of vinyl groups to ethyl, 821
Reductive alkylation, 659
—, degradation of the porphyrin nucleus, 659—691

Removal of iron from hemins, 49, preparative methods, 800—803
—, of vinyl groups from porphyrins, preparative method, 822
Resonance pathway in porphyrins, 338—341
Resorcinol fusion of vinylhemins, 50, 655, preparative method, 822
Reversible reactions of porphyrins and metalloporphyrins, 593—623
R_F values, lutidine method, 842
— —, n-propanol method, 845
Rhodins, formation, 657
Rhodin-g_7, preparation, 55, preparative method, 777
Rhodium porphyrins, scheme of chemistry, 217
Rhodo type absorption spectra, 21
— — — —, reversal of rhodofying effect, 21, 22
Rhodoporphyrin-XV, from chlorophyll, 53, preparative method, 777
—, synthesis, 46
Ring cleavage of hemes, preparative method, 813
—, current, 399, 402—410
— —, in ^{13}CMR, 412
— —, in macrocycles related to porphyrins, 405—409, 730, 736
— —, and structure, 409
Role of axial ligands in heme cleavage, 131
Ruffling of porphyrin core, 323
Ruthenium porphyrins, *cis* and *trans* effects, 220
— —, scheme of chemistry, 216

Sapphyrins, 8—9, 750
S_4 axis, 325
Scavenging of metal ions in mass spectrometry, 384, 396
Self-aggregation of porphyrins, 494
Sensitization of photochemical reactions, 708
—, of singlet oxygen, 676
Separation of aminolevulinic acid and porphobilinogen, 787
—, of *a* and *b* series of chlorophyll derivatives, 53, preparative method, 775
Sepharose-bound aminolevulinic acid dehydratase, 72
—, porphobilinogen deaminase, 96
Shale, porphyrins from, 172—173, 785
S_i, stability index, 197—199, 243
Side-chain abbreviations, 4
— —, fragmentations in mass spectra, 388—394
— —, modification in enzymic formation of protoporphyrin-IX, 96—104
— —, reactions, preparative methods, 819—829
Silicic acid, for column chromatography, 855—857
Silicon complexes, mass spectra, 395
Site of heme catabolism, 129
Skeletal vibrations of porphyrins, table, 528
Sitting-atop complexes, 248, 280, 295
Slow protonation of *meso*-tetraphenylporphyrin and N-methylporphyrins, 13
Solvent extraction for analysis of natural porphyrins, 781—785
— —, of hemes from tissues, 807
Solvents with high dielectric constant in metal insertion, 287
Solvolysis reactions of metalloporphyrins, 243—247
Solubilities, 829—833
Solubility, in acidified organic solvents, 833
—, in aqueous acids, 829
—, in aqueous alkalis, 830
—, in aqueous detergents, 831
—, in organic solvents, 832
Soret band, 10, 19
Special techniques in porphyrin chemistry, 829—839
Specificity of bridge cleavage in heme degradation, 137—142
Spectral data and stability of metalloporphyrins, correlations, 203—205
Spectrophotometric analysis of natural porphyrins, 782
Spin Hamiltonian, 558
Spin state equilibria, 549
— —, of iron porphyrins, 500
— — — — —, dependence on stereochemistry, 320, 327
Spin relaxation, 558
Spin—spin couplings, ^{13}C-^{13}C, 490
— —, ^{1}H-^{13}C, 489
— —, Tl-^{13}C, 490
Spiro hypothesis for type-III skeleton, 85—86

Spirographis porphyrin, synthesis from protoporphyrin-IX, 52
Stability classes of metalloporphyrins, 196
—, constants for metalloporphyrins, 259—264
—, index, S_i, 197—199, 243
—, order of metalloporphyrins, 197—199, 243
— —, for substituents in mass spectra, 389
—, and spectral data of metalloporphyrins, correlations, 203—205
—, of structurally modified ligands, 205—207
Static coordination chemistry of metalloporphyrins, 157—231
Stereochemistry of coordination groups in metalloporphyrins, 343—373
—, of core in metalloporphyrins, 327—335
—, of porphyrins and metalloporphyrins, 317—380
—, of macrocycle, by NMR, 505
—, of metal-free porphyrins, 336—343
—, of metalloporphyrins, by NMR, 505—509
—, and spin state in iron porphyrins, 320, 327
—, unconventional, 373
Steric effects on reactivity, 627
Stern-Volmer relationship, 674
Strategy of porphyrin synthesis, 29, 47
Structural analogs of porphyrins, 729—754
—, determinations of porphyrins and metalloporphyrins, 317—380
Structure of oxophlorins, 630—633
—, of unusual metalloporphyrins, 288—310
Sublimation of porphyrins, 15
Substituent effects on absorption spectra, 20—24
— —, in ^{1}HMR spectra, 422
meso-Substituents, mass spectral fragmentations, 391—394
Substituents, reactions of, 654—659
—, stability order in mass spectra, 389
—, vibrations, 530
Substituted deuteroporphyrins, p*K*'s, table, 236
—, porphyrins, effect on stability of metal complexes, 206
— —, ^{1}HMR, 418—426
Substitution reactions, of cobalt tetradehydrocorrins, 748
— —, of deuteroporphyrin-IX, 51
— —, of ligands, 268—271
— —, of metalloporphyrins, 240—243
— —, of nickel tetradehydrocorrins, 747
Succinyl coenzyme A, binding, 70
Sulfuric anhydrides of porphyrins, 657
Superoxide dismutase, 134
Symmetry considerations in porphyrin and metalloporphyrin geometry, 321—327
Synthesis of coproporphyrin-III tetramethyl ester, 40, synthetic method, 761—765
—, of corroles, 732—736
—, of deuteroporphyrin-IX, 34
—, of 2,3-diacetyldeuteroporphyrin-III, 44
—, of etioporphyrin-I, preparative method, 765—766
—, of hemin, 34
—, of isocoporphyrin, 45
—, of octaethylporphyrin, 33, preparative methods, 766—769
—, of oxophlorins, 36, preparative meth-of, 812
—, of porphobilinogen, preparative method, 758—761
—, of *meso*-acetoxyporphyrins from oxophlorins, 41, preparative method, 816
—, of mesoporphyrin-IX, 39
—, of metalloporphyrins, 282—288, preparative methods, 795—799, 803—804
—, of phylloporphyrins related to *Chlorobium* chlorophylls, 43
—, of porphyrins, 32—51, preparative methods, 761—770
— — —, from *a,c*-biladienes, 44—47
— — —, from *b*-bilenes, 41—44
— — —, from oxophlorins, 41, preparative method, 816
—, of pyrromethanes, 31
—, of pyrromethenes, 30
—, of rhodoporphyrin-XV, 46
—, of tetradehydrocorrins, 732—736
—, of *meso*-tetraphenylporphyrin, 32, preparative method, 769—770
—, of tripyrrenes, 46—47
Synthetic procedures, 757—770
π-Systems, aggregation, 618—620
Systems with interrupted conjugation, 448—457

Talc method for concentration of natural porphyrins, 781
Tautomerism, NH, 10, 340—341, 489, 501—503
Temperature dependence of magnetic susceptibility, 548—549
Tension in hemoglobin axial connection, 369—370
—, model for hemoglobin, 369—370
Tetradehydrocorrins, chemical properties, 740—749
—, cobalt salts, redox reactions, 748
— — —, substitution reactions, 748
—, hydrogenation, 743—746
—, hydroxylation, 746
—, nickel complexes, redox reactions, 747
— — —, substitution reactions, 747
—, physical properties, 736—737
—, protonation, 741
—, removal of angular ester groups, 741
—, structure, 8
—, synthesis, 732--736
—, thermolysis, 742
Tetrahydrocoproporphyrin-III, 106
Tetrahydroporphyrins, 6, 643—644
Tetrahydroprotoporphyrin-IX, 100—101, 105—106
meso-Tetraphenylchlorin, 32
—, as a contaminant in the preparation of *meso*-tetraphenylporphyrin, 769—770
meso-Tetraphenylporphyrin, ^{1}HMR, 416
—, slow protonation, 13, 458—459
—, synthesis, 32, preparative method, 769—770
Thermodynamic and stability constants of metalloporphyrins, 259—264
Thermolysis of tetradehydrocorrins, 732
Thiacorroles, 749
Thiaporphyrins, 730—734
—, ^{1}HMR, 449
Thiasapphyrins, 751
Thin layer chromatography, 858
Thiocyanation, 653
meso-Thiolation of porphyrins, preparative method, 819
"Three rearrangements" hypothesis for type-III isomer biosynthesis, 86—87
Total synthesis, preparative methods, 757—770
trans-effects in ruthenium and osmium porphyrins, 220
—, in iron porphyrins, 262
Transference from aqueous acid to ether, 830
Transmetalation, 195, 201—202
Trimetallic porphyrins, 308, 310
Trimethylsilyl ethers, mass spectra, 390
Trioxoporphomethenes, 456
Triplet energies, table, 669
Triplet states of porphyrins and metalloporphyrins, 581
Tripyrrenes in porphyrin synthesis, 44, 46—47
—, synthesis, 44—45
Tripyrrole, enzymic studies with, 96
Trivial names of porphyrins, 4
Tryptophane dioxygenase, 629
Type-III isomer formation, analysis of hypotheses, 85—87
Type isomers, mass spectra, 389
Type-III macrocycle, integrity during biosynthesis of heme, 87
Type-III problem, conclusions of biosynthetic work, 95—96
— —, ^{13}C studies, 87—92
— —, general biosynthetic considerations, 75

Unconventional coordination geometry, 373
"Unstable chlorin", 53, preparative method, 776
Unusual dimetallic porphyrins, 300—310
—, geometries in metalloporphyrins, 295—310
—, metalloporphyrins, 279—313
— —, ^{1}HMR, 468—471
—, monometallic porphyrins, 295—300
Urinary porphyrinogens, analysis, 794
Urine, isolation of porphobilinogen, 788
Uroporphyrins, 9
—, from natural materials, 778
Uro-, copro-, and protoporphyrins, fluorimetric determination, 783
Uroporphyrin-III and coproporphyrin-III as artefacts in porphyrin biosynthesis, 75
Uroporphyrin, detection in natural materials, 783
—, isomers, 75, 76
— —, separation by paper chromatography, dioxan method, 846
Uroporphyrin-III, natural occurrence, 17
Uroporphyrinogens from porphobilinogen with acid, 75, 82
Uroporphyrinogen-I, enzymic formation, 78—83

—, formation, possible mechanistic scheme, 82
—, intermediates in enzymic formation, 79
—, synthetase, 77
Uroporphyrinogen-III, as a biosynthetic precursor of vitamin B_{12}, 115
—, cosynthetase, 78
— —, inhibition, 78
— —, as a specifier protein, 96
—, decarboxylation, 96—99, preparative method, 825—826
— —, intermediates, 97—99
—, enzymic formation, 77, 78, 83—85
—, photo-oxidation, 688
—, from porphobilinogen, 74—96
—, preparative method from uroporphyrin-III, 815

Vanadyl and molybdyl porphyrins, EPR, 567
—, porphyrins, EPR of oxidation products, 583
Verdoheme, 136
Verdohemin, 638
Vinyl groups, reactions of 655, preparative methods, 821—824
2-Vinylpheoporphyrin-a_5 dimethyl ester, preparation, 54, preparative method, 778
Vinylporphyrins, protection of vinyl groups, 51, preparative method, 823
—, photolability, 689
—, reactions of, 655
—, reaction with diazoacetic ester, preparative method, 821
2-Vinylrhodoporphyrin-XV from chlorophylls, 53, preparative method, 777
Voltammetry with rotating platinum electrode, 599—603
Vibrations of axial ligands, 533
—, metal-ligand, 532
—, metal-N, 531—533
—, of non-porphyrin macrocycles, 527
—, of porphyrin macrocycle, 526—528
—, of pyrromethenes, 529
Vibrational spectroscopy, 525—535
Vilsmeier formylation of copper octaethylporphyrin, preparative method, 818
Visible absorption spectra, tables, 871—889
Vitamin B_{12}, biosynthesis, 112—116
— —, common pathway with porphyrins, 112—113
— —, incorporation of methionine, 113,
— —, incorporation of uroporphyrinogen-III, 115—116

Warburg's green hemin, 131
Water soluble porphyrins, basicity, 238
Willstätter number, 14, 833

Xanthoporphyrinogens, 638
—, ^{1}HMR, 456
—, preparative method, 813
X-ray parameters, tables, 328, 329, 330
X-ray studies, 317—380
X-ray studies of metal-free porphyrins, 336—343

Zeeman splitting, 541
Zero field splitting, EPR, 556
Zinc coproporphyrin for analysis of coproporphyrin from natural materials, 782
Z_{ox}, oxidation number, 191—195

Bayerische
Staatsbibliothek
München